THE PHOTOLYSIS OF CALCIUM, BARIUM, STRONTIUM AND LITHIUM AZIDES AND THE CO-IRRADIATED DECOMPOSITION OF CALCIUM AZIDE

A thesis submitted to the

UNIVERSITY OF CAPE TOWN

in fulfilment of the requirements for the degree of

DOCTOR OF PHILOSOPHY

by

CYRIL THOMAS O'CONNOR B.Sc.(Hons.) (Cape Town)

School of Chemistry,
University of Cape Town,
Rondebosch, Cape,
South Africa.

August, 1978.

ACKNOWLEDGEMENTS

The author wishes to express his sincere thanks to

Prof. E.G. Prout, D.Sc., Professor of Physical Chemistry, University of Cape Town, for his invaluable advice, direction and interest throughout the period of this research project.

Sincere thanks are also extended to

Mr D. Lensen, for his expert assistance with all the technical aspects of the project,

Mr C. Ledger, the glassblower, for his constant helpfulness and competent handling of glassblowing problems,

Mr B. Orlandi of the Department of Clinical Medicine and Immunology, U.C.T. Medical School, for his assistance in developing the low temperature control system, and

Ms. E. Stenton for her patience and helpfulness during the typing and proofreading of this thesis.

CONTENTS

1 SUMMARY

The effect of very high intensity ultraviolet radiation on powdered calcium, barium, strontium and lithium azides in the temperature range -80,0° - 35,0°C has been studied. Powdered and pelleted calcium azide was also irradiated with ultraviolet radiation in the temperature range 35,0° - 90,0°C and powdered lithium azide in the temperature range 24,0° - 170,0°C. All these decompositions were purely photolytic. Powdered and pelleted calcium azide was also subjected to ultraviolet radiation in the temperature range 110,0° - 140,0°C. This latter decomposition was termed co-irradiation due to the fact that both thermal and photolytic mechanisms were operative in this temperature range. Except at low temperatures, the extent of the decomposition was almost the same as that of a simple thermal decomposition.

Kinetic analyses, determination of activation energies, studies of the dependence of reaction rates on light intensity, the effect of introducing water vapour to the sample at various stages of decomposition and the observance of the colour of the sample at various stages of reaction have been carried out. Analogous results were obtained for all four azides at low temperatures and the results obtained for calcium and lithium azides at ambient and higher temperatures were analogous to those obtained for barium and strontium azides under similar conditions by previous workers.

During photolysis the activation energy underwent transitions, in all four azides, in the region of 0°C and in the region of 60°C.

Co-irradiation studies of calcium azide commenced at temperatures greater than 100°C. Similar studies were not carried out on lithium azide since even at temperatures in the region of 180°C the rate of photolytic decomposition was very much greater than that of a purely thermal decomposition at the same temperature.

2 INTRODUCTION

The work presented in this thesis involves a study of the photolytic and co-irradiated decompositions of various azides. Before presenting the results obtained in this study it is necessary to discuss the effects of the interaction of light with solids and the mechanisms of thermal decomposition. The effects of irradiation prior to thermal decomposition (pre-irradiation) and of irradiation during thermal decomposition (co-irradiation) will then be reviewed.

3 THE PHOTOLYSIS OF SOLIDS

(i) THE EFFECTS OF THE INTERACTION OF ULTRAVIOLET LIGHT WITH SOLIDS

A large number of crystals of inorganic solids can be decomposed by exposure to intense ultraviolet light e.g. azides and oxalates.[1] This photochemical decomposition or photolysis is favoured when the irradiation corresponds to a characteristic absorption band of the solid. The reaction is usually followed by pressure measurements of the evolved gas at fixed time intervals during photolysis. When this photolytic decomposition is examined in detail two general features become obvious.[2] Firstly, in most of the cases the photolysis-producing light is not absorbed at the crystal surface but in a distribution below the surface. Secondly, in a number of cases, the decomposition process clearly takes place on the surface. Ultimately, however, some decomposition begins to take place in the interior, especially after prolonged exposure to light. When decomposition takes place inside the crystal, it is not uniformly distributed but occurs at well defined individual locations. These observations have been interpreted from two viewpoints. Firstly,

the solid properties are regarded as relatively unimportant except as a matrix for holding the reacting interface. Secondly, all the properties associated with solids, in particular the electronic properties, are considered. This latter viewpoint, in which the electronic properties usually associated with that of semi-conductors and non-metals are assumed to be involved, provides a natural explanation for a large number of the effects observed in the photolytic process.

By using ultraviolet light just within the fundamental absorption edge, the radiation is, for the most part, uniformly absorbed within the first few microns below the incident surface. Such stimuli are then transferred to specific surface sites at which decomposition is initiated.[3] This has been observed in the photolysis of sodium[4] and potassium[5] azides. These surface sites are specific crystallographic locations that closely resemble etch pits. They also exist at crystal edges, and at the intersection of dislocations, and slip and twin planes, with the surface.

The transference of the stimuli referred to above implies the presence of an energy or charge carrier which transports the energy imparted by the individual photon to the point in the crystal where the decomposition occurs.[2] The basic fact to be considered is that by the absorption of a photon, the total energy of the crystal has been increased, and the crystal, being now in an excited state, may dispose of this energy in various ways. Before considering the means whereby the energy is transferred, it is necessary to consider the behaviour of electrons in solids.[6,7]

Consider an extra electron introduced into an ionic crystal. If we imagine the electron to migrate from a metal ion to a neighbouring metal ion, then the potential field in which the electron moves is the average of the field created by all the other nuclei and electrons. A

reasonably approximate treatment of such a field can be achieved by considering a constant potential inside the crystal modified by a superimposed periodic potential having the periodicity of the lattice. For a one-dimensional periodic potential field, the solutions of the Schrödinger equation have the form

$$\psi(x) = u_k(x)\, e^{\pm ikx}$$

where $u_k(x)$ is periodic with a periodicity equal to that of the lattice, and k is the wave number corresponding to the number of wavelengths contained in one full period, that is,

$$k = 2\pi/\lambda.$$

The function $u_k(x)$ depends generally on k. At values of k equal to $\pm\pi/a$, $\pm 2\pi/a$, $\pm 3\pi/a$, etc., where a is the lattice constant, discontinuities occur in the energy thus giving rise to energy bands and forbidden energy gaps. This arises since the condition for Bragg reflection of the electron wave in the crystal is met, i.e.

$$k = n\pi/a$$

becomes equivalent to the Bragg condition

$$2a \sin\theta = n\lambda.$$

The zones defined by values of k which are integral multiples of π/a (in one dimension) are Brillouin zones. The energy gaps occur at the zone boundaries. The first zone includes the segment between $-\pi/a$ and $+\pi/a$; the second includes the two segments $-2\pi/a < k < -\pi/a$ and $\pi/a < k < 2\pi/a$, etc.

The energy states within these bands are distributed in a quasi-continuous fashion. Electrons progressively fill all the allowed states starting with those lowest in energy and continuing until the supply of electrons is exhausted. In ionic solids, all the energy states in the first band are occupied hence it is termed a 'full' band. The full band is separated by several electron volts from the next band which is completely empty. In the full band, every state contains its maximum number of two electrons and, in accordance with the Pauli Exclusion Principle, electronic conductivity is impossible. Such substances are, therefore, insulators apart from possible ionic conductivity. If an insulator is irradiated with light of suitable wavelength, frequently in the ultraviolet region, an electron in the full band may be given sufficient energy to be raised into the next band where there is an abundance of empty states. The excited electron can, therefore, move freely through the crystal in the so-called 'conduction' band.

When an electron is elevated from the full band into the conduction band, the gap in the full band from which an electron is missing is called a positive hole. When, for example, a positive hole is localized on any halogen ion, the latter becomes a halogen atom. An electron on a neighbouring ion can tunnel through to the atom, thus exchanging places with the positive hole. Thus mobile electrons in the conduction band and mobile positive holes in the full band can contribute to the electronic conductivity of insulators.

The chemical activity within solids is closely connected to physical properties such as transport of matter, electrical conductivity, optical behaviour, and magnetic, thermal and mechanical properties. These physical properties in turn depend upon defects in electronic structure

and deviation from ideal atomic arrangements in solids. Lattice defects which are arbitrarily scattered throughout the crystal give rise to regions of disturbance localized about individual points. Crystal defects, such as inhomogeneities, point and line defects, influence the energy levels available for electrons and the properties of growth of new phases. In addition these defects act as traps for energy carriers. Consideration will now be given to the various imperfections present in solids.

Seitz has classified six primary types of crystal imperfections[8]:

(a) Phonons

(b) Electrons and holes

(c) Excitons

(d) Vacant lattice sites and interstitial atoms

(e) Foreign atoms in either interstitial or substitutional positions

(f) Dislocations.

In addition to these he lists three transient imperfections:

(a) Light quanta

(b) Charged radiations

(c) Uncharged radiations.

Seitz states that it is possible to generate the primary types of imperfections listed above by irradiating the perfect or imperfect solid with the above three radiations and that two or more imperfections of the same or different types may interact to generate other imperfections. Some of the properties of the crystal imperfections will be discussed with special emphasis given to those particularly relevant to the phenomenon of photolysis.

(a) *Phonons*: A phonon is a particle associated with unit quantum excitation of one of the modes of elastic vibration of an ideal crystal. Phonons of a given frequency are introduced into a crystal by linking the specimen with a piezo-oscillator.

(b) *Electrons and holes*: At low temperatures, an insulating crystal does not display appreciable ohmic conductivity. If however one excites electrons thermally, or otherwise, the crystal will behave like an ohmic electronic conductor. The electron is excited from the filled valence band to the empty conduction band, leaving behind a hole. Successive jumps of valence electrons into empty positions produce an opposite net motion of the hole, in the direction of the electric field. Hence the term positive hole is used to indicate that the entity moves in a field as though it has a positive charge, although what actually happens is a net shift of the valence band electrons in the opposite direction.

(c) *Exciton:* On irradiating an insulator with light of wavelength less than that of the gap between the valence and conduction bands, electrons from an anion may be excited to exciton levels which exist between the valence and conduction band. These levels can be thought of as corresponding to possible Bohr orbits with their convergence limit at the lowest level of the conduction band. An electron-hole pair is produced and the electron is bound to the positive hole by coulombic attraction. If this excited electron-hole pair remains fixed at a specific location in the crystal it is usually called a molecular exciton. If, however, it migrates throughout the crystal it is called an exciton. These mobile excitons have the important property that they can transport energy without any charge transport occurring. Once formed the mobile excitons migrate throughout the

crystal until they interact with any centre or defect which upsets the coulombic attraction between the two charges. Once this interaction occurs, the two charges recombine, or neutralize, with the release of a certain amount of energy. Usually the energy released when an exciton is destroyed is tenths of an electron-volt less than the band-gap energy. Excitons can also dissociate thermally to yield positive holes and electrons in the conduction band and thus aid photoconductivity. The exciton levels referred to above can be observed from the long wavelength edge in the low temperature optical absorption spectra. Exciton transitions have been observed in the optical absorption spectra of sodium, potassium, rubidium and caesium azides[9] as well as silver and thallous azides[10,11] in the wavelength range 140 - 200 nm. From these spectra the spacings between the exciton levels and their separation from the valence band have been calculated.

(d) *Vacant lattice sites and interstitial atoms*:

(i) Imperfect crystals: The simplest defect solids are imperfect crystals which are defined as having a stoichiometric composition, but having misplaced atoms or ions throughout the structure[12]. Such crystals do not have every atom in a position of minimum potential energy. Schottky defects consist of a vacant cation site and a vacant anion site. The two missing atoms are considered to have migrated to the surface of the crystal. Frenkel defects consist of a vacant lattice site with the atom which ideally should have occupied that site occupying a different position in the lattice such as is vacant in the perfect crystal. The concentration of defects of either type is dependent upon the energy required to produce them and upon the absolute temperature.

(ii) Non-stoichiometric crystals: Non-stoichiometry is characterised by a solid showing an excess or deficiency of one component, as indicated by composition. In order to satisfy charge balance, any excess or deficit of cations is accompanied by a corresponding excess or deficit of electrons. Cation and anion vacancies will tend, other things being equal, to form a vacancy pair by being attracted to each other. These vacancy pairs can capture an electron to form the so-called 'F-centre' and a cation vacancy in the bulk of the crystal.

(e) *Foreign Atoms*: These are included in the crystal, occupying either interstitial sites or normal lattice sites, in the latter case substituting for the atoms of the host crystal.

(f) *Dislocations*: These are line defects and two basic types can be distinguished. One type is an edge dislocation in which an extra half plane of atoms is inserted into the crystal lattice. The other kind is a screw dislocation which results from a displacement of the atoms in one part of a crystal relative to the rest of the crystal, forming a spiral ramp around the dislocation line.

As a result of the production of imperfections such as excitons or free electrons and their conjugate positive holes, by the absorption of light of characteristic wavelengths, the total energy of the crystal is increased. This excess energy can now be disposed of in various ways. Thus these imperfections can be considered as energy carriers for the transport of energy imparted by an individual photon.

When an exciton is formed, the excited ion will interact differently with its neighbours so that, at first, the lattice in its vicinity is not in its configuration of minimum energy. Consequently, the excited atom will vibrate about its new equilibrium position, and some

of the absorbed energy will be communicated thermally to the lattice. There are two main possibilities for the relative positions of the potential energy curves for the ground and excited states.[13] Either the excited state has a minimum inside or outside the curve representing the ground state. In the former case the electron is excited optically and then loses energy to the lattice while the ions take up new equilibrium positions. An electron can remain in an excited state for about 10^{-8} seconds after which it reverts to the ground state by an optical transition. Since the re-emission of radiation has never been observed in the first absorption band, the excited electron must make a radiationless transition to the ground state in less than 10^{-8} seconds. In the latter case, the electron could remain in the excited state until a radiationless transition occurs.

The exciton is in fact moving through the lattice at about the same speed as a thermal electron, interacting with the vibrational modes of the crystal and thus undergoing considerable scattering and losing kinetic energy. According to Seitz,[14] unless the exciton becomes trapped in a metastable state, it may transfer its energy to imperfections since it must pass over at least 10^7 ions in a lifetime of 10^{-8} seconds.

An electron can also revert to the ground state by luminescence i.e. emission of radiation. This includes fluorescence and phosphorescence. The former involves a spontaneous re-emission of quanta of the same transition or of photons resulting from a return to the ground state by a different route. Phosphorescence occurs when the excited electron is transferred to a metastable state from which a direct transition to the ground state cannot occur.

When a photon is absorbed by a crystal the absorption process usually involves one or more defect centres. The defect centres include colour centres, trapping centres, impurity ions, etc. When an interband absorption occurs an electron is removed from the valence band and, providing the energy is sufficient, is injected into the conduction band. In the conduction band the electron then migrates until trapped by one of a variety of different kinds of trapping centres. The hole may also migrate and be trapped by a hole trap. The lifetime of the migrating hole is usually less than that of the migrating electron. Hole traps have a high probability of capturing electrons. Hence holes and electrons recombine and energy is released.

Owing to the electron traps, hole traps and/or recombination centres on the surfaces of crystals, electronic processes occurring at these surface sites or surface states can release sufficient energy to produce reactions at the crystal surface. Also defects or impurities in the crystal lattice or Tamm states[15] (a consequence of the quantum mechanical nature of the electronic properties of the crystal) are responsible for trapping free electrons and their conjugate positive holes, and excitons.

In a photolytic reaction, the nature of the trap, i.e. the particular defect, impurity or surface state acting as a decomposition site, need not be identified. The electronic processes associated with the decomposition site are, however, quite specific. The first step in the electronic process occurs when the site traps an electron, a hole or an exciton after which it is considered to be in its first excited state which may last for a few nanoseconds or even a few

days. The excited site is now capable of trapping an oppositely charged carrier, for example, or an exciton and of releasing sufficient exciton potential energy to facilitate a photolytic reaction.

An electron excited into the conduction band can be trapped immediately or migrate through the band and then be trapped at a trapping centre. The pertinent defect responsible for this trapping is the absence of an anion from its normal negative lattice site. The result of the trapping is the production of an F-centre, one of the simplest colour centres. The existence of F-centres was first suggested by de Boer.[16] Evidence that anion vacancies are actually formed was derived from precise density measurements[17] and theoretical calculations[18] which showed that the number of F-centres determined optically agrees with the number of anion vacancies required to give the observed changes in density. An F-centre absorbs in the visible region of the spectrum and is observed when ionic solids, in particular the alkali halides, are exposed to ultraviolet light, X-radiation or electronic bombardment, exhibiting a deep colouration characteristic of the crystal as a whole. The optical absorbtion of an F-centre arises from an electronic dipole transition to a bound excited state of the F-centre.[19,20] Extensive work carried out by Pohl[21] has shown this colouration to be due to a bell shaped absorption band in the region 400 - 800 nm. A structure of an F-centre as an electron bound to an anion vacancy has been confirmed also by e.s.r. data[14] and the centres have been identified by e.s.r. methods in sodium azide when irradiated with ultraviolet light at 77K.[22,23,24]

When, for example, a stoichiometric alkali halide crystal is coloured, electrons are elevated from the full band into the conduction band by radiation and are subsequently trapped at anion vacancies. Each F-centre must be accompanied by the formation of a positive hole in the full band. By analogy, we would expect that the holes could become trapped at cation vacancies and thus give rise to a different type of absorbing centre. Similarly, crystals containing a stoichiometric excess of the electronegative constituent ought to contain the same centres. Potassium bromide was annealed in bromine vapour and a new set of absorption bands at the short wavelength side of the F-band appeared.[25,26] These have since been called the V-bands (V_1 to V_5 have been distinguished)[14] and identified with centres formed by the interaction of positive holes with cation vacancies. V-centres have been observed from the ultraviolet absorption spectrum of sodium azide at 77K.[23]

Photoconductivity can arise when crystals containing F-centres are irradiated within the F-band. The excited state must therefore be sufficiently close to the conduction band for the electrons to be ionized thermally. The free electrons will then wander through the crystal in a Brownian motion manner until retrapped. In the presence of an applied field, the effective distance travelled in the direction of the field to the point of retrapping will have a certain average value w. In potassium chloride at 170K, the value of w is inversely proportional to the concentration of F-centres, and consequently it follows that an anion vacancy can trap two electrons. Irradiation in the F-band has confirmed this.[14] The band is bleached, and at sufficiently low temperatures, a broad band called the F'-band appears on the long wavelength side with a peak between 600 and 800 nm.[27,28]

The band decomposes on warming, the F-band being regenerated. The quantum efficiency for the destruction of F-centres is found to be two[27] as it should be since each electron liberated combines with a second F-centre to form an F'-centre. If the crystal is now irradiated in the F'-band, the F-band is regenerated and the quantum yield for the conversion of F'- to F-centres is again two. Thus we have

$$\boxdot' \xrightarrow{h\nu} \boxdot + e$$

$$e + \square \rightarrow \boxdot$$

where $\square$ = anion vacancy $\boxdot$ = F-centre $\boxdot'$ = F'-centre (This symbolism for anion vacancy, F-centre and F'-centre will be adhered to throughout this thesis unless otherwise stated.)

It has been shown that a potassium iodide crystal possesses an absorption peak just on the edge of the fundamental absorption band.[29] When the crystal is irradiated in the F-band such that F'-centres are formed, the β-band, as it is called, is also bleached. Simultaneously a new band called the α-band emerges on the long wavelength side of the β-band, but still close to the main lattice absorption edge. Heating to decompose the F'-centres causes the α-band to disappear and results in an increase of the β-band and the F-band, which are restored to their original value. Crystals irradiated at very low temperatures show an α-band but no F'-band, hence excluding the possibility of these two bands being due to the same centre. The β-absorption band is caused basically by an exciton being trapped at an F-centre, whereas the α-absorption band results from an exciton being trapped at an anion vacancy.[30] This α-absorption band is due to a perturbation caused to the exciton levels by a neighbouring anion vacancy, leading

to exciton levels somewhat lower than the normal exciton level so that a new peak, the α-band, appears superimposed on the normal lattice absorption edge. The β-band occurs between the α-band and the main exciton level and is due to promotion of electrons to perturbed exciton levels in the immediate neighbourhood of F-centres. Thus exciton formation occurs in the α-band and not the β-band on irradiation within the F-band, owing to enhancement of perturbations on ions adjacent to those bleached F-centres or anion vacancies.

Absorption within the α-band is accompanied by fluorescence. This observation implies that the exciton formed is trapped by the anion vacancy and the resulting complex does not dissociate into an F-centre and a free positive hole.

The α- and β-bands were first found in potassium iodide where the polarizing effects of the vacancies on the anion would be most important, but they have since been observed in potassium chloride and bromide as well as in rubidium chloride.[31]

After irradiation within the F-band at room temperature a rather broad band at the long wavelength side of the F-band is often developed simultaneously. This band has been called the M-band.[32] Usually other absorption bands, situated between the F-band and the M-band, the so-called R- and N- bands are formed simultaneously. The R_1-, R_2- and M-centres are found to be clearly associated with various combinations of electrons with vacancies. An M-centre is formed by the combination of an F-centre with a cation-anion vacancy pair.[14] If an M-centre captures a second electron it will be unstable and the cation vacancy may diffuse away leaving a double F-centre, identified with the R_2-centre. If an R_2-centre loses one of its electrons to a nearby trap e.g. an anion vacancy, M-centre or a vacancy pair by the tunnel effect,

it becomes the R_1-centre. Thus we have:

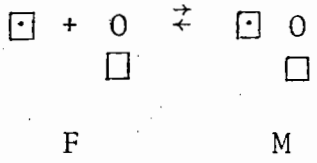

F M

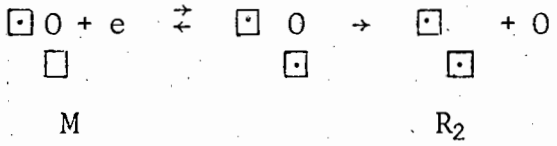

M R_2

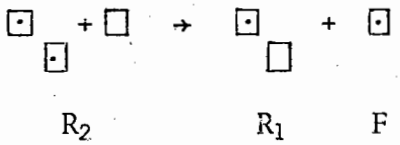

R_2 R_1 F

where O = cation vacancy ⊡ = F-centre □ = anion vacancy

These R-, M- and N-bands have been found in potassium chloride[32,33] and in sodium azide.[24] At about 373K irradiation in the F-band yields a very broad band called the R'-band on the long wavelength side of the F-band. At low temperatures it is not resolved and probably contains a large number of components formed by the combination of electrons with groups of vacancies including the R_1-, R_2- and M-centres. The rate of conversion of F-centres to R'-centres increases with temperature but beyond the equilibrium point at about 773K the dissociation of R'-centres into F'-centres and vacancies is virtually complete.

Irradiation within the F-band also causes some bleaching of the V-bands. A V_1-centre appears when a crystal is irradiated with X-rays at liquid air temperatures, but warming to 128K causes this band to be bleached with a marked reduction in the size of the F-band. This results in the photoconductance and luminescence - thus supporting the

model of a positive hole trapped at a cation vacancy for the V_1-centre. Bleaching of the F- and V_1-bands occurs with low quantum yield owing to the low probability of thermal ionization of an electron from the excited state of an F-centre. These free electrons annihilate the trapped holes. V_1- and F-bands are bleached simultaneously by irradiation within the V_1-band through recombination of electrons and holes. The V_2-centres are bleached by irradiation within the F-band at room temperature which is too high a temperature for the V_1-centres to be stable. Temperatures greater than room temperature are needed to bleach the V_3-band. This band is bleached when the crystal is irradiated simultaneously with F- and V-light. This supports the theory that V_2- and V_3-centres comprise two holes trapped by two cation vacancies, and one hole trapped by two cation vacancies respectively. The V_1-centre is the antimorph of the F-centre, the V_2- and V_3-centres are the antimorphs of the R-centres and the V_4-centre is the antimorph of the M-centre. Other centres which have also been investigated are H-centres,[34] which are possibly holes trapped by vacancy pairs, U-centres[35] and Z-centres[14] which consist of electrons captured by divalent ions.

In order to free electrons thermally from F-centres, energies of about 2 eV in the alkali halides are required.[36] Thus no bleaching is expected at room temperatures because of the small probability that a trapped electron can escape from an F-centre on acquiring a small amount of thermal energy. Bleaching can occur by tunnelling through the potential barrier. A process of recombination with nearby positive holes and with V_2- and V_3-centres then occurs.

The phenomena described above all represent effects of irradiation on crystals. The significant feature of prolonged photolysis of salts such as azides, for example, is that uniform illumination of the

surface results in the separation of discrete metallic nuclei. The rate of photolysis is constant and is unaffected either by discontinuous irradiation or by the continued separation of the metallic product. The basic fact to be explained is how uniform illumination results in the growth of discrete nuclei. Mott[37] in 1939 was the first to put forward a real theoretical explanation of photolysis when he proposed a photolytic mechanism for the photolysis of barium azide, based on the work of Garner, Maggs and Wischin.[38,39]

Mott treated the solid barium azide as an ionic conductor with mobile metal ions in interstitial positions. On irradiation, electrons and positive holes were formed, which were able to diffuse through the crystal lattice. Unspecified 'sensitivity specks' caused trapping of the electrons, resulting in neutralization of the mobile metal ions at these trapping sites. This led to an accumulation of metal atoms, producing product nuclei which grew. He then postulated a secondary growth mechanism whereby further electrons were trapped by the metal to form metal anions, which then neutralized the mobile metal cations, leading to further product formation.

Mott's mechanism was able to account for the observed formation of nuclei on the surface of crystals, accompanied by the evolution of a gas. Subsequent workers have criticized and modified Mott's original mechanism and many other mechanisms have been postulated.

A review will now be made of the work done on the photolysis of barium, strontium, calcium and lithium azides. The photolysis of other inorganic azides in particular and inorganic compounds in general will then be discussed.

(ii) THE PHOTOLYSIS OF THE ALKALI-EARTH AZIDES

(a) Photolysis of Barium Azide

Thomas and Tompkins made a detailed analysis of Mott's theory[37] of the mechanism of decomposition of metallic azides and proposed an alternative approach involving the production and trapping of excitons.[40] Using a low pressure mercury arc in the temperature range -106° – 45°C they found that, when light of wavelength 253,7 nm was used, the rate of photolysis was constant at constant temperature and constant light intensity. The rate varied as the square of the light intensity at constant temperature but increased in a complex manner with variation of temperature at constant intensity. The primary excitation process was considered to be exciton formation and the production of nitrogen. This resulted from the bimolecular reaction of excitons at imperfections which were identified tentatively as vacant lattice sites. The metal product apparently played no significant part in the reaction.[40] Boldyrev *et al.*[45] have proposed that the minimum processes in the photolysis of any azide are

$$N_3^- \underset{k_2}{\overset{k_1}{\rightleftarrows}} N_3^0 + e$$

$$N_3^0 \xrightarrow{k_3} N_2$$

The rate of these elementary steps depends on energy criteria, the lifetime of the excitations and the concentration and mobility of the excitations.

Baidins suggested that the metallic reaction product of the photolysis of barium azide is not photochemically inert.[41] Further investigations were made of the photolysis of barium azide[42,43,44] and new kinetic measurements were made using high and low pressure mercury lamps

over the temperature range -25° - 25°C. The barium product formed as a result of photolysis was found to play an important role. Jacobs *et al.*[44] consequently proposed two mechanisms. The first mechanism, found to occur chiefly in fresh salt, concerned the formation of barium atoms (pre-nuclei) and the second mechanism concerned the thermal production of holes by the transfer of electrons to barium pre-nuclei which have been ionized by the photoemission of an electron into the conduction band. The rate of photolysis first decreased and then increased after which it became constant, when light of wavelength 253,7 nm or a lamp emitting a more or less continuous spectrum with the principal mercury lines superimposed was used.

The initial rate was found to be proportional to the square of the intensity and initially the activation energy was about 5 Kcal./mol. This is interpreted in terms of the bimolecular recombination of excitons at an unidentified trap T,

$$N_3^- \; T \overset{h\nu}{\rightleftarrows} N_3^{-*} \; T \rightleftarrows [N_3T]^{-*}$$

Repetition of this process within the (relatively long) life-time of $[N_3T]^{-*}$ gives two adjacent excited azide ions,

$$N_3^- \; [N_3T]^{-*} \overset{h\nu}{\rightleftarrows} N_3^{-*} \; [N_3T]^{-*} \rightleftarrows [N_3TN_3]^{-*}$$

which can either revert to the ground state or undergo chemical decomposition,

$$[N_3TN_3]^{-*} \; Ba^{2+} \xrightarrow[5 \text{ Kcal./mol.}]{} Ba + 3N_2 + \square T \square$$

where $\square$ = anion vacancy * = excited state of the anion or complex.

As photolysis proceeds, the rate decreases to a minimum value at which stage the square law ceases to apply. It is thus clear that the

number of traps T decreases steadily. After the minimum, the rate of evolution of nitrogen increases again at constant intensity to a constant rate proportional to the intensity.

Developing Baidins' suggestion, the possibility of photoemission from barium atoms was considered the reason for the increasing rate period, the generated electrons causing an acceleration of the reaction by facilitating the combination of excitons and radicals. Barium metal was thought to form via aggregation of barium atoms.

$$Ba \overset{h\nu}{\underset{}{\rightleftarrows}} Ba^{+} + e$$

$$Ba^{+} + N_3^{-} \overset{\Delta}{\rightarrow} Ba + N_3 \qquad 20 \text{ Kcal./mol.}$$

$$N_3^{-} \overset{h\nu}{\rightleftarrows} N_3^{-*}$$

$$N_3^{-*} + N_3 \rightarrow 2N_3 + e$$

$$2N_3 \rightarrow 3N_2$$

$$Ba + Ba^{2+} + 2e \rightarrow Ba_2$$

A study of the dark rate indicates the following purely thermal mechanism.

$$Ba + Ba^{2+} \overset{kT}{\rightarrow} (Ba_2)^{2+}$$

Electrons are then transferred from azide ions to the positively charged barium and the positive holes react together.

$$(Ba_2)^{2+} + 2N_3^{-} \rightarrow Ba_2 + 2N_3$$

$$2N_3 \rightarrow 3N_2$$

This cycle of events can continue until all the pre-nuclei have grown into large specks of barium.

The importance of the wavelength of the ultraviolet light on the photochemical decomposition of barium azide has been widely

investigated. In the study by Jacobs *et al.* referred to above,[44] the effect of filtering the 253,7 nm wavelength from the source was investigated. It was concluded that the 253,7 nm wavelength was responsible for the acceleratory reaction. Verneker[46] found that light of wavelength 184,9 + 253,7 nm or light of wavelength 200 - 300 nm gave rise to the rate-time plot reported by Jacobs *et al.* above. However, he found that, unlike the results of Jacobs *et al.*, light of wavelength 253,7 nm produced no acceleratory reaction and the product after each reaction, regardless of temperature, gave a positive nitride test. Barium nitride showed an acceleratory reaction when photolysed with light of wavelength between 200 - 300 nm. Verneker stated that firstly, the initial decrease in photolytic rate seemed to be caused by the gradual consumption of defects originally present which are helpful to the reaction. As the reaction proceeds metallic specks are produced which initiate a second process. This process is based on the photoemission of electrons from the metal and keeps the photolytic process going. After reaching the minimum, an acceleration in the photolytic process is caused by the photodecomposition of the nitride. Thus an acceleration in the photolytic rate can be expected if light capable of photoionizing the metal atoms (formed during photolysis) is used as a photolyzing source. During irradiation with $\lambda > 170$ nm, no photocurrent was detected and thus the transition is to a bound excited or exciton state. Moreover, since the band has vibrational structure, the excitons must be trapped on the molecule on which they are formed, i.e. the excitation is probably an internal transition to a low lying excited state of the azide ion. Irradiation at below 155 nm gives a temperature-independent photocurrent that probably results from a direct electron transition from the valence to the conduction band

Tompkins[3] has suggested that the photolysis of barium azide could involve the trapping of excitons at anion vacancies. This incorporates the production of the N_2^- ion which is stable at room temperature and of which the rate of production is linearly dependent at first on intensity. The existence of the N_2^- ion has been identified by e.s.r. methods.[47] Thus the trapped exciton is formed as follows:

$$N_3^- \overset{h\nu}{\rightleftarrows} N_3^{-*} \overset{\square}{\rightarrow} N_3^{-*}\,\square$$

and can then decay in two ways:

$$\text{(i)} \qquad N_3^{-*}\,\square \rightarrow N_2^-\,\square + N$$

$$\text{(ii)} \qquad N_3^{-*}\,\square + N_3^{-*} \rightarrow 3N_2 + \boxdot'$$

where $\square$ = anion vacancy

$\boxdot'$ = two electrons trapped at an anion vacancy (F'-centre).

The F'centre may now react with a lattice Ba^{2+} to give the embryo nucleus, the Ba atom. At the surface, bimolecular combination of nitrogen atoms produces gaseous nitrogen.

Prout and Sears[48] have studied the photolysis of the pellets of powdered dehydrated barium azide monohydrate in the temperature range -197° - 20°C using both high and low pressure mercury lamps. Under certain conditions good reproducibility was obtained. The resulting pressure-time plots always displayed periods of acceleration and protracted decay. The acceleratory reaction varied as the square of the light intensity implying a bimolecular reaction involving two excited ions. The following mechanism was proposed for the initial acceleratory reaction in the temperature range 0° - 20°C, initiation occurring at points such as emergent grain boundaries and dislocations.

$$N_3^- \overset{h\nu}{\rightleftarrows} (N_3^-)^* \qquad \text{(excited ion)}.$$

These excited ions are trapped at anion vacancies

$$(N_3^-)^* + \square \rightarrow (N_3\square)^{-*}.$$

These entities may react on neighbouring sites,

$$2(N_3\square)^{-*} \rightarrow (N_3\square_2 N_3)^{-*}.$$

Then,

$$(N_3\square_2 N_3)^{-*} \rightarrow N_2^- + 2N_2 + 3\square + e$$

The formation of separate anion vacancies and electrons are postulated rather than isolated F-centres owing to the instability of the latter at the temperature of irradiation. Barium atoms are formed by the reaction

$$Ba^{2+} + 2e \rightarrow Ba.$$

This mechanism has been supported by e.s.r. measurements which have detected N_2^- ions.[47,49] The reaction accelerates because of the production of new anion vacancies. The layer of product consists of colloidal Ba in a matrix of $Ba(N_2)_2$. Aggregation will eventually take place followed by the formation of discrete nuclei of the metal. Photoemission then occurs[44]

$$Ba_n \overset{h\nu}{\rightleftarrows} Ba_n^+ + e$$

$$N_2^- \overset{h\nu}{\rightleftarrows} N_2^{-*}$$

$$Ba_n^+ + N_2^{-*} \rightarrow N_2 + Ba_n \quad .$$

This is a unimolecular reaction with respect to N_2^- ions in accordance

with the observed dependence of the decay reaction on the first power of the light intensity. No dark rate was observed when the light was switched off, but an increase in the rate of photolysis was observed following the dark period. This fact was explained by assuming that during the dark period aggregation of Ba atoms continues and some aggregation occurs.

At the lower temperature range (0° - -197°C) a free radical type of reaction was proposed:

$$N_3^- \overset{h\nu}{\rightleftarrows} N_3^{-*}$$

$$2N_3^- \rightarrow 2N_3 + 2e$$

$$e + \square \rightarrow \boxdot$$

$$N_3 + N_3^- \rightarrow N_4^- + N_2$$

$$N_3 \rightarrow N + N_2$$

$$N + N_3^- \rightarrow N_2^- + N_2.$$

Prout and Shephard[50] have recently studied the photolysis of barium azide in the temperature range 27° - 100°C. Two definite temperature dependent regions were studied i.e. 27° - 60°C and 60° - 100°C. In the 27° - 60°C region, and indeed over the whole range, the most effective wavelengths for the photolysis of barium azide were in the region 220 - 280 nm. These wavelengths were of less energy than that required for the formation of positive holes and electrons and it was assumed that absorption leads to excited azide ions rather than excitons. Ba atoms were formed on the surface and on the planes of the crystal, each plane starting at the surface at an emergent grain boundary. Nuclei were formed by aggregation at the end of the induction period. Between 27° and 60°C the following mechanism was

proposed:

$$N_3^- \overset{h\nu}{\underset{}{\rightleftarrows}} N_3^{-*}.$$

The excited azide ion adjacent to a ground state azide ion at a surface defect S (probably an anion vacancy) then reacted with a barium ion:

$$N_3^- S N_3^{-*} + Ba^{2+} \overset{\Delta}{\rightleftarrows} Ba + 3N_2 + S .$$

Formation of barium metal nuclei during the induction period in the 60° – 100°C range was thought to occur according to the following mechanism:

$$N_3^- \overset{h\nu}{\rightleftarrows} N_3^{-*}$$

$$Ba^{2+} + N_3^- \overset{\Delta}{\rightarrow} Ba^+ + N_3$$

$$N_3 + N_3^{-*} \rightarrow 3N_2 + e$$

$$Ba^+ + e \rightarrow Ba$$

Below 60°C the rate of nucleus growth was found to be dependent on the square of the light intensity, indicating that the overall mechanism must involve the decomposition of two excited azide ions. The mechanism proposed involves the formation of barium ions and electrons via the photoelectric effect and subsequent reaction with excited azide ions:

$$Ba_n \overset{h\nu}{\rightleftarrows} Ba_n^+ + e \qquad (1)$$

$$N_3^- \overset{h\nu}{\rightleftarrows} N_3^{-*} \qquad (2)$$

$$Ba_n^+ + N_3^{-*} \overset{\Delta}{\rightarrow} Ba_n + N_3 \qquad (3)$$

$$N_3 + N_3^{-*} \rightarrow 3N_2 + 2\square + e \qquad (4)$$

$$\rightarrow 3N_2 + \square + \boxdot$$

The F-centres collapse as follows:

$$2\,\boxdot \rightarrow 2\,\square + 2e \qquad (5)$$

and then the barium metal nuclei grow,

$$Ba_n + 2e + Ba^{2+} \rightarrow Ba_{n+1} \qquad (6)$$

Between 60° and 100°C the mechanism proposed for the acceleratory period is identical to that shown above except for step (3). At temperatures above 60°C there is sufficient thermal energy for the thermal transfer of an electron from the ground state azide ion to a Ba^+ ion formed via the photoelectric effect. Thus in this step we have:

$$Ba_n^+ + N_3^- \rightleftharpoons Ba_n + N_3 \qquad \text{Rate determining step.}$$

This mechanism is in accordance with the observed linear dependence of the rate of photolysis on light intensity.

Over the whole temperature range the decay period was simply considered to be a continuation of the process occurring during the acceleratory period. Similar mechanisms were proposed for the decomposition of pellets in this temperature range.

There is much speculation on the existence of the various radicals proposed in the different mechanistic pathways suggested whereby azides undergo photolytic decomposition. The radical N_3 still eludes e.s.r. spectroscopists. It is well known in the gas phase and has probably been formed in liquid phase pulse experiments with aqueous azide ions. At 77 K, using glassy aqueous solutions, no N_3 was obtained, possibly due to molecules dissociating to give nitrogen molecules and atoms.[51] N_3 has been reported in an infrared study of

discharged nitrogen deposited at 4,2K.[52] N_3^{2-} has been characterized in a study of barium azide irradiated with ultraviolet light.[53] According to Symons *et al.*[54,55] N_3 radicals have life times long enough for them to interact with neighbouring azide ions:

$$N_3 + N_3^- \rightarrow N_4^- + N_2$$

and

$$N_3 + N_3^- \rightarrow N_2^- + 2N_2$$

Both these reactions have a similar probability of occurring and both are considered more probable than

$$N + N_3^- \rightarrow N_4^-$$

and

$$N + N_3^- \rightarrow N_2^- + N_2$$

The existence of the N_2^- and N_4^- species has been well established.[47,61,62] Thus, in the case of barium azide, the following initial process was proposed:

$$N_3^- \overset{h\nu}{\rightleftarrows} N_3 + e$$

$$N_3^- + e \rightarrow N_3^{2-}.$$

(b) Photolysis of Strontium and Calcium Azides

Most of the studies on strontium azide have been done in conjunction with barium azide and analogies sought between the two in their modes of decomposition.[56,38,43,57] Prout and Shephard[50] have recently investigated the photolysis of strontium azide in the temperature range 30° - 90°C. The process of photolysis differs in the regions 30° – 50°C and 50° – 90°C. In the temperature range 30° – 50°C, the rate of photolysis is found to be proportional to the square of the light intensity throughout the reaction. In the range 50° – 90°C the

same relationship is observed. The plate-like nuclei are considered to grow two-dimensionally, increasing from a fixed number of centres as was found for barium azide. The formation of the strontium metal nuclei at the end of the induction period of photolytic decomposition in the temperature range 30° – 50°C was assumed to proceed as follows:

$$N_3^- \overset{h\nu}{\rightleftarrows} N_3^{-*} \ .$$

Reaction then takes place with an Sr^{2+} ion when there are two singly excited azide ions at a surface defect S

$$N_3^{-*} \ S \ N_3^{-*} + Sr^{2+} \overset{\Delta}{\rightarrow} 3N_2 + Sr + S \ .$$

This mechanism is in accordance with the dependence of the rate of photolysis on the square of the light intensity. In the temperature range 50° – 90°C, the following mechanism is proposed for the corresponding period of decomposition.

$$N_3^- \overset{h\nu}{\rightleftarrows} N_3^{-*}$$

$$Sr^{2+} + N_3^{-*} \overset{\Delta}{\rightarrow} Sr^+ + N_3$$

$$N_3 + N_3^{-*} \rightarrow 3N_2 + e$$

$$Sr^+ + e \rightarrow Sr \ .$$

Two mechanisms are postulated for the growth of the strontium nuclei during the acceleratory period of photolysis in the temperature range 30° – 50°C. Both are in accordance with the dependence of rate on the square of the light intensity. The first mechanism is as follows:

$$Sr_n \overset{h\nu}{\rightleftarrows} Sr_n^+ + e \qquad (1)$$

$$N_3^- \overset{h\nu}{\rightleftarrows} N_3^{-*} \qquad (2)$$

$$N_3^{-*} \overset{h\nu}{\rightleftarrows} N_3^{-**} \qquad (3)$$

$$N_3^{-**} + Sr^{+} \overset{\Delta}{\rightarrow} Sr + N_3^{*} \qquad (4)$$

$$N_3^{*} + N_3^{-} \rightarrow 3N_2 + e + 2\square \qquad (5)$$

$$\rightarrow 3N_2 + \boxdot + \square \qquad (6)$$

$$2\boxdot \rightarrow 2\square + 2e \qquad (7)$$

$$Sr_n + 2e + Sr^{2+} \rightarrow Sr_{n+1} \qquad (8)$$

where $\square$ = anion vacancy $\boxdot$ = F-centre.

In the second mechanism, step (3) above is replaced by

$$N_3^{-*} + N_3^{-*} \rightleftarrows N_3^{-**} + N_3^{-}$$

i.e. energy is transferred from an excited ion to an adjacent excited azide ion.

In the temperature range 50° – 90°C an increase in the activation energy requires a modification to the mechanism postulated above:

$$Sr_n \overset{h\nu}{\rightleftarrows} Sr_n^{+} + e$$

$$N_3^{-} \overset{h\nu}{\rightleftarrows} N_3^{-*}$$

$$Sr_n^{+} + N_3^{-*} \overset{\Delta}{\rightarrow} Sr_n + N_3$$

$$N_3 + N_3^{-*} \rightarrow 3N_2 + e + 2\square$$

$$\rightarrow 3N_2 + \boxdot + \square$$

$$2\boxdot \rightarrow 2\square + 2e$$

$$Sr_n + 2e + Sr^{2+} \rightarrow Sr_{n+1} \quad .$$

The decay period is considered to be a continuation of the acceleratory period and the same mechanisms are proposed.

Little work has been done on the photolysis of calcium azide although Tompkins and Young [58,59] have studied the thermal decomposition of the salt after pre-irradiation with ultraviolet light. The result of the pre-irradiation was, firstly, to increase the number of growth nuclei as a result of the additional production of anion vacancies. Secondly, it was found that the growth, as well as the formation, of these nuclei took place during irradiation.

Prout *et al.*[137,168] have also made a study of the thermal decomposition of unirradiated calcium azide as well as of the azide pre-irradiated with γ-, X- and ultraviolet radiation.

(iii) THE PHOTOLYSIS OF THE ALKALI-METAL AND OTHER INORGANIC AZIDES

Mechanisms for the observed photolytic decompositions of sodium, potassium and lithium azides have been postulated with correlations to the already proposed mechanisms for the photolysis of barium azide. Jacobs *et al.*[60] have compared the kinetics of sodium and potassium azides with data previously obtained for barium azide.[44] Potassium and sodium azides both showed an initial deceleratory reaction. Potassium azide showed a subsequent acceleration after which the rate of photolysis became constant. Sodium azide showed no subsequent acceleration. Filtering the arc with water made no difference to the rate-time plot of sodium azide but completely removed the acceleratory period of potassium azide. Presumably the acceleratory period of the latter depends on light of wavelength 184,9 nm and the initial deceleratory reaction on light of wavelength 253,7 nm. Two mechanisms appeared to be involved in the photolysis of these azides. A mechanism was proposed based on measurements from absorption spectra,[43] photo-electric properties,[43,63] colour centre absorption bands[64,65,66,23] and e.s.r. data[22,24,67,68,69,70,71,53] to date. The primary process involved 253,7 nm radiation and produced the excited azide ion N_3^{-*}. These excited ions were destroyed at adjacent imperfections as follows:

$$N_3^- \overset{h\nu}{\underset{}{\rightleftarrows}} N_3^{-*}$$

$$N_3^{-*} + N_3^{-*} \rightarrow N_4^- + \boxdot + N_2 \qquad (1)$$

$$N_3^{-*} + N_3^{-*} \rightarrow N_2^- + \boxdot + 2N_2 \qquad (2)$$

$$N_3^{-*} + N_3^{-*} \rightarrow \boxdot\square + 3N_2 \qquad (3)$$

where $\boxdot$ = F-centre $\qquad$ $\boxdot\square$ = F_2^+-centre .

In route (3) the extra electron must be trapped by the site or by a metal atom. The e.s.r. evidence indicates that (2) dominates in potassium azide at low temperatures.[53,69,70] Route (3) is important in sodium azide.[24] N_4^- and N_2^- have not been identified in sodium azide but F- and F_2^+-centres have been detected. Symons *et al.*[55] have proposed that in the case of sodium azide the following occurs:

$$N_3^- \overset{h\nu}{\rightleftarrows} N_3 + e$$

$$N_3 + e + \square \rightarrow N_3 + \boxdot \quad .$$

On warming irradiated potassium azide from low temperatures V-centres bleach, the N_2^- resonance decreases, the N_4^- resonance increases but nitrogen is not evolved. Possibly the following reaction occurs:

$$N_2^- + N_2^- \rightarrow N_4^- + \boxdot$$

followed by aggregation of F-centres with eventual formation of metal. For sodium azide aggregation of F- and F_2^+-centres leads to the formation of metal specks. The measured life-time of the N_4^- ion in potassium azide at room temperature means that it is in all probability responsible for the dark reaction:

$$N_4^- \rightarrow N_3^- + N$$

$$N + N \rightarrow N_2 \quad .$$

The acceleratory process in potassium azide involves the metallic product. In crystals containing metal specks, photons of the requisite energy will result in photoemission of electrons from the metal into the conduction band. Presumably azide ions adjacent to the specks then decompose and nitrogen is produced. Owens[72] has found that the rate of growth of paramagnetic centres in potassium azide is proportional to the

square of the light intensity. He proposed that the first step in the photolytic process is the excitation of the azide ion by light of wavelength 225 nm. The ability of this ion to decompose is determined by the density of the excitations, involving presumably an exciton and an associated impurity defect .

The absorption spectra[9] of sodium and potassium azides are very similar and thus it seems unlikely that the explanation for the lack of the acceleratory process in sodium azide lies in the energy band structure of the salt. Jacobs and Tariq Kureishy[73] showed that two mechanisms are operative for the decomposition of sodium azide. The salt showed that, after exposure to nitrogen gas, an acceleratory reaction, followed by a constant rate, occurred. Exposure of the photolyzed azide to nitrogen resulted in diffusion into the partly decomposed crystal and reaction with the metallic product. This surface chemisorption is sufficient to prevent the catalysis of the photolysis by sodium metal until the metal has been reformed.

The deceleratory reaction was proportional to the square of the light intensity and the following mechanism was proposed:

$$N_3^- \overset{h\nu}{\rightleftarrows} N_3^{-*}$$

$$N_3^{-*} + S \rightleftarrows N_3 \, e \, S$$

$$N_3^{-*} + N_3 \, e \, S \rightarrow 3N_2 + \boxdot\square + S^-$$

where S = special trapping site $\boxdot\square = F_2^+$-centre.

F_2^+-centres have been shown by absorption spectra and e.s.r. measurements[24] to be the major product at low temperatures. This centre is unstable at room temperature and we get:

$$Na^+ + \boxdot\square \rightarrow Na + 2\square$$

where $\square$ = anion vacancy .

Whether or not the site S can hold an extra electron permanently depends on its nature. It may shed it to form a second Na atom.

$$S^- + Na^+ \rightarrow Na + S'$$

where S' differs from S since it is now associated with two sodium atoms and two anion vacancies. Eventually a stable nucleus of sodium forms, the rate of formation being a deceleratory process since potential nucleus-forming sites S are being steadily consumed during the reaction.

The subsequent constant-rate reaction in the photolysis of sodium azide is due to the growth of these nuclei and the formation of colloid centres.[67] Photoemission from the sodium specks occurs and electrons may tunnel from excited azide ions to be trapped by nuclei which have become ionized by the light.

$$Na_n \overset{h\nu}{\rightleftarrows} Na_n^+ + e$$

$$N_3^{-*} + Na_n^+ \rightarrow Na_n + N_3$$

$$N_3^{-*} + N_3 \rightarrow 3N_2 + 2\square + e \quad .$$

The electrons produced are trapped by anion vacancy pairs forming F_2^+-centres which then react with Na^+ to form Na atoms, the net result being

$$Na_n + 2e + 2Na^+ \rightarrow Na_{n+2} \quad .$$

Repetition of this cycle leads to growth of the nucleus.

Jacobs and Tariq Kureishy[73] have studied the photolysis of rubidium and caesium azides. Rubidium azide resembles potassium azide in that the rate of photolysis at first decreases, passes through a minimum and then increases, finally attaining a constant value. The rate of photolysis of caesium azide decreases, becomes constant for a brief period and then decreases again before becoming constant. Three mechanisms are thought to be responsible for the rate-time curves. The first two mechanisms as proposed above for barium azide are considered valid.[44] The third is considered to involve the reaction of excitons and excited azide ions at metal nuclei and to produce N_4^- ions. The subsequent thermal decomposition of these ions is responsible for the dark reaction that occurs on switching off the lamp. The following mechanism was proposed for the acceleratory reaction:

$$N_3^- \overset{h\nu}{\rightleftarrows} N_3^{-*} \qquad \text{(exciton)}$$

$$M_n \overset{h\nu}{\rightleftarrows} M_n^+ + e \qquad (M_n = \text{metal nucleus})$$

$$N_3^- \overset{h\nu}{\rightleftarrows} N_3^{-*} \qquad \text{(excited azide ion)}$$

$$N_3^{-*} + M_n^+ \rightarrow N_3M_n$$

$$N_3^{-*} + N_3M_n \rightarrow M_n + N_4^- + N_2 + \square$$

(anion vacancy formed)

$$M_n + M^+ + e \rightarrow M_{n+1} \; .$$

Prout and Sears have studied the photolysis of lithium azide.[74] The azide was photolyzed in the temperature range -60° – 20°C and a markedly sigmoid, highly reproducible plot was obtained. Activation energies in the region 1 Kcal/mol were obtained over the whole range

for both the acceleratory and decay period. The rate constant varied as the square of the light intensity indicating a bimolecular reaction involving two excited azide ions. The following mechanism was proposed:

$$N_3^- \overset{h\nu}{\rightleftarrows} N_3^{-*}$$

$$N_3^{-*} + \square \rightarrow (N_3\square)^{-*}$$

These entities react when on neighbouring sites as follows:

$$2(N_3\square)^{-*} \rightarrow (N_3\square_2 N_3)^{-2*}$$

$$(N_3\square_2 N_3)^{-2*} \rightarrow 2N_3 + 2\boxdot$$

$$2N_3 \rightarrow 3N_2 + 2\boxdot$$

where N_3^{-*} = excited azided ion $\square$ = anion vacancy .

The lithium metal then formed as follows:

$$2Li^+ + 2\boxdot \rightarrow 2Li + 2\square \quad .$$

The effect of the pre-irradiation with X-rays and γ-rays was to decrease the acceleratory reaction only - probably by forming F-centres and thus decreasing the concentration of vacancies which are propagating entities in the above mechanism.

The effect of radiation of different wavelengths on the photolysis of sodium, potassium, barium, lead and silver azides has been investigated by Verneker.[75] The common feature of the photolytic decomposition of these azides is that when irradiated with the above sources, the rate of gas evolution initially decreases to a minimum value. Irradiation with light of wavelength 184,9 nm + 253,7 nm causes the potassium, sodium and barium salts to show an acceleration which is missing when

the latter two are irradiated with light of wavelength 253,7 nm. Silver azide showed an acceleratory reaction only when light of wavelengths between 200 and 300 nm was used. Lead azide showed no acceleratory reaction when light of either 184,9 nm + 253,7 nm or 200 - 300 nm was used. All these azides, except lead azide, showed a positive nitride test. As explained previously, photoemission from metal specks produced through the consumption of defects prevented the photolytic rate from decreasing to zero. The work functions of the metals of all these azides are such that light of wavelength 184,9 nm is sufficient to cause the photoemission of electrons from the metal. Thus the acceleration in the rate-time plot could not be attributed to this process. However, since no acceleration was observed with light of wavelength 184,9 nm + 253,7 nm in lead and silver azides, the ionization potential of the metal atoms were thought to be important. A study of the relation between acceleration rates and ionization potentials then clearly indicated that the absence of acceleration in lead and silver azides is due to the inability of light of wavelength 184,9 nm to ionize Pb and Ag atoms. Further, light of wavelength 253,7 nm alone is enough to ionize K atoms hence accounting for the acceleration of potassium azide when irradiated with this wavelength alone. Irradiation in the range 200 - 300 nm caused an acceleration to occur and this was thought to be due to the decomposition of the nitride formed.

The partially covalent, conducting azides have not been studied as intensively as barium azide. However lead, thallous and silver azides have been investigated and their photolytic decompositions will be discussed. The rate of photolysis of lead azide has been found to be proportional to the intensity but pre-irradiation has not been found to enhance the rate of thermal decomposition. The rate of photolysis of

thallous azide was found to assume a constant value proportional to the intensity of the radiation.[10] The mechanism proposed by Deb *et al.* involved, as the essential step, the promotion of an electron to the conduction band thus forming an azide radical. The mechanism postulated for the photolysis at long wavelengths ($\lambda > 400$ nm)[1] is:

$$N_3^- \overset{h\nu}{\rightleftarrows} N_3^{-*} \qquad \text{(exciton formation)}$$

$$N_3^{-*} \rightarrow N_3^- + q \qquad \text{(reversion of exciton to ground state)}$$

$$N_3^{-*} \rightarrow N_3 + e \qquad \text{(thermal dissociation of exciton)}$$

$$N_3 + e \rightarrow N_3^- + q' \qquad \text{(recombination of exciton and hole)}$$

$$2N_3 \rightarrow 3N_2 + Q \qquad \text{(combination of two positive holes)}$$

$$Tl_n + Tl^+ + e \rightarrow Tl_{n+1} \qquad \text{(e-trapping and metal formation)} .$$

At short wavelengths ($\lambda \approx 330$ nm) the first three steps are replaced by:

$$N_3^- \overset{h\nu}{\rightleftarrows} N_3 + e \quad .$$

With silver azide an exciton can also be dissociated thermally. Silver specks distributed throughout the azide can be thermally ionized:

$$Ag_n\, N_3^- \rightarrow Ag_n^+\, N_3^- + e \quad .$$

An electron from an adjacent ion can tunnel through the interface and be trapped

$$Ag_n^+\, N_3^- \qquad Ag_n\, N_3 \quad .$$

Two mechanisms are then postulated:

(i) Interfacial excitation:

$$Ag\,N_3N_3^- \underset{\leftarrow}{\overset{h\nu}{\rightarrow}} AgN_3N_3^{-*} \rightarrow 3N_2 + Ag_{n+1}\square$$

$$Ag_{n+1}\square + e \overset{Ag^+}{\rightarrow} Ag_{n+2}$$

(ii) Mobile exciton:

$$N_3^- \underset{\leftarrow}{\overset{h\nu}{\rightarrow}} N_3^{-*}$$

$$Ag_n\,N_3 + N_3^{-*} \underset{\leftarrow}{\overset{\rightarrow}{}} Ag_nN_3N_3^{-*} \overset{Ag^+}{\rightarrow} Ag_{n+1}\square + 3N_2 \quad .$$

Both these mechanisms are consistent with the observed steady fall in the rate of photolysis as the photolysis proceeds, and the initial dependence of the rate on the square of the intensity.

The photolysis of ammonium azide has also been investigated.[76] The reaction mechanism incorporates the species N_2^-, N_4^-, N and N_3^{2-} all identified by e.s.r. measurements as already referred to above. The scheme proposes:

$$N_3^- \underset{\leftarrow}{\overset{h\nu}{\rightarrow}} N_3^{-*}$$

$$N_3^{-*} \rightarrow N + N_2^-$$

$$N + N_3^- \underset{\leftarrow}{\overset{\rightarrow}{}} N_4^- \rightarrow N_2^- + N_2 \quad .$$

The N_3^{-*} and N_2^- then react with the ammonium ion, producing ammonia which reacts with N_2^- to produce nitrogen and NH_3^-.

Then follows:

$$NH_3^- + NH_4^+ \rightarrow 2NH_3 + H\cdot$$

$$N + H\cdot \rightarrow NH$$

$$2NH \rightarrow N_2 + H_2$$

$$NH + NH_3 \rightarrow NH_2NH_2$$

$$2N \rightarrow N_2$$

Deb *et al.*[77] have investigated the photolytic decomposition of mercurous azide. The rate of decomposition is proportional to the light intensity. Nitrogen gas and a brown product, probably a nitride, are formed. Decomposition probably takes place by bond fission within the azide group.

A study has also been made of the photolytic decomposition of zinc azide.[78] The rate of decomposition was found to be proportional to the first power of the intensity and the following initial mechanism was proposed:

$$N_3^- \overset{h\nu}{\rightleftarrows} N_3^{-*}$$

$$S + N_3^{-*} \rightleftarrows N_3\ S\ e^*$$

$$N_3\ S\ e^* + N_3^- \rightarrow 3N_2$$

$$N_3\ S\ e^* \rightleftarrows N_3 + S + e$$

where S is a trapping site.

Pai Verneker *et al.*[197] have studied the photolysis of α-lead azide at ambient and low temperatures. Metal present in the form of nuclei or small specks and produced during the photolysis, presumably initiates a new process. The photolytic reactions in sequence are:

$$N_3^- \overset{h\nu}{\rightleftarrows} (A\ N_3^-)^* \qquad A = \text{trap}$$

$$(A\ N_3^-)^* + N_3^- \rightarrow 3N_2 + (e\ A\ e) + 2 \text{ vacancies}$$

$$Pb^{2+} + (e\ A\ e) \rightarrow Pb^0 + \text{aggregate of traps}$$

$$Pb_n \overset{h\nu}{\rightleftarrows} Pb_n^+ + e \qquad \text{photo-electric effect}$$

$$Pb_n^+ + N_3^- \rightarrow Pb_n + N_3$$

$$N_3 + N_3^- \rightarrow 3N_2 + e + \text{vacancies.}$$

The mechanism as proposed is in accordance with the experimentally determined linear dependence of the rate on the light intensity. Speculations were made regarding the mechanisms at low temperatures. It was postulated that N_4^- and N_2^- ions were present, although they were not detected. It was thought that the reaction

$$N_4^- \rightarrow 2N_2$$

occurs at 10°C and the reaction

$$N_2^- \rightarrow N_2$$

occurs at 25°C.

(iv) THE PHOTOLYSIS OF OTHER INORGANIC COMPOUNDS

(a) Halides

In certain salts, notably the silver halides, the effect of irradiation is permanent and results in a definite chemical change, in this case the separation of photolytic silver. Experimental and theoretical work on the photochemical reduction of solids has been dominated by the attention given to the silver halides. The prolonged exposure of dry crystals of silver halides to irradiation is accompanied by the release of halogen and the separation of silver.[79] The radiation is considered to be absorbed principally within the volume elements of the sub-structure. This energy produces mobile excitons which can either decay, transferring their energy to lattice vibrations, or interact with phonons and dissociate into a free electron and positive hole or, thirdly, interact with atoms, ions or molecules on the bounding surfaces of the volume elements to produce photochemical changes. In the case of silver bromide, excitons are assumed to transfer their energy to bromide ions occupying kink sites on the free surface of the crystal or jogs along edge dislocation sites. These ions then eject electrons to form bromine atoms and an adjacent silver ion would then represent a localized excess positive charge with which an electron might ultimately combine to produce a silver atom. The probability of this happening immediately is small so that an interval will be available during which the silver ion can diffuse away from the bromine atom most probably into and along an adjacent sub-boundary. It may there combine with the electron to form a silver atom.[80] It has been shown that, in the photolysis of silver halides, silver particles form in the first seconds of irradiation. This is followed eventually by a definite decay period in which the particles reach maximum size,

are round, coalesce and become mobile.[81] If bromide ions associated with jogs along the internal surface dislocation lines interact with excitons a similar process to that shown above occurs. This requires, however, that the bromine atom diffuses to the surface and escapes without combining with a previously separated silver atom. Precisely the same changes would result if electrons and positive holes were created directly by the absorption of energy in the crystals and the holes were then trapped before the electrons by bromine ions on the free surface or on internal surfaces. Atoms of bromine would again be produced together with excess silver ions which could combine with the electrons. Saunders[82] has shown that, in the photolysis of silver halides, holes escape as halogen from a certain diffusion layer which is dependent upon the type of halide, the intensity of the light and the absorption constant. The rate of photolysis has been found to be proportional to the square of the light intensity[83] and in the case of the bromide the activation energy of dissociation to be equal to approximately 1 eV.[84]

In a study of the photolysis of silver bromide in vacuum,[85] it was found that a decrease in wavelength was accompanied by an increase in quantum yield. At short wavelengths the incident radiation is absorbed in a thin surface layer of silver bromide. The concentration of positive holes and electrons in the region of the crystal in which photolysis occurs is much greater at short wavelengths and considerable recombination should take place. The high yields at short wavelengths show, however, that such recombination does not occur and that vacuum is a very good halogen acceptor. The increase in yield has been attributed to increased absorption of the incident radiation at the surface with decrease in wavelength, since the most effective absorption

occurs in a thin surface layer, about one-third of a micron thick. High yields at long wavelengths were only observed in thin crystals with thickness comparable to that of the active layer. With an increase in the temperature of irradiation there is a decrease in the stability of the trapped electrons thus leading to decreased quantum yields. This is most marked at short wavelength where the surface concentration of holes and electrons is the greatest. Therefore the number of electrons in shallow traps will be greater at short wavelengths than at long wavelengths, the rate of recombination with bromine will be greater, and the yield will decrease.

The photochemical behaviour of the lead halides has been shown to be very similar to that of the silver halides. The Mott-Gurney mechanism proposed for the latter has been used in explaining the photolysis of lead halides. Absorption of a photon causes an electron to be excited into the conduction band where it combines at a trapping site with a metal ion, the holes being trapped at surface halogen ions followed by the desorption of halogen atoms. Verwey[86] has proposed that following absorption of a photon to give an electron-hole pair, three modes of photolysis may be discerned. The first mode, the colour centre mode, consists of the transport and trapping of photo-generated electrons and holes. At liquid nitrogen temperature reaction products of electrons and holes with lattice defects have been detected by e.s.r. measurements.[87] The second mode, the print-out mode, results from mass transport by ionic motion. On irradiation at room temperature small lead particles inside the crystal near the surface are produced. Thirdy, the photo-enhanced evaporation mode is where the substance is completely evaporated from the surface.

In lead bromide and chloride the photo-generated hole is trapped at a surface halogen ion giving a halogen atom which is desorbed. The electrons are trapped at Pb^{2+} ions, giving ultimately aggregates of lead atoms. A higher concentration of anion vacancies facilitates photolysis in three ways. Firstly, they carry the mass transport current of anions to the surface, secondly, an enhanced anion vacancy concentration is accompanied by a reduced concentration of cation vacancies because the latter trap holes, and, thirdly, annihilation of anion vacancies supplies room for the lead nuclei since lead atoms have a larger radius than the lead ions.

In the photolysis of lead chloride[88] a transition from one mode of photolysis to another has been observed, the mechanism operating during photolysis being dependent on the intensity of irradiation. At low intensities holes are trapped at surface halogen ions producing surface halogen atoms which can be desorbed. The excess lead condenses inside the crystal. At higher intensities more or less complete $PbCl_2$ molecules are desorbed from the surface. This has been explained in the following way.[89] Holes trapped at the surface during the photochemical process develop a potential barrier causing an acceleration of photogenerated electrons towards the surface. When the lifetime of an electron is shorter than the transit time to cross the barrier, the electrons will not reach the surface. This transit time is reduced with an increase in intensity of radiation. When electrons produced during the photolysis of lead chloride cross the potential barrier and become trapped at surface states connected with Pb^{2+} ions, called Pb^{+} states,[90] recombination centres for holes and electrons may form. These states have been identified from e.s.r. measurements.[87] An electron trapped at a Pb^{+} state and a hole at a nearby Cl^{-} state form

a surface Cl atom and a Pb^+ ion. These in turn may form a molecular-like structure facilitating the surface breakdown by evaporation. Reber *et al.*[91] have recently proposed a mechanism for the photolysis of lead chloride which is very similar to those proposed above. After absorption of a photon to yield an electron and a hole, the latter diffuses to the crystal surface where it is trapped by a surface chloride ion and is desorbed as chlorine. The photoelectron is trapped at the crystal surface by one of the numerous chloride ion vacancies to form an F-centre. These, being unstable at room temperature, are discharged on to the Pb^{2+} ions to form unstable [$\square$. Pb^+] complexes which aggregate to form a lead atom, two chloride ion vacancies and a Pb^{2+} ion:

$$2\ [\square . Pb^+] \rightarrow Pb^0 + Pb^{2+} + 2\square .$$

For both lead chloride and lead bromide the intensity dependence of photolysis was found to be a function of irradiation time. At low intensities the rate of photolysis of the chloride was proportional to $I^{0,17}$ and at high intensities to $I^{3,2}$.[92] The rate of photolysis of lead bromide was proportional to intensity for irradiation times shorter than one second.

Dawood *et al.*[93] have studied the photolysis of lead iodide. The rate of photolysis was found to vary as the square root of the irradiation time. Assuming the radiation is centred on 500 nm, excitons are produced which are free to migrate in the specimen. The concentration of these excitons will be greater near the surface. One of these excitons may be trapped at a suitable site (probably at the surface) and will be stable for a certain period before reverting to the ground state. If, before this happens, a second exciton is trapped at the same site, then a finite probability exists that the two will

react since most of the activation energy for the reaction is present as excitation energy. If reaction occurs we get:

$$I^- \overset{h\nu}{\rightleftarrows} I^{-*}$$

$$I^{-*} + I^{-*} \rightarrow I_2 + 2\square + 2e \quad .$$

Then either

$$2\square + 2e \rightarrow 2\boxdot$$ if F-centres are stable (1)

or

$$Pb^{2+} + 2e \rightarrow Pb$$ if F-centres are unstable (2).

In (1), aggregation of F-centres will lead to the formation of lead nuclei which is therefore the net result in both cases. This mechanism includes the possibility that the reaction of two excitons proceeds through intermediate stages.

Albrecht *et al.*[94] have recently also made a study of the photolysis of lead iodide. They found the rate to be dependent on the first power of the light intensity and proposed the following mechanism. A hole created by irradiation is trapped at a surface cation vacancy, O,

$$h^{\cdot} + O \rightarrow O'$$

This species, O', is the well-known V_1-centre which then reacts with an adjacent iodide ion

$$O' + I^-_{adj} \overset{\rightarrow}{\leftarrow} I^{\cdot} + O$$

producing ultimately an excess of anion vacancies at surface sites.

$$I^{\cdot} \rightleftarrows \square + I$$

The iodine atoms combine to form molecular iodine which desorbs:

$$2I \rightleftarrows I_2(g) \ .$$

Electrons are then trapped at anion vacancies within a space charge region to create F-centres

$$\square + e \rightleftarrows \boxdot \ .$$

Also anion vacancies diffuse from surface sites into the bulk

$$\square_s + I^- \rightarrow I^-_{adj} + \square$$

where I^-_{adj} indicates an iodide ion adjacent to the surface anion vacancy $\square_s$.

Finally metallic lead is formed by the reaction of lead ions with the unstable F-centres:

$$Pb^{2+} + 2\,\boxdot \rightarrow Pb + 2\,\square \ .$$

The sites where decomposition occurs are considered to be anion vacancies situated at kink sites, cracks, etc. The importance of anion vacancies in the decomposition has been demonstrated by experiments on films of lead iodide doped with suitable impurities such as Ag^+ ions. The growth of the lead nuclei can proceed by at least two mechanisms. Firstly, electrons produced by the decomposition of excitons may react with trapped interstitial lead ions although at low temperatures this process is rather slow. Secondly, pairs of excitons decompose at a surface site adjacent to a nucleus of lead. This process requires the transport of neutral excitons and not charged lattice ions and is considered the predominant process at low temperatures.

(b) Bromates

Herley and Levy[2,95,96] have made a study of the photolysis of sodium bromate. The rate of decomposition or production of oxygen decreased until a constant rate was attained in a manner analogous to the photolysis of sodium azide. The constant rate was almost dependent on the second power of the light intensity. The absence of photoconductivity indicated that the photolytic process probably involves excitons. The analogy with sodium azide's behaviour, led to the assumption that initially the concentration of the entities that become excited decomposition sites (which could be reaction products) is high and approaches an equilibrium concentration during the photolysis process. The following sequence of decomposition reactions were proposed:

$$BrO_3^- + * \text{ (excitation)} \rightleftarrows BrO_3^{-*}$$

$$BrO_3^{-*} + * \rightleftarrows BrO_3^{-**}$$

or

$$BrO_3^{-*} + BrO_3^{-*} \rightleftarrows BrO_3^{-**} .$$

The doubly excited site may now generate an additional singly excited site i.e.

$$BrO_3^{-**} + BrO_3^- \rightarrow 2BrO_3^{-*}$$

or it may produce decomposition

$$BrO_3^{-**} \rightarrow BrO^- + O_2 .$$

The generation of new decomposition sites from existing sites is similar to the process observed in the alkali halides for the generation of vacancies from centres that resume their initial characteristics after each additional vacancy is formed.

(c) Perchlorates

Verneker *et al.* have studied the photolytic decomposition of nitronium[97] and silver[98] perchlorates. In the former case the effects of irradiation as a function of intensity, temperature and time of irradiation have been investigated. The predominant gaseous products found have been O_2 and NO. The results indicated that two photolytic processes were taking place. The rate of decomposition increased initially to a maximum and then fell to a constant value. It was also found to be dependent throughout on the square of the light intensity. The first mechanism proposed occurs rapidly and depends on the existence of impurity or trapping centres which are consumed in this reaction. Hence we have

$$ClO_4^- \overset{h\nu}{\rightleftarrows} (ClO_4^-)^*$$

$$(ClO_4^-)^* + T \rightleftarrows (T\ ClO_4^-)^*$$

$$ClO_4^- \overset{h\nu}{\rightleftarrows} (ClO_4^-)^*$$

$$(T\ ClO_4^-)^* + (ClO_4^-)^* \rightarrow T + Cl_2 + 4O_2 + 2e$$

$$2NO_2^+ + 2e \rightarrow 2NO_2 + 2\ \text{vacancies}$$

where T = trap (electron acceptor).

The amount of oxygen evolved is proportional to the square of the light intensity. The traps, associated at the end with two anion vacancies, can no longer participate in the mechanism and the rate then decreases. This procedure probably accounts for the acceleratory and deceleratory parts of the rate-time curve. This process causes two electrons to enter the conduction band where they are eventually captured by other traps or by the nitronium ion.

The second mechanism proposed occurs simultaneously with the first. It is slower but does not have the self-consuming features of the first mechanism. In this case, the following mechanism is proposed:

$$NO_2^+ \overset{h\nu}{\rightleftarrows} (NO_2^+)^*$$

$$ClO_4^- \overset{h\nu}{\rightleftarrows} (ClO_4^-)^*$$

$$(NO_2^+)^* + (ClO_4^-)^* \rightarrow NO + ClO + 2O_2 \ .$$

The existence of this second mechanism was supported by the absence of a deceleratory period when an already photolysed sample was subjected to a second photolysis.

In a similar investigation of the photolysis of silver perchlorate[98] three different mechanisms were considered to be operating. The rate of gas evolution increased initially to a maximum and then fell to a constant value. The first mechanism proposed involved the creation of defect centres leading to an acceleration in the rate of photolysis:

$$ClO_4^- + \square \overset{h\nu}{\rightarrow} ClO_4\cdot + \boxdot$$

$$ClO_4^0 \rightarrow \text{products} + \square$$

$$Ag^+ + \boxdot \rightarrow Ag^0 + \square \ .$$

The deceleratory mechanism depends on the existence of trapping centres which are consumed in carrying out their part of the reaction mechanism. Doping experiments indicated that the trapping centre is likely to be an anion vacancy. Since the deceleratory reaction did not decrease to zero but became a finite constant value, a new mechanism was thought to become active, in which no consumable trapping centres are involved and which presumably continues until the crystal is consumed. The rate is proportional to the intensity of light and the silver metal formed in the

first mechanism is thought to initiate the reaction by photoemitting an electron.

$$Ag_m^0 \xrightarrow{h\nu} Ag_m^+ + e$$

$$Ag_m^+ + ClO_4^- \rightarrow Ag_m^0 + ClO_4^{\cdot}$$

$$ClO_4^{\cdot} \rightarrow \text{products}$$

$$Ag_m^0 + Ag^+ + e \rightarrow Ag_{m+1}^0$$

where Ag_{m+1}^0 is representative of the growth of colloidal metal. Thus the three mechanisms are (i) the creation of defect centres, (ii) the consumption of defect centres, and (iii) a steady-state rate.

Boldyrev[99] has recently made a study of the photolysis of ammonium perchlorate and found that, during the acceleratory period, ClO_3^-, ClO_2^- and ClO^- are formed. He also found that the induction period decreases on the introduction of proton - donor additives and increases with proton acceptor additives. In a study of sodium chlorate[100] no photoconductivity was detected which implied the absence of the existence of any holes or electrons. The following mechanism was proposed:

$$ClO_3^- \xrightarrow{h\nu} ClO_3^{-*}$$

$$ClO_3^{-*} + ClO_3^{-*} \rightarrow ClO_3^{-**} + ClO_3^-$$

$$ClO_3^{-**} \rightarrow ClO^- + O_2$$

$$ClO_3^{-**} + ClO_3^- \rightarrow 2ClO_3^{-*}$$

where the last reaction is the regeneration step. In the photolysis of sodium perchlorate the following mechanism has been postulated[101]:

$$ClO_4^- \xrightarrow{h\nu} ClO_4^{-*}$$

$$ClO_4^{-*} \rightarrow ClO_3^- + O^\cdot$$

$$O^\cdot + O^\cdot \rightarrow O_2.$$

The overall reaction is

$$NaClO_4 \rightarrow NaCl + 2O_2.$$

(d) Permanganates

Prout and Lownds[102] have investigated the photolysis of potassium permanganate in the form of crystals, powdered crystals and pellets in the temperature range 20° – 180°C. Initially a small volume of gas was rapidly liberated, followed by a short acceleration of the reaction and then a decay period. The initial "puff" was thought to be associated with reaction at highly defect surface sites where the MnO_4^- ions are more easily raised to excited states than at positions of greater crystal perfection. Excitation proceeds until the ion dissociates. The main decay reaction represents the reaction at less reactive, but still favoured, sites which are steadily consumed during photolysis. The rate of the reaction showed a dependence on the square and the cube of the intensity.

The reaction mechanism proposed involved the successive excitation and de-excitation of MnO_4^-, MnO_4^{-*} and MnO_4^{-**} culminating in the decomposition

$$MnO_4^{-***} \rightarrow \text{Products}.$$

The number of excitations was dependent on the relationship between the rate of the reaction and the light intensity. The overall photolytic

reaction below 110°C was proposed as

$$MnO_4^- \xrightarrow{3h\nu} MnO_2^- + O_2 \ .$$

Between 120° and 180°C only two photons are required to raise the energy of the permanganate ion to a level at which the excited ion dissociates thermally. Thus the following was proposed:

$$MnO_4^{-**} \xrightarrow{\Delta} MnO_4^0 + e$$

$$MnO_4^0 \rightarrow MnO_2 + O_2$$

$$MnO_4^- + e \rightarrow MnO_4^{2-}$$

the species MnO_4^{2-} having been detected at high flash intensities.[103] The activation energies found over the indicated temperature ranges were considered to be associated with the thermal dissociation of the excited ions.

(e) Oxalates

Finch *et al.*[104] have investigated the photolytic decomposition of silver oxalate. The kinetics of photolysis are explained by an exciton mechanism similar to, but not identical with, that previously applied to the decomposition of barium and potassium azides.[40] On prolonged photolysis by ultraviolet light, the oxalate decomposed into silver and carbon dioxide. After an initial rapid rate, the rate of gas evolution was practically constant. The rate was found to vary as the square of the intensity. The process envisaged was the capture of a singly excited oxalate ion at an anion vacancy. This complex could either be further excited by light absorption so that a second electron is captured by the anion vacancy or it may be destroyed by the electron returning by tunnel effect from the anion vacancy back to the singly-

charged ion. The possible processes are given by the following reaction scheme:

$$Ox^{2-} \xrightarrow{h\nu} [Ox^{-}]^{-} \quad \text{(stabilized exciton)}$$

$$[Ox^{-}]^{-} \rightarrow Ox^{2-}$$

or

$$[Ox^{-}]^{-} \xrightarrow{h\nu} [Ox]^{2-} \quad \text{(double exciton)}$$

$$[Ox]^{2-} \rightarrow [Ox^{-}]^{-}$$

$$[Ox]^{2-} \rightarrow 2CO_2 + \square + 2e.$$

4 THE THERMAL DECOMPOSITION OF SOLIDS

Since it was proposed to examine the simultaneous effects of thermal decomposition and photolysis (i.e. co-irradiation) it is necessary to discuss the thermal decomposition of solids. The majority of reactions which have been studied are of the type

$$A(s) \rightarrow B(s) + C(g)$$

where the start of the reaction involves the formation of a new phase B at special points in the lattice of A. Decomposition commences when local fluctuations provide favourable circumstances for the formation of B.

An experimental study of a thermal decomposition usually commences with the determination, isothermally, of a curve representing the plot of the fraction decomposed, α, (usually a measure of the pressure of gas evolved) as a function of time, t. The general features of typical α vs t curves are shown in Fig. 1.

In general they are sigmoid as shown in (a). Some substances e.g. lead styphnate and mercuric oxalate, have a relatively shorter acceleratory period and a more pronounced final decay period as shown in (b). Curve (c) is typical of lead azide where there is virtually no induction period. Curve (d) shows all the general features which can be present:

(i) initial rapid evolution of gas, represented by A;

(ii) an induction period in which gas may or may not be evolved, represented by B;

(iii) an acceleratory period following the induction period, represented by C; and

(iv) a decay period, represented by D.

Boldyrev[105] has divided thermal decomposition into two groups.

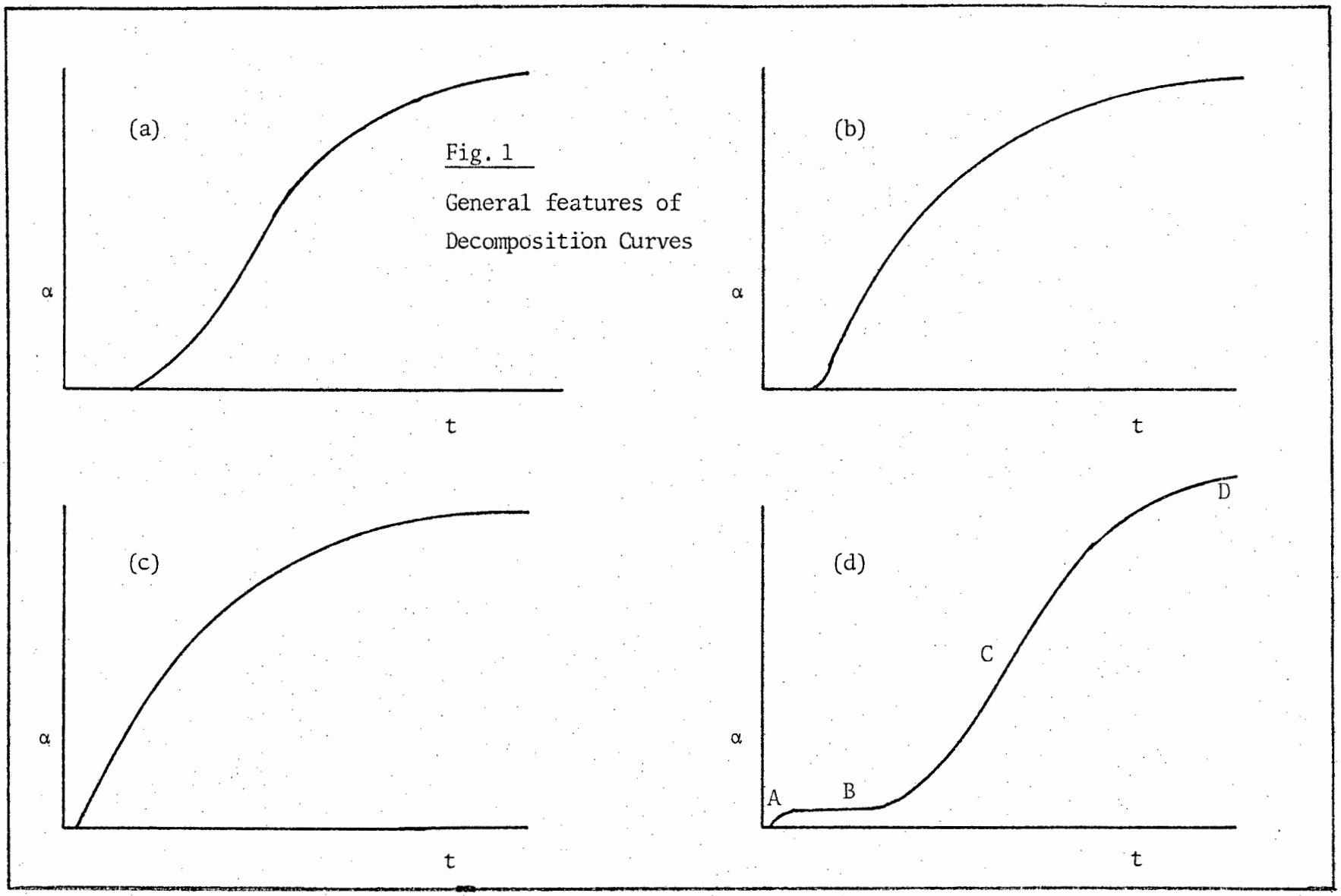

Fig. 1

General features of Decomposition Curves

(i) Thermal decomposition proceeding via cleavage of bonds in an anionic or cationic lattice component and accompanied by no transfer of charge. This mechanism depends mainly on defects on the surface and along lines (edge or screw dislocations). An example of this type of decomposition is that of $KMnO_4$.[106,107]

(ii) Thermal decomposition proceeding as a result of the transfer of an electron from an anion to a cation. This mechanism is mainly dependent on point defects such as vacancies, interstitials, impurity atoms, excitons, free electrons and holes. An example of this type of decomposition is that of the inorganic azides.[108]

In both of these cases the electronic environment at the site of decomposition of an individual molecule will influence the activation energy of its decomposition.

Line defects play an important role in the thermal decomposition of solids since reaction commences at the point of emergence of dislocations at the crystal surface and at the boundaries of groupings.[64,109,110,111] The emergence of edge dislocations, bent crystals, twisted crystals, incipient cleavage cracks, and similar families of edge dislocations at the surface of crystals of platinum phthalocyanine have been observed by Menter.[112] The concentration of these line defects is dependent on the age of the crystal, and consequently so is the rate of thermal decomposition dependent on age. With ageing in a crystal, the formation of groupings of dislocations is annihilated. The thermal decomposition of carbonates[113] and azides[114,115] has been shown to be favoured at dislocations, growth defects and mosaic block boundaries.

The process of thermal decomposition may also be influenced by point defects in the lattice, such as anionic or cationic vacancies, interstitial

ions, impurity atoms or ions and electronic defects (free electrons, excitons, colour-centres and positive holes).

The charge transfer scheme in the thermal decomposition of ionic solids was first postulated by Mott.[37] Electrons from the conduction band of the crystal are captured by an impurity centre. An adjacent ion almost immediately hands over an electron to this newly formed radical and the positive hole so formed diffuses away to the surface, escapes and decomposes. The impurity centre which has received an electron grows by attracting interstitial positive ions. This scheme has been used to explain topochemical processes accompanied by charge transfer although changes and additions have been made as in the case of mechanisms proposed for photolysis.

Charge transport within an ionic lattice is dependent on the defect structure of the solid and is achieved by ionic conductivity i.e. migration of ions. Ionic conductivity through the crystal is a result of migration of interstitials or a counter-migration of vacancies. Migration rates, for both interstitial and vacancy mechanisms,are directly dependent on the concentrations of these point defects. The result of ionic mobility is the migration of product atoms or molecules through the lattice.

Semi-conductivity also influences charge transport in crystals. When electrons are thermally excited from the valence to the conduction band, leaving positive holes in the valence band, we have intrinsic semi-conductivity. The phenomenon of impurities either accepting or donating electrons is known as extrinsic semi-conductivity. The energy levels of these donors and acceptors lie in the forbidden energy gap near the conduction and valence band respectively. Promotion of an electron from a level within the forbidden zone into the conduction band is n-type

semi - conductivity ; promotion of an electron from the valence band into a nearby level within the forbidden zone is p-type semi-conductivity. With reference to the solid decompositions it is important to note that type of semi-conductivity resulting from the product phase having a different work function to the reactant phase. In this case the phases act as proton donors or acceptors depending on their relative work functions.[116]

Exciton formation during thermal decomposition results from thermal excitation of an electron to a non-conducting excited state or alternately from the partial combination of an electron and a positive hole, without reversion to the electronic ground state. As discussed under photolysis, where they play a more important role, excitons are mobile and can dissociate into free electrons and positive holes, thus aiding charge transport.

A characteristic feature of the thermal decomposition of solids is the initiation and propagation of the reaction from a number of preferred sites termed nuclei formed at the abovementioned imperfections in the lattice. These nuclei may be distributed over the surface of, or embedded in, the bulk of the reactant matrix and their activation energy of decomposition is lowest at these sites. Further decomposition is localized at the interface between the nuclei and the reactant matrix, so that the nuclei grow in size as the reaction proceeds. As the nuclei grow, the area of this interface increases. Photographs have been obtained which show discrete, random nucleation on crystal surfaces. It has been observed from these photographs that the nuclei form in the regions of emergence of dislocations and grain boundaries on the crystal surface. Herley *et al.*[181] have shown that this occurs during the thermal decomposition of ammonium perchlorate.

These nuclei are thought to be composed of solid reaction products. Differences in the physical properties between product and reactant phases cause strain which results in movement of reaction through the lattice. Chemical transformation is facilitated at defects on the internal and external surfaces of the crystal because both the chemical potential and the stereochemical environment of ionic species in the immediate vicinity of these points differ from those of similar species at 'ideal' lattice sites.

Nuclei may be classified as (i) diffuse and (ii) compact.

(i) Diffuse nuclei. These are spread throughout the solid and are not directly observable since they do not grow to a visible size. This occurs, for example, in the thermal decomposition of mercury fulminate.[140]

(ii) Compact nuclei. Generally the activation energy for nucleus formation is greater than that for nuclear growth with the consequence that compact nuclei are formed. They are directly observable and have characteristic shapes dependent on the physical properties of the solid. In sodium azide pellets[117] they were observed to be 2-dimensional and approximately circular and were formed on preferred crystallographic faces. Spherical nuclei have been observed in the thermal decomposition of barium azide,[39] horn-shaped nuclei in the dehydration of $CuSO_4.5H_2O$[118] and hexagonal nuclei in the thermal decomposition of potassium hydrogen phthlate.[119]

The number of nuclei formed during thermal decomposition may be greatly influenced by the pre-reaction treatment of the sample, thereby increasing greatly the number of potential nucleus forming sites. Grinding[58,120], scratching of the crystal surface[121] and the method of sample preparation[122] have been shown to play an important role in this respect. Pre-irradiation of the solid prior to decomposition with ionizing radiations (γ- and X-rays),[123,124,125,126] UV light,[38] electron[127] or reactor radiation[128,129] has been found in general to enhance the subsequent thermal decomposition of the solid as a

result of the formation of crystal defects and decomposition of radiolysis products in the crystal lattice.

Nucleus formation is considered to take place during the induction period (B in Fig. 1(d)). At the end of the induction period the production of nuclei is at a critical stage, and the reaction becomes auto-catalytic during the acceleration. At the end of the induction period the crystal is a function of the number of nuclei and their spatial distribution, the size and shape of the nuclei and a variety of properties of the nuclei themselves e.g. their chemical, crystallographic and electronic structure. Growth of these nuclei takes place during the acceleration, although some nucleus formation may also occur during this stage of the reaction.

Beyond the inflection point, the decay stage begins. Nucleus growth ceases and the rate of reaction decreases when the nuclei have expanded far enough to begin to overlap and thereby decrease the interfacial area between reactant and product.

The mechanism of a particular decomposition and the kinetic equation which describes the acceleration of the reaction depends on two factors:

(i) the rate of nucleus formation, and

(ii) the rate and mode of growth of the nuclei.

When nucleus formation involves a single step it can be described as a linear or exponential function of time. When it involves multiple steps it can be described as a power of the time. A linear increase in the number of nuclei with time has been observed with the dehydration of $CuSO_4.5H_2O$.[130] Photographs of nucleation in ammonium perchlorate crystals have been obtained by Herley, Levy and Jacobs.[131,132,133,134] Discrete nuclei on the surface of the crystal were observed in preferred crystallographic directions, the nuclei being different on different

crystal faces. Nucleus growth stopped once the nuclei reached a critical size. At the same time the smaller nuclei continued to grow until they too had reached the critical size. When decomposition over the external faces was complete nucleation on the subsurfaces was observed.

A. *Analysis of Acceleratory Period*

The kinetics of simultaneous nucleus formation and growth, or the growth of a constant number of nuclei, i.e. the acceleratory region, can be described by the following mathematical relationships:

(i) The Power Law,

(ii) The Exponential Law,

(iii) The Prout-Tompkins equation, and

(iv) The Avrami-Erofeyev equation.

(i) The Power Law

This class of thermal decomposition comprises those in which multiple steps are required for nucleus formation. Nucleus growth is assumed constant and overlap of the growing nuclei is neglected. It can then be shown[13] that

$$p = kt^n \qquad (1)$$

where p = the gas pressure at time t during an isothermal decomposition,

k = the rate constant,

and $n = \beta + \lambda$ β is an integer representing the number of successive molecular decompositions at a single site required to form a stable growth nucleus,

λ has values 1, 2, or 3 depending on whether the nuclei grow 1-, 2-, or 3-dimensionally i.e. linear, plate-like or spherical.

The power law has been applied successfully in the above form, and in the form $p^{1/n} = kt$, to a number of compounds. Its usefulness is enhanced in that the final pressure is not required. The acceleratory reaction of the thermal decomposition of lithium,[135] calcium[58,59,136,137] and strontium azides have been analysed using the power law with $n = 3$. It has been applied to zinc oxalate[138] with $1 \leq n \leq 2$, to silver oxalate[139] with $3{,}02 \leq n \leq 5{,}30$ and to barium azide[39] with $n = 6$.

(ii) The Exponential Law

This law, derived by Garner and Hailes[140], in the process of studying the concept of linear branching chains, assumes a constant rate of nucleation and a constant branching chain coefficient k. We thus have

$$p = c \exp(kt) \qquad (2)$$

where c = constant, is a function of temperature, and contains the constants for nucleation, growth and branching.

Although the equation was applied with success to the decomposition of mercury fulminate and large crystals of lead styphnate[141] it is now generally accepted that the concept of linear chains requires some modification. The rapid propagation of linear chains through the crystal would tend to separate it into mosaic blocks, which would then decompose slowly. This was not considered to be a favourable mechanism and thus a modification was postulated whereby the branching plate-like nuclei were propagated throughout the crystal.[142] This concept was applied to silver oxalate[104] and it was suggested that decomposition

proceded along grain boundaries and dislocation lines, with branching occurring at intersections of these defects in the crystal lattice.

(iii) The Prout-Tompkins Equation

Prout and Tompkins noted that the original form of Garner's linear branching chain theory did not take into account the overlap of branching chains at higher degrees of decomposition. They thus introduced a term for the probability of chain termination into Garner and Hailes'[140] linear branching chain formula. The Prout-Tompkins equation was obtained on integrating the equation derived to represent the rate of decomposition $d\alpha/dt$ and has the form

$$\log \frac{p}{p_f - p} = kt + c \qquad (3)$$

where p = pressure at time t

p_f = final pressure

k = branching coefficient.

This equation has been applied to the thermal decomposition of unirradiated and pre-irradiated permanganates,[143] the co-irradiation decomposition of potassium permanganate[144], the analysis of the entire thermal decomposition of nitronium perchlorate[145] and lead oxalate[125], and the acceleratory reactions of potassium metaperiodate,[146] lithium perchlorate[147] and pre-irradiated ammonium perchlorate.[148]

Prout and Tompkins found that analysis of the decomposition of silver permanganate was improved if the following modified form was used:

$$\log \frac{p}{p_f - p} = k \log t + c \qquad (4)$$

This equation takes into account the fact that the branching coefficient k was not constant but varied inversely with time.

(iv) The Avrami-Erofeyev Equation

Avrami,[149] in attempting to obtain a more general kinetic equation, dealt with the nucleation process in a study of the kinetics of phase change. He assumed that the new phase, as a result of the thermal decomposition of the solid, is nucleated by tiny "germ nuclei" which already exist in the old phase. These germ nuclei are capable of developing into observable "growth nuclei" after commencement of the transformation. The number of germ nuclei decreases in two ways as the reaction preceeds. The first effect is the normal activation and growth of the nuclei and the second effect is the ingestion of germ nuclei by actively growing growth nuclei, which thus renders the germ nuclei inoperative.

Avrami developed an equation which represents a general solution to the problem of random nucleation followed by 3-dimensional growth. It had the form:

$$-\log(1-\alpha) = \frac{6\ S\ N_0\ k_2'^3}{V_0\ k_1'^3}\left[e^{-k_1' t} - 1 + k' t - \frac{(k' t)^2}{2!} + \frac{(k' t)^3}{3!} \right] \quad (5)$$

where S = Shape factor,

V_0 = final volume of product obtained from complete decomposition of reactant,

N_0 = total number of germ nuclei at time $t = 0$,

k_1' = constant,

and α = frational decomposition (p/p_f).

Several limiting cases were obtained from this equation.

(i) α small: When $\alpha << 1$, the contribution of overlapping and phantom nuclei will be negligible and the general equation reduces to the power law i.e.

$$\alpha = ct^n \qquad (6)$$

where n has the same meaning as before.

In particular n = 4 corresponds to random nucleation of three-dimensional nuclei, n = 3 corresponds to instantaneous nucleation followed by three-dimensional growth and n = 2 corresponds to linear growth.

(ii) α large: When α is large i.e in the decay period, the general equation reduces to

$$-\log(1-\alpha) = [S N_0 k_2'^3/V_0]t^3 \qquad (7)$$

$$= kt^3 \qquad (8)$$

Using a different approach Erofeyev[150] first derived a general kinetic equation

$$\alpha = 1 - \exp(-\int_0^t p\, dt) \qquad (9)$$

or $$-\log(1-\alpha) = \int_0^t p\, dt \qquad (10)$$

where α = fractional decomposition,

and p = probability of the reaction of an individual molecule in an interval dt.

The equation was then applied to the formation and growth of nuclei in the solid state. He obtained the equation

$$\alpha = 1 - \exp(-kt^4) \qquad (11)$$

corresponding to 3-dimensional nuclei increasing in number at a constant rate. For cylindrical nuclei

$$\alpha = 1 - \exp(-kt^3) \qquad (12)$$

and for flat nuclei

$$\alpha = 1 - \exp(-kt^2) \quad . \qquad (13)$$

Thus in general according to the shape of the nuclei and their rate of increase

$$\alpha = 1 - \exp(-kt^n) \qquad (14)$$

$$\text{or} \quad -\log(1-\alpha) = kt^n \qquad (15)$$

which is the same general form as derived by Avrami. Equations 7, 8 and 15 are general equations for the kinetics of reactions which proceed by way of formation and growth of reaction nuclei in a solid. These are forms of the Avrami-Erofeyev equation.

The Avrami-Erofeyev equation is versatile because of the variable n[151,154,115,155-157,148] and has been used in the analysis of the acceleratory region in the thermal decomposition of sodium and potassium hydrogen carbonates,[154] nickel terephthalate,[156] sodium nitrate,[158] barium azide,[115] ammonium perchlorate[159] and silver oxalate[160] where n has assumed values of 2, 3 and 4.

B. *Analysis of Decay Period*

During the decay period, overlap of the compact nuclei has occurred and the reaction then proceeds from a shrinking of the interface between the reactant and product phases. In certain cases the product phase may catalyze the reaction as a result of intimate

contact between the two solid phases. Topokinetic equations applicable to the decay period thus describe a contracting envelope of product enclosing a volume of reactant which is free of defects such as dislocations since these represent sites of preferential decomposition and are usually consumed by the product during the acceleratory period.

The decay period may be analyzed by use of the following equations:

(i) Avrami-Erofeyev equation

(ii) Unimolecular Decay Law

(iii) Prout-Tompkins equation, and

(iv) Contracting sphere equation.

(i) The Avrami-Erofeyev Equation

The form

$$\alpha = 1 - \exp(-kt^3) \qquad (16)$$

is used in the analysis of the decay period providing the contracting interface remains intact. Because of the difference in molecular volume between product and reactant phases, a collapse of the interface may occur leaving isolated blocks of material in which no nuclei are present. The rate is thus proportional to the amount of substance undecomposed.

Hence

$$\frac{d\alpha}{dt} = k(1-\alpha) \qquad (17)$$

(ii) Unimolecular Decay Law

From equation (17) we get the unimolecular decay law

$$-\log(1-\alpha) = kt \qquad (18)$$

$$\text{or} \quad \log \frac{p_f}{p_f - p} = kt \quad . \qquad (19)$$

(iii) Prout-Tompkins Equation

This equation considers the decay reaction to be proportional to the number of unreacted molecules.[161] Only those molecules adjacent to product molecules will be able to decompose. Thus the rate of reaction is

$$\frac{dp}{dt} = k(p_f - p)\, P \qquad (20)$$

where P = the probability of the favoured situation and is determined by $\alpha = p/p_f$.

Thus

$$\frac{dp}{dt} = k(p_f - p)\, p/p_f \qquad (21)$$

Integration between limits led to the equation

$$\log \frac{p}{p_f - p} = kt + c \qquad (22)$$

which is the Prout-Tompkins equation as found for acceleratory reactions with a different rate constant k.

(iv) Contracting Sphere Equation

In the cases where there is rapid and efficient surface nucleation of particles, the surfaces of the particles become coated with a layer of product in the early stages of the reaction. The rate determining step could then be the rate of penetration of this interface into the particles. The form of the equation is then

$$1 - (1-\alpha)^{1/3} = kt \, . \qquad (23)$$

A similar method to the contracting sphere method may be applied for contracting interfaces in geometrical shapes other than spherical.

Many applications have been found for the above equations. The Avrami-Erofeyev equation with n = 3 has been used in the study of the decay reaction of sodium nitrate[158] and ammonium perchlorate,[159] and the equation with n = 1 in the study of the decay stage of lithium perchlorate[147] and pre-irradiated ammonium perchlorate.[148] The contracting sphere equation has been used by Prout and co-workers in the study of the decay of lithium azide,[135] calcium azide,[136] nickel oxalate[162] and barium azide.[115]

When none of the standard equations has been found suitable, empirical equations have been used[128,159] or a general method for the calculation of rate constants as described by Jacobs and co-workers[163] have been used. The rate constant in these cases has no physical meaning however.

Mathematical analysis of the acceleratory and decay periods of pressure-time plots for isothermal decomposition of solids can thus yield much information on the reaction mechanisms, such as the process of nucleation, shape of nuclei and mechanism by which they grow in size. Applicability of an equation, however, does not necessarily imply that the model, from which the equation was derived, is relevant but rather as a postulate upon which experimentation designed to support this postulate can be based. Furthermore, it is possible for more than one equation to apply to some given data. For example both the Prout-Tompkins equation[161] and the Avrami-Erofeyev equation with n = 4[164] have been applied to the kinetics of thermal decomposition of potassium permanganate.

The theoretical approach to the decomposition kinetics of solids has led to a greater understanding of the macro-processes occurring during the reactions, and has also provided equations which yield rate

constants. These in turn, regardless of their significance, can be used to investigate the dependence of reaction rate on a variety of experimental variables such as temperature of decomposition, size of particles and age or history of the material.

5 THE EFFECTS OF PRE-IRRADIATION WITH ULTRA-VIOLET LIGHT ON THE THERMAL DECOMPOSITION OF SOLIDS

The results and conclusions of pre-irradiation studies are naturally of significance in any study involving co-irradiation effects and thus a review of the former is appropriate at this point.

The effect of pre-irradiation on the thermal decomposition of many crystalline solids, in particular the azides, has been studied in considerable detail.[5,37,38,57,58,165] These studies have led to an increased knowledge of the mechanism of the thermal decomposition of unirradiated solids and also to a better understanding of the nature of radiation damage. Almost every type of radiation has been used but a large fraction of the published work describes effects produced by ultraviolet light, X-ray, γ-ray, and reactor irradiations. Studies on irradiated material are usually performed for one or both of two reasons. Firstly, the material may have been irradiated to investigate one or more features of the decomposition process. Ultraviolet light may, for example, produce effects which would indicate whether a particular decomposition involves one or more electronic processes. Secondly, it may have been included in a "radiation damage" study in order to determine if irradiation can modify one or more properties of the material in any important way. For example, irradiation could possibly introduce lattice defects or trapped charges.[166]

The general effects of pre-irradiation on the subsequent thermal decomposition of the solid are:

(i) shortening of the induction period,

(ii) acceleration of the reaction,

(iii) changes in the activation energies associated with the decomposition process, and

(iv) changes in the mathematical analysis governing the pressure-time plots, and their extent of fit.

The effects of the pre-irradiation are generally of long duration but may undergo aging. Some substances such as silver permanganate[167] are insensitive to pre-irradiation whereas others such as strontium azide are extremely sensitive.[168] Since thermal decomposition of many inorganic solids has been thought to proceed via an electron transfer, the effects of the interaction of ultraviolet light on ionic solids leads to the conclusion that pre-irradiation with ultraviolet light will have a positive effect on the subsequent thermal decomposition. The inorganic azides are a clear illustration of this. When barium and strontium azides were subjected to pre-treatment with ultraviolet light, the induction periods were found to be shortened in the subsequent thermal decomposition[38] and in the case of barium azide an increase in the rate constant k, in the equation $\alpha = k(t - t_0)^6$, was observed. No attempts were made to measure the activation energies when the pre-irradiated specimens were thermally decomposed, and it was assumed that the nature of the reaction mechanisms was not markedly affected by the pre-irradiation with ultraviolet light. It was postulated that ultraviolet irradiation produced "holes" and diffusion of barium atoms, in the case of barium azide, to these "holes" resulted in the formation of nuclei from which the reaction started. Mott[37] proposed that the ultraviolet irradiation caused electrons from azide ions to enter the conduction band where they wandered until trapped by a metallic barium speck which thus grew by a process of internal photolysis.

Later investigation by Thomas and Tompkins[40] into the effect of ultraviolet light at room temperature on the subsequent thermal decomposition of barium azide confirmed the above findings. The induction period

decreased and an increase in the rate of the acceleratory reaction was observed. With large doses of irradiation the exponent in the rate equation changed from six to three. This was explained by proposing that at low doses, more potential nucleus forming sites are created, these sites being assumed to be anion vacancies. At higher doses these sites were thought to become activated by trapping electrons and thus relaxing the requirement for thermal activation. Eventually all the potential nucleus forming sites become both activated and equivalent and thus a cubic acceleratory period is obtained.

When barium azide was pre-irradiated with ultraviolet light, the exponent in the Avrami-Erofeyev equation was found to change from four to six.[168] Prout and Moore proposed the formation of large numbers of F-centres on irradiation, which aggregate and collapse on heating, with the formation of barium atoms. These then migrate and crystallize at favourable sites to yield metallic nuclei, from which the reaction then proceeds. They proposed the same growth mechanism for these nuclei as they proposed for the unirradiated azide.[115] The exponential change was accounted for by assuming that after irradiation the number of nuclei no longer increased linearly with time but rather with the cube of time.

Pre-irradiation of potassium azide[120] had no subsequent effect on the thermal decomposition. The salt was coloured blue but this rapidly faded on heating. It was postulated that mobile excitons are formed and the electron from the exciton tunnels to a vacant site forming a single entity, the colouration complex, which comprises an F-centre and a positive hole. A second exciton then forms a complex adjacent to the first and a reaction takes place in which three molecules of nitrogen are formed. On heating it was proposed that the reverse process in fact occurred when both the bimolecular combination of positive holes and the

unimolecular recombination of electrons from F-centres with positive holes took place by the tunnelling effect. This accounted for the absence of photoconductance.

Treatment of sodium azide with ultraviolet light at room temperature followed by thermal decomposition results in the development of centres of colloidal sodium.[67] These particles are thought to form as a result of the photochemical reduction by irradiation, leaving an excess of sodium in the lattice which forms clusters during thermal diffusion. Aggregation of the metal was proposed via vacancy or electron diffusion.

Prout and Liddiard[169] have studied the effect of pre-irradiation on the thermal decomposition of lithium azide. The irradiation effect is confined to the irradiated face only. The thermal decomposition is accelerated by pre-irradiation with ultraviolet light and the induction period is drastically reduced. The changes in lithium azide were considered analogous with those in potassium[69] and sodium[67] azides. The excited azide ions are trapped at anion vacancies and react together to yield F-centres and F-centre aggregates, the latter possibly collapsing to form lithium atoms. Excited azide ions may also react with an adjacent azide ion to produce N_4^- ions. High doses of pre-irradiation result in the elimination of the induction and acceleratory periods, indicating the creation of a large number of "thermal decomposition" nuclei which touch soon after heating commences. The observed exponential change in the Avrami-Erofeyev equation from three with unirradiated to two with pre-irradiated azide is a result of the high concentration of nuclei at the start of the acceleration. The thermal decomposition of pre-irradiated lithium azide thus proceeds via two-dimensional growth of nuclei, growth occurring from a fixed number of nuclei. Since the decay showed little dependence on irradiation it was concluded that the topochemistry of this stage of the reaction was similar to that of the

unirradiated material, and after surface nucleation and coverage the product reactant interface moves inwards on the particles of the powder.

Calcium[58,136,168] and strontium[38,168,57] azides have shown similar results on being pre-irradiated. Garner and Reeves[57] found that the power law with the exponent n = 3 held for the unirradiated and pre-irradiated decomposition of both these azides. Pre-irradiation resulted in a shortening of the induction period and an increase in the rate constant for the acceleratory period. Pre-irradiation with ultraviolet light was thought to result in the development of sites into nuclei of approximately the same size, the end result being the same as that observed at the end of the induction period of thermal decomposition. Tompkins and Young[58] examined the effects of pre-irradiation on aged and annealed calcium azide and on the fresh material. The former yielded a rate constant which was constant for all doses up to 10^{14} photons/cm^2 whereas the latter yielded a rate constant increasing continuously with the irradiation dose. The differences observed were attributed to the activation of excess bulk vacancies in the fresh azide. In the case of the aged material an excess of electrons due to irradiation were thought to be captured by surface clusters and these transformed into growth nuclei. In fresh azide containing excess grown-in vacancies, pre-irradiation was reported to activate germ nuclei throughout the system.

Prout and Moore[168] investigated further the effects of ultraviolet pre-irradiation on calcium and strontium azide and found the results for both salts to be very similar. Heavy ultraviolet doses resulted in pressure-time curves for thermal decomposition which could be analyzed using the power law with n = 2. No darkening occurred, the induction period was shortened and an increase in the rate constant for the acceleratory region was observed. The inflection point was found to

decrease with an increase in the pre-irradiation dose. It was suggested that surface damage occurred with the resultant two dimensional nucleus growth for the highly irradiated azides. Heavy irradiation doses caused a change in n from three to two presumably due to the high concentration of surface nuclei. A study of the effects of pre-irradiation on the thermal decomposition showed no detectable change in the induction period or the rate of the reaction.[114]

Prout and Tompkins[170] have investigated the pre-irradiation effects on mercuric oxalate. The irradiated azide decomposed at a higher rate, the acceleratory period showing an initial burst of gas followed by a short constant rate period. Later investigation[115] showed that the unirradiated and irradiated decomposition could be represented by the power law with $n = 2$. An unidentified irradiation product created by an electron transfer process which formed and grew under the action of light on the surface of the mercuric oxalate was postulated, the product tentatively thought to be mercurous oxalate.

The effects of pre-irradiation on the thermal decomposition of silver oxalate have also been investigated.[171,172] It was found that pre-irradiation caused an increase in the rate constant of the acceleratory period with a decrease in the value of n in the expression $\alpha = k(t - t_0)^n$ from approximately four to three. These effects were attributed to the first-order formation at certain sites of compact nuclei which grow in three dimensions, the number of unfertilized sites decreasing as the intensity of the ultraviolet light increases. Other researchers[104,142] proposed a branching chain mechanism for the silver oxalate decomposition. The rate constant was unchanged after the pre-irradiation but the pre-exponential factor varied. Haynes and Young[173] have proposed that in irradiated silver oxalate the number of starting points on the surface are increased by pre-irradiation. These then develop into growth nuclei,

with simultaneous decomposition along a line joining two of these nuclei, hence explaining the use of the exponential equation. Russian workers[151, 152] have concluded that the effect of pre-irradiation on silver oxalate is a purely surface one and affects only the initial decomposition.

6 THE CO-IRRADIATED DECOMPOSITION OF SOLIDS

Co-irradiated decomposition is the term used to describe the simultaneous thermal and photolytic decompositions of solids. Photolytic decompositions of solids imply the absence of any dark rate i.e. removing the source of radiation causes the decomposition to cease, there being no thermal decomposition taking place or the rate of thermal decomposition being negligible compared to that of photolysis. Garner and Moon[175] have made a study of the effect on the rate of decomposition of placing 1 mg of radium in close proximity to a crystal of barium azide at a temperature of 110°C. They found that the induction period halved and the rate of decomposition increased fourfold compared to that of a straight thermal decomposition. In the accelerated reaction the nuclei present on the face of the crystal nearest to the radioactive source were found to be much larger than those of the other faces of the crystal. The main influence of the emission was thought to lie not in nuclear formation but in an acceleration of the rate of propagation of the reaction through the solid.

Boldyrev *et al.*[176-178] have studied the co-irradiated decomposition of a number of ionic salts including barium, silver, calcium and strontium azides. In all cases X-ray irradiation was used. The effect of irradiation was to increase the rate of decomposition. The acceleration of thermal decomposition by irradiation in the case of barium azide was found to be related to the formation, during irradiation, of incipient decomposition centres. These centres may occur as stable interstitial aggregates formed according to the mechanism of Mott[36] or aggregates of F-centres formed according to the mechanism of Frenkel.[179] X-ray irradiation causes the concentration of free electrons in the crystal lattice to increase thus leading to the formation of large numbers of

stable aggregate nuclei. When the irradiation is carried out at the threshold decomposition temperature, the high concentration of free electrons in the lattice is accompanied by a rise in the concentration of ion defects interacting with electrons, and their mobility thus increases. Consequently, a large number of stable aggregate nuclei are formed with a greater probability of critical dimensions for each. This is evidently the cause of the increase in the rate of decomposition achieved by irradiation at this threshold decomposition temperature. In another study[178] Boldyrev found that co-irradiation accelerates decomposition only of substances for which the dissociation is accelerated by pre-irradiation. Calcium, strontium and barium azides show an increase in rate of decomposition but silver azide shows no change with co-irradiation. From the data obtained experimentally it was concluded that all the effects observed during decomposition in a radiation field can be explained from the viewpoint of the mechanism proposed for explaining the effect of pre-irradiation on the thermal decomposition kinetics. The mechanism of the irradiation effect is due to activation of the solid phase by the X-rays, for example by formation of radiolysis products which activate thermal decomposition. The absence of a specific irradiation effect during decomposition, as opposed to pre-irradiation, is considered to be an indication that during thermal decomposition of these substances the electron-excitation stage is not the limiting stage. Pre-irradiation with X-rays had a greater effect than co-irradiation on the thermal decomposition of calcium and strontium azides, whereas co-irradiation of barium azide had a more marked effect on the thermal decomposition than pre-irradiation. The proportional effect of pre-irradiation and co-irradiation on the thermal decomposition is dependent on the sensitivity of the salt to irradiation and the temperature dependence of the pre-irradiation effect.

Pre-irradiation of barium azide was found to have a larger temperature dependence than strontium or calcium azides which could account for the greater sensitivity of the former to co-irradiation.

Permanganates of potassium and silver have also been subjected to X-radiation during thermal decomposition. Boldyrev *et al.*[178] found that no effect on the thermal decomposition resulted from either pre-irradiation or co-irradiation of the potassium salt with an X-ray dose of 400 rad/min. The rate of thermal decomposition of silver permanganate increased five times when pre-irratiated or co-irradiated with this dose.

Prout and Lownds[144] have also studied the co-irradiated decomposition of potassium permanganate. They proposed that photolytic decomposition and thermal decomposition occurred concurrently and postulated the following mechanism:

$$\text{(i)} \qquad MnO_4^- \xrightarrow{h\nu} (MnO_4^-)^*$$

$$\text{(ii)} \qquad (MnO_4^-)^* \xrightarrow{\Delta} MnO_4^0 + e$$

The activation energies for the co-irradiated decomposition were found to lie between those found for photolytic decompositions and those for thermal decompositions.

Prout and Shephard[50] have recently made a study of the co-irradiated decomposition of barium and strontium azides. In the former case the percentage decomposition was unaltered. At low light intensities the activation energies approximated those of the thermal decomposition of the azide and with increased light intensity the values of the activation energies decreased. They proposed that parallel reactions took place i.e. the photolytic reaction proposed for the lower temperature ranges and the thermal reaction occurring in the temperature range under discussion. Analysis of equations used implied the occurrence of two-dimensional growth

of plate-like nuclei increasing from a fixed number of centres. During the induction period atoms are formed on the surface and on the planes of the crystal, each plane starting at the surface at an emergent grain boundary. Nuclei are formed by aggregation at the end of the induction period. The following mechanisms were proposed to take place concurrently:

(i) $N_3^- + N_3^- \xrightarrow{\Delta} 3N_2 + 2e$

$Ba^{2+} + 2e \rightarrow Ba$

(ii) $N_3^- \overset{h\nu}{\rightleftarrows} N_3^{-*}$

$Ba^{2+} + N_3^- \xrightarrow{\Delta} Ba^+ + N_3$

$N_3 + N_3^{-*} \rightarrow 3N_2 + e$

$Ba^+ + e \rightarrow Ba$.

The process of nuclear growth over the acceleratory period was explained by the following concurrently occurring mechanisms:

(i) $N_3^- + Ba\ (metal) \xrightarrow{\Delta} N_3 +$ (electron in conduction band of barium metal)

$N_3 + N_3^- \rightarrow 3N_2 + e + 2\square$

$\rightarrow 3N_2 + \boxdot + \square$

$2\boxdot \rightarrow 2\square + 2e$

$Ba_n + 2e + Ba^{2+} \rightarrow Ba_{n+1}$

(ii) $Ba_n \overset{h\nu}{\rightleftarrows} Ba_n^+ + e$

$N_3^- \overset{h\nu}{\rightleftarrows} N_3^{-*}$

$Ba_n^+ + N_3^- \xrightarrow{\Delta} Ba_n + N_3$

$N_3 + N_3^{-*} \rightarrow 3N_2 + e + 2\square$

$$\rightarrow \quad 3N_2 + \boxdot + \square$$

$$2\,\boxdot \rightarrow \quad 2\,\square + 2e$$

$$Ba_n + 2e + Ba^{2+} \rightarrow \quad Ba_{n+1} \quad .$$

For the decay period the same mechanisms were postulated as those for the acceleratory period. In the case of strontium azide the same mechanisms were proposed in all three stages of the decomposition as for barium azide.

7 OBJECTS OF RESEARCH

The object of this research was to make a detailed study of the photolysis of calcium, strontium, barium and lithium azides as well as the co-irradiated decomposition of calcium azide. A new technique, used by Prout and Shephard[50], involving the use of very high intensity lamps was to be employed. With this method the samples, hitherto only studied in terms of surface decomposition, decomposed throughout the mass, resulting in a high percentage decomposition. Work had been done by Prout and Shephard on barium and strontium azides at ambient and higher temperatures. The programme here was to extend the range of temperatures to between approximately -70,0°C and ambient temperature. Prout and Moore[168] and Prout and Brown[137] have studied the thermal decomposition of calcium azide and the effect thereon of pre-irradiating the sample with ultraviolet radiation. It was proposed that the photolysis and co-irradiated decomposition of calcium azide between approximately -70,0°C and 140,0°C should be studied. It was also considered to be of value to make a study of the photolysis of lithium azide in order to draw comparisons, if any, between the azides of divalent metals, normally barium, strontium and calcium, and a monovalent metal, namely lithium.

8 APPARATUS AND EXPERIMENTAL METHODS

(i) HIGH VACUUM SYSTEMS

The course of all photolytic decompositions of powdered and pelleted material were followed using a high vacuum constant volume line. The vacuum line consisted essentially of a pumping system, a pressure measuring device and a decomposition cell. The line is illustrated in Fig. 2.

The pump used in evacuating the line was a Pfeiffer TVS 250 turbo-molecular pump. This was capable of producing a vacuum of $1,0 \times 10^{-6}$ torr. In the case of decomposition of powdered material the pressure was measured using an Edwards "Speedivac" Pirani Gauge Control Unit Model 8-2 with gauge head G5C-2. The gauge was linked to a Phillips PM 8100 flat-bed recorder for automatic recording of pressure changes with time. The Pirani gauge was calibrated against a McLeod gauge. The ranges of the recorder used in the study (5 mV and 10 mV) were then calibrated against the Pirani gauge. It was found that above 0,02 torr the relationship between pressure and millivolt reading was non-linear and thus decompositions were limited to the pressure range 0,00 to 0,02 torr. Fig. 3 illustrates a plot of pressure against the recorder millivolt reading.

In the case of the decomposition of pelleted material the pressures involved were greater than the maximum of 0,02 torr allowed for accurate measurement using the Pirani gauge. In these decompositions the pressure was measured using a McLeod gauge of volume 123,1 cm^3. The McLeod gauge was joined to the line at the same position used by the Pirani gauge head.

The vacuum line consisted of three ten litre bulbs. This allowed the volume of the line to be varied for different decomposition conditions and different compounds. In this way the pressures were always maintained

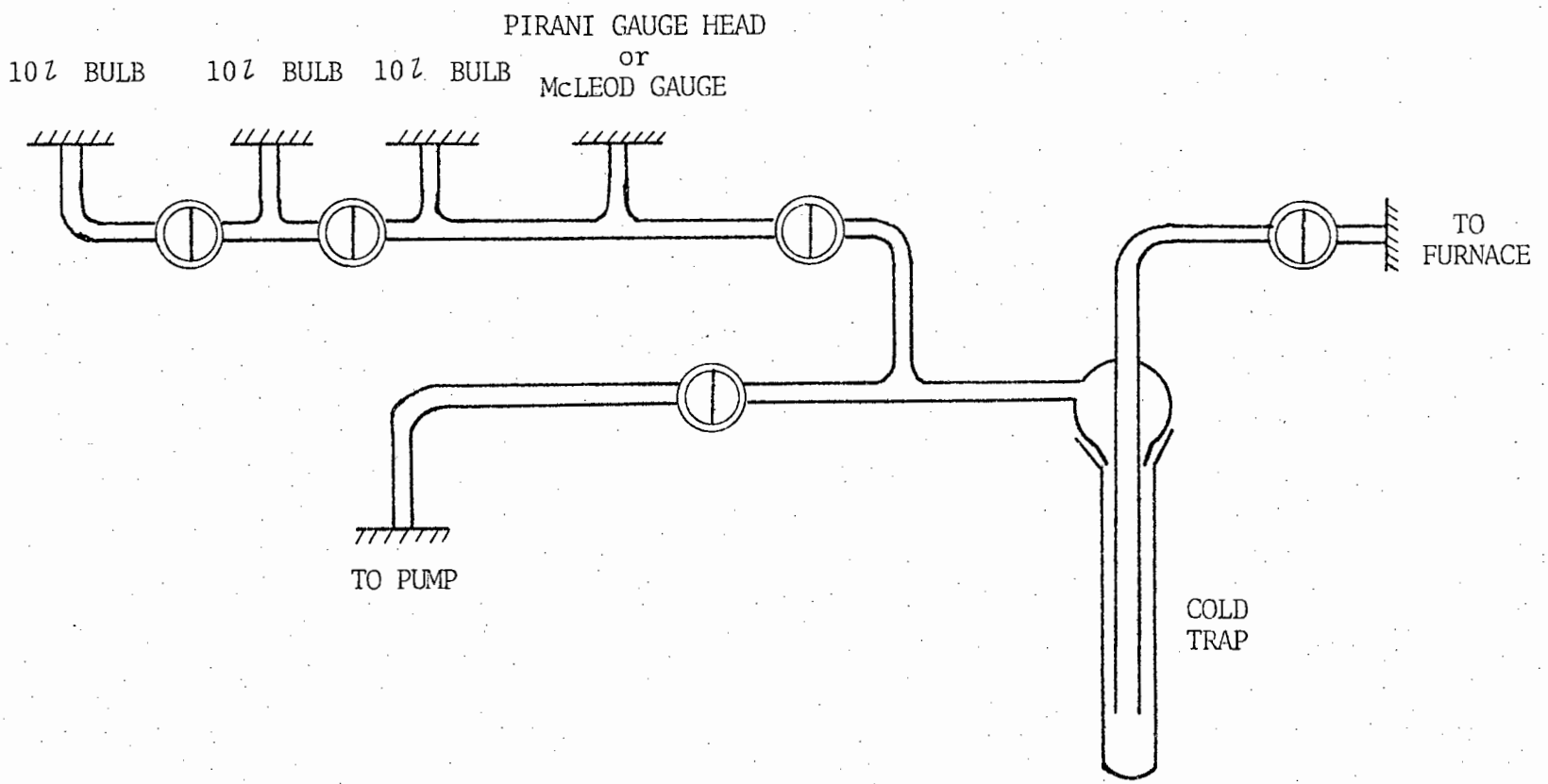

Fig. 2

Vacuum line used for decompositions.

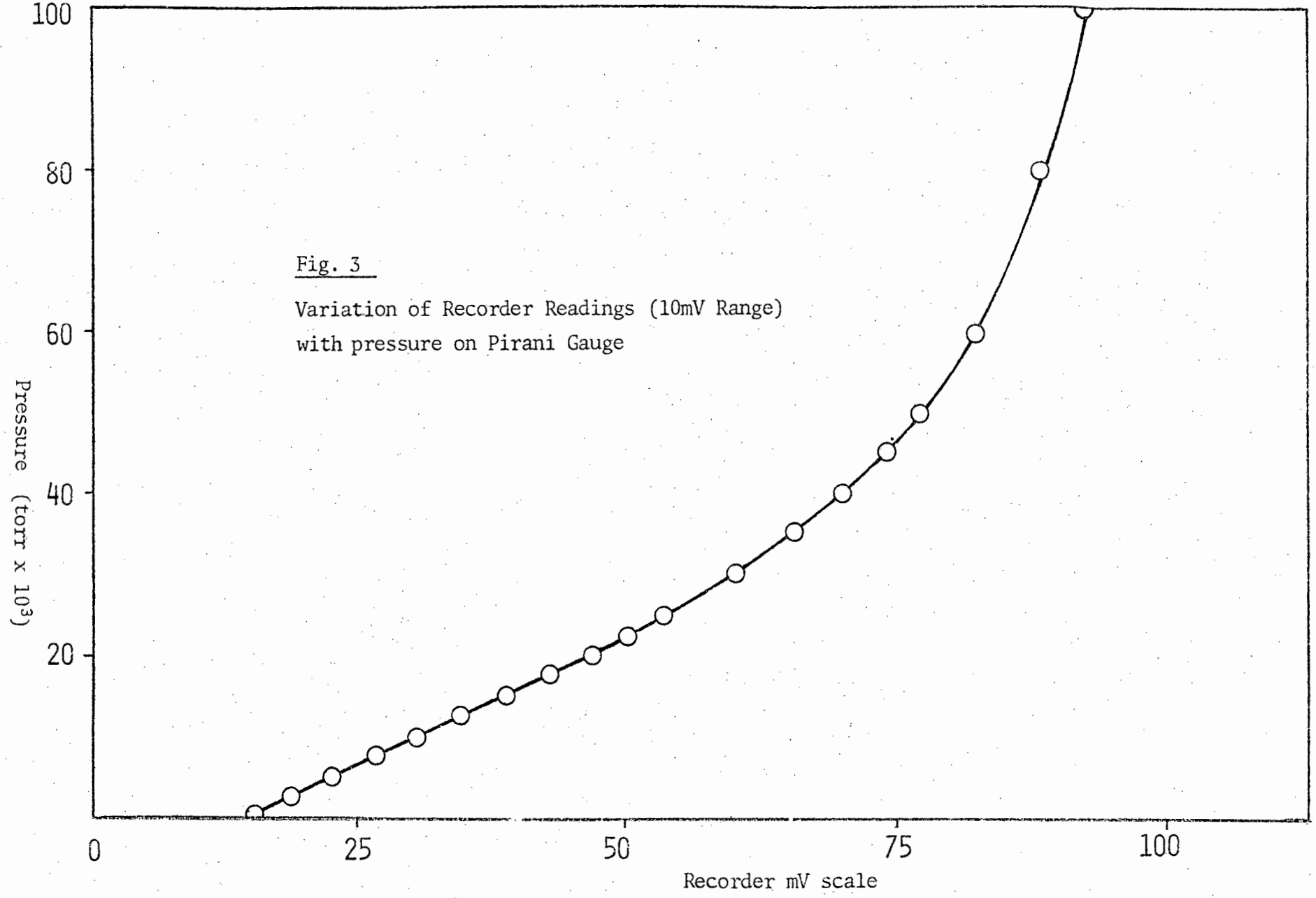

Fig. 3

Variation of Recorder Readings (10mV Range)
with pressure on Pirani Gauge

within the correct range for optimum accuracy. The bulbs were positioned so as to ensure that, when the rate of decomposition was at its maximum, the time required for pressure equilibration to take place throughout the large volume was negligible.

A quartz glass decomposition cell was used for all decompositions. The cell was specifically designed to fit exactly into the furnace used in the high temperature work. The cell was 80,0 mm in length and 18,0 mm in diameter. It was tapered over the bottom 10,0 mm to a diameter of 10,0 mm as shown in Fig. 4. A silica quartz cylinder 10,0 mm in height was glassblown on top of the cell with an inlet and outlet tube. This served as a water filter. The windows (upper and lower) of the cell were vitreosil optically polished quartz discs. The cell was attached to the line by means of a ball and socket joint with a neoprene ring.

(ii) TEMPERATURE CONTROL SYSTEMS

Two different systems were used in order to obtain accurate temperature control during decompositions. The high temperature system involved a furnace consisting of a solid cylindrical brass block (diameter 60 mm, height 90 mm) bored through the centre (19 mm diameter) and machined so as to accomodate exactly the decomposition cell. The outer surface of the brass cylinder was wound with nichrome wire and insulated with asbestos and plaster of paris. The furnace was mounted on a silver steel rod so that it could be moved freely in a vertical direction and swing freely in a horizontal plane. The cell fitted midway into the furnace and rested on a brass plug which was machined to the shape of the bottom of the cell. The furnace was held in position around the cell by means of a tapered pin (Fig. 4). The temperature was controlled by means of a CNS Versicon

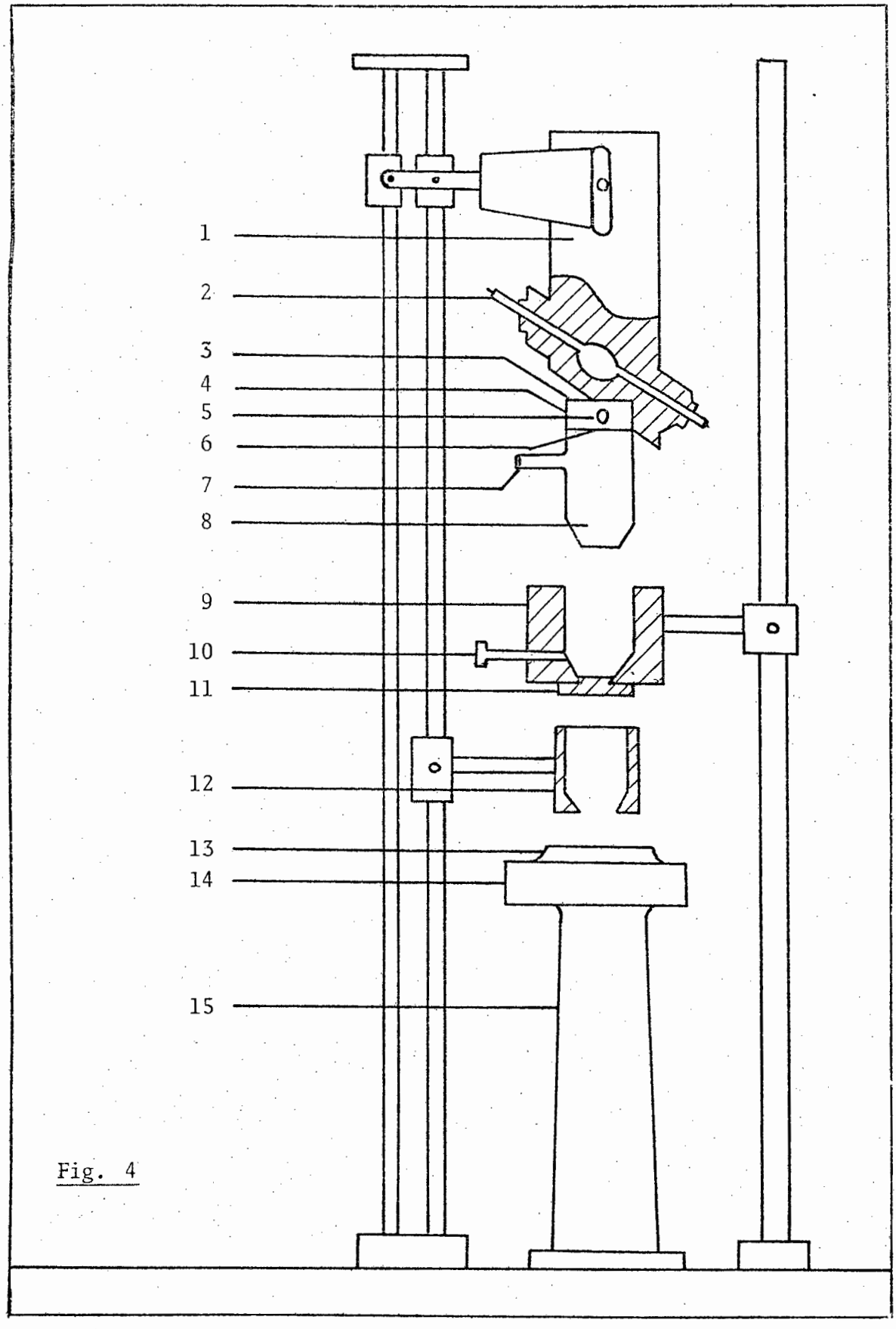

Fig. 4

Key to Fig. 4

Cross-sectional view of lamp housing, decomposition cell, furnace, cell holder for intensity determinations and perspex support for photometer detector.

1 Lamp housing
2 Ultraviolet lamp
3 Plane window
4 Water filter
5 Inlet flow of water through filter
6 Plane window
7 Ball and socket joint with neoprene ring
8 Decomposition cell
9 Furnace
10 Platinum resistance thermometer
11 Brass plug
12 Holder for cell for intensity measurements
13 Collar over window of detector
14 Photometer detector
15 Perspex support for photometer detector

Temperature Controller Type 101. This consisted of a source of electrical power for heating and a platinum resistance thermometer which was inserted into the side of the furnace so as to be as close as possible to the bottom of the decomposition cell. The temperature of the furnace was measured by a copper-constantan thermocouple placed in an evacuated pyrex cell identical in shape to the decomposition cell. The thermocouple was connected to a pre-calibrated Scalamp Thermocouple Galvanometer with a range of 0-300°C. The temperature was controlled in this manner to within ±0,5°C over the temperature range 0° - 200°C.

The low temperature system is illustrated in Fig. 5. The furnace used in the high temperature work was replaced by a 5 litre Dewar flask. Liquid nitrogen was passed through a copper coil inside the flask which was filled with absolute alcohol. Immersed in the flask was a stirrer which was operated by means of a belt driven by a variable speed induction motor. This stirrer was crucial in ensuring minimum fluctuations in temperature. The temperature was controlled by a sensitive temperature controller, the circuit of which is shown in Fig. 6. The sensor consisted of two G22 thermistors in parallel each having a resistance of 172Ω at 22°C. At temperatures above -70,0°C only one thermistor was required but both were connected for temperatures lower than -70,0°C. The control of the temperature was effected by means of an Alco 100RA solenoid valve which opened or closed according to the fluctuation in temperature. The temperature was measured by means of a -120° - 10°C thermometer immersed into the liquid so that the bulb was at the position normally occupied by the bottom of the decomposition cell. The temperature was monitored by means of a Thermocoax iron-constantan thermocouple connected to a Phillips PM 8100 flat-bed recorder. Attempts were made to measure the temperature by converting the emf to °C using appropriate tables, but this method was not found to be accurate. The degree of temperature

Fig. 5

Sectional view of Low Temperature Apparatus

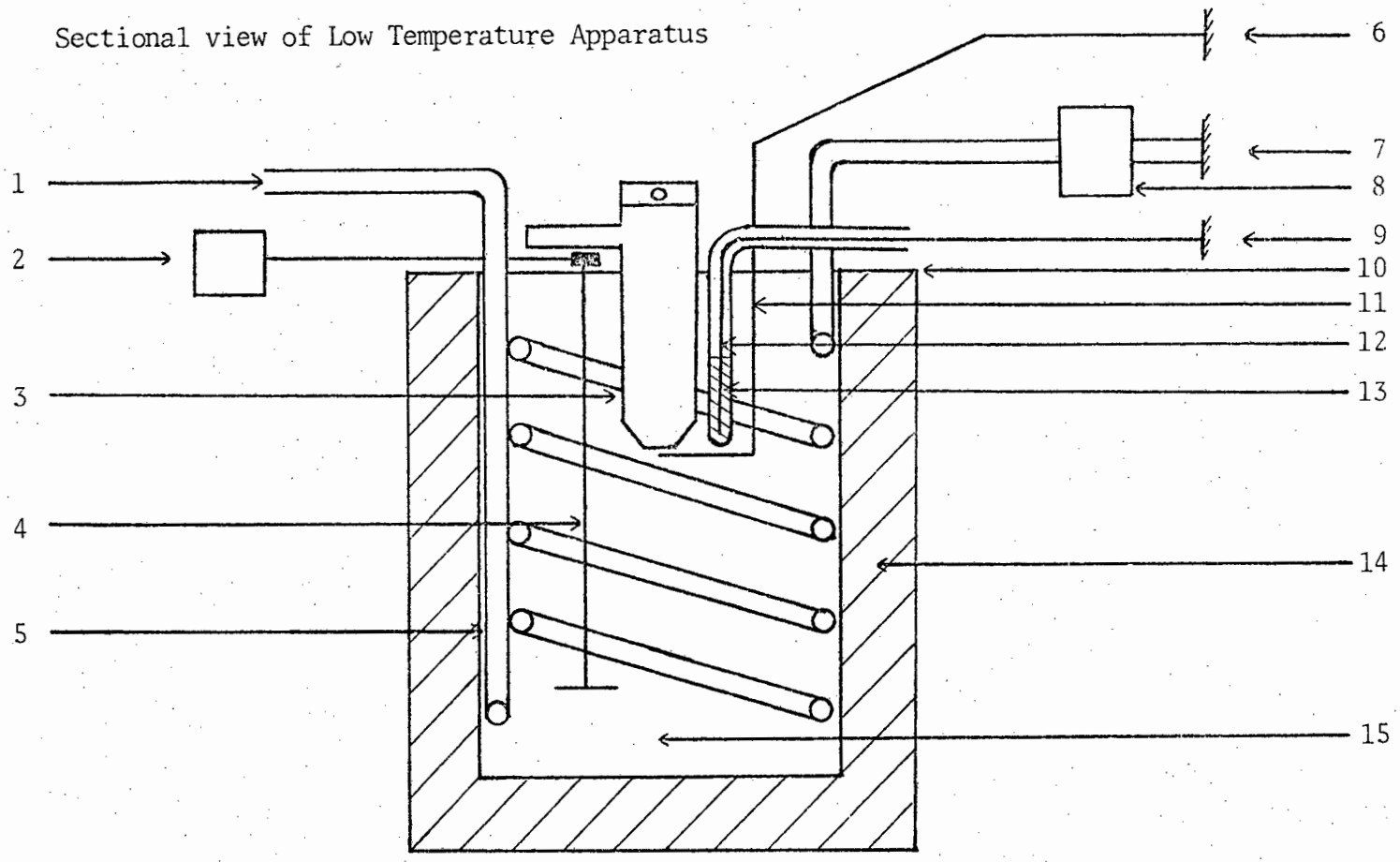

Key to Fig. 5

Low Temperature Apparatus

1 Outlet for liquid nitrogen

2 Induction Motor to drive stirrer

3 Decomposition cell

4 Stirrer

5 Copper coil through which liquid nitrogen passes

6 Thermocouple connected to recorder for monitoring temperature changes during decomposition

7 Liquid nitrogen supply feeding liquid nitrogen to copper coil via solenoid valve

8 Solenoid valve

9 Thermometer lead to circuit shown in Fig. 6

10 Thermocouple

11 Aluminium plate

12 Thermistor

13 Silicon grease in which thermistors are embedded

14 Dewar flask (volume 5 ℓ)

15 Flask filled with absolute alcohol.

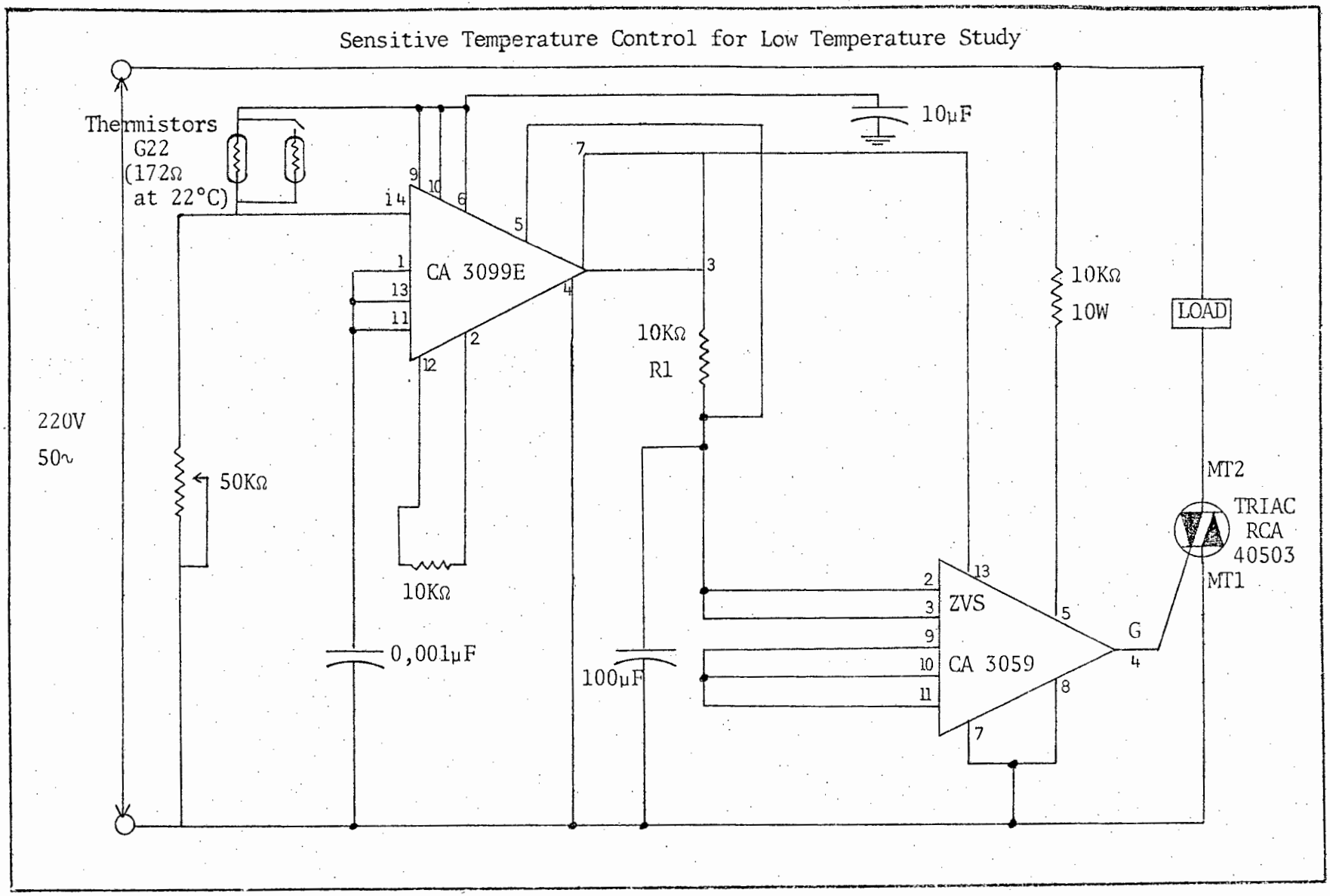
Sensitive Temperature Control for Low Temperature Study
Thermistors
G22
(172Ω
at 22°C)
10µF
CA 3099E
10KΩ
10W
LOAD
R1
220V
50∿
50KΩ
MT2
TRIAC
RCA
40503
MT1
10KΩ
ZVS
CA 3059
G
0,001µF
100µF

Fig. 6

control obtained was excellent and the temperature was accurate to well within ±0,5°C. The top of the flask was covered with a circular aluminium plate with the necessary apertures to allow entries for the various components. The cell was positioned as illustrated in the figure. The aluminium plate was attached to the flask in such a way as to achieve optimum insulation.

Temperatures in the range 5,0° - 20,0°C were controlled by using a Lauda K4R electronic cooler. Water at the required temperature was circulated through the copper coil in the same way as the liquid nitrogen was in the lower temperature range.

(iii) DECOMPOSITION AND MONITORING PROCEDURES

Different ultraviolet sources were used for the high temperature and low temperature work. The ultraviolet source used for ambient and high temperature photolysis and co-irradiation studies was a 100 W short arc mercury lamp. The power came from a Hanovia D.C. compact power supply. The luminous intensity of this lamp was 260 candelas with an efficacy of 22 lm/W. The lamp was housed in a copper pipe, 40 mm in diameter, in such a way that it was positioned at an angle of 45°. This was done to ensure that droplets of unvapourized mercury did not sit in the bowl of the lamp while it was in operation. The pipe was open to the air at the top and air holes were drilled into the pipe to facilitate cooling. The construction is illustrated in Fig. 4.

The low temperature photolysis studies were conducted with an HBO 200 W/4 super pressure mercury lamp using an HBO 200 W power supply. The luminous intensity of this lamp was 1000 candelas and it had an efficacy of 50 lm/W. This lamp was housed in a copper pipe similar to that used for the 100 W lamp but was positioned at an angle of 60° with the horizontal. In both cases an aluminized concave mirror was placed

approximately 50 mm above the centre of the lamp to reflect back any light propagated away from the sample. The above arrangement enabled the lamp to be brought within 5 mm of the decomposition cell. The intensity was varied by varying the distance of the lamp from the sample.

The intensity of the ultraviolet radiation was measured by using a "Photovolt" photometer, model 520A, incorporating a photomultiplier probe head. Accurate readings were facilitated by mounting a brass cylinder half the length of the furnace on a rack. This cylinder was capable of moving in the same manner as the furnace. The cylinder and rack were positioned by means of a tapered pin so that the bottom of the cylinder was then in the exact same position as the sample was during decomposition. The inside of the cylinder was machined to the shape of the decomposition cell, the aperture at the bottom being 5 mm in diameter this being the diameter of the bottom of the decomposition cell. The window of the detector (probe head) was covered with a brass collar machined to fit the brass cylinder so that the bottom of the decomposition cell fitted over the aperture in the collar when the detector was in position. Intensity readings were taken with the cell, under vacuum, surrounded by the brass cylinder. The probe head was supported under the cell by means of an accurately constructed perspex stand. The readings on the photometer were found to vary unduly if the opening of the shutter on the probe head was too large. It was also found necessary to store the probe head in a desiccator at all times. New lamps were used for all the activation energy determinations and studies of the variation of the rate of decomposition with intensity. Intensity measurements were made after each run.

Decompositions were carried out in the quartz decomposition cell attached to the line. The powdered sample was introduced into the cell

by means of a glass rod at the end of which was a carefully constructed trough designed to hold ≈2,0 mg. of the powder. In the case of lithium azide this process was carried out in a dry box and the cell sealed off until attached to the evacuated line. The vacuum line was pumped down until the minimum possible pressure was reached and then, after isolating the pump, the pressure was monitored for approximately 10 mins. to ensure the absence of leaks. The furnace, or the alcohol in the flask in the case of the low temperature studies, was preset at the desired temperature and then brought into position around the cell. The shutter separating the lamp housing from the decomposition cell was closed and the ultra-violet lamp switched on. At least fifteen minutes were allowed for the lamp to warm up to its maximum intensity and for the sample to attain the temperature of the furnace or alcohol. The suction was then opened and decomposition commenced. The pressure was monitored by a Pirani gauge coupled to a recorder in the case of powders and by a McLeod gauge in the case of pellets. The Pirani was used together with the McLeod gauge for pellet runs for the purpose of measuring the induction period. During the course of decomposition the liquid nitrogen around the cold trap was kept at a constant level by means of an automatically controlled feeding device incorporating a solenoid valve and a thermistor. The latter was fixed at 20 mm below the top of the Dewar flask surrounding the trap. The light intensity was measured at the end of each run. The cell was cleaned by using a dilute solution of hydrofluoric acid. It was then rinsed with distilled water and acetone and pumped dry. The procedures involved in interrupting a decomposition and admitting water vapour onto the salt are discussed in section 9.

(iv) PREPARATION OF HYDRAZOIC ACID

Hydrazoic acid was prepared by an ion exchange process using "Analar" cationic resin viz. Permutit "Zeo-karb" 225 (SRC 13) cation exchange resin. Impurities were removed from the column by alternate washings with 2M HCl and 2M NaOH, and washing with glass distilled water between each acid or alkali washing. The resin was converted to the H^+ form by passing two bed volumes of 2M HCl through the column followed by six bed volumes of glass distilled water. 500 ml. of a 10% solution of B.D.H. "Analar" grade sodium azide was then passed through the bed of resin followed by 400 ml. of glass distilled water. The middle portion of the eluent was collected and found to be an approximately 3% solution of hydrazoic acid. Ferron reagent and flame photometry tests indicated the absence of ions of sodium or iron.

(v) PREPARATION OF THE AZIDES

The barium azide and strontium azide used in this study were taken from samples prepared two years prior to this work. The method whereby it was prepared is described in reference 50. It had been stored in vacuo over P_2O_5.

Calcium and lithium azides were prepared in a similar manner to the above azides. To a slurry of approximately 10,0 g of the hydroxide of calcium or lithium (A.R.), was added 3% hydrazoic acid until the solution was acidic to phenolphthalein. The colour was pale orange with a small amount of precipitate present. All indicator tests were performed externally. The solution was transferred to a Rotavapor immersed in a water bath at 60,0°C. Hydrazoic acid was continually added in order to ensure that the solution was acidic. When the solution had been reduced to a slurry, the latter was transferred to an evaporating dish and placed

in an oven at 45°C. Dry air was allowed to bleed through the oven to a vacuum pump. In the case of calcium azide clear white crystals were formed and in the case of lithium azide two separate preparations produced clear white crystals and straw coloured crystals respectively. The former batch alone was used. The crystals were then pumped to dryness, in a blackened desiccator, over P_2O_5. The P_2O_5 was regularly replaced and the desiccator pumped down regularly. The lithium azide was very hygroscopic and was handled at all times in a dry box under a positive pressure of dry air. The desiccator was placed in the box and pumped down continuously.

(vi) GRINDING AND PELLETING PROCEDURES

In order to obtain powders of the various azides small quantities of the crystals were ground for 5 min. in a grindex using an agate capsule and a nylon ball. The resulting powder was passed through a selection of Endecott test sieves. The powder between mesh size 63μ and 125μ was collected and stored over P_2O_5 in a black vacuum desiccator. This whole procedure was carried out inside a dry box in the case of lithium azide. The sieved powder was placed in an evacuable KB-R die. The die was evacuated for 10 min. and then a pressure of 2000 lb./sq.in. was applied for 15 min. by a 10 ton Apex Type 341/4 hydraulic press. The resulting pellets were 5 mm in diameter and 0,25 mm thick.

9 RESULTS

Decompositions of the various azides are divided into two categories i.e. photolytic decompositions (photolysis), which take place at temperatures below those at which a dark rate can be detected, and co-irradiated decompositions, which take place at temperatures where dark rate is observed. In the case of calcium azide co-irradiation commences at about 105,0°C and in the case of lithium azide at above 180,0°C.

Photolytic decompositions at low temperatures i.e. from below -70,0° – 30,0°C were carried out on calcium, strontium, barium and lithium azides. At temperatures higher than these only calcium and lithium azides were studied, the former in powder and pellet form and the latter in powder form only.

The variables plotted in the decomposition diagrams are α and time where $\alpha = p/p_f$ (p = pressure at time t and p_f = observed final pressure). In some instances the final pressure used in the calculations was other than that observed.

Throughout this study powder refers to material of particle size ranging from 63μ to 125μ. Pelleted material is powder pressed at 1500 lb./sq.in. (or in some instances 2000 lb./sq.in.) in a 5 mm die for approximately 10 minutes whilst simultaneously evacuating the die. For all powder decompositions ±2,0 mg of compound was used and in the manufacture of pellets ±8,0 mg of powdered material was used resulting in pellets 5,0 mm in diameter and 0,25 mm thick. Percentage decompositions were calculated assuming the equations for decomposition to be $M(N_3)_2 \rightarrow M + 3N_2$ for barium, strontium and calcium azides where M represents the metal and $2LiN_3 \rightarrow 2Li + 3N_2$ for lithium azide. Intensity units are arbitrary and are only comparable in a particular set of runs.

(i) PHOTOLYSIS OF POWDERED CALCIUM AND LITHIUM AZIDES AT AMBIENT AND HIGHER TEMPERATURES

The photolysis of calcium azide was studied in the temperature range 35,0° – 95,0°C as no dark rate was detected in this temperature range and hence it could be safely assumed that the thermal effects were negligible. Similarly the photolysis of lithium azide was studied in the range 24,0° – 170,0°C for the same reasons. In the latter case the thermal effects, as shown by the thermal decomposition of lithium azide at 180°C, were considerable but the photolytic decompositions in this temperature range were completed in a time shorter than the induction period of the thermal decomposition. For this reason it was not found possible to make a study of the co-irradiation of lithium azide. The percentage decomposition for calcium azide was 90,0% and for lithium azide 77,9%.

(i.a) Reproducibility

In the case of both calcium and lithium azides large particles or even those ground in a grindex gave irreproducible results. Crystals of calcium azide were ground in a grindex and then seived between seives of mesh size 63μ and 125μ. The powder thus obtained yielded reproducible results. In the case of lithium azide, the compound was found to be extremely hygroscopic and it was necessary to handle the salt at all times in a dry box which was under positive pressure from air which had initially passed through phosphorus pentoxide, calcium chloride and silica gel. Initially the method of grinding and pelleting set out by Liddiard[174] was used in which the ground powder was pelleted and re-ground. It was later found, however, that equally good reproducibility was obtained when the powder was ground and sieved in a manner identical to that described for

calcium azide. The reproducibility of calcium azide was tested by analyzing three successive photolytic decompositions at a temperature of 75°C and an intensity of 24 units. The sets of curves in which α is plotted against time were superimposed and satisfactory reproducibility was obtained. The three superimposed curves are shown in Fig. 7. In a similar manner the reproducibility of lithium azide powder was tested by analyzing three successive photolytic decompositions at temperatures of 30°C and 127°C and light intensities of 37 units and 35 units respectively. As in the case of calcium azide the three plots of α against time in each set were superimposed and the resulting curves are shown in Fig. 8 and 9. As can be seen, satisfactory reproducibility was obtained. The rate constants for calcium azide are tabulated in Table 1 and those for lithium azide in Table 2. In both cases the Avrami-Erofeyev equation with n = 2 was used for the acceleratory period and the unimolecular law was used for the decay period. The applicability of these equations and the determination of the final pressures will be discussed in the next section. The above conditions with respect to size and handling of powder were adhered to in all subsequent tests since they were found to yield reproducible results.

It will be observed from a study of the tables showing reproducibility constants as well as the figures illustrating the reproducibility of the photolysis of calcium and lithium azides, that the induction period is not as reproducible as are the values of k_{acc} and k_{decay}. This was found to be especially so at lower temperatures. Nevertheless, throughout this work, analyses are always made of the induction periods if only to to illustrate, in some instances, the irreproducibility of this part of the decomposition process. Clearly results obtained from sets of experiments, in which the analysis of the induction period indicates considerable irreproducibility, should be treated with caution.

Table 1 Reproducibility constants for the photolysis of calcium azide powder

Temperature °C	Intensity Units	Induction Period min.	$k_{acc} \times 10^2$ min^{-1}.	$k_{decay} \times 10^2$ min^{-1}.
75,0	24	6,80	3,45	3,29
		5,40	3,58	3,33
		5,30	3,75	3,32

Table 2 Reproducibility constants for the photolysis of lithium azide powder

Temperature °C	Intensity Units	Induction Period min.	$k_{acc} \times 10^2$ min^{-1}.	$k_{decay} \times 10^2$ min^{-1}.
30,0	37	3,60	11,70	5,60
		3,00	12,00	5,50
		4,40	12,40	5,80
127,0	35	0,90	6,40	2,00
		0,90	6,30	1,70
		1,00	6,10	1,80

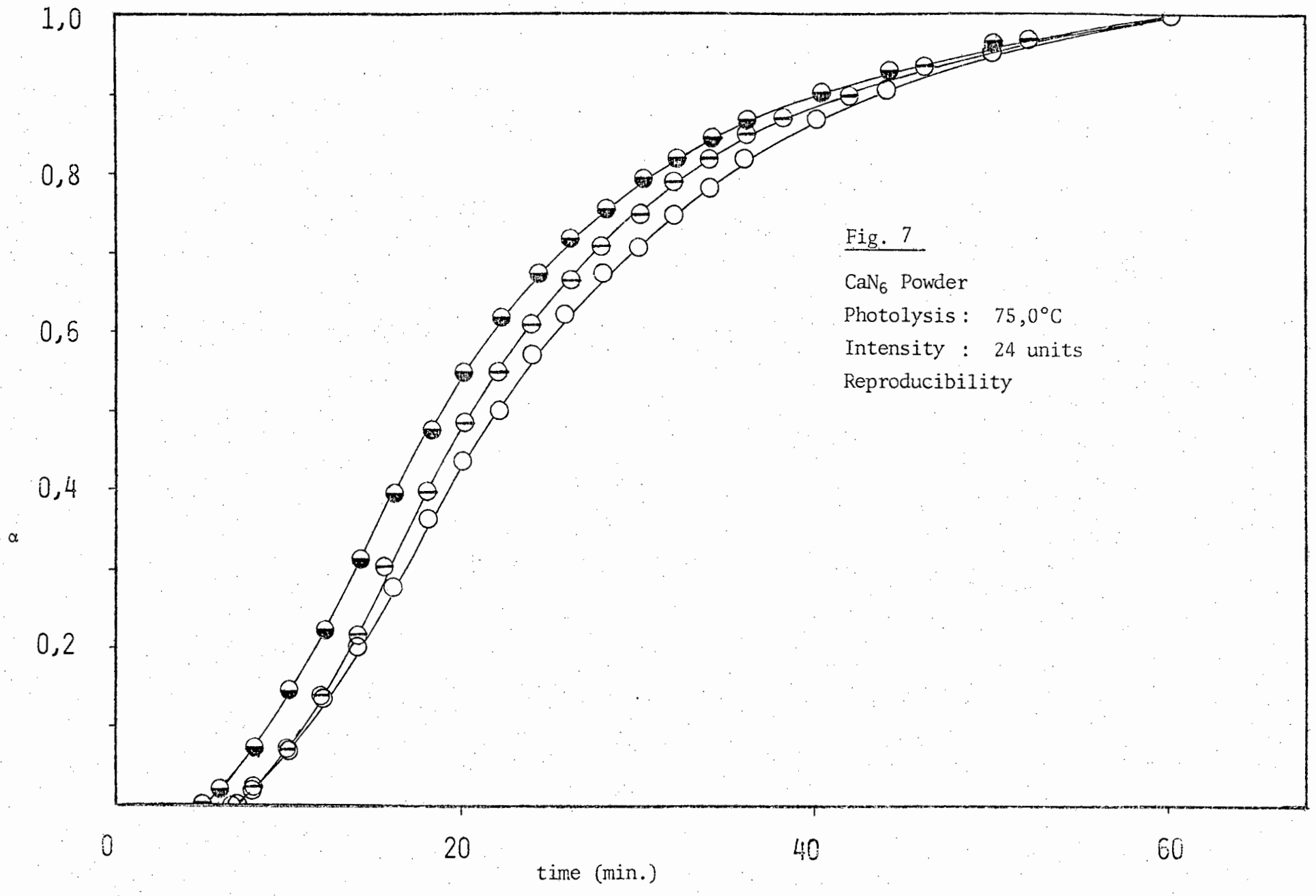

Fig. 7

CaN_6 Powder
Photolysis : 75,0°C
Intensity : 24 units
Reproducibility

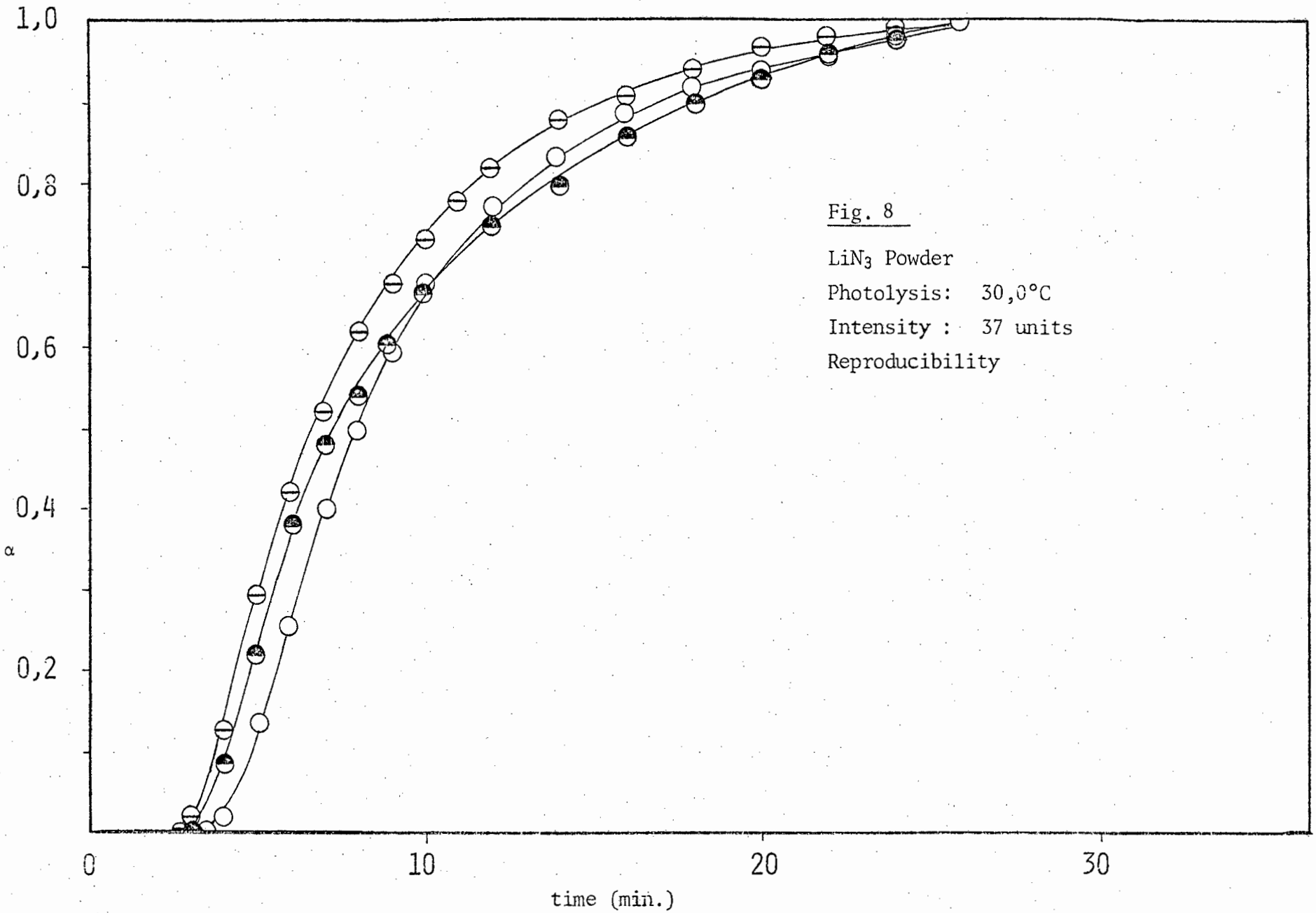

Fig. 8

LiN_3 Powder
Photolysis: 30,0°C
Intensity : 37 units
Reproducibility

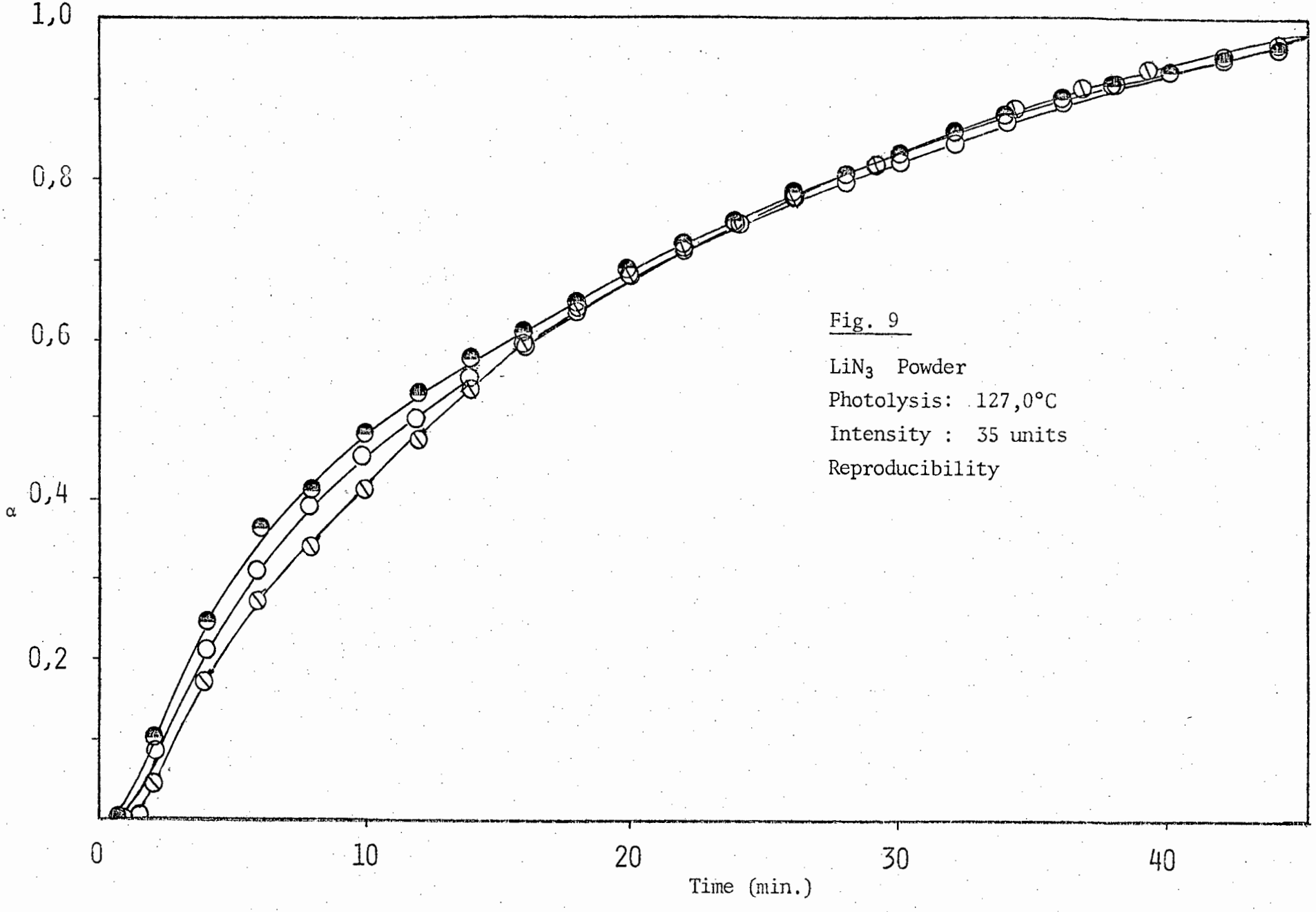

Fig. 9

LiN_3 Powder
Photolysis: 127,0°C
Intensity : 35 units
Reproducibility

In all mathematical analyses where slopes of graphs had to be determined, a least squares method was used whereby slope and intercept were obtained.

(i.b) Mathematical Analyses

Photodecomposition curves of calcium azide in the temperature range 35,0°- 95,0°C showed a well defined induction period during which there was no evolution of gas. There then followed an acceleratory period and a decay period. The inflection point occurred in the region of $\alpha = 0,35$.

No mathematical analysis of the induction period was possible since there was no measurable evolution of gas. For purposes of comparison, however, the inverse of the duration of the induction period i.e. the time taken for the reaction to reach $\alpha = 0,01$ was used as a rate constant.

The acceleratory reaction was described by the Avrami-Erofeyev equation with n = 2

$$\text{i.e.} \quad [-\log(1-\alpha)]^{\frac{1}{2}} = k_{acc}t + c \qquad \alpha = p/p_f.$$

This equation fitted the curve in the region $0,01 < \alpha < 0,35$.

The decay reaction was analyzed using the unimolecular law

$$\text{i.e.} \quad -\log(1-\alpha) = k_{decay}t + c \qquad \alpha = p/p_f \ .$$

This equation fitted the curve in the region $0,35 < \alpha < 0,90$.
A typical α vs t curve for the photolysis of calcium azide powder, with mathematical analyses, at a temperature of 75°C and light intensity of 24 units is shown in Fig. 10.

The photolytic decomposition of lithium azide in the temperature range 25° – 170°C showed the same characteristics as that of calcium azide powder. An induction period was present which was followed by a definite acceleratory period and finally a decay period. The decay period was found

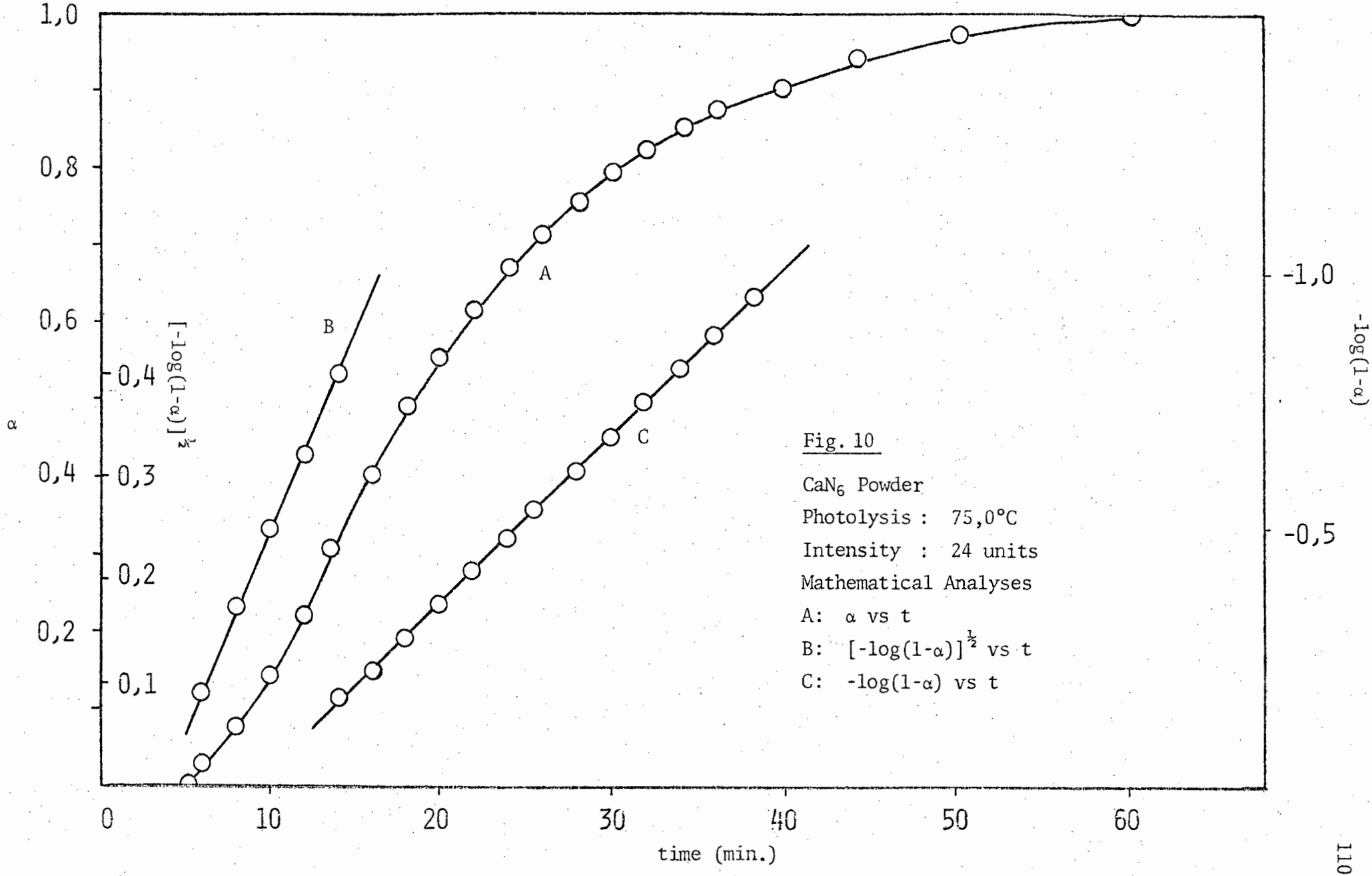

Fig. 10

CaN_6 Powder
Photolysis : 75,0°C
Intensity : 24 units
Mathematical Analyses
A: α vs t
B: $[-\log(1-\alpha)]^{\frac{1}{2}}$ vs t
C: $-\log(1-\alpha)$ vs t

to be very protracted particularly at lower light intensities. The kinetic equations which were tested were the Avrami-Erofeyev equation, the Prout-Tompkins equation, the contracting sphere equation, the exponential laws of acceleration and the unimolecular decay equations, including the power laws of acceleration and decay. The Avrami-Erofeyev equation with n = 2 was found to fit the acceleratory reaction. The prolonged decay period presented a problem regarding the value of the final pressure to be used in normalizing the pressures. By using the observed final pressure, even after a prolonged period, no highly satisfactory fit of equation could be obtained. This necessitated estimating a value of the final pressure. This estimated value was given the value p'_f as opposed to the observed final pressure p_f. The estimated value was obtained by plotting the pressure-time curve on graph paper using a compressed scale on the time axis and then tapering off the decay period at a point where α had a value of approximately 0,90. This method is illustrated in Fig. 11. Care had to be taken that in analyzing a series of runs this estimation of p'_f was done in as highly reproducible a manner as possible. Using this estimated value of the final pressure the Avrami-Erofeyev equation with n = 2 (where $\alpha = p/p'_f$) was found to fit the acceleratory period in the region $0,01 < \alpha < 0,25$. This represented no change from the analysis of the acceleratory period using the observed final pressure. The decay reaction was analyzed using the unimolecular decay law as in the case of calcium azide except that $\alpha = p/p'_f$ in the case of lithium azide. This equation was found to fit the decay period in the region $0,25 < \alpha < 0,90$. The inflection point thus occurred at $\alpha = 0,25$. Of particular interest in analyzing the decay period was the equation

$$\frac{1}{(-\log \alpha)} = kt$$

which had been used by Prout and Sears in a previous study of lithium azide[74]. Ultimately the unimolecular law was found to fit equally well and was used in the analyses for the sake of consistency in view of the fact that Prout and Shephard[50] had used it in the analysis of barium and strontium azides and that it had been found to fit calcium azide in the present study.

The protracted decay reaction remained a source of interest, however, and a study was made of this part of the reaction using the split-run technique. The methods involved and the results obtained in this study will be discussed in the next section. The unimolecular law was also used in the analysis of the split-runs. In the plots shown of α vs t in the case of lithium azide the values of α were obtained using the observed final pressure and not the estimated final pressure.

Typical α vs t curves of the photolysis of lithium azide powder, with mathematical analyses at temperatures of 30°C and 127°C and light intensities of 37 units and 35 units respectively are shown in Fig. 11 and 12. Curve A shows a plot of α vs t ($\alpha = p/p_f$). The position in the decay reaction where the final pressure was estimated is indicated on this curve (p'_f). Curve B is a plot of the Avrami-Erofeyev equation ($n = 2$) against time with p_f, the observed final pressure, being used in the equation. Curve B' shows a plot of the same equation except that p'_f was used as the final pressure value. Curves C and C' are plots of the unimolecular law against time. C was obtained by using the observed final pressure p_f in the equation while the curve C' was obtained by using the estimated final pressure p'_f. Thus for the determination of all rate constants for the photolytic decompositions of lithium azide powder, a final pressure p'_f was estimated.

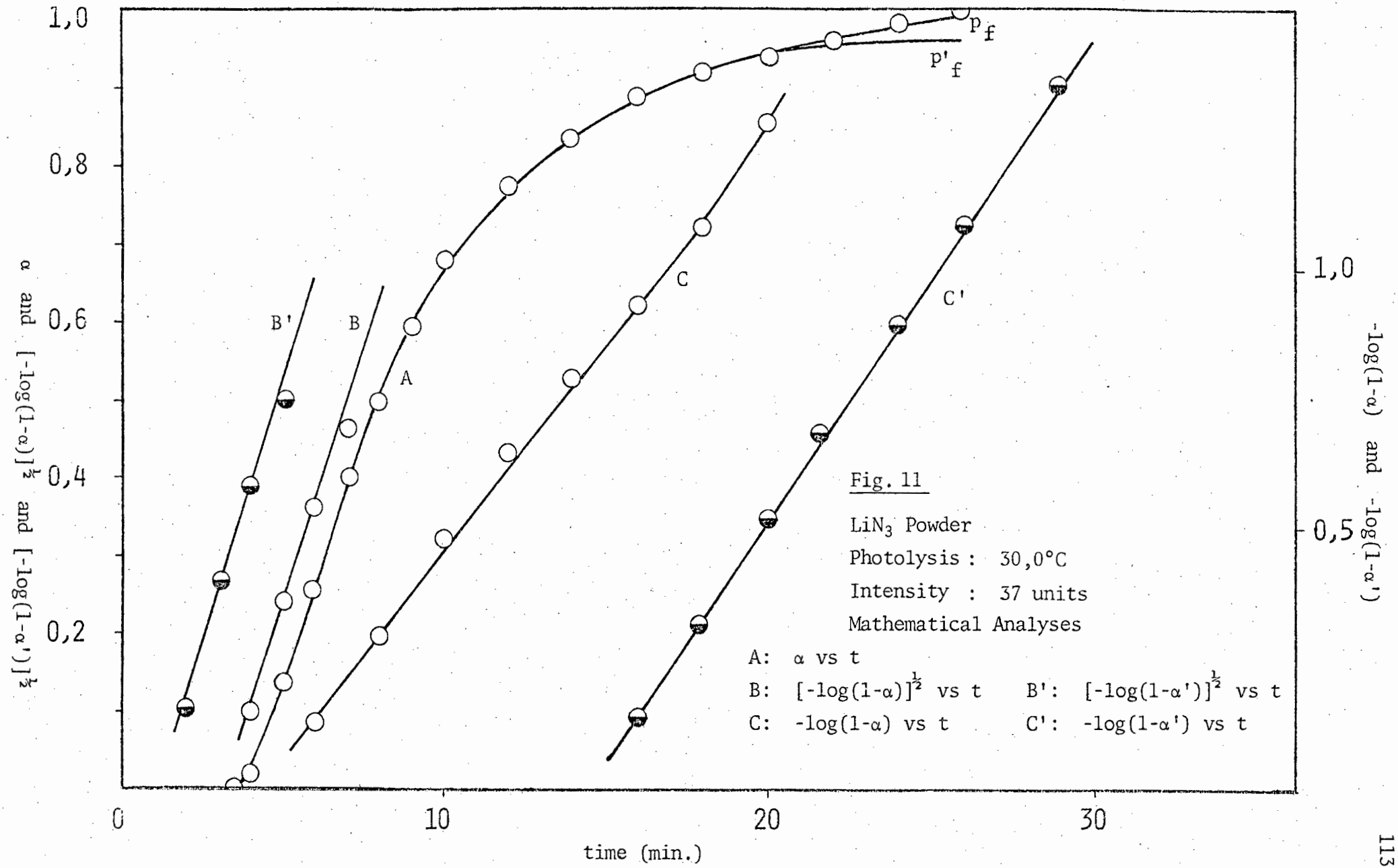

Fig. 11

LiN_3 Powder
Photolysis : 30,0°C
Intensity : 37 units
Mathematical Analyses

A: α vs t
B: $[-\log(1-\alpha)]^{\frac{1}{2}}$ vs t B': $[-\log(1-\alpha')]^{\frac{1}{2}}$ vs t
C: $-\log(1-\alpha)$ vs t C': $-\log(1-\alpha')$ vs t

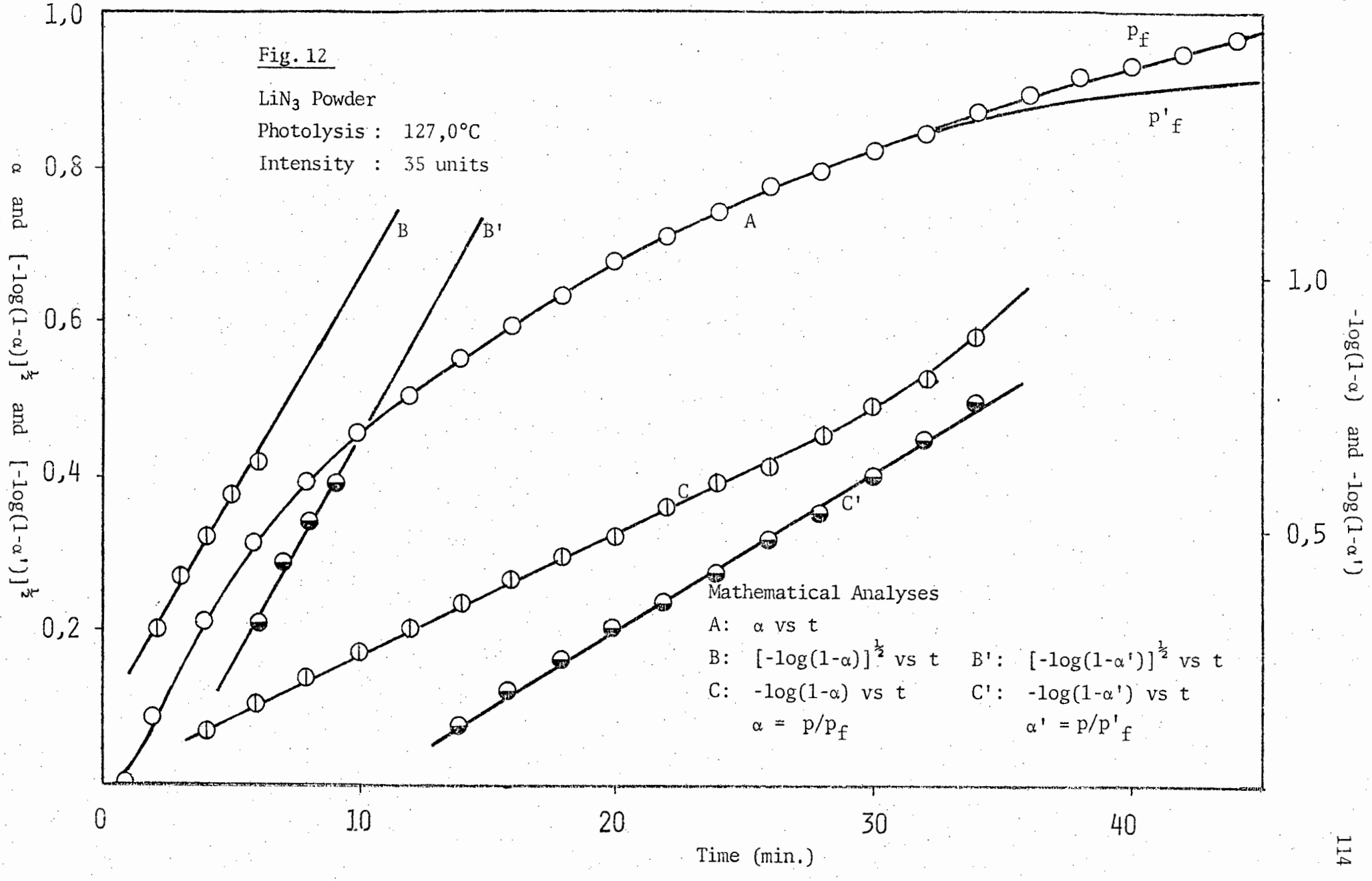
Fig. 12
LiN3 Powder
Photolysis : 127,0°C
Intensity : 35 units
α and [-log(1-α)]½ and [-log(1-α')]½
-log(1-α) and -log(1-α')
Time (min.)
1,0
0,8
0,6
0,4
0,2
0,5
0
10
20
30
40
A
B
B'
C
C'
pf
p'f
Mathematical Analyses
A: α vs t
B: [-log(1-α)]½ vs t
B': [-log(1-α')]½ vs t
C: -log(1-α) vs t
C': -log(1-α') vs t
α = p/pf
α' = p/p'f

(i.c) Evaluation of Activation Energies

Activation energies for calcium and lithium azides were obtained by decomposing samples at various temperatures in the photolytic temperature range. The light intensity was kept at a constant value throughout the determination. In order to obtain the critical increment of the process(es) occurring during photolysis, the Arrhenius equation was applied. For the induction period the logarithm of the reciprocal of the induction period was plotted against $10^3/T$, and for the acceleratory and decay reactions the logarithms of k_{acc} and k_{decay} respectively were plotted against $10^3/T$ where T is the temperature of decomposition in K.

A constant light intensity of 24,0 units was chosen for calcium azide and a value of 35,0 units for lithium azide for the determination of rate constants throughout the respective temperature ranges.

In the case of calcium azide it was found that a change occurred in the activation energy at 60,0°C and activation energies were calculated separately for the 35,0 - 60,0°C amd 60,0 - 95,0°C ranges. For lithium azide the change in activation energy occurred at 71,8°C and thus activation energies were calculated in the ranges 24,6° - 71,8°C and 71,8° - 170°C.

As already mentioned the photolytic decomposition of lithium azide was extremely rapid at the temperature of 170,0°C and for this reason the possibility of co-irradiation was disregarded. Fig. 13 illustrates the difference between the thermal decomposition and photolysis of lithium azide at 180°C. The decomposition curves shown in this figure indicate clearly that at this temperature thermal effects are negligible.

Table 3 gives the rate constants for calcium azide and Table 4 those for lithium azide. The activation energies for the photolysis of calcium azide are shown in Table 5 and the activation energies for the photolysis of lithium azide in Table 6.

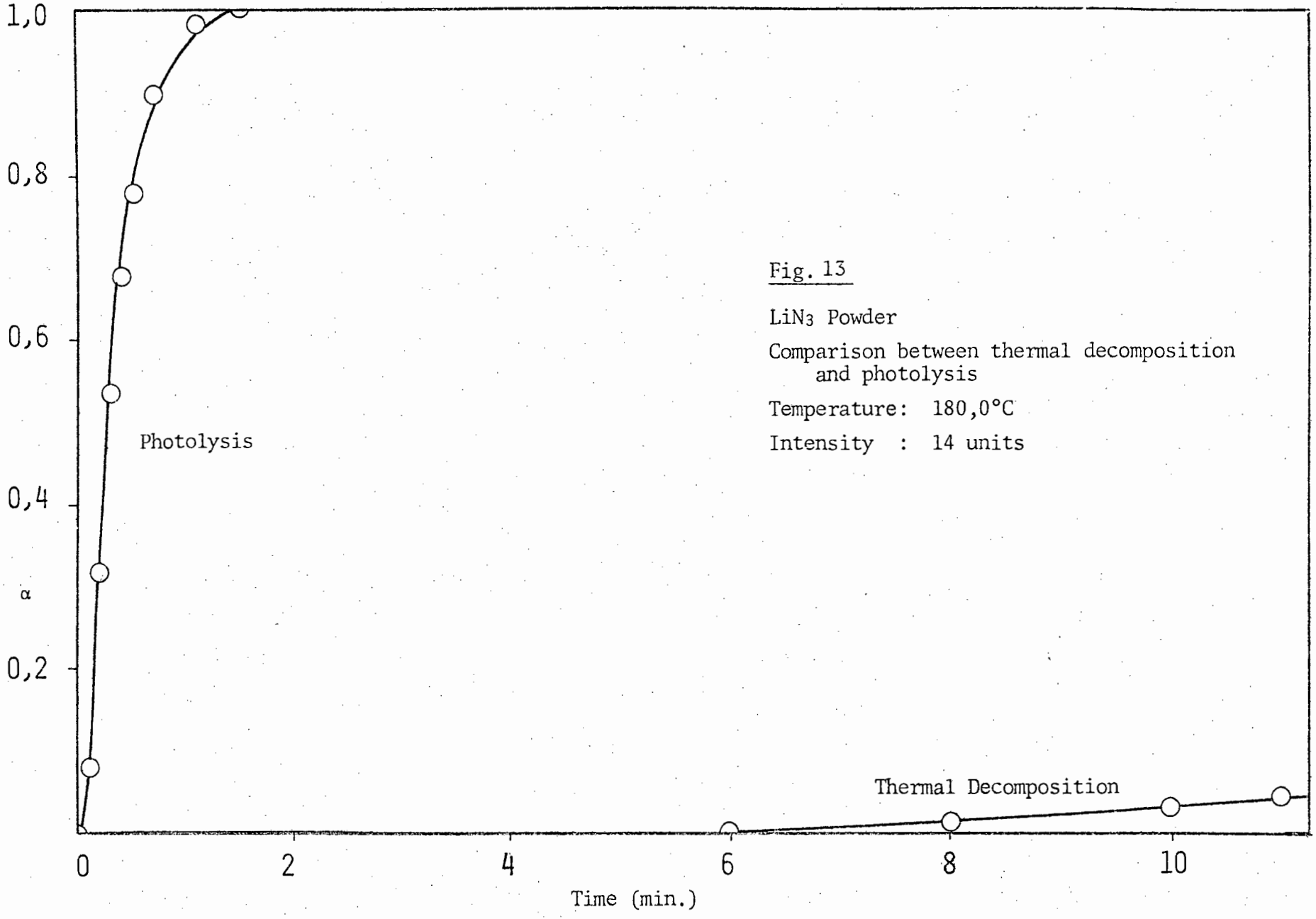

Fig. 13

LiN_3 Powder

Comparison between thermal decomposition and photolysis

Temperature: 180,0°C

Intensity : 14 units

Table 3 Rate constants for the photolysis of calcium azide powder

Temperature range: 35,0° - 95,0°C

Light intensity : 24 units

Temperature °C	Induction Period min.	$k_{acc} \times 10^2$ min^{-1}.	$k_{decay} \times 10^2$ min^{-1}.
35,0	52,0	0,85	0,44
40,0	31,8	1,05	0,59
45,0	31,0	1,50	0,60
50,0	21,5	1,62	0,74
55,0	25,5	1,77	0,68
60,0	16,6	2,20	0,88
65,0	11,7	2,80	1,30
70,0	12,0	4,10	2,20
75,0	8,0	5,20	3,00
80,0	7,0	6,50	3,20
85,0	6,0	7,70	5,40
90,0	4,0	8,90	7,90
95,0	3,5	14,70	11,40

Table 4 Rate constants for the photolysis of lithium azide powder

Temperature range: 24,6° - 170,0°C

Light intensity : 35 units

Temperature °C	Induction Period min.	$k_{acc} \times 10^2$ min^{-1}.	$k_{decay} \times 10^2$ min^{-1}.
24,6	13,8	1,61	0,56
33,2	16,0	1,70	0,48
44,8	6,0	2,36	1,10
53,5	9,0	2,67	1,19
60,0	5,8	3,13	1,06
66,0	3,6	4,72	1,53
71,8	4,0	3,43	1,44
76,2	2,8	4,32	1,18
82,5	1,6	5,08	1,55
88,1	3,8	6,12	1,87
90,0	1,85	8,04	2,02
95,2	1,6	8,34	2,24
100,2	1,0	10,00	3,02
101,0	1,4	10,81	3,08
106,0	0,7	13,00	3,10
112,2	0,75	15,14	6,14
117,2	1,0	17,86	12,25
134,8	0,32	33,81	16,48
146,5	0,12	42,95	19,10
153,0	0,06	60,26	21,93
158,0	0,07	54,95	36,22
164,0	0,06	65,77	26,06
170,0	0,05	90,99	48,19

Table 5 Activation energies for the photolysis of calcium azide powder

Intensity : 24 units

Temperature Range °C	Induction Period Kcal./mol.	Acceleratory Period Kcal./mol.	Decay Period Kcal./mol.
35,0 - 60,0	7,78	7,30	4,67
60,0 - 95,0	10,80	12,52	17,36

Table 6 Activation energies for the photolysis of lithium azide powder

Intensity : 35 units

Temperature Range °C	Induction Period Kcal./mol.	Acceleratory Period Kcal./mol.	Decay Period Kcal./mol.
24,6 - 71,8	6,10	4,20	3,20
71,8 - 170,0	11,50	9,90	11,60

The plots of -log I.P., log k_{acc}, and log k_{decay} against $10^3/T$ in the various temperature ranges for the photolysis of calcium azide are shown in Fig. 14-16. The corresponding plots for the photolysis of lithium azide are shown in Fig. 17-20.

A split-run study was made of the decay reaction in the photolysis of lithium azide. With this method the decomposition was allowed to proceed at the lowest temperature at which the first rate constant was to be calculated. After an appropriate time the run was interrupted by shutting off the ultraviolet radiation and removing the furnace from the sample. The temperature of the furnace was then adjusted to a higher temperature while the sample was allowed to cool to room temperature. When the furnace had reached the new temperature it was replaced in position around the decomposition cell and photodecomposition was started after the sample had been given 5 minutes in which to reach the temperature of the furnace. Five or six rate constants could be found for the decay reaction using one sample of lithium azide powder.

Before the split-run technique was used to determine the activation energy, it was necessary to ensure that the interruption in the run had no subsequent effect on the photolytic decomposition of the compound. To this end a decomposition was allowed to proceed to a certain point and then interrupted in the manner described in the previous paragraph. It was found that the subsequent reaction continued as though no interruption had taken place.

The activation energy for the decay reaction in the photolysis of lithium azide powder was thus determined. The range of temperatures over which the rate constants were calculted was 55,0° - 126,6°C and a light intensity of 35,0 units was used. The change in the activation energy was found in the region of 78,0°C. Table 7 gives the rate constants for the

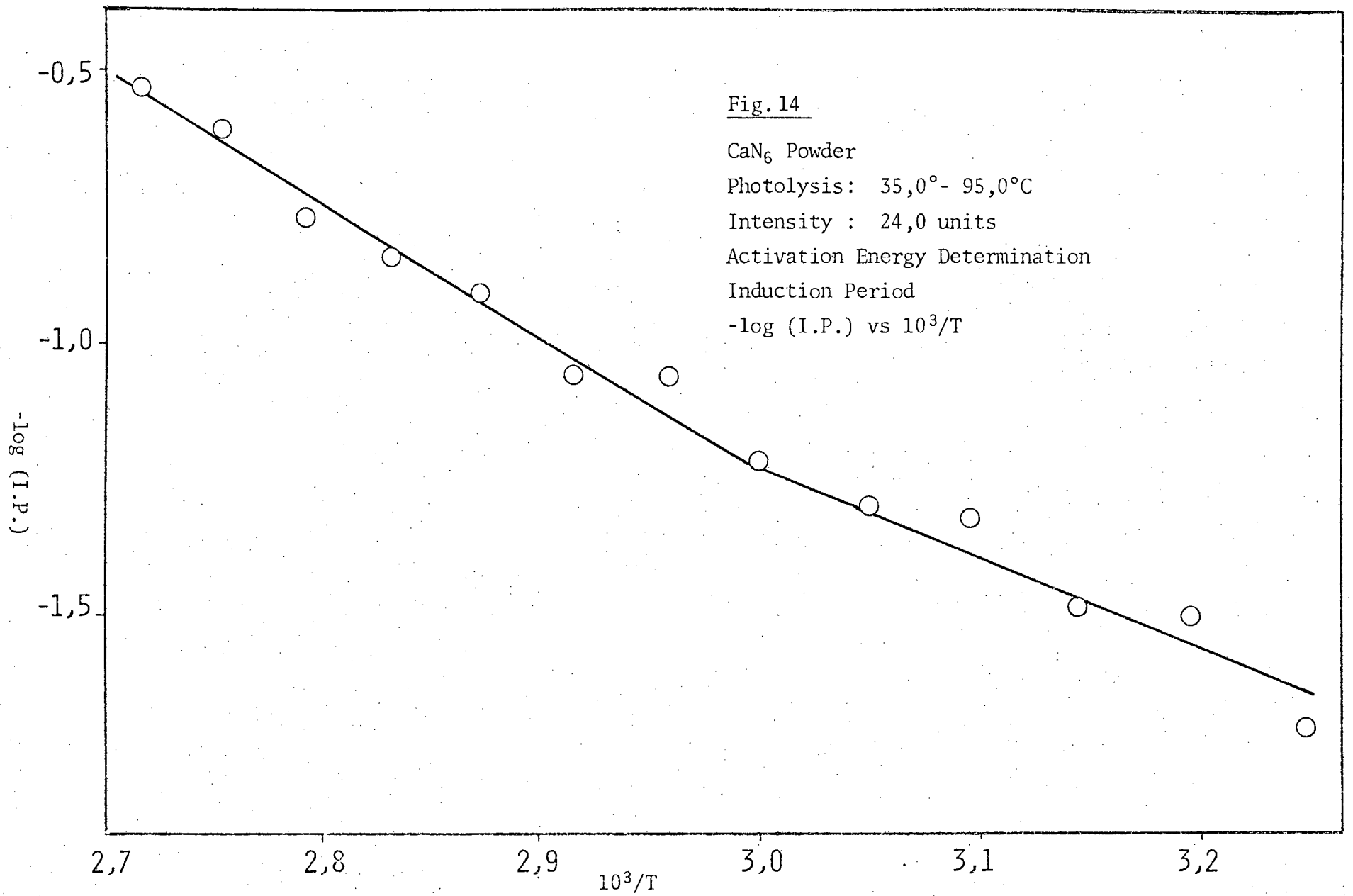

Fig. 14

CaN_6 Powder
Photolysis: 35,0°- 95,0°C
Intensity : 24,0 units
Activation Energy Determination
Induction Period
-log (I.P.) vs $10^3/T$

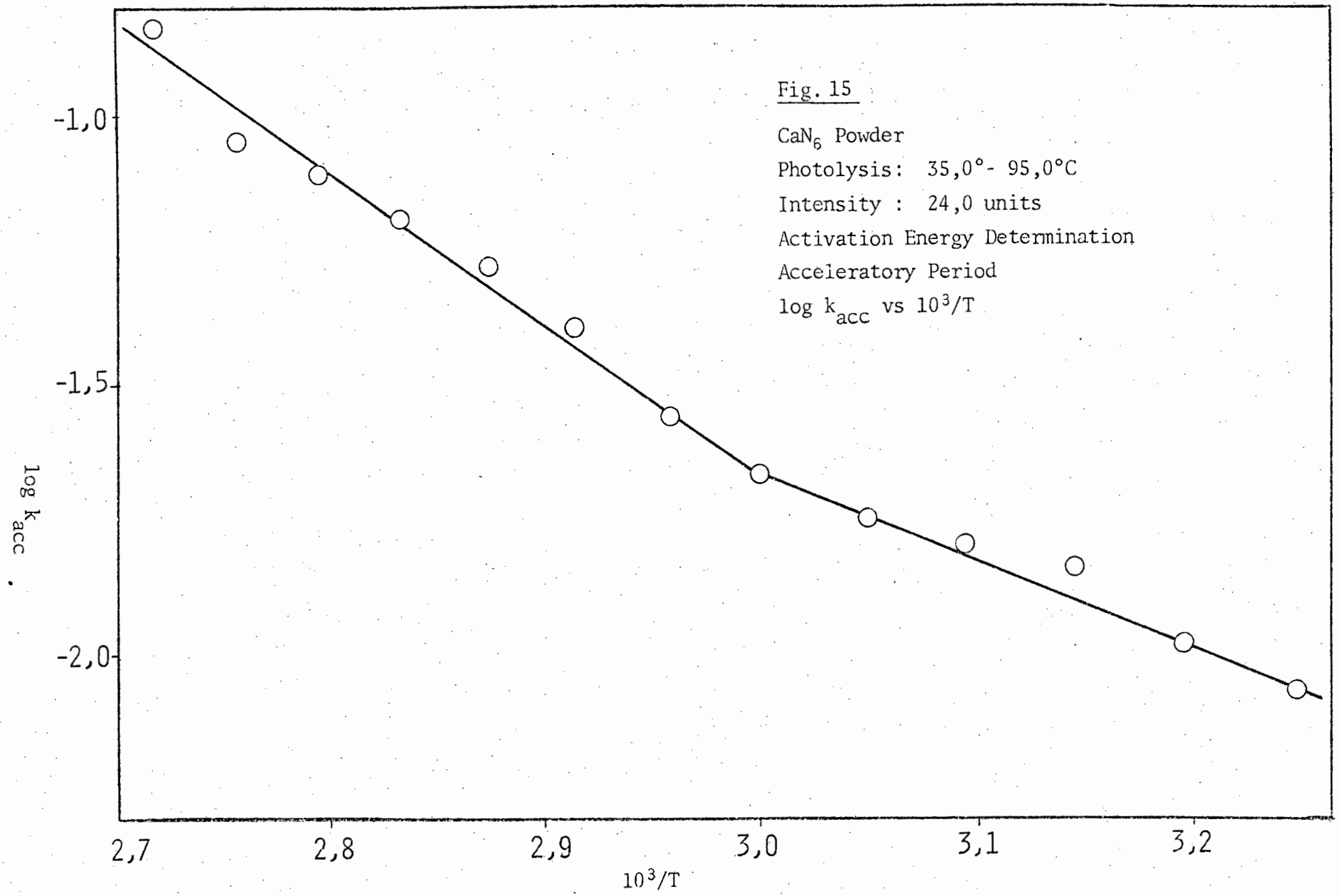

Fig. 15

CaN_6 Powder
Photolysis: 35,0°- 95,0°C
Intensity : 24,0 units
Activation Energy Determination
Acceleratory Period
log k_{acc} vs $10^3/T$

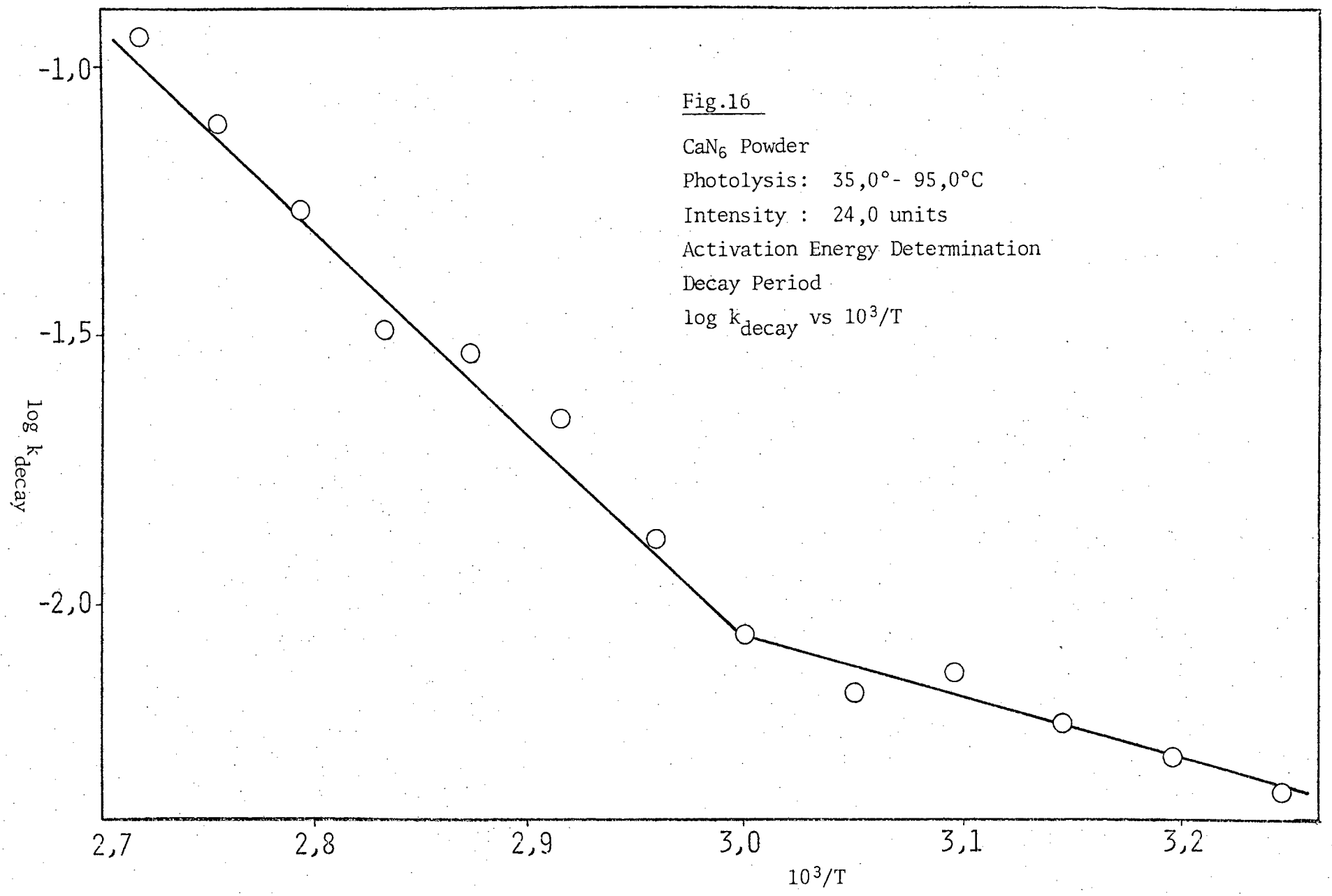

Fig.16

CaN_6 Powder

Photolysis: 35,0°- 95,0°C

Intensity : 24,0 units

Activation Energy Determination

Decay Period

log k_{decay} vs $10^3/T$

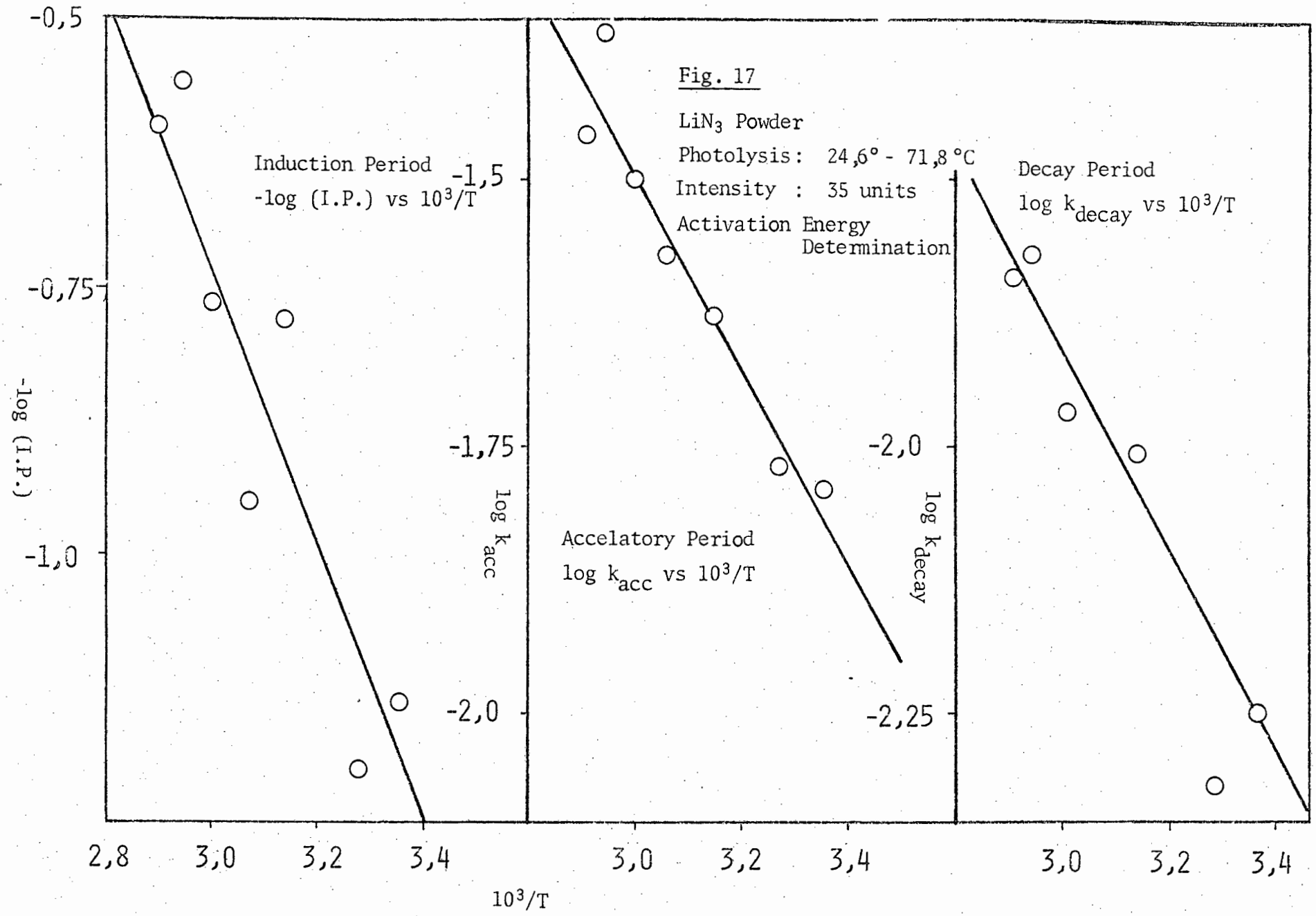

Fig. 17

LiN_3 Powder

Photolysis: 24,6° - 71,8 °C

Intensity : 35 units

Activation Energy Determination

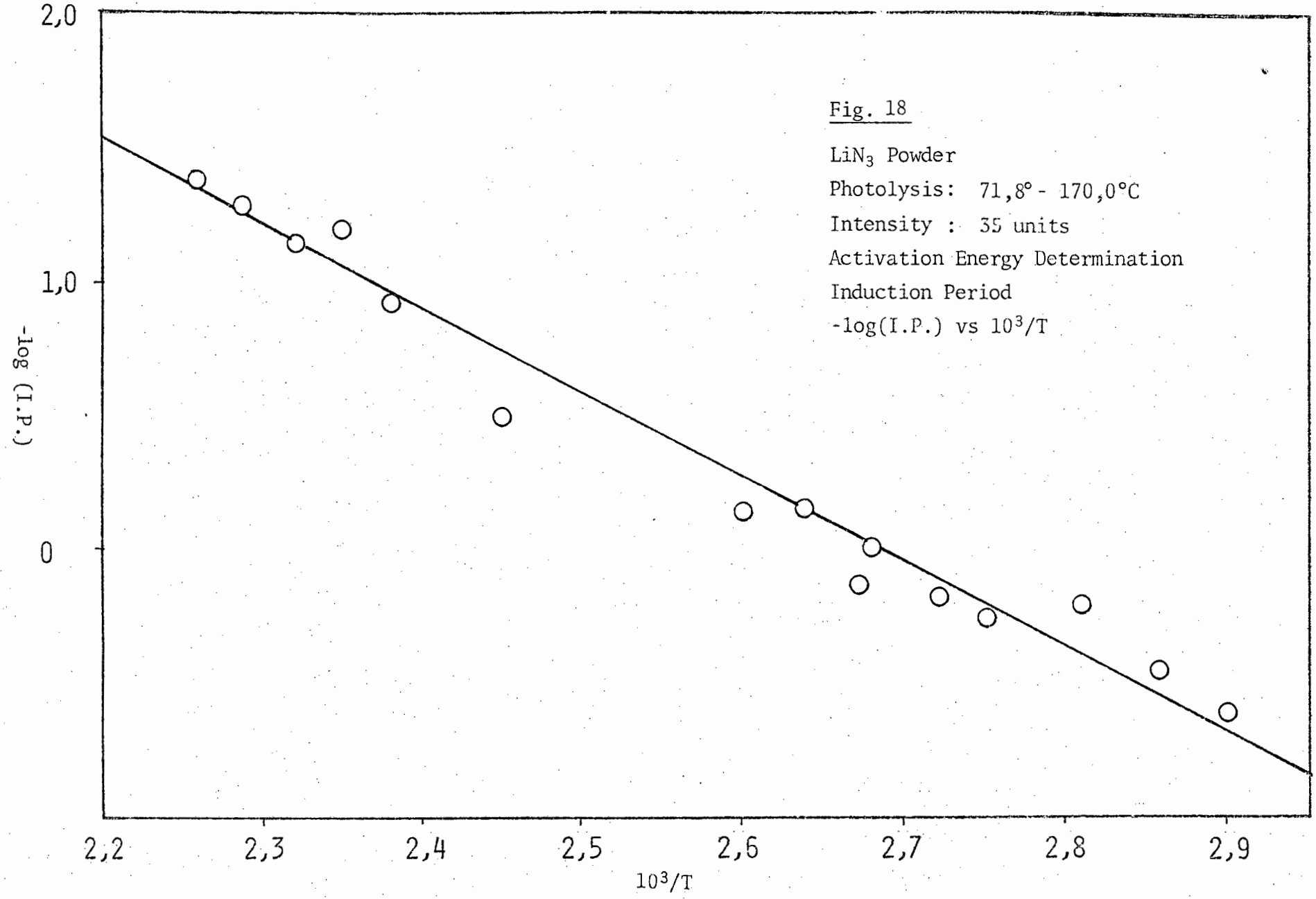

Fig. 18

LiN_3 Powder
Photolysis: 71,8° - 170,0°C
Intensity : 35 units
Activation Energy Determination
Induction Period
$-\log(I.P.)$ vs $10^3/T$

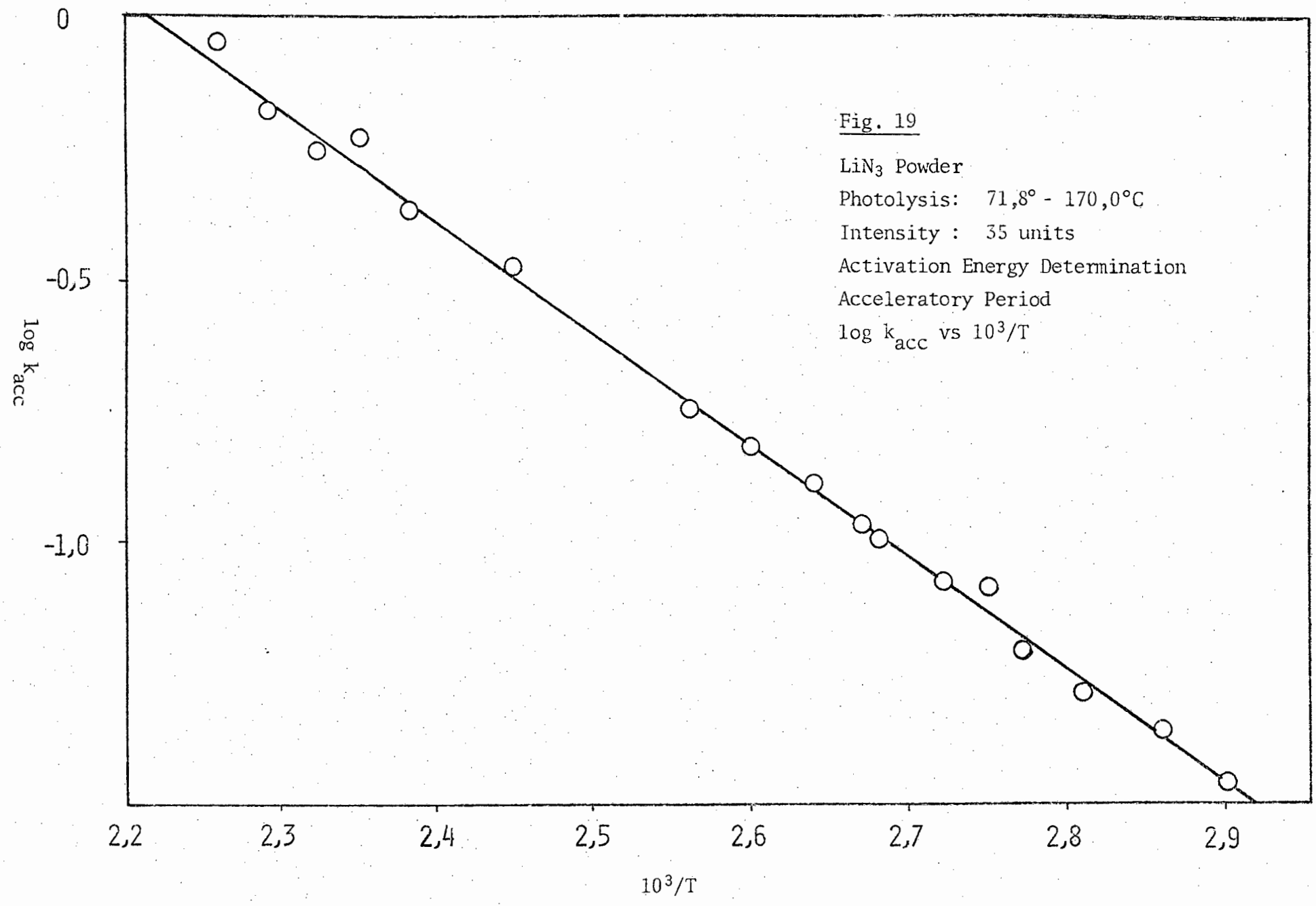

Fig. 19

LiN_3 Powder
Photolysis: 71,8° - 170,0°C
Intensity : 35 units
Activation Energy Determination
Acceleratory Period
log k_{acc} vs $10^3/T$

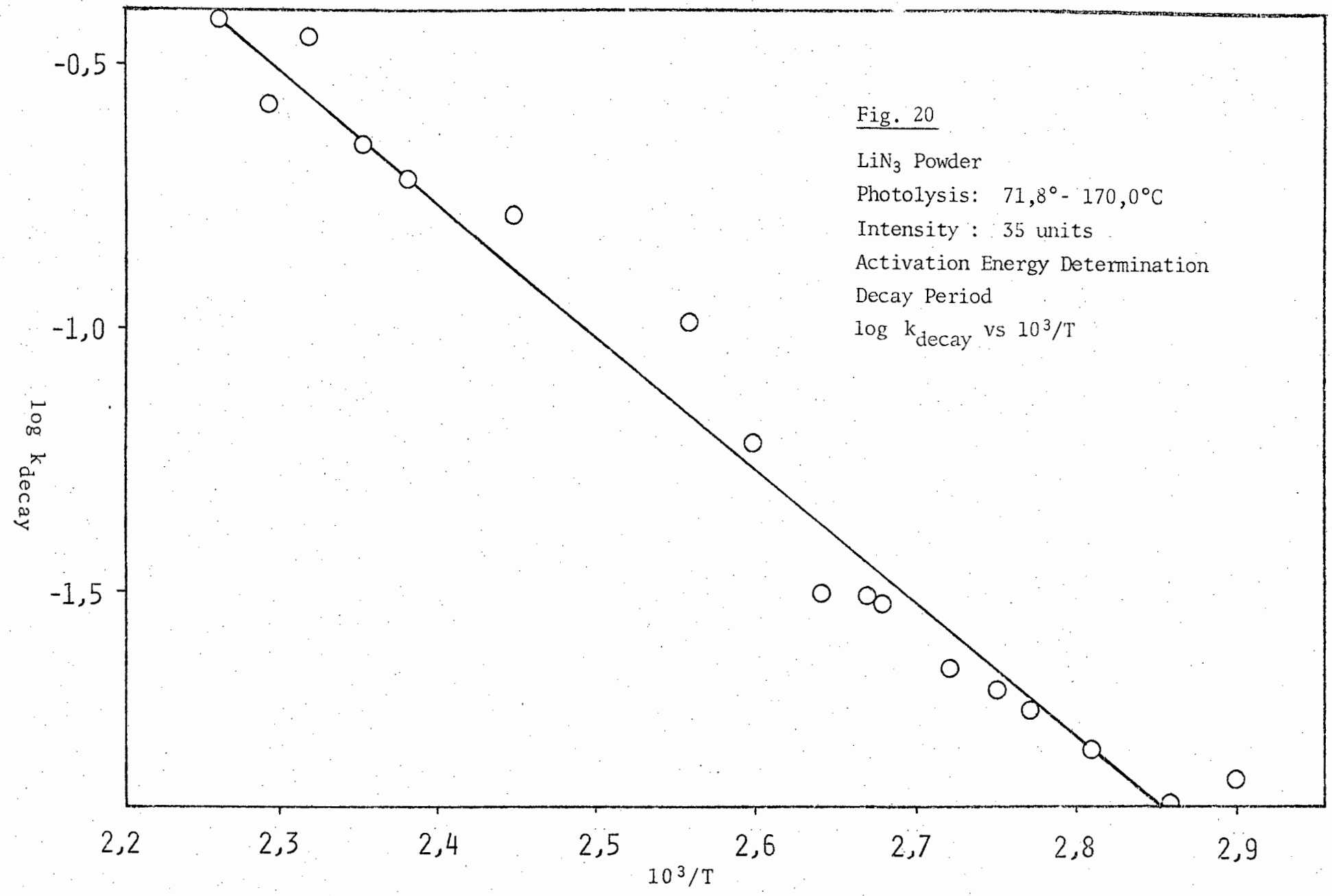

Fig. 20

LiN_3 Powder
Photolysis: 71,8°- 170,0°C
Intensity : 35 units
Activation Energy Determination
Decay Period
log k_{decay} vs $10^3/T$

Table 7 Rate constants for the decay reaction of photolysed lithium azide powder (Split Run Technique)

Temperature range : 55,0° - 126,6°C

Light intensity : 35 units

Temperature Range of Split Run °C	Temperature °C	$k_{decay} \times 10^3$ min^{-1}.
55,0 - 78,0	55,0	1,3
	65,0	1,4
	74,0	1,6
78,0 - 126,6	85,0	2,1
	95,0	4,4
	106,0	4,1
	116,0	5,4
	126,6	7,0

Table 8 Activation energies for the decay reaction of photolysed lithium azide powder (Split Run Technique)

Intensity : 35 units

Temperature Range °C	Decay Period Kcal./mol.
55,0 - 78,0	2,48
78,0 - 126,6	8,44

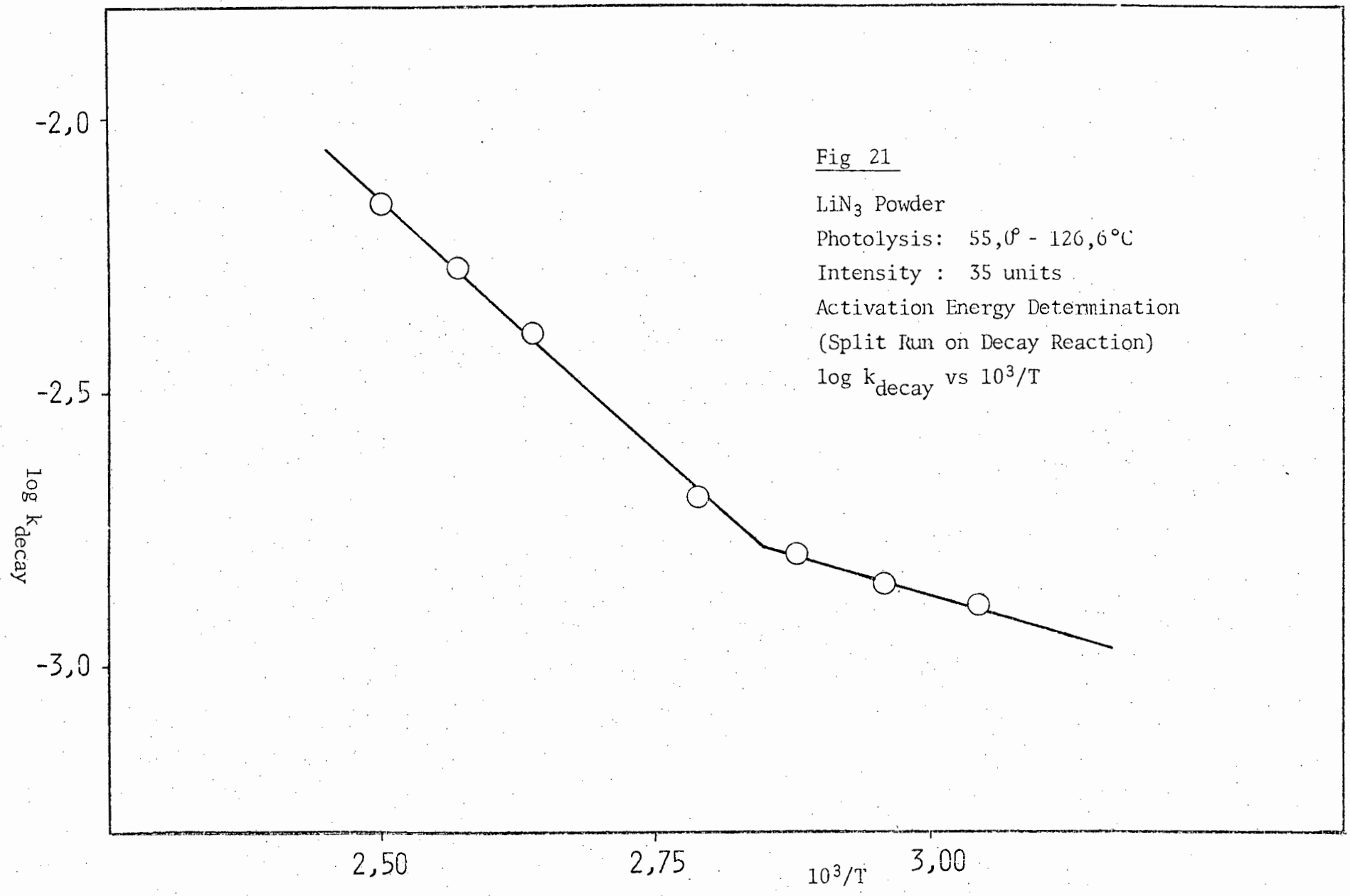

Fig 21

LiN_3 Powder
Photolysis: 55,0° - 126,6°C
Intensity : 35 units
Activation Energy Determination
(Split Run on Decay Reaction)
log k_{decay} vs $10^3/T$

decay reaction using the split run technique and Table 8 the corresponding activation energies. Fig. 21 shows the plot of log k_{decay} vs $10^3/T$ for these runs.

(i.d) The effect of variation of intensity of ultraviolet light source

The rates of photolysis of calcium and lithium azides were measured at different light intensities with the temperature being kept constant for the purpose of determining the molecularity of the processes taking place. The method used to vary the intensity of the light has already been explained in section 8(iii). The effect of variation of light intensity in the photolysis of calcium azide was studied at 55,0°C and 90,0°C and, in the case of lithium azide, at 30,0°C and 127,0°C.

The equation

$$k = I^m + c$$

where k = rate constant

I = intensity

m = molecularity

c = constant

was used to analyze the results and thus a value for m was obtained for each of the induction, acceleratory and decay periods by ignoring c, and rearranging the equation to

$$\log k = m \log I.$$

Log k was then plotted against log I.

Table 9 gives the rate constants for the photolysis of calcium azide at 90,0°C and 55,0°C at various light intensities and Table 10 gives the rate constants for the photolysis of lithium azide at 127,0°C and 30,0°C also at various light intensities. Tables 11 and 12 give the values of m for calcium azide and lithium azide respectively. Fig. 22-25 and Fig. 26-28 show plots of k against I^m for calcium and lithium azides respectively. In all graphs the value of m has been corrected to the nearest whole number.

Table 9 Rate constants for the photolysis of calcium azide powder at various light intensities

Temperature °C	Intensity Units	Induction Period x10 min.	$k_{acc} \times 10^2$ min^{-1}.	$k_{decay} \times 10^2$ min^{-1}.
90,0	8,5	10,7	3,8	3,3
	12,5	7,7	5,4	3,8
	14,0	5,7	6,0	4,7
	16,0	5,5	6,4	3,6
	19,0	4,5	9,9	6,5
	20,0	4,4	8,0	4,2
	24,0	4,8	9,5	8,4
	30,8	3,0	11,8	7,5
	36,0	2,8	12,7	10,6
	38,0	3,4	13,6	9,9
	41,0	1,6	13,6	13,1
	65,0	1,3	23,2	17,7
55,0	20,0	34,8	1,2	0,65
	23,0	26,6	1,6	0,77
	25,0	25,2	2,0	0,74
	30,0	17,4	2,4	0,80
	32,0	17,4	2,6	1,70
	37,0	23,2	3,8	2,10
	42,5	10,4	4,9	2,70
	47,0	9,3	4,5	2,70
	50,0	8,0	6,2	4,10
	56,0	8,2	7,2	4,00

Table 10 Rate constants for the photolysis of lithium azide powder at various light intensities

Temperature °C	Intensity Units	Induction Period x 10 min.	k_{acc} x 10^2 min^{-1}.	k_{decay} x 10^2 min^{-1}.
127,0	7,5	6,5	4,3	0,62
	13,5	6,1	5,3	1,10
	22,0	5,0	9,9	1,70
	29,5	6,0	19,2	2,80
	35,0	3,4	22,6	4,10
30,0	4,0	52,0	0,46	0,22
	6,5	67,6	0,70	0,50
	12,3	8,2	2,87	1,70
	13,1	15,2	3,50	1,70
	18,0	7,2	6,17	3,80

Table 11 Value of m in the equation $k = I^m + c$ for calcium azide powder

Temperature °C	Induction Period	Acceleratory Period	Decay Period
90,0	0,99	0,84	0,90
55,0	1,46	1,70	2,00

Table 12 Value of m in the equation $k = I^m + c$ for the lithium azide powder

Temperature °C	Induction Period	Acceleratory Period	Decay Period
127,0	1,14	1,14	1,18
30,0	1,54	1,81	1,86

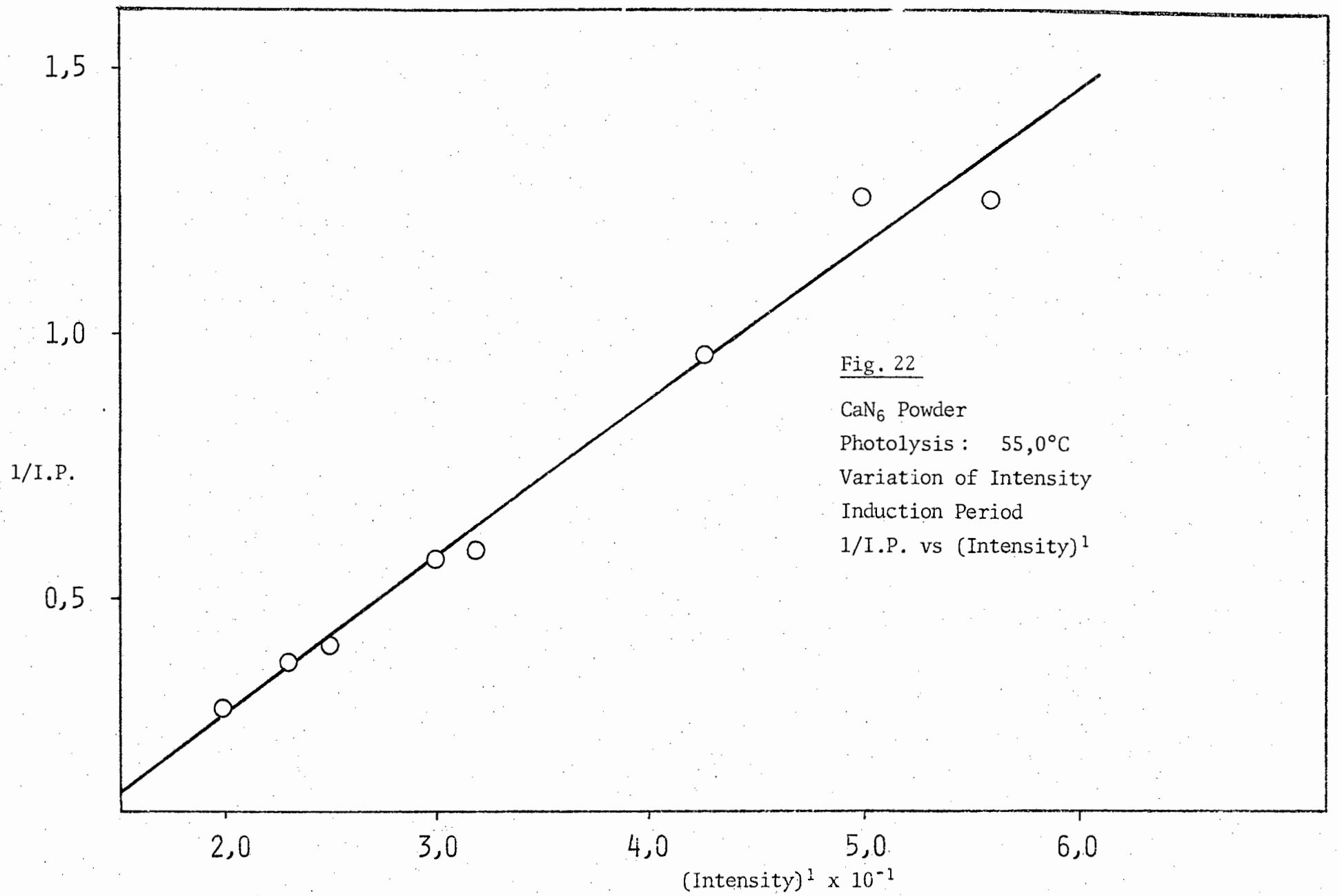

Fig. 22

CaN_6 Powder
Photolysis : 55,0°C
Variation of Intensity
Induction Period
1/I.P. vs (Intensity)^{1}

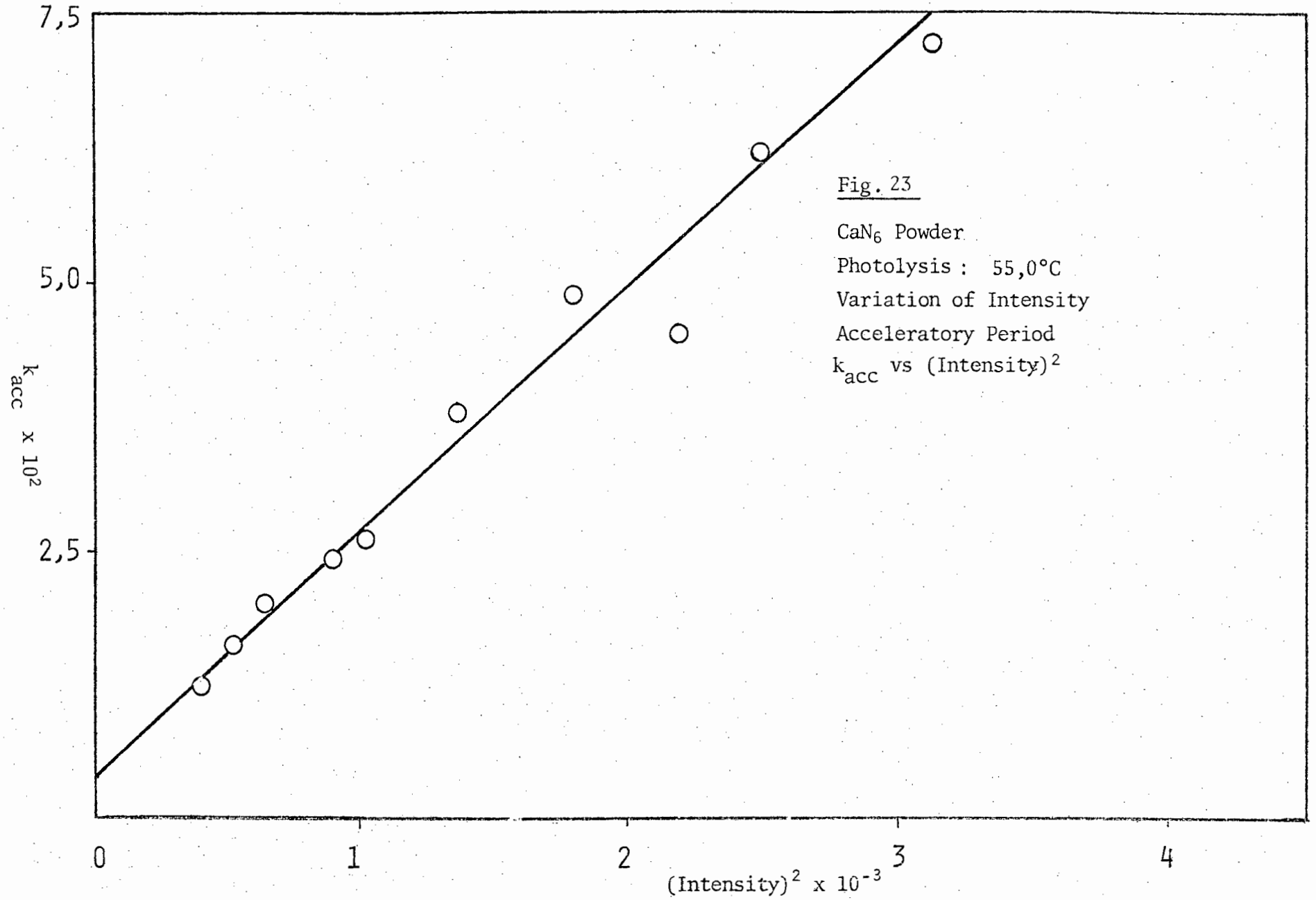

Fig. 23

CaN_6 Powder
Photolysis : 55,0°C
Variation of Intensity
Acceleratory Period
k_{acc} vs (Intensity)^2

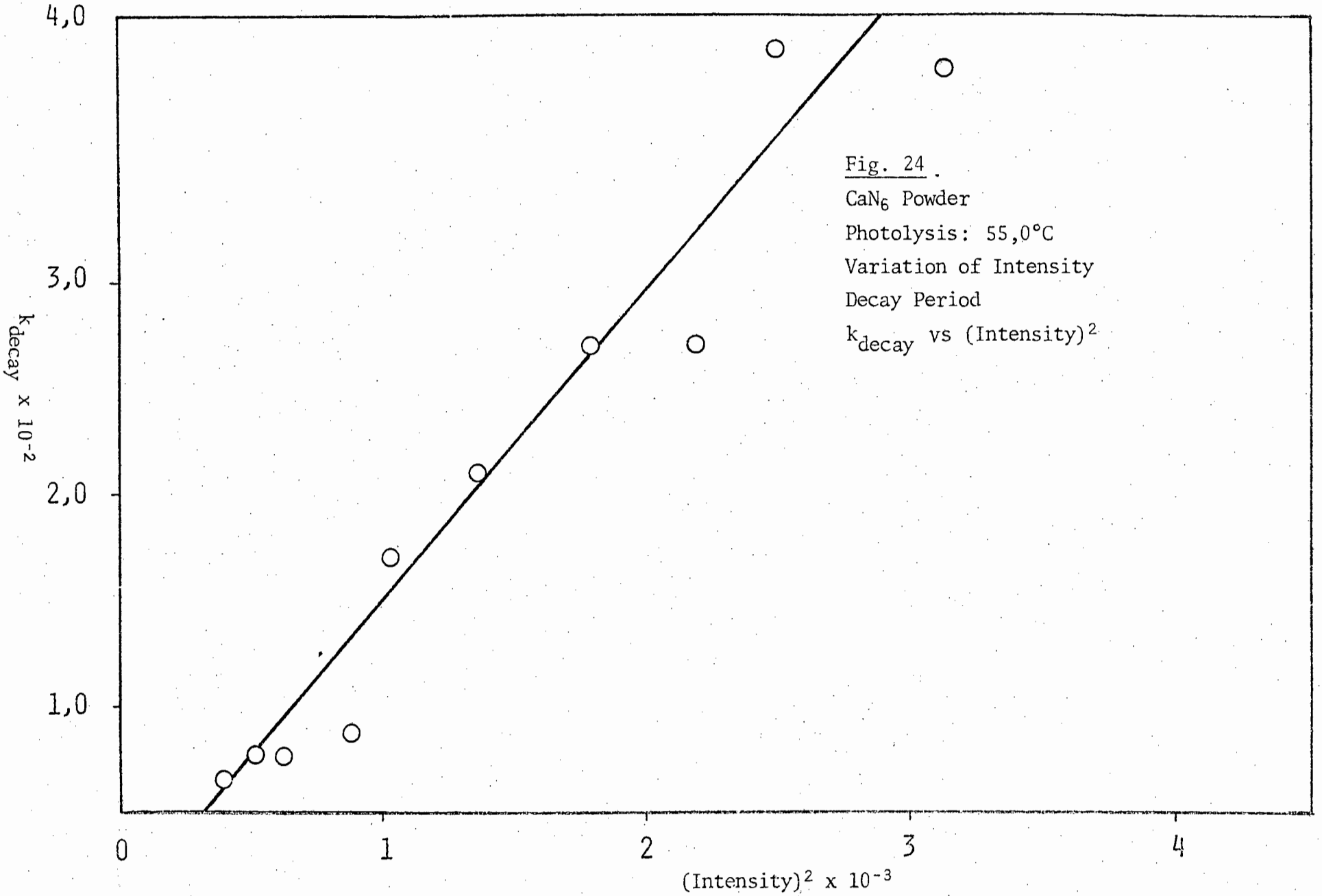

Fig. 24 .
CaN_6 Powder
Photolysis: 55,0°C
Variation of Intensity
Decay Period
k_{decay} vs $(Intensity)^2$

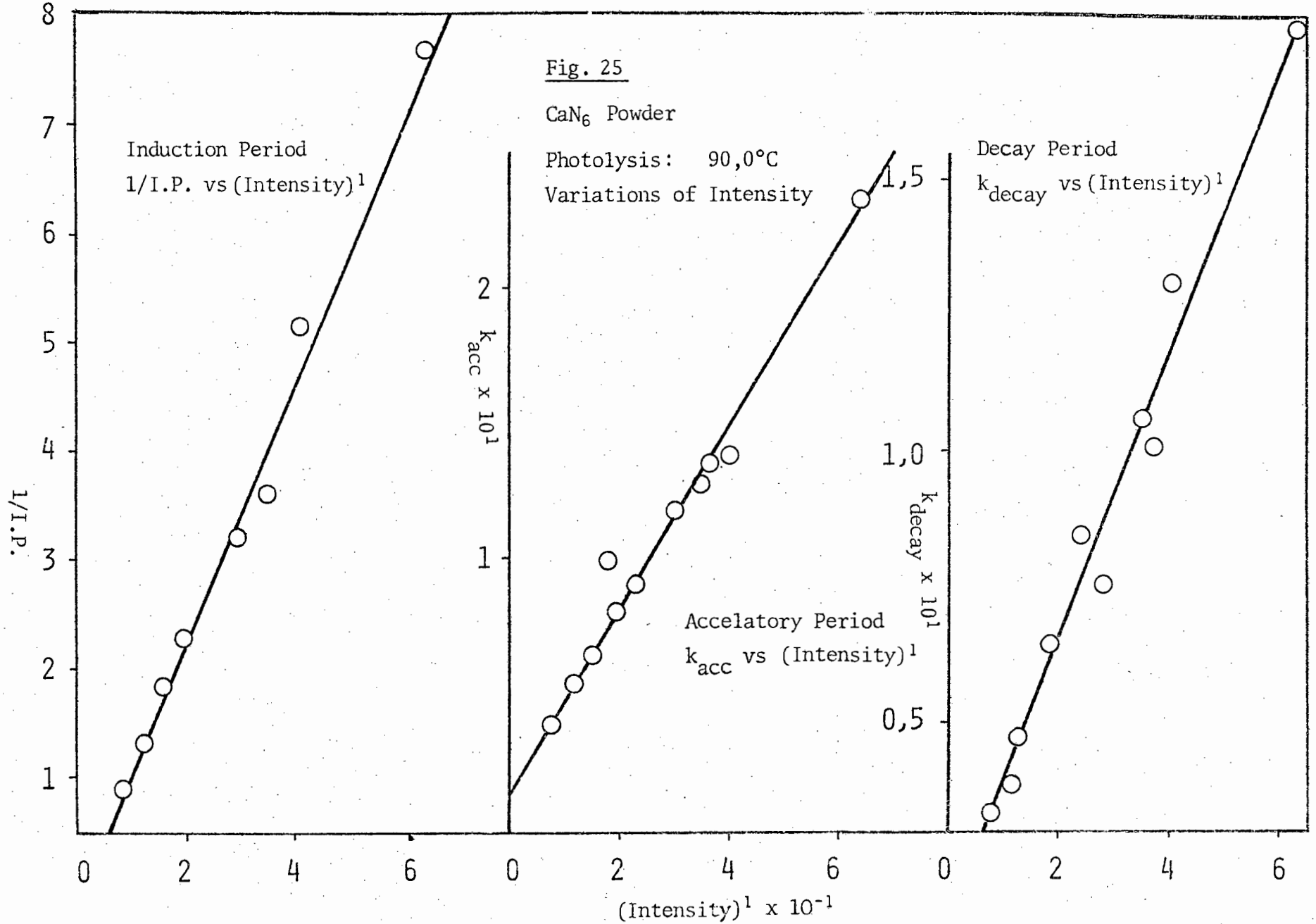

Fig. 25

CaN_6 Powder

Photolysis: 90,0°C

Variations of Intensity

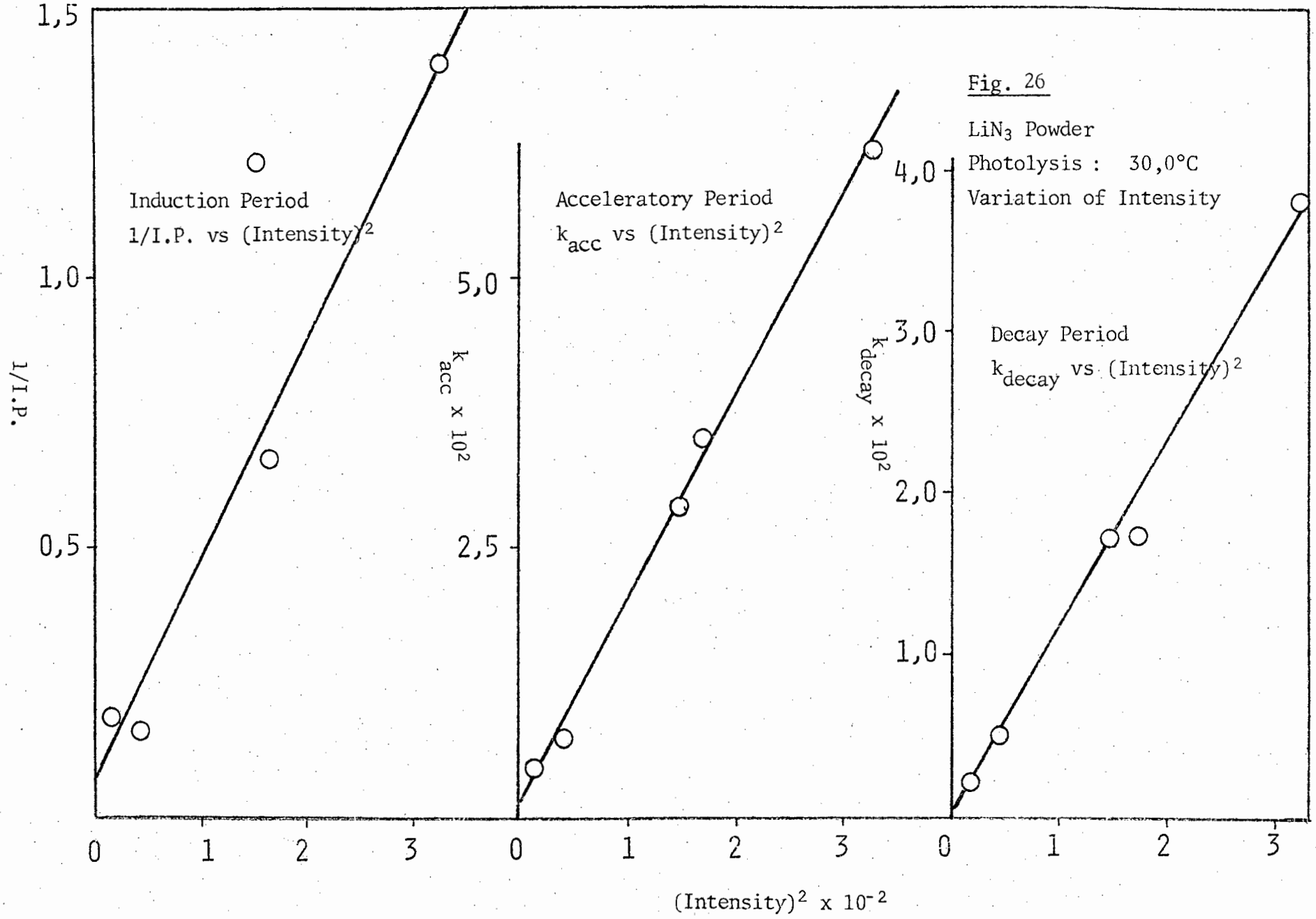

Fig. 26

LiN_3 Powder
Photolysis : 30,0°C
Variation of Intensity

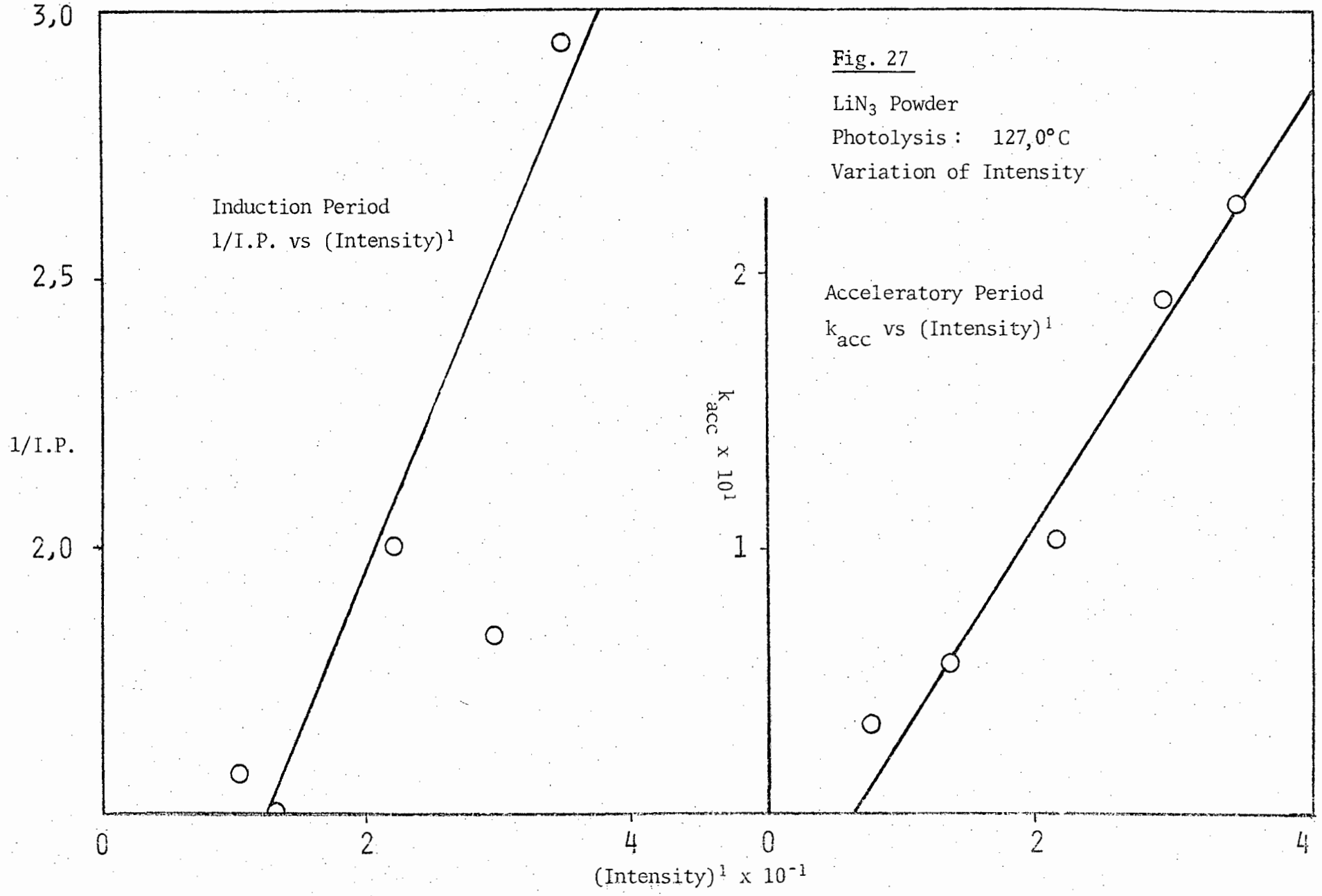

Fig. 27

LiN_3 Powder
Photolysis : 127,0°C
Variation of Intensity

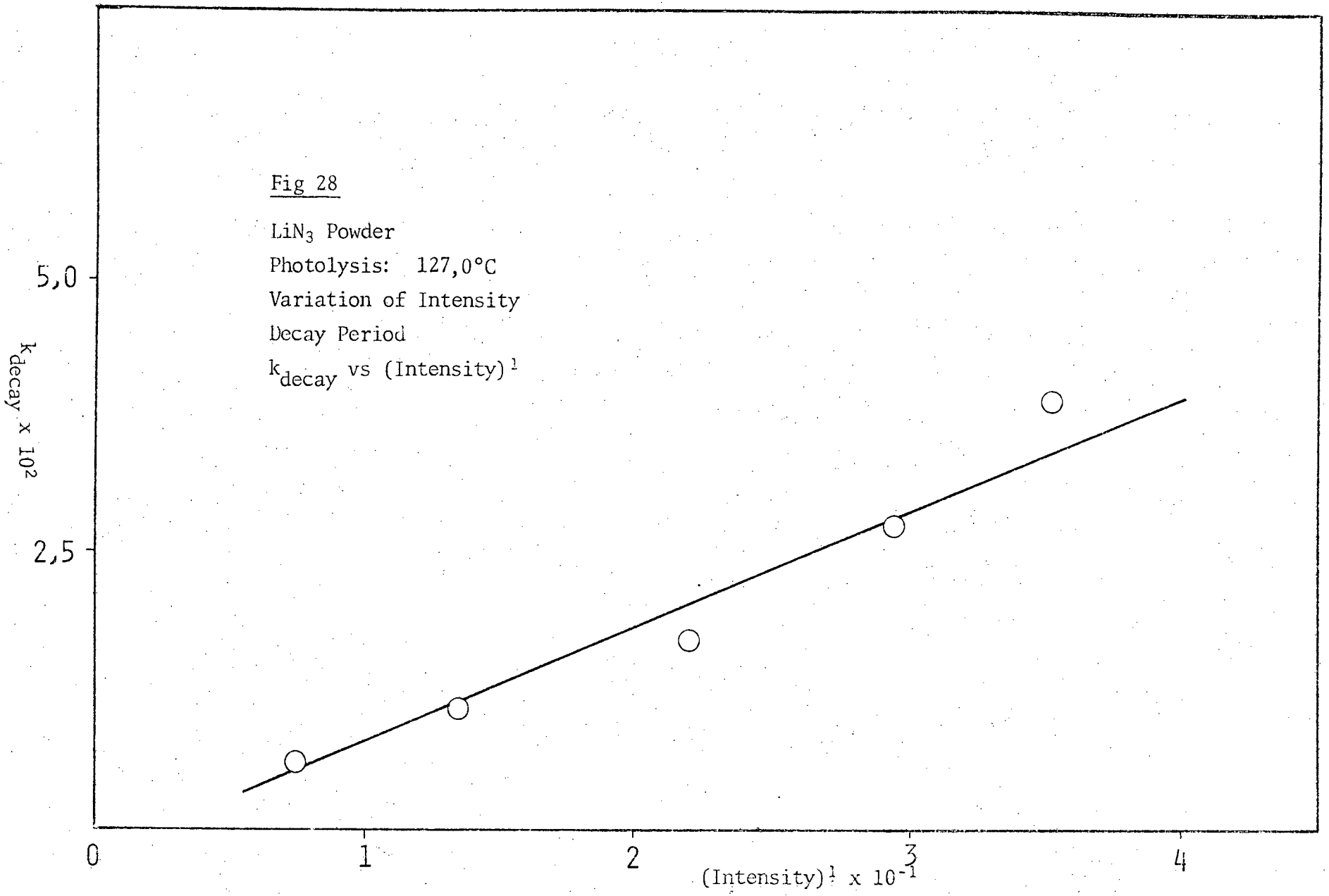
Fig 28
LiN_3 Powder
Photolysis: 127,0°C
Variation of Intensity
Decay Period
k_{decay} vs $(Intensity)^{\frac{1}{3}}$
5,0
2,5
$k_{decay} \times 10^2$
0
1
2
3
4
$(Intensity)^{\frac{1}{3}} \times 10^{-1}$

(i.e) Visual observations

The colour of the calcium and lithium azide powders was observed at various stages of photolysis. Observations were carried out on calcium azide at a temperature of 47,0°C and a light intensity of 5 units. An opthalmascope was used in order to improve the quality of the observation. At α = 0,01 very little change had taken place and when α = 0,07 the powder had become light brown on top but was still white underneath. At α = 0,14 the sample had become light brown throughout progressively becoming a darker brown colour until at α = 0,28, which was near the inflection point, the powder was almost black on top with individual particles becoming clearer. This process of blackening, with the presence of what appeared to be large particles, continued until at α = 0,61 the sample was black throughout and continued as such to the end. The final product reacted violently on exposure to the atmosphere or to a weak acid solution.

The sample of lithium azide was observed at a temperature of 30,0°C and an intensity of 35 units. At the end of the induction period the sample started to turn a light brown colour. Immediately after the end of the induction period one or two small "explosions" occurred. The colour of the sample then became a darker brown. Throughout the photolytic decomposition process at this stage the "explosions" became progressively more violent. At $\alpha \approx 0,20$ the state of perturbation, as it were, reached a maximum. The peak of activity at $\alpha \approx 0,20$ was just prior to the inflection point. Subsequently the sample became a darker brown and the activity subsided. When the sample had re-settled dark brown spots formed and at the end of the decomposition a dark brick red to black sample remained which reacted violently on the addition of a weak acid solution.

Lithium azide was also observed at a temperature of 127,0°C and an intensity of 35 units. The observations were basically the same as those

made at 30,0°C. The final product was a black colour and, like the final product of calcium azide, reacted violently on exposure to the atmosphere, a bright flash and white fumes being observed.

(i.f) Interruption of a photodecomposition: dark rate determination

All photolytic decompositions of calcium azide below 110,0°C and of lithium azide in the temperature range studied ceased the moment the ultraviolet radiation was removed. No measurable dark rate could be observed in these ranges. On recommencing photolytic decompositions the runs continued as though no interruption had occurred.

(i.g) Admittance of water vapour following an interruption

In order to investigate the presence of metallic nuclei at various stages of the photolytic decomposition of calcium and lithium azides, water vapour (17 torr pressure) was introduced after the reaction had reached a certain point. These decompositions are called 'water interruptions'. This was achieved by introducing 1 ml of distilled water into the cold trap before the decomposition cell was connected to the line. The water was then solidified by the liquid nitrogen surrounding the trap. After the cell had been connected to the line, the system was pumped down and decomposition commenced in the normal manner. At the selected point of interruption the ultraviolet radiation was shut off and the furnace removed from the sample. The expansion bulbs and the decomposition cell were then isolated and the liquid nitrogen flask removed. When at least half of the water present had vapourized it was allowed to come into contact with the sample for a period of 1 minute, after which the water vapour was pumped from the line. The pump was then isolated, the liquid nitrogen trap replaced and the furnace repositioned around the sample. The sample was then allowed 5 min. in which to reach

the decomposition temperature, the expansion bulbs were opened, the sample exposed to the ultraviolet radiation and the decomposition continued.

Prior to carrying out the water interruption tests the effect of interrupting a decomposition was examined. The method of studying this effect has already been explained in section 9(*i.e.*). This test was carried out on both compounds at a variety of temperatures and light intensities. It was found in the case of both calcium and lithium azide that the interruption had no effect on the subsequent reaction which continued as if no interruption had taken place.

Water interruption tests were carried out on calcium azide at a temperature of 75,0°C and a light intensity of 6,5 units as well as on lithium azide at a temperature of 30,0°C and light intensity of 35 units and at a temperature of 96,5°C and a light intensity of 22 units. In the case of calcium azide the water vapour was introduced at time t = 0, midway along the induction period and at α values of 0,01; 0,13; 0,27; 0,40 and 0,59. With lithium azide at 96,5°C the water vapour was introduced at time t = 0, midway along the induction period, and at α values of 0,02; 0,17; 0,37 and 0,61.

The results of these investigations were similar for both calcium and lithium azides. The interruptions during the induction period had virtually no effect on the subsequent reaction other than to lengthen the induction period slightly compared to that of an uninterrupted run. When water vapour was introduced at α = 0,01 a new induction period, somewhat shorter than that for an uninterrupted run, was observed. Interruptions at other positions along the decomposition curve caused this new induction period, observed at α = 0,01, to become more protracted. In all cases the subsequent reaction showed the usual acceleratory and decay regions although the values of k_{acc} and k_{decay} decreased as the point of interruption along the curve increased. When water vapour was

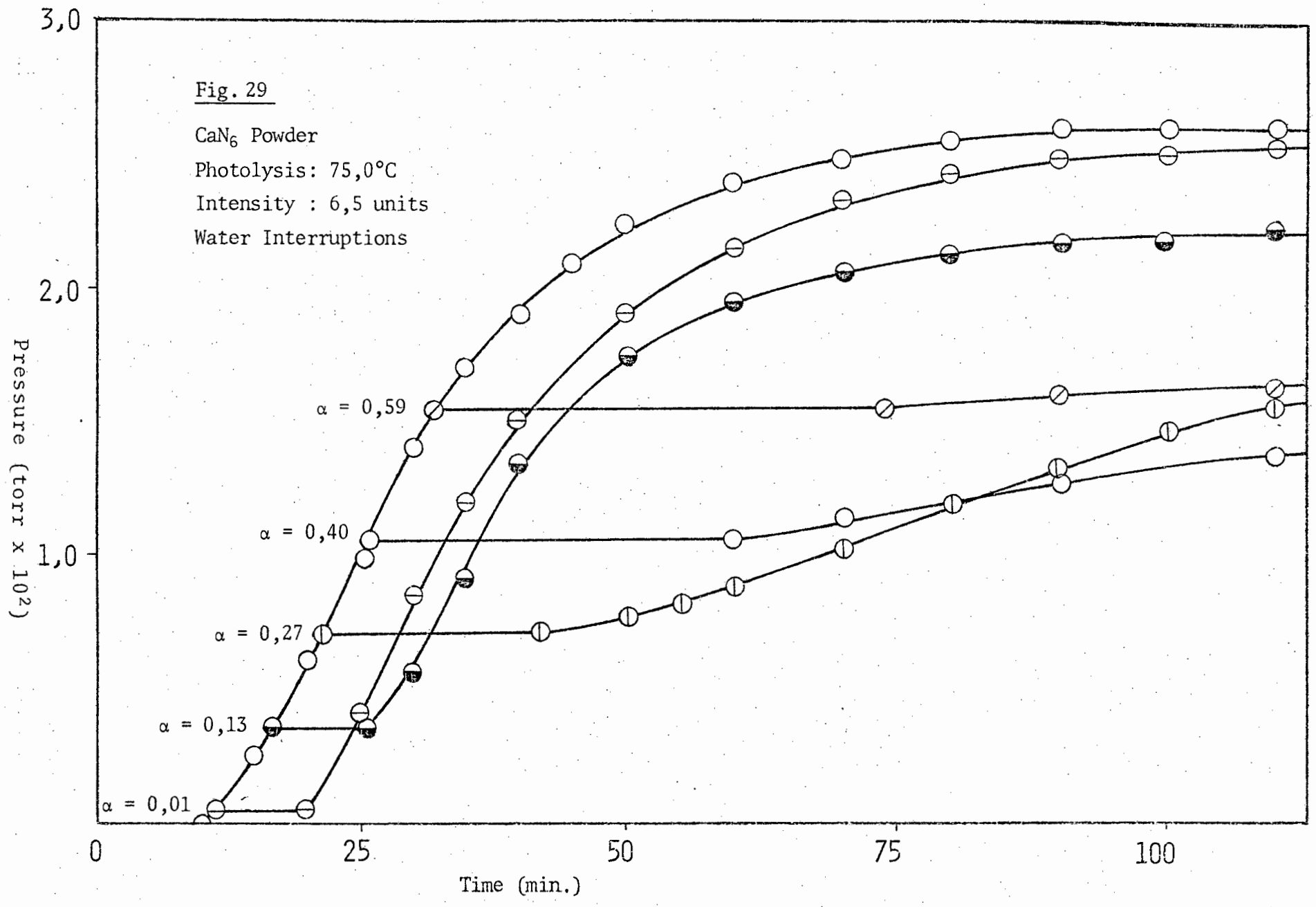
Fig. 29
CaN_6 Powder
Photolysis: 75,0°C
Intensity : 6,5 units
Water Interruptions
α = 0,59
α = 0,40
α = 0,27
α = 0,13
α = 0,01
3,0
2,0
1,0
0
25
50
75
100
Pressure (torr x 10^2)
Time (min.)

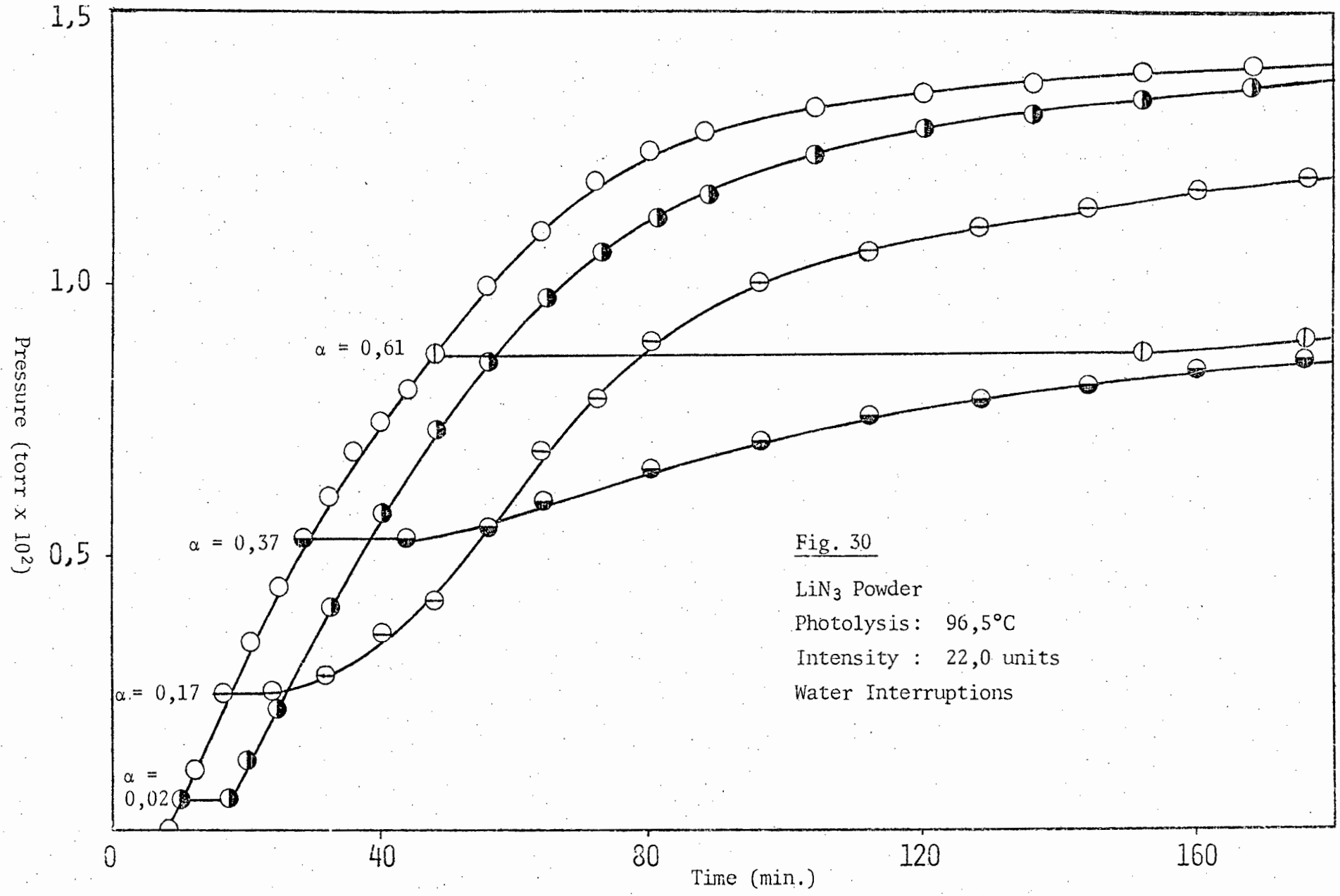

Fig. 30

LiN_3 Powder
Photolysis: 96,5°C
Intensity : 22,0 units
Water Interruptions

introduced at values of α greater than that of the inflection point, the induction period became extremely long relative to that of an uninterrupted run and the subsequent reaction reduced to a point where it could be considered to have been virtually destroyed. In all cases of interruptions taking place after the normal induction period, the final pressure was observed to be less than that of an uninterrupted run, the reduction being greater the later the interruption. The results for calcium azide are shown in Fig. 29 and those for lithium azide at 96,5°C in Fig. 30. The pressures have not been normalized so that the effect of the interruptions on the final pressure can be observed.

(i.h) The effect of filtering the high intensity arc with blue and ultraviolet transmission filters

In order to determine which wavelengths of ultraviolet radiation were most effective for the photolysis of calcium and lithium azides, various Schott filters were used.

Photodecompositions were carried out on calcium azide at temperatures of 55,0°C and 90,0°C and a light intensity of 35,0 units in both cases. The effect of filters on lithium azide was studied at temperatures of 30,0°C and 127,0°C and light intensities of 27,5 and 23,0 units respectively. The Schott filters and their Chance equivalents as well as the radiation and the light intensities transmitted by these filters are listed in Table 13.

The effect of the filters was found to be similar for both compounds. The 5 mm BG12 filter caused the reaction to slow down drastically, its decreasing effect on the reaction relative to a normal reaction being very much more than that of the other two filters. The 3 mm UG5 and the 1 mm UG1 filters both caused a reduction in the reaction rate, the latter more so than the former although, in the case of calcium azide, the difference in the effects of these two filters was not as great as in the case of lithium

Table 13 Filters used in the photolysis of calcium and lithium azide powders.

Schott filter	Chance filter	Transmitted λ nm	Transmitted Intensity
3 mm UG5	OX 7	220 - 420	0,16
1 mm UG1	-	280 - 420	0,20
5 mm BG12	OY 10	330 - 490	0,26

azide. These results are illustrated in Fig. 31 and 32 for calcium azide and in Fig. 33 and 34 for lithium azide.

(i.i) The determination of the nature of photolytic nuclei

At the end of the induction period the crystal is a function of the number of nuclei, their spatial distribution, the size and shape of the nuclei and the variety of properties of the nuclei themselves (e.g. chemical, crystallographic and electronic structure). In order to determine whether the photolysis of calcium and lithium azides involved similar reaction centres, i.e. nuclei, to those involved in thermal decomposition the following tests were performed.

The compound was decomposed thermally (at 119,0°C for calcium azide and 147,0°C for lithium azide) until the reaction had reached the end of the induction period. The furnace was then removed from the sample. Once the furnace had cooled to a lower temperature (85,0°C in the case of both calcium and lithium azides)it was replaced in position around the cell. A warm-up time of 5 min. was allowed and then photolysis commenced (the light intensities were 10 units for calcium azide and 22 units for lithium azide). It was found that photolysis commenced without an induction period and that

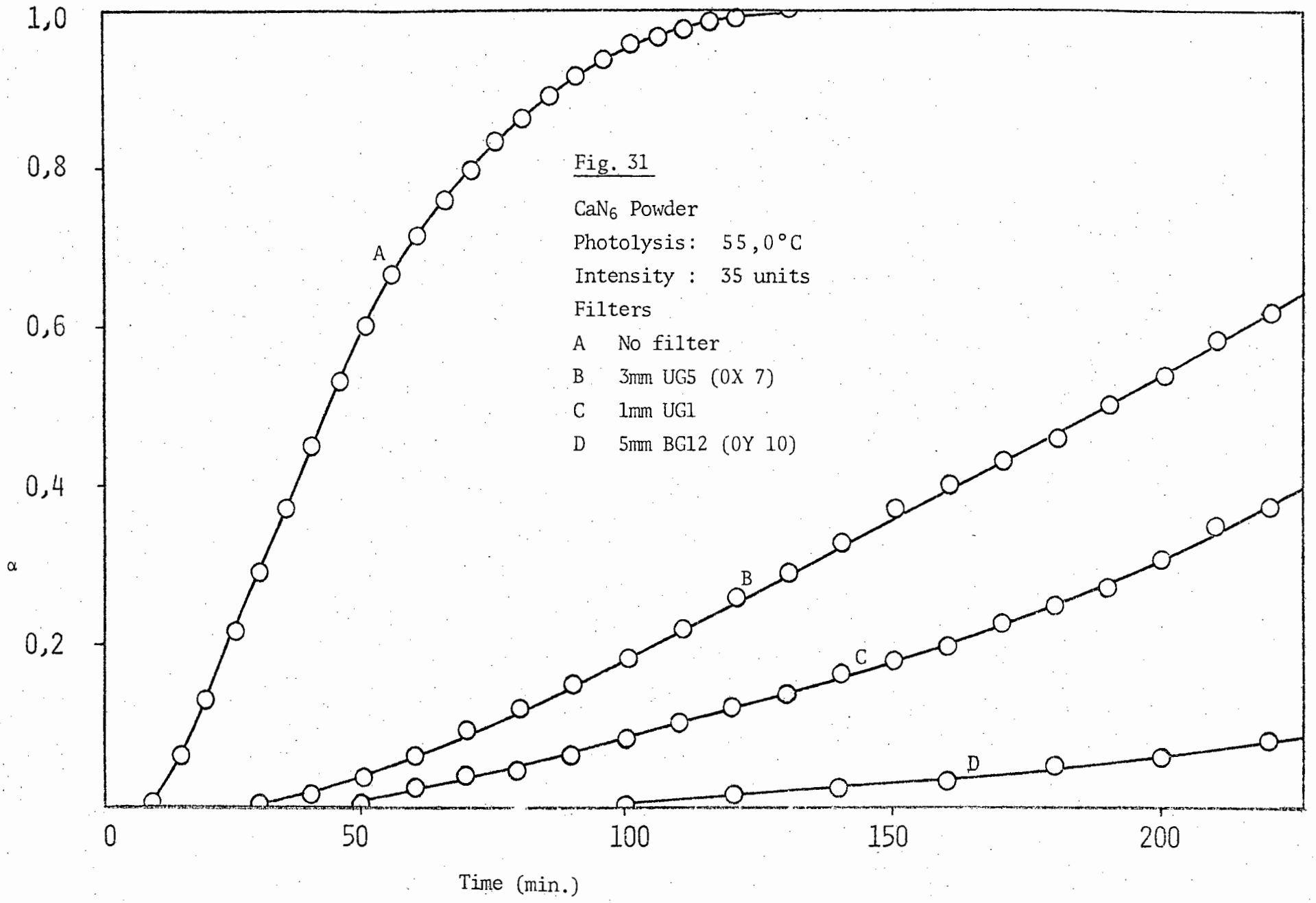

Fig. 31

CaN_6 Powder
Photolysis: 55,0°C
Intensity : 35 units
Filters
A No filter
B 3mm UG5 (0X 7)
C 1mm UG1
D 5mm BG12 (0Y 10)

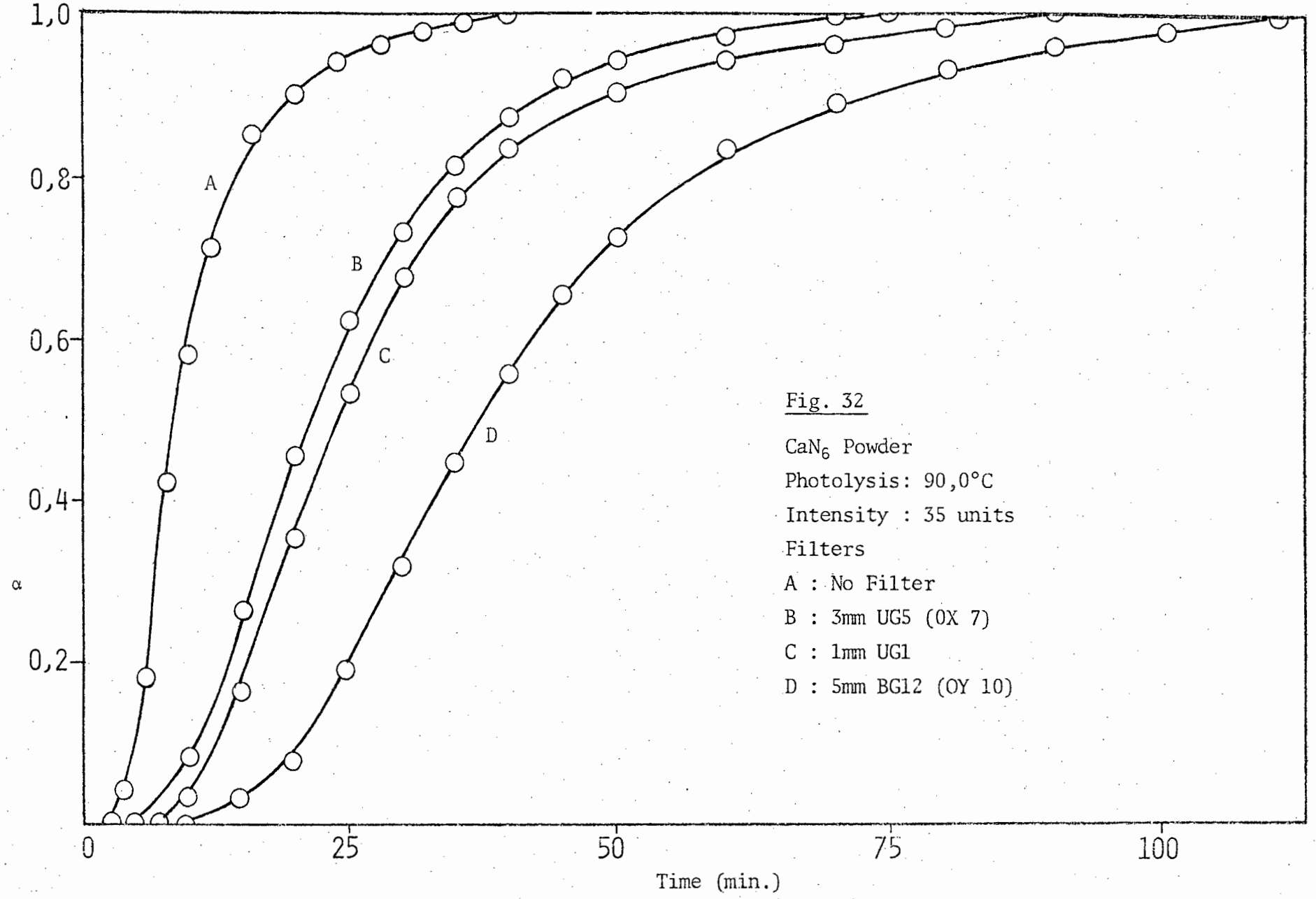

Fig. 32

CaN_6 Powder
Photolysis: 90,0°C
Intensity : 35 units
Filters
A : No Filter
B : 3mm UG5 (0X 7)
C : 1mm UG1
D : 5mm BG12 (OY 10)

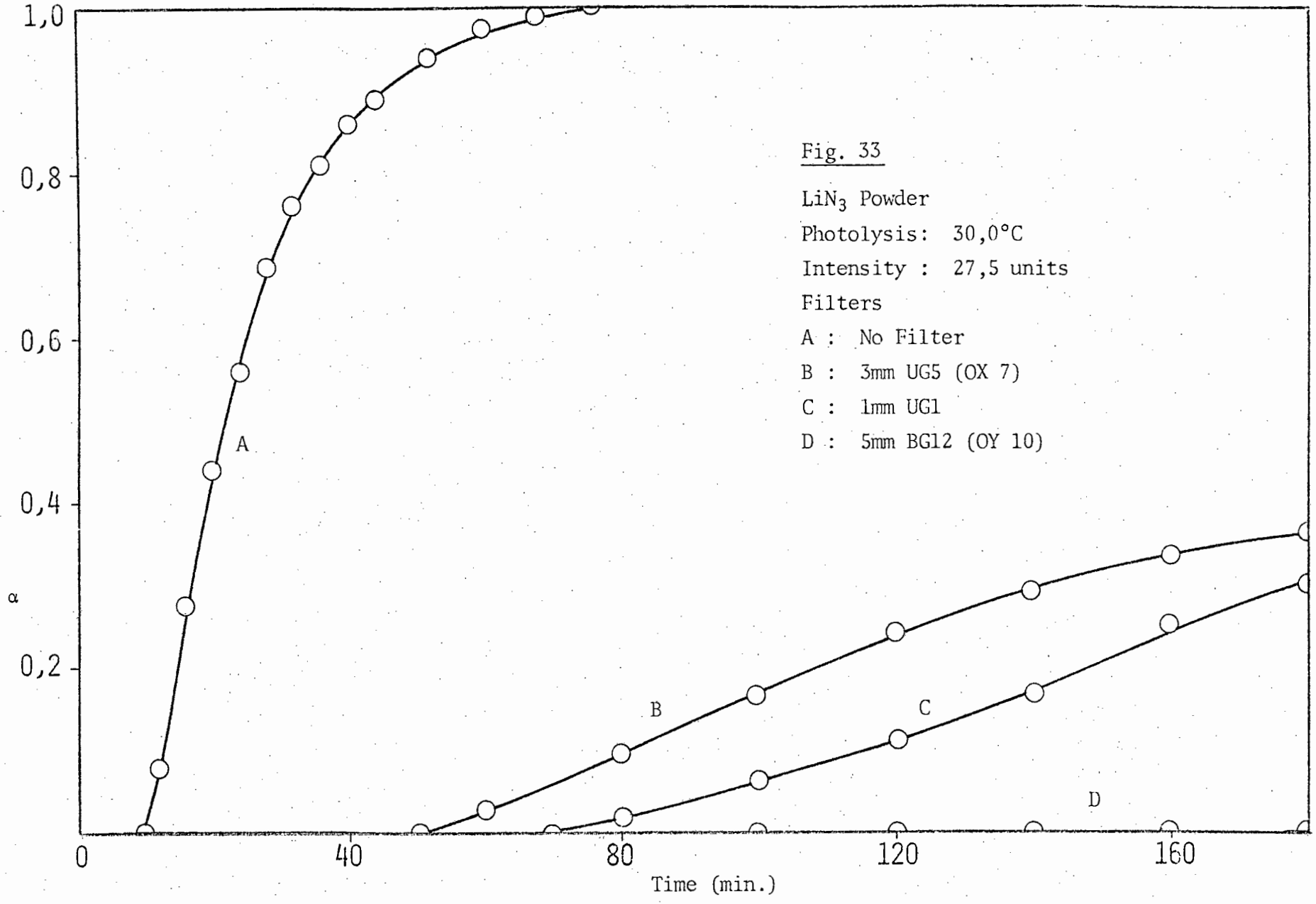

Fig. 33

LiN_3 Powder

Photolysis: 30,0°C

Intensity : 27,5 units

Filters

A : No Filter

B : 3mm UG5 (OX 7)

C : 1mm UG1

D : 5mm BG12 (OY 10)

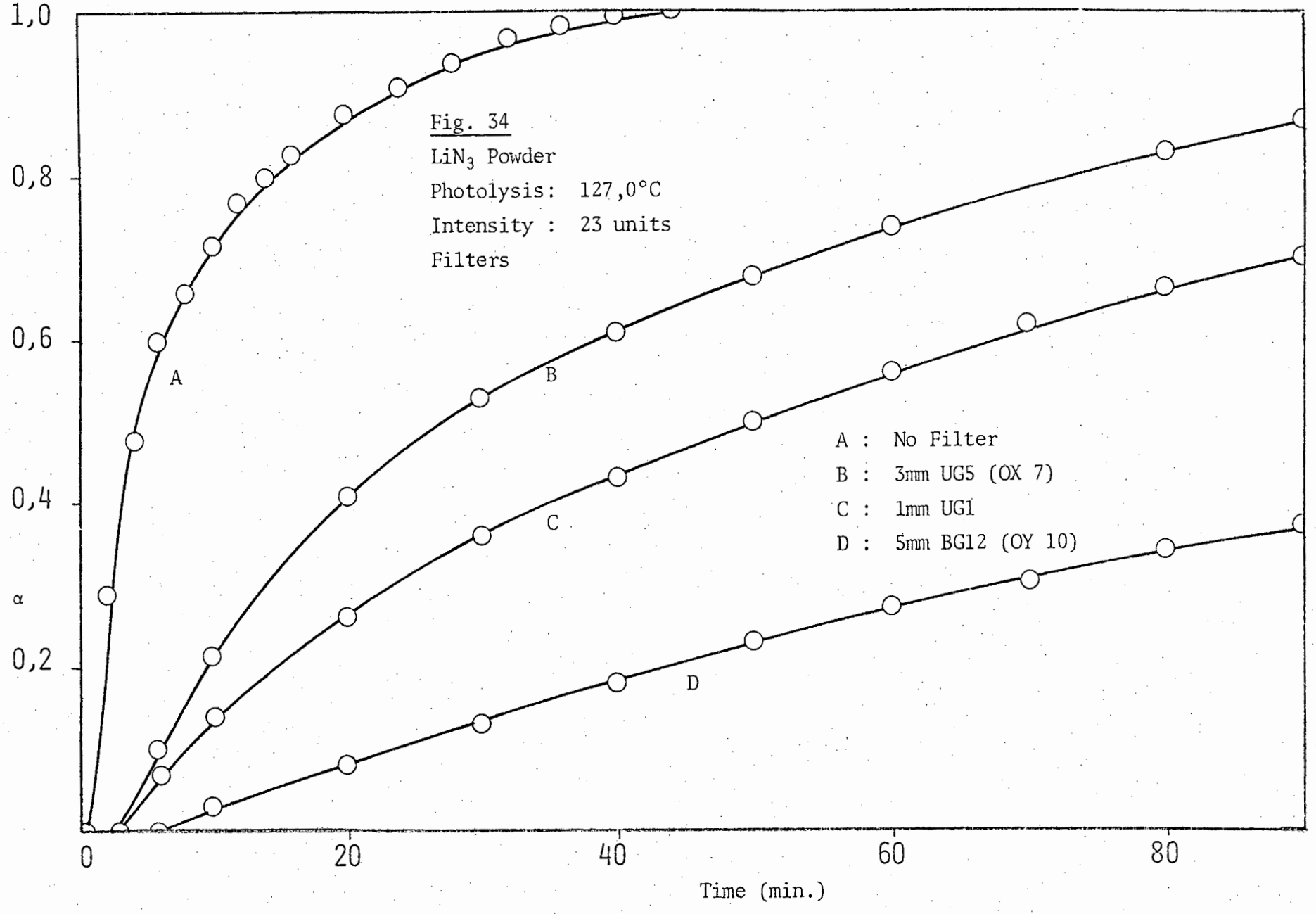

Fig. 34

LiN_3 Powder

Photolysis: 127,0°C

Intensity : 23 units

Filters

the rate of the reaction was the same as that expected for a purely photolytic decomposition. The reverse procedure of photolysis until the end of the induction period followed by thermal decomposition at the higher temperature showed a similar effect in that the thermal decomposition commenced without an induction period.

(ii) PHOTOLYSIS OF PELLETED CALCIUM AZIDE AT AMBIENT AND HIGHER TEMPERATURES

The photolysis of calcium azide pellets was studied in the temperature range 25,0°- 90,0°C. The pellets had a mass of±8,0 mg, were 5 mm in diameter and 0,25 mm thick. The method of preparing these pellets has been described in section 8(vi). The percentage composition was found to be 73,4%.

(ii.a) Reproducibility

The shape of the decomposition curve obtained from the photolysis of pelleted calcium azide differed from that obtained for photolyzed powder. The most marked change was a less distinctive acceleratory period. The inflection point in photolytic decompositions of pelleted calcium azide was at α = 0,27. Fig. 35 illustrates three typical α vs t curves for the photolysis of calcium azide pellets at a temperature of 55,0°C and a light intensity of 30,0 units. The induction period and acceleratory period are not as reproducible as in the case of the powdered form and, as will be seen from the reproducibility constants in Table 14, the reproducibility obtained is not as good as that for the powder. On a number of occasions the pellet fractured during or shortly after the end of the induction period. This was particularly frequent at high temperatures or light intensities. The fracturing was accompanied by a sudden burst of gas often to an α value of ≈0,50 and was followed by a smooth decomposition curve. Such decompositions were never used in this study.

(ii.b) Mathematical Analyses

The decomposition curve of the unfractured pellet was analyzed as for the powdered calcium azide. The inverse of the duration of the induction period was used as a rate constant for this part of the reaction.

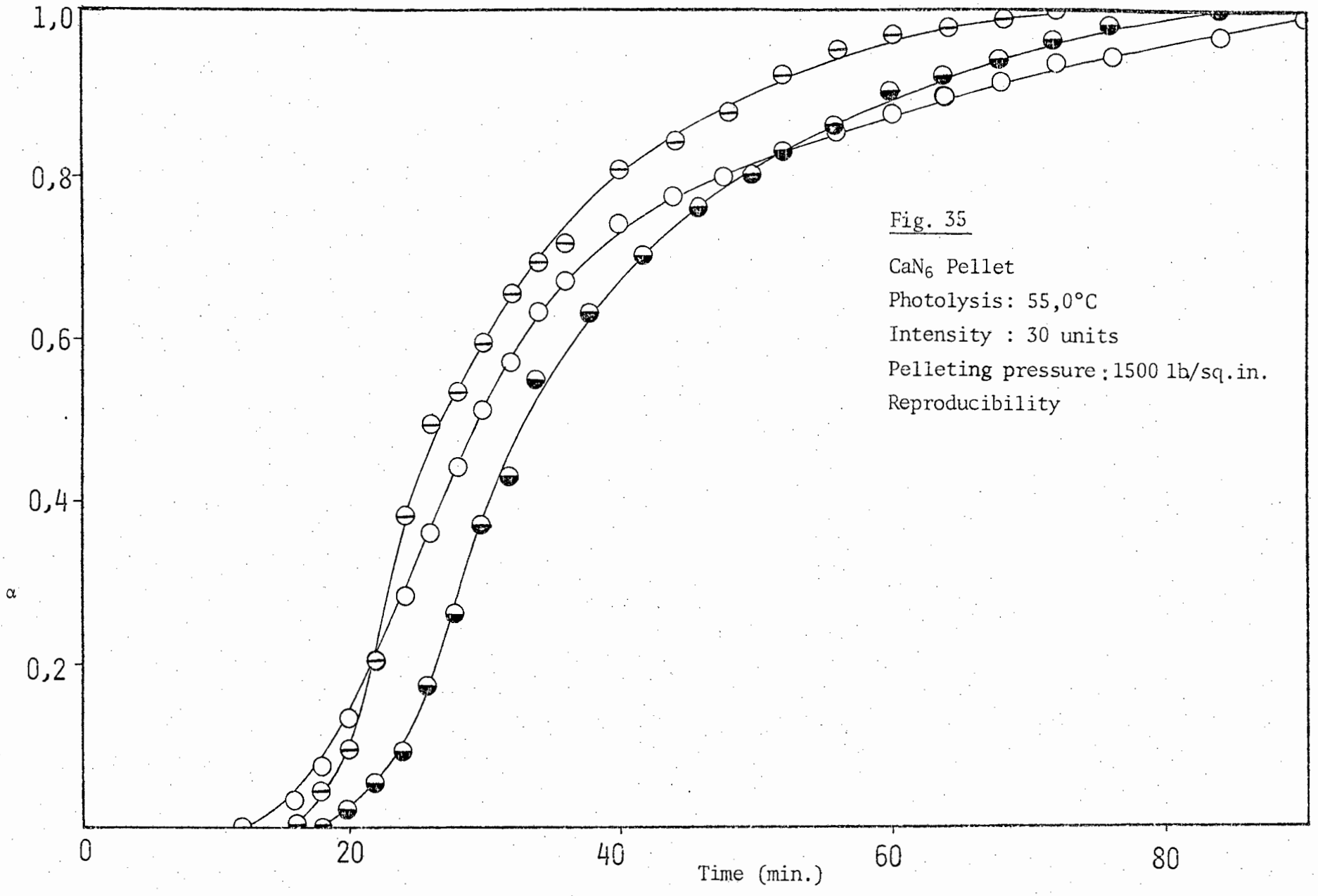

Fig. 35

CaN_6 Pellet
Photolysis: 55,0°C
Intensity : 30 units
Pelleting pressure : 1500 lb/sq.in.
Reproducibility

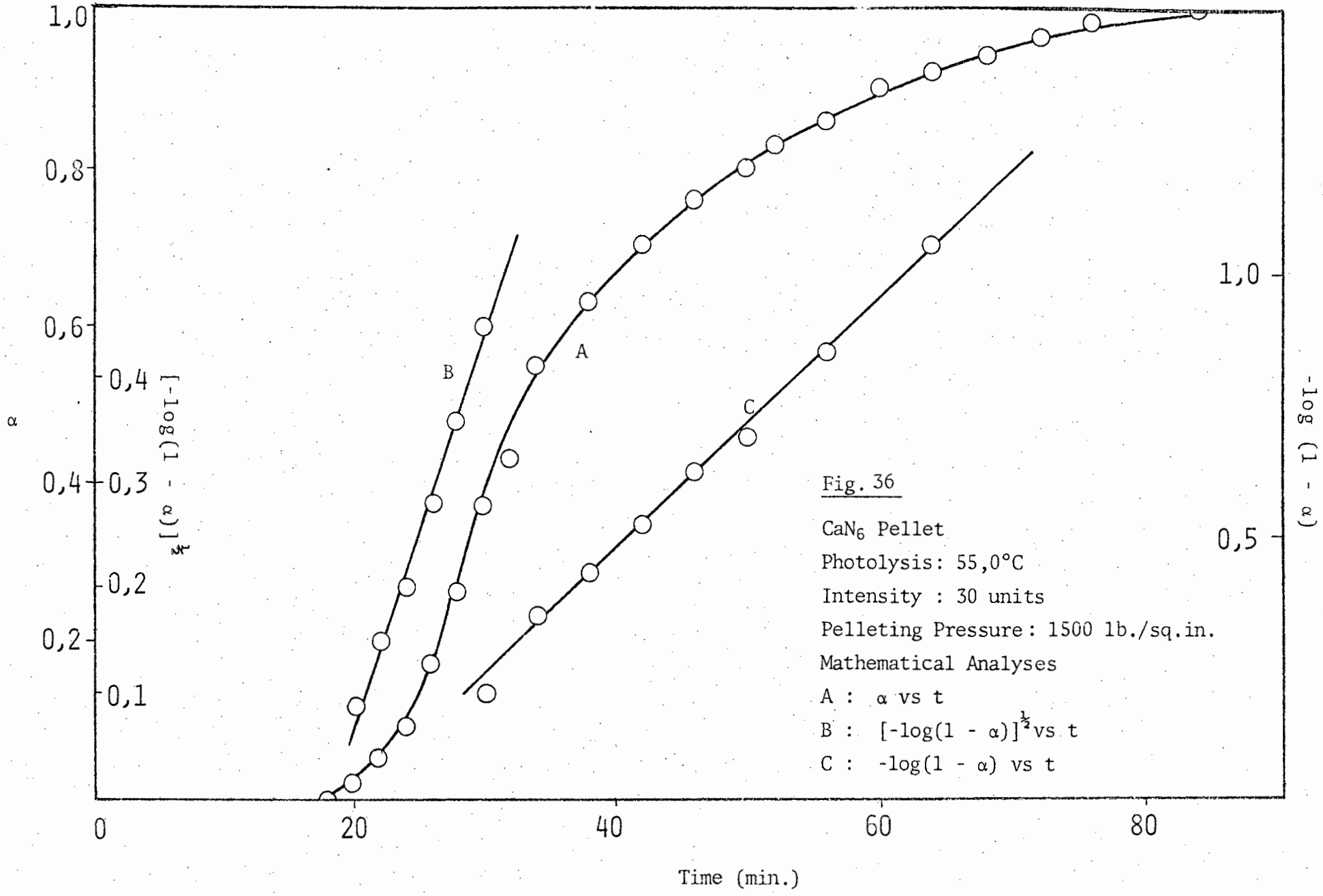

Fig. 36

CaN_6 Pellet
Photolysis: 55,0°C
Intensity : 30 units
Pelleting Pressure : 1500 lb./sq.in.
Mathematical Analyses
A : α vs t
B : $[-\log(1 - \alpha)]^{\frac{1}{2}}$ vs t
C : $-\log(1 - \alpha)$ vs t

The acceleratory reaction was found to obey the Avrami-Erofeyev equation with n = 2 and the decay reaction was analyzed using the unimolecular law. The former equation fitted the curve in the region $0,01 < \alpha < 0,27$ and the latter equation fitted the curve in the region $0,27 < \alpha < 0,90$. No significant difference was found to arise in the mathematical analyses of the decomposition curve when the pelleting pressure was varied. In general a pelleting pressure of 1500 lb./sq.in. was used but in some instances a pressure of 2000 lb./sq.in. was used mainly for the purpose of illustrating the similarity of the results. The rate constants obtained using the above methodsof analysis are listed in Table 14 and Fig. 36 shows a typical α vs t curve for the photolysis of a calcium azide pellet, with mathematical analyses, at a temperature of 55,0°C and a light intensity of 30,0 units.

Table 14 Reproducibility constants for the photolysis of calcium azide pellets.

Pelleting pressure: 1500 lb./sq.in.

Temperature °C	Intensity Units	Induction Period min.	$k_{acc} \times 10^2$ min^{-1}.	$k_{decay} \times 10^2$ min^{-1}.
55,0	30	17,0	4,6	7,0
		13,6	4,5	7,2
		17,2	3,7	4,5

(ii.c) Evaluation of activation energies

Activation energies were determined in the usual manner as described in the case of the powder. However, in view of the relatively poor reproducibility obtained in the case of the pelleted calcium azide, activation

energies were also determined using a split-run technique. This latter method implied necessarily a study of the decay reaction only. As previously mentioned the results of any decomposition in which a pellet fractured were discarded. The technique involved in the split-run study has already been described in Section 9(*i.c*) with respect to the study of the decay period of lithium azide powder. The necessary tests to ensure that interrupting a run had no adverse effect on the subsequent decomposition were performed. It was found that the decomposition continued as if no interruption had taken place.

Activation energies were determined for the induction period, the acceleratory period and the decay period for calcium azide pellets pressed at 1500 lb./sq.in. These pellets were decomposed separately and were photolyzed in the temperature range 25,0°- 50,0°C with a light intensity of 30,0 units. Table 15 gives the rate constants obtained from this set of runs. The activation energies were obtained using the Arrhenius equation and these values are listed in Table 18. Fig. 37 illustrates the plots of -log(I.P.), log k_{acc} and log k_{decay} against $10^3/T$ for the abovementioned light intensity and temperature range.

Activation energies were determined for the decay reactions at pelleting pressures of 1500 lb./sq.in. and 2000 lb./sq.in. respectively. It was assumed, from the results obtained for powdered calcium azide, that a change in activation energy would be expected at ±60,0°C. Activation energies were determined in the temperature range 30,0°- 60,0°C at light intensities of 41,0 and 30,0 units, and in the temperature range 60,0°- 90,0°C at light intensities of 30,0 and 12,0 units. Table 17 lists the rate constants for these various sets of runs and Table 18 gives the activation energies obtained for the various temperature ranges over the decay period by plotting log k_{decay} against $10^3/T$. Fig. 38 illustrates the plot of log k_{decay}

Table 15 Rate constants for the photolysis of calcium azide pellets (Separate runs)
Pelleting pressure: 1 500 lb./sq.in.
Temperature range : 25,0°- 50,0°C
Light intensity : 30,0 units

Temperature °C	Induction Period min.	$k_{acc} \times 10^2$ min^{-1}.	$k_{decay} \times 10^2$ min^{-1}.
25,0	44,2	1,30	1,20
30,0	35,6	1,60	1,60
35,0	42,0	1,40	1,20
40,0	31,2	2,00	3,40
45,0	22,6	1,70	1,40
50,0	18,0	4,50	5,60

Table 16 Rate constants for the photolysis of calcium azide pellets over the decay period (Split Runs)
Pelleting pressure: 2 000 lb./sq.in.
Temperature range : 30,0° - 80,0°C

Intensity Units	Temperature Range of Split Run °C	Temperature °C	$k_{decay} \times 10^2$ min^{-1}.
41	30,0 - 60,0	29,5	0,12
		35,0	0,13
		40,5	0,19
		47,0	0,32
		51,5	0,41
		56,0	0,44
15	60,0 - 80,0	61,0	0,24
		67,5	0,37
		73,5	0,71
		79,5	1,28

Table 17 Rate constants for the photolysis of calcium azide pellets over the decay period (Split Runs)
Pelleting pressure: 1 500 lb./sq.in.
Temperature range : 30,0° - 90,0°C

Intensity Units	Temperature Range of Split Run °C	Temperature °C	$k_{decay} \times 10^2$ min^{-1}.
41	30,0 - 60,0	34,9	0,62
		40,0	0,89
		45,5	1,15
		50,0	1,69
		55,5	6,83
		60,0	7,26
30	60,0 - 80,0	61,0	1,30
		66,7	1,50
		73,0	3,40
		79,0	6,70
30	30,0 - 60,0	30,0	0,16
		35,0	0,24
		40,0	0,33
		46,2	0,49
		50,0	0,74
		55,5	1,26
		61,0	3,27
12	60,0 - 90,0	60,0	0,12
		65,5	0,18
		72,0	0,31
		78,0	0,86
		84,0	1,99
		90,2	2,35

Table 18 Activation energies for the photolysis of calcium azide pellets

Pelleting pressure: 1 500 lb./sq.in.

Intensity Units	Temperature Range °C	Induction Period Kcal./mol.	Acceleratory Period Kcal./mol.	Decay Period Kcal./mol.
30	25,0 - 50,0	6,39	7,07	12,11
30	30,0 - 60,0	-	-	12,87
41	30,0 - 60,0	-	-	15,34
30	60,0 - 80,0	-	-	22,75
12	60,0 - 90,0	-	-	26,06

Table 19 Activation energies for the photolysis of calcium azide pellets (Split run)

Pelleting pressure: 2 000 lb./sq.in.

Intensity Units	Temperature Range °C	Decay Period Kcal./mol.
41	30,0 - 60,0	12,25
15	60,0 - 80,0	22,75

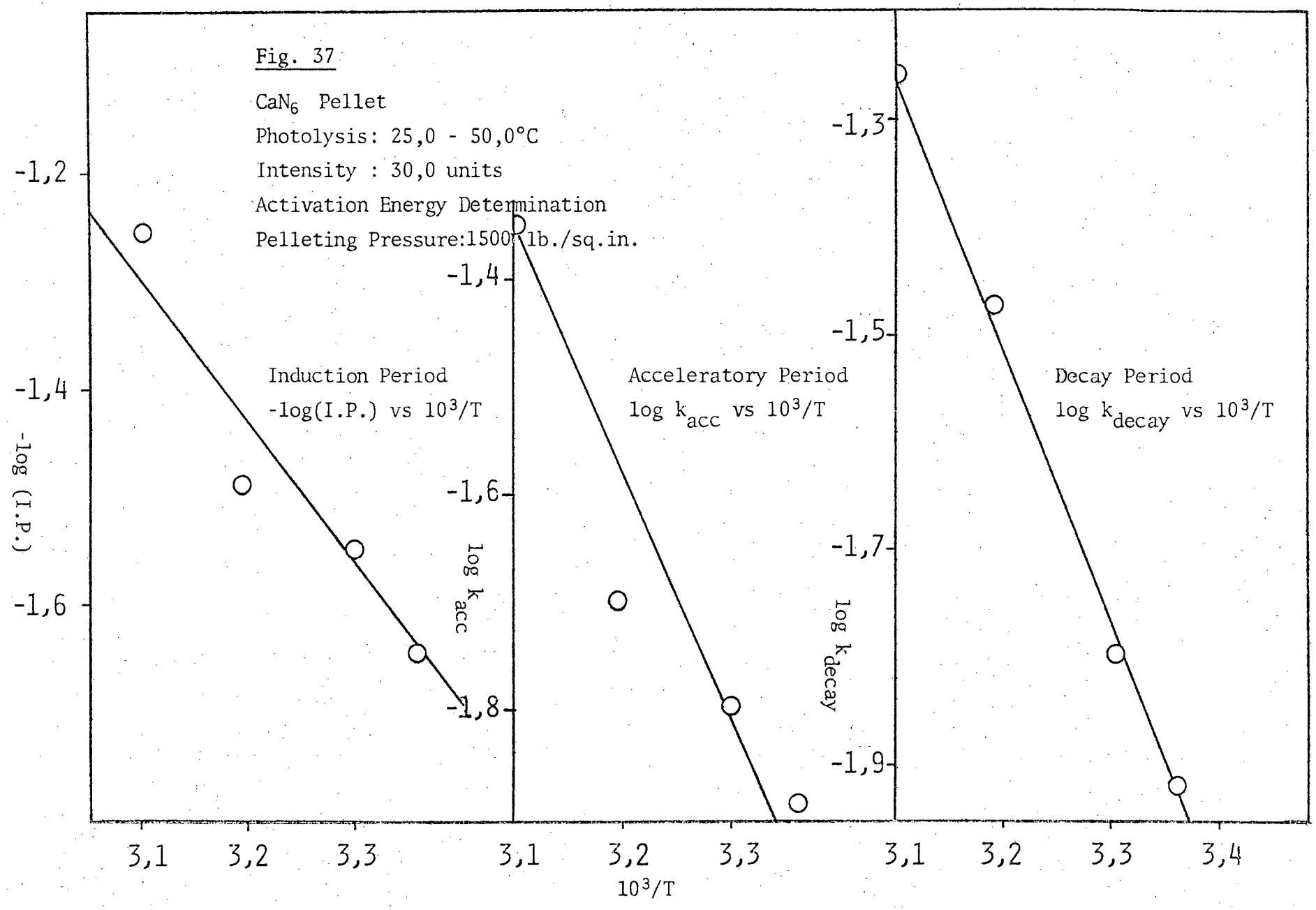
Fig. 37
CaN_6 Pellet
Photolysis: 25,0 - 50,0°C
Intensity : 30,0 units
Activation Energy Determination
Pelleting Pressure:1500 lb./sq.in.
Induction Period
-log(I.P.) vs $10^3/T$
Acceleratory Period
log k_{acc} vs $10^3/T$
Decay Period
log k_{decay} vs $10^3/T$
-log (I.P.)
log k_{acc}
log k_{decay}
$10^3/T$
-1,2
-1,4
-1,6
-1,8
-1,3
-1,5
-1,7
-1,9
3,1
3,2
3,3
3,4

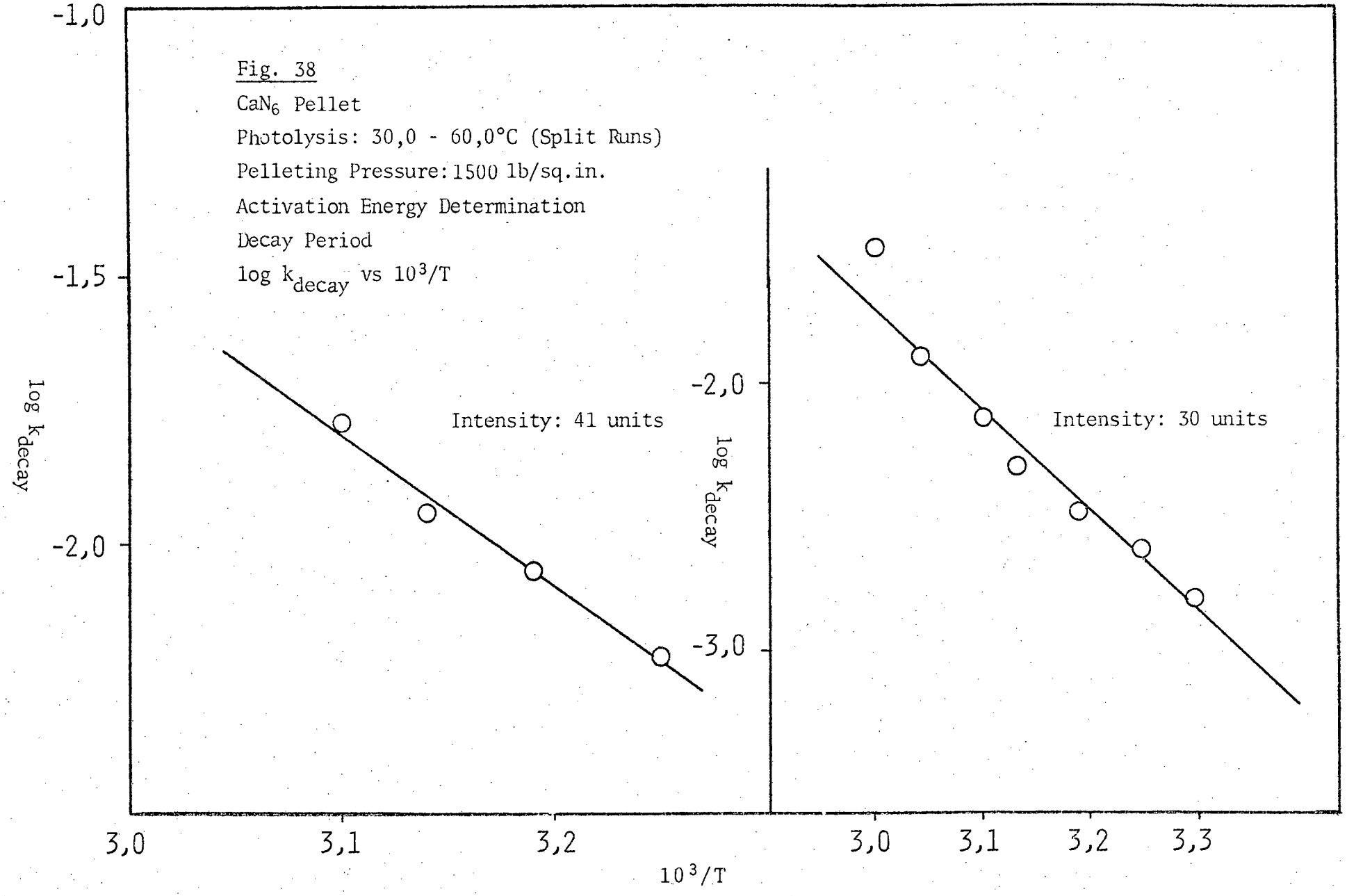

Fig. 38

CaN_6 Pellet

Photolysis: 30,0 - 60,0°C (Split Runs)

Pelleting Pressure: 1500 lb/sq.in.

Activation Energy Determination

Decay Period

log k_{decay} vs $10^3/T$

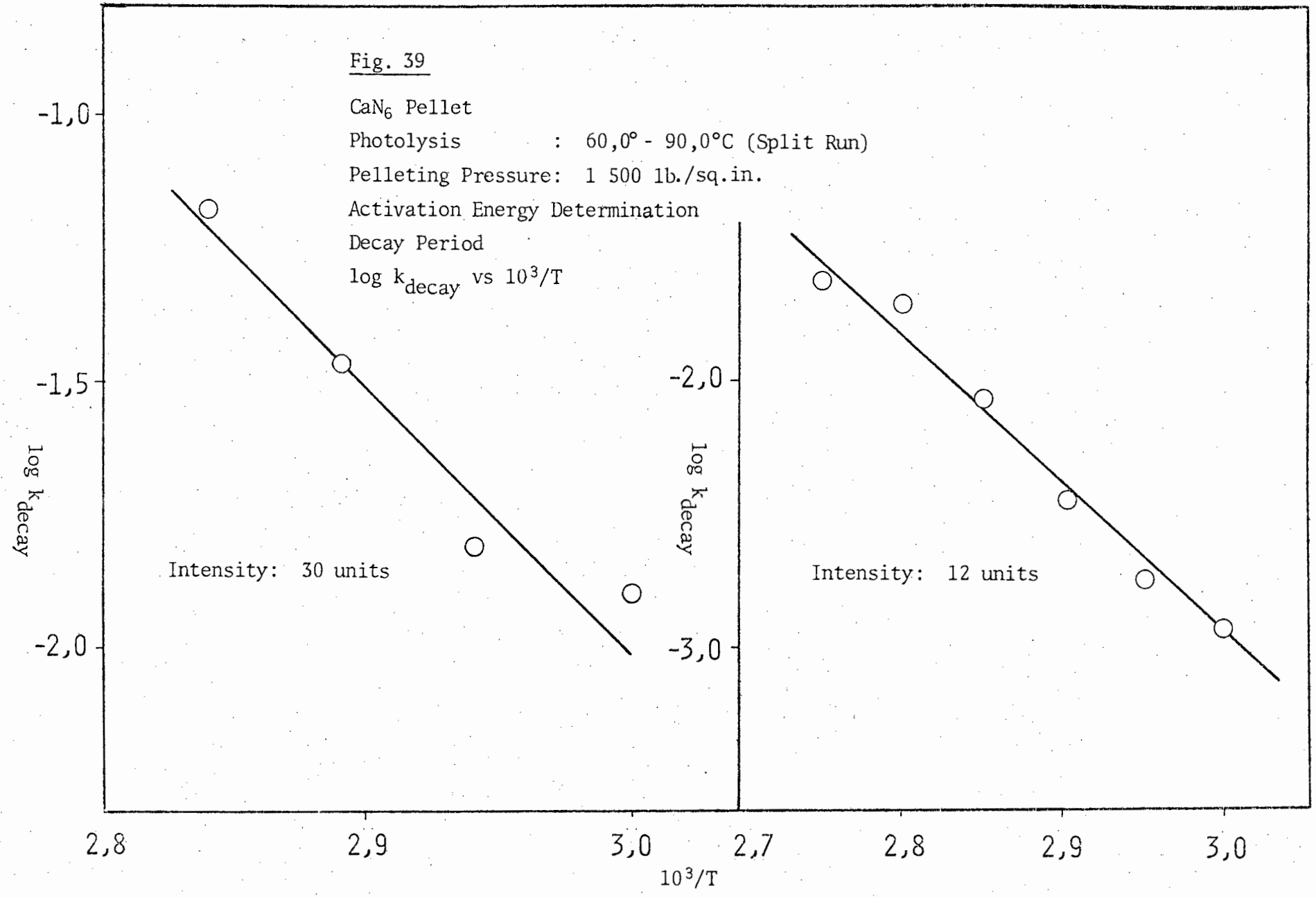
Fig. 39
CaN_6 Pellet
Photolysis : 60,0° - 90,0°C (Split Run)
Pelleting Pressure: 1 500 lb./sq.in.
Activation Energy Determination
Decay Period
log k_{decay} vs $10^3/T$
-1,0
-1,5
-2,0
log k_{decay}
Intensity: 30 units
-2,0
-3,0
log k_{decay}
Intensity: 12 units
2,8
2,9
3,0
2,7
2,8
2,9
3,0
$10^3/T$

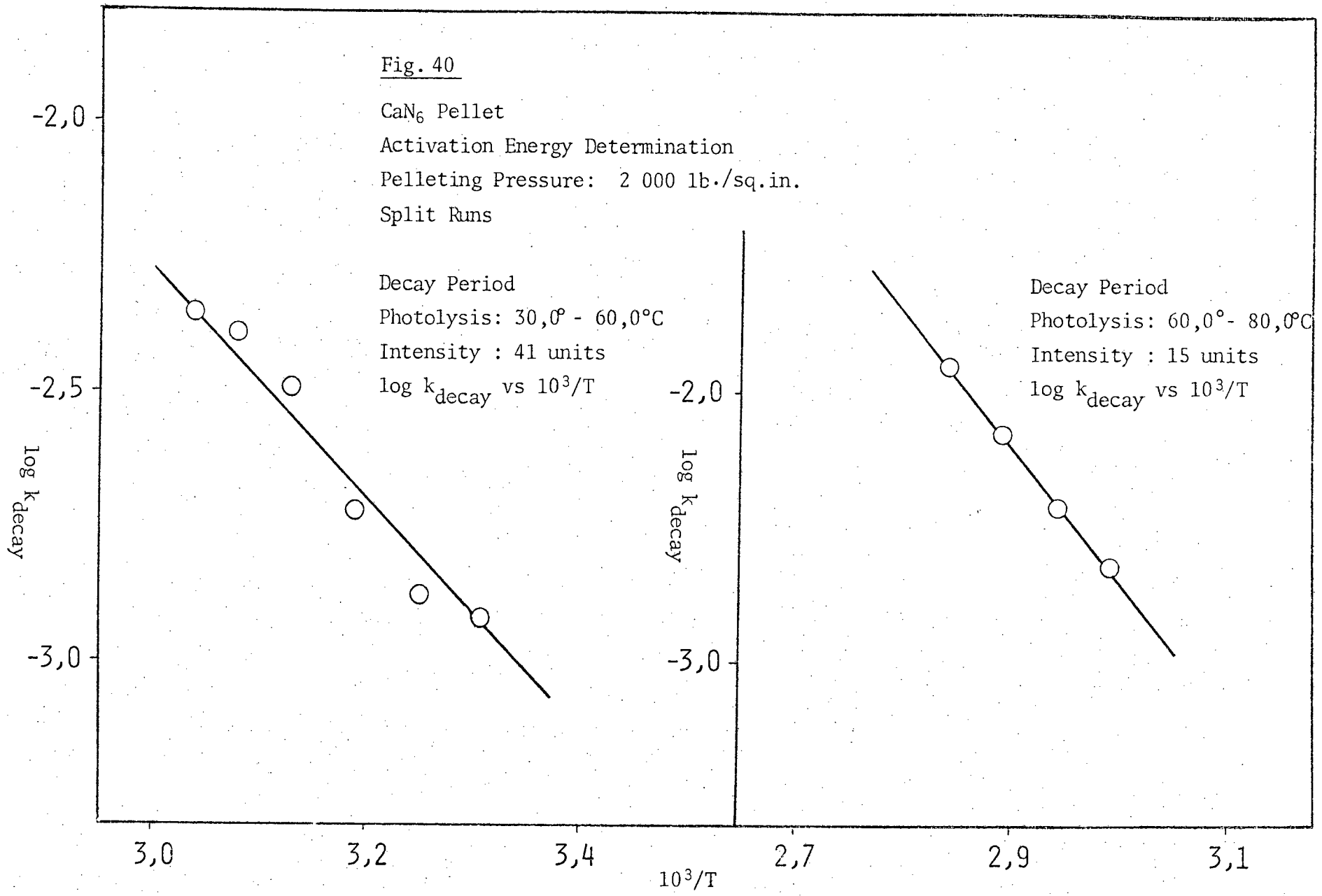
Fig. 40
CaN_6 Pellet
Activation Energy Determination
Pelleting Pressure: 2 000 lb./sq.in.
Split Runs
Decay Period
Photolysis: 30,0° - 60,0°C
Intensity : 41 units
log k_{decay} vs $10^3/T$
Decay Period
Photolysis: 60,0°- 80,0°C
Intensity : 15 units
log k_{decay} vs $10^3/T$
-2,0
-2,5
-3,0
log k_{decay}
3,0
3,2
3,4
2,7
2,9
3,1
$10^3/T$

vs $10^3/T$ for the temperature range 30,0° - 60,0°C and the relevant light intensities and Fig. 39 the same plots for the temperature range 60,0° - 90,0°C and the relevant light intensities.

Another set of split-runs over the decay period was carried out at a pelleting pressure of 2000 lb./sq.in. and over the temperature range of 30,0° - 80,0°C. The light intensity was 41,0 units in the range 30,0° - 60,0°C and 15,0 units in the range 60,0° - 80,0°C. Table 16 lists the rate constants obtained for the decay period. The activation energies for this decay reaction at a pelleting pressure of 2000 lb./sq.in. are listed in Table 19. Fig. 40 illustrates the plots of log k_{decay} against $10^3/T$ over the temperature range 30,0° - 60,0°C and 60,0° - 80,0°C at the abovementioned light intensities.

(ii.d) Visual observations

A pellet of calcium azide was observed visually during various stages of the photolytic decomposition. The decomposition took place at a temperature of 47,0°C and a light intensity of 20,0 units. The pelleting pressure was 1500 lb./sq.in. During the course of the induction period the surface facing the light source turned a brownish colour and the opposite side of the pellet showed the appearance of brown spots. By the end of the induction period the whole upper surface had turned dark brown whereas the lower surface was covered with large brown patches. At α = 0,30 the upper surface of the pellet had turned almost black on top and the lower surface dark brown in patches. By breaking a pellet open inside the cell at this stage, the interior of the pellet was seen to be white. At α = 0,62 the external surfaces of the pellet were black. At the end of the reaction, a broken pellet revealed some very small edges still white.

(ii.e)Interruption of a photodecomposition; dark rate determination

No measurable dark rate could be observed at any stage in a photolytic decomposition of a pellet of calcium azide in the given temperature range. The reaction ceased the moment the light was switched off but commenced as though no interruption had taken place once the light was switched on again.

(ii.f)Admittance of water vapour following an interruption

In order to investigate the presence of metallic nuclei, water vapour (17 torr pressure) was admitted at various stages of the decomposition. The method used was identical to that for 'water interruptions' in the powder. Pellets of calcium azide pressed at a pressure of 1500 lb./sq.in. were photolyzed at a temperature of 74,0°C and a light intensity of 2,5 units and subjected to water interruptions at time t = 0, midway along the induction period and at α values of 0,05; 0,41 and 0,48. Prior to the 'water interruptions' it was confirmed that an interruption in a decomposition had no effect on the subsequent reaction. As can be seen from Fig. 41 interruptions at points beyond the inflection point of α = 0,27 virtually caused the subsequent reaction to be completely destroyed. Interruptions at points prior to α = 0,27 caused the appearance of a new induction period, followed by a normal decomposition with a slight reduction in the value of the acceleratory and decay rate constants as well as of the final pressure. Interruptions at time t = 0 and during the induction period had virtually no effect on the subsequent reaction compared to that for an uninterrupted run.

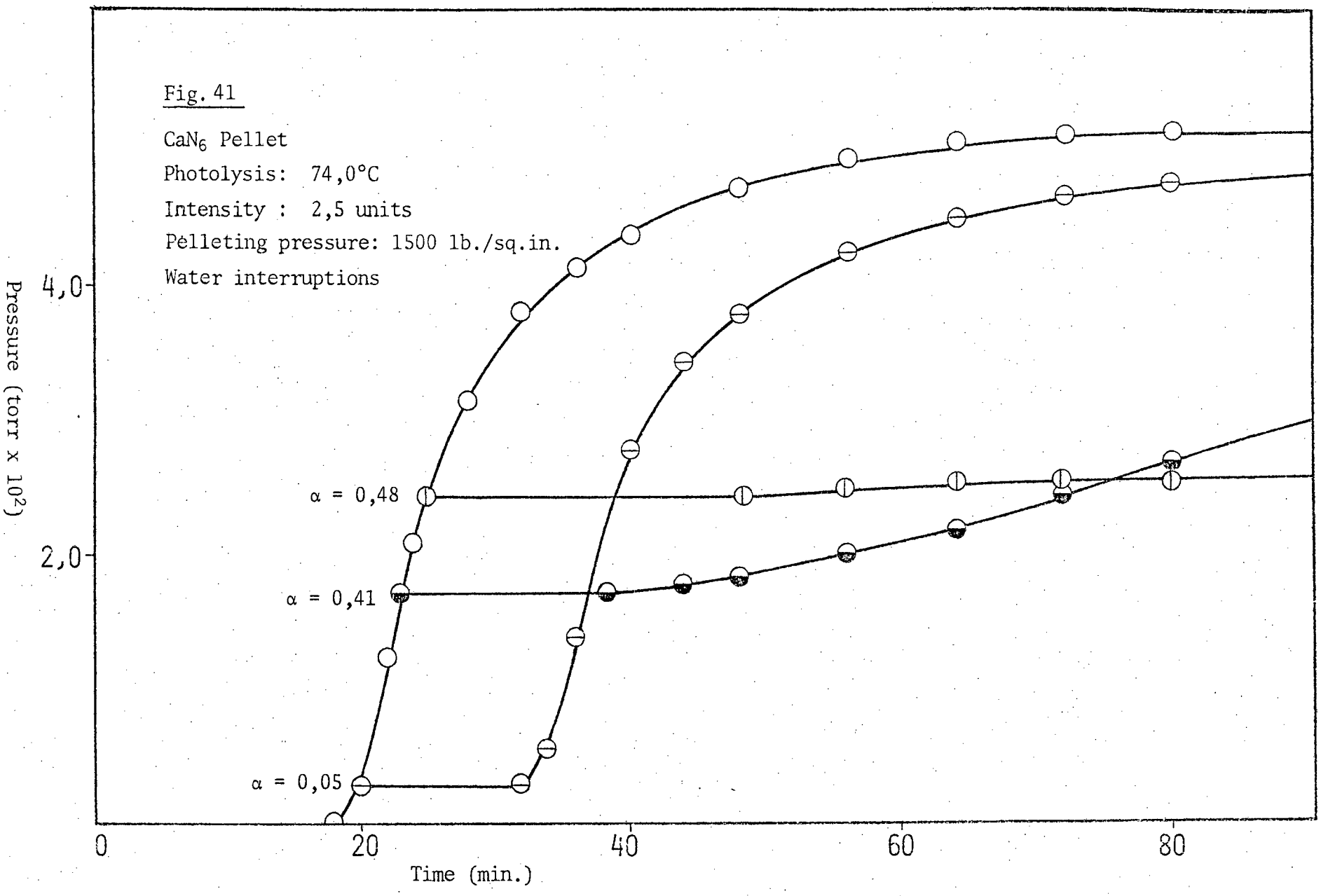
Fig. 41
CaN_6 Pellet
Photolysis: 74,0°C
Intensity : 2,5 units
Pelleting pressure: 1500 lb./sq.in.
Water interruptions
Pressure (torr x 10^2)
4,0
2,0
α = 0,48
α = 0,41
α = 0,05
0
20
40
60
80
Time (min.)

(iii) IRRADIATION OF POWDERED CALCIUM AZIDE WITH ULTRAVIOLET LIGHT DURING THERMAL DECOMPOSITION (CO-IRRADIATION)

Co-irradiation is the term used to describe photolytic decompositions which take place in the temperature range in which a dark rate exists i.e. where thermal decomposition is taking place at a comparable rate. The temperature range over which the co-irradiation of calcium azide was studied was 110,0° - 140,0°C. Irradiation with ultraviolet light during thermal decomposition had a marked effect on the rate of decomposition. The induction period decreased and the rates of the acceleratory and decay reactions increased. Fig. 42 depicts the difference between the thermal decomposition of calcium azide powder at 122,0°C and the co-irradiated decomposition of calcium azide powder at the same temperature and with a light intensity of 11,5 units. The abovementioned effects are clearly illustrated. The percentage decomposition was found to be 91,0%.

(iii.a) Reproducibility

To investigate the reproducibility of co-irradiated decompositions, three decompositions of calcium azide were carried out at a temperature of 122,0°C and a light intensity of 11,5 units. The resulting decomposition curves were superimposed and satisfactory reproducibility was obtained for the induction and acceleratory periods but the decay period did not yield equally good results. The curves obtained are illustrated in Fig. 43.

(iii.b) Mathematical analyses

The decomposition curves for co-irradiation of calcium azide powder were analyzed as for the photolyzed powdered and pelleted forms. The inverse of the duration of the induction period was considered as the rate constant for this part of the reaction. The acceleratory reaction was

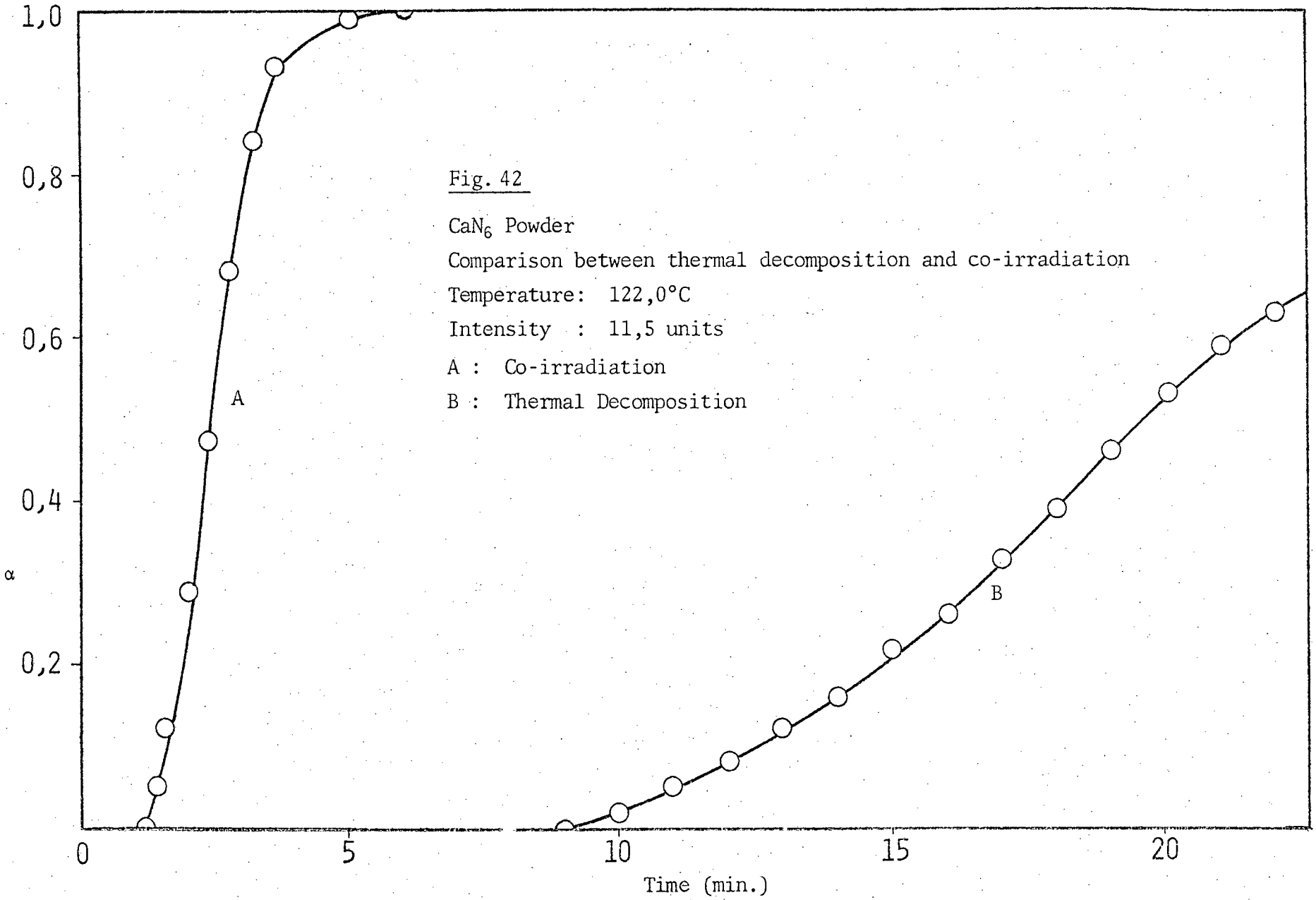

Fig. 42

CaN_6 Powder

Comparison between thermal decomposition and co-irradiation

Temperature: 122,0°C

Intensity : 11,5 units

A : Co-irradiation

B : Thermal Decomposition

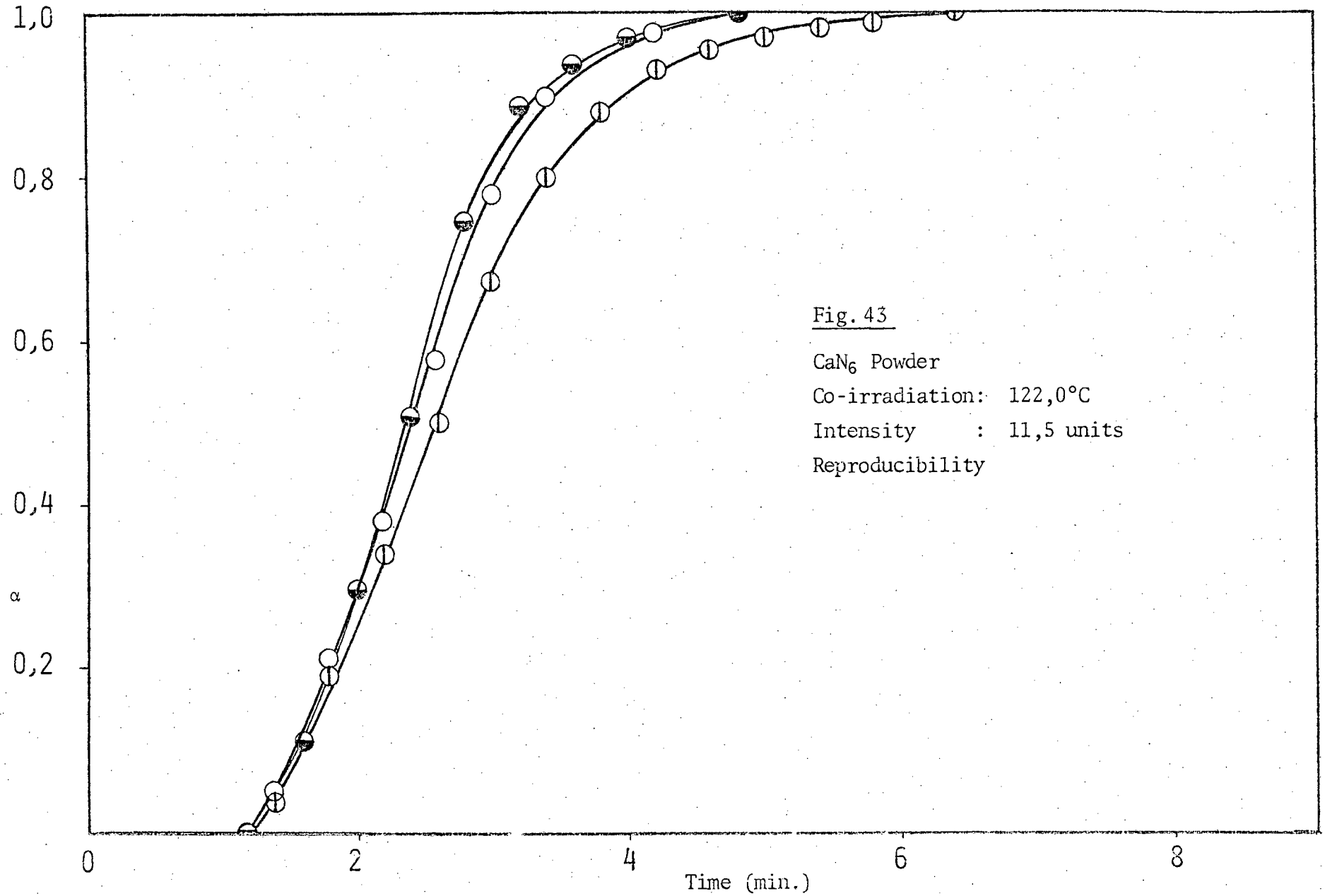

Fig. 43

CaN_6 Powder
Co-irradiation: 122,0°C
Intensity : 11,5 units
Reproducibility

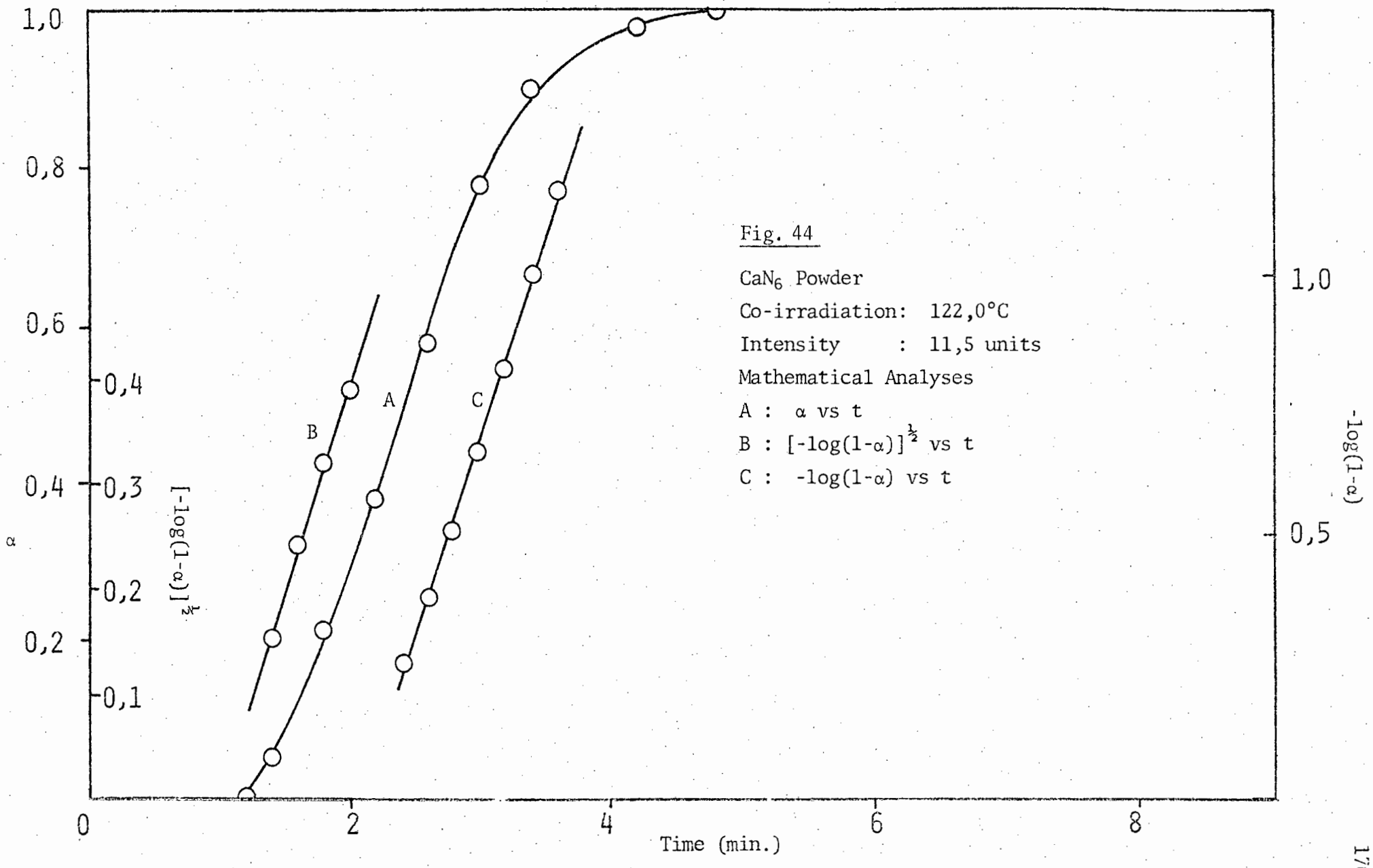

Fig. 44

CaN_6 Powder

Co-irradiation: 122,0°C

Intensity : 11,5 units

Mathematical Analyses

A : α vs t

B : $[-\log(1-\alpha)]^{\frac{1}{2}}$ vs t

C : $-\log(1-\alpha)$ vs t

analyzed using the Avrami-Erofeyev equation with n = 2 and the decay reaction was analyzed using the unimolecular law. The former equation fitted the decomposition curves in the range $0,05 < \alpha < 0,52$ and the latter equation fitted the curve in the range $0,52 < \alpha < 0,95$. The inflection point occurred at $\alpha = 0,52$. A typical α vs t curve for co-irradiated calcium azide at a temperature of 122,0°C and a light intensity of 11,5 units is illustrated in Fig. 44 together with analyses of the acceleratory and decay periods. Reproducibility constants using the method of analysis for the co-irradiated decompositions described in section 9*(iii.a)* are listed in Table 20.

Table 20 Reproducibility constants for co-irradiated calcium azide powder

Temperature °C	Intensity Units	Induction Period min.	$k_{acc} \times 10^2$ min^{-1}.	$k_{decay} \times 10^2$ min^{-1}.
122,5	11,5	1,20	5,31	7,20
		1,24	5,46	8,40
		1,22	5,39	5,40

(iii.c) Evaluation of activation energies

A series of runs was carried out in which the intensity was kept constant and the decomposition temperature varied over the temperature range 110,0° - 132,0°C. Rate constants were determined and the Arrhenius equation used in the usual manner to determine the values of the activation energies for the various stages of the reaction. Three sets of runs were carried out, each at a different but constant light intensity, in order to

Table 21 Rate constants for the co-irradiation of calcium azide powder

Temperature range : 109,0°- 132,0°C

Intensity Units	Temperature °C	Induction Period min.	$k_{acc} \times 10^1$ min^{-1}.	$k_{decay} \times 10^1$ min^{-1}.
7,0	110,0	3,26	1,36	1,88
	114,6	2,20	1,77	2,31
	119,9	1,68	3,02	5,59
	125,9	1,17	4,88	7,72
	131,5	0,68	6,89	11,40
11,5	110,5	2,51	2,44	2,75
	113,9	2,00	3,20	4,14
	120,0	1,40	5,06	6,08
	125,4	0,86	6,81	9,20
	131,0	0,66	8,10	1,64
17,5	109,0	2,20	1,54	3,52
	113,1	2,15	2,13	5,10
	120,0	1,20	4,05	8,59
	124,7	1,07	4,38	11,20
	128,5	0,80	7,10	13,80

examine the effect of a more intense radiation on the activation energy of the co-irradiated compound. Activation energies were thus determined using light intensities of 7,0; 11,5 and 17,5 units respectively. Higher intensities were of no value since the decomposition took place so rapidly that the time taken for the reaction to go to completion was less than the time taken for the pressure equilibration throughout the line. Table 21 lists the rate constants obtained for the co-irradiated decomposition of calcium azide powder in the temperature range 110,0° - 132,0°C and light intensities of 7,0; 11,5 and 17,5 units. Table 22 lists the activation energies obtained at each light intensity. As can be seen from these values, the activation energy tends to decrease slightly in all stages of the reaction with an increase in light intensity. Fig. 45 shows plots of the logarithms of the rate constants against the reciprocals of the absolute temperatures at a light intensity of 7,0 units in the temperature range 110,0°- 132,0°C. Fig. 46 shows a similar plot at a light intensity of 11,5 units in the temperature range 110,0°- 131,0°C, and Fig 47 a plot at a light intensity of 17,5 units in the temperature range 109,0°- 130,0°C.

Table 22 Activation energies for the co-irradiation of calcium azide powder.

Temperature range: 110,0° - 140,0°C

Intensity Units	Induction Period Kcal./mol.	Acceleratory Period Kcal./mol.	Decay Period Kcal./mol.
7	21,31	24,01	27,51
11,5	20,65	22,64	25,60
17,5	14,04	23,18	21,66

Fig. 45

CaN_6 Powder

Co-irradiation: 110,0°- 132,0°C

Intensity : 7,0 units

Activation Energy Determination

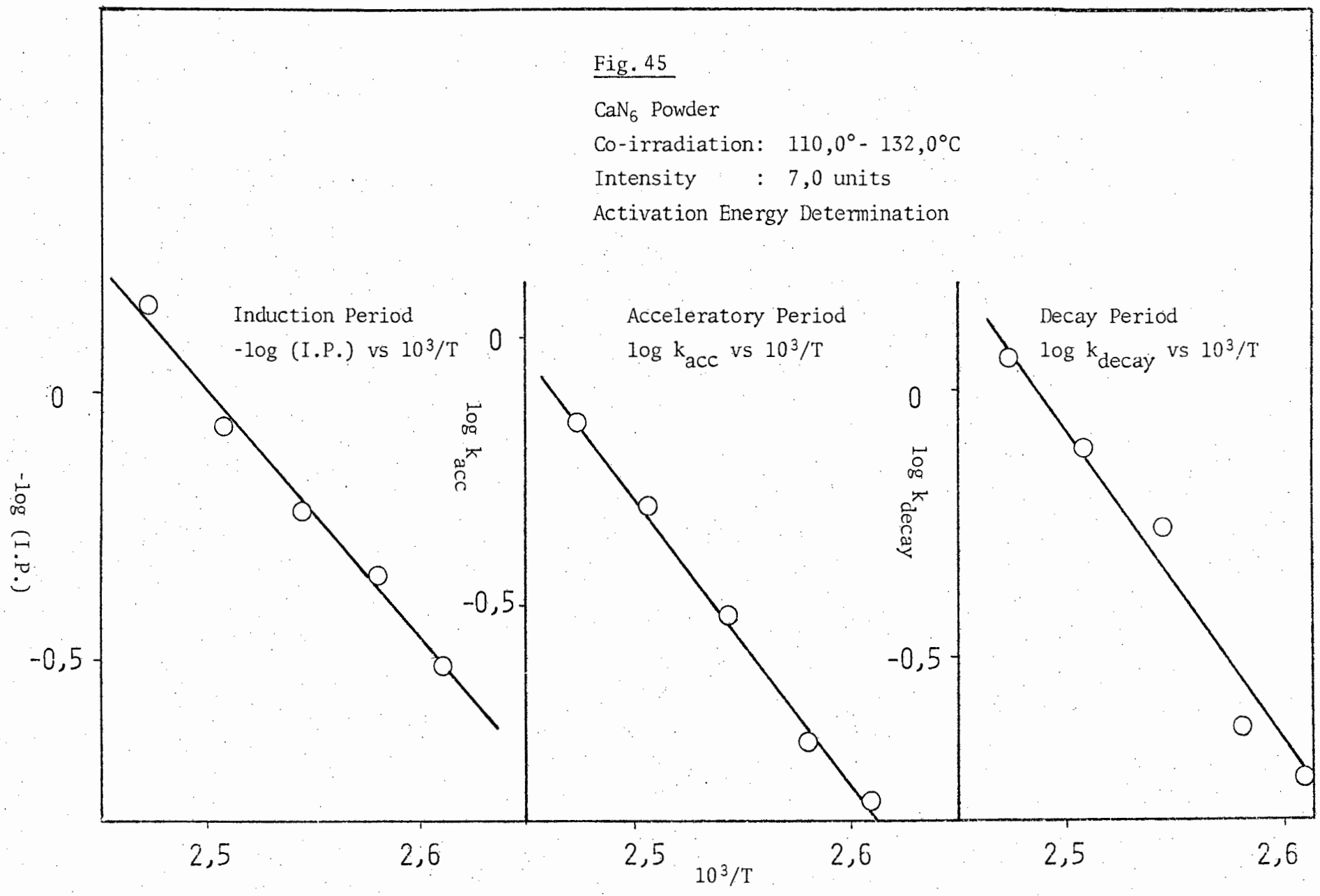

Fig. 46

CaN_6 Powder

Co-irradiation: 110,0° - 131,0°C

Intensity : 11,5 units

Activation Energy Determination

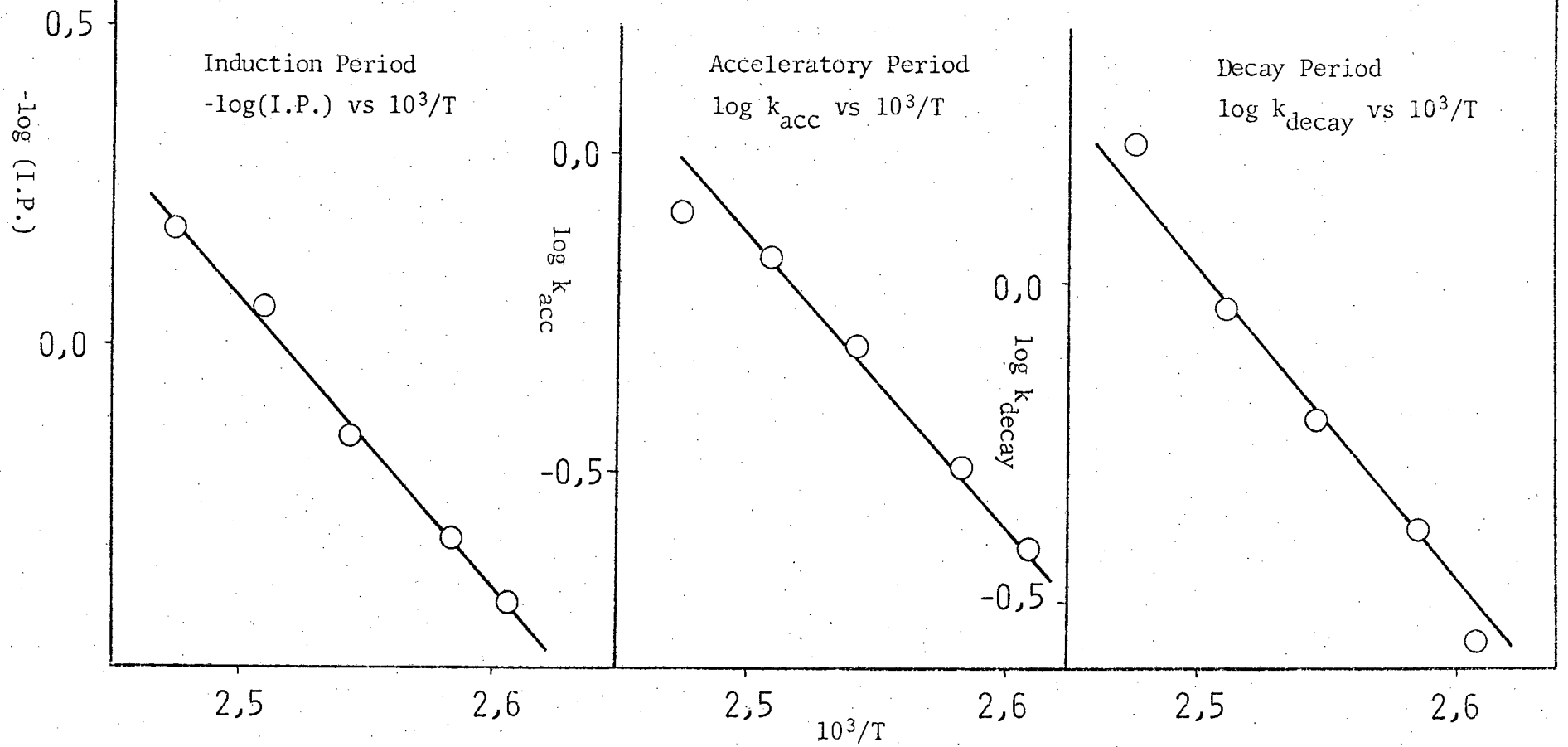

Fig. 47

CaN_6 Powder

Co-irradiation: 109,0° - 130,0°C

Intensity : 17,5 units

Activation Energy Determination

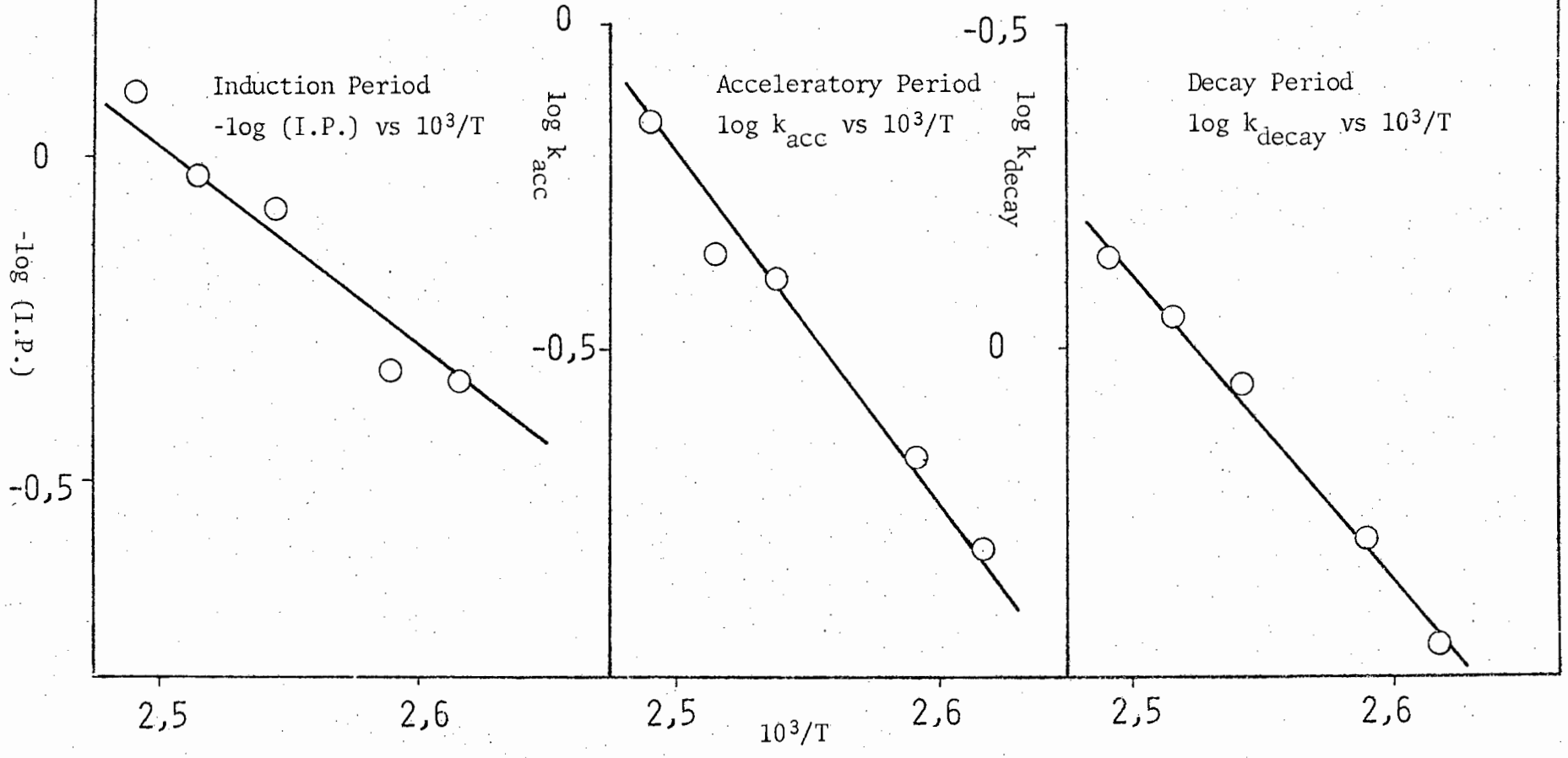

(iii.d) The effect of variation of intensity of ultraviolet light source

The molecularity of the mechanism involved in the co-irradiation of calcium azide powder was determined by examining a series of decompositions at a constant temperature of 115,0°C at various light intensities. In this way it was possible to determine the dependence of the induction period and the subsequent acceleratory and decay reactions of co-irradiated calcium azide on the intensity of the light source. The method involved in this study has been described in section 8.

The molecularity, m, of the process of co-irradiation was calculated from the equation

$$k = I^m + c.$$

For the purpose of determining m, c was ignored and the equation rewritten in the form

$$\log k = m \log I.$$

A plot of log k vs log I yielded a graph of slope m which was determined by a method of least squares. Table 23 lists the rate constants at various light intensities and Table 24 gives the value of m for each period. Plots of k vs I^m for each period are shown in Fig. 48.

(iii.e) Visual observations

A sample of calcium azide powder, decomposed at 120,0°C and at a light intensity of 7,0 units, was observed at various stages of decomposition. At the end of the induction period the powder had started to darken in colour and at $\alpha \approx 0,20$ the upper surface of the sample had turned a greyish brown colour. The colour then changed rapidly to dark brown/black and at α values beyond 0,60 the sample had turned black throughout. No further changes could be observed visually during the remainder of the decomposition.

Table 23 Rate constants for co-irradiated calcium azide powder at various light intensities

Temperature: 115,0°C

Intensity Units	Induction Period min.	$k_{acc} \times 10^1$ min^{-1}.	$k_{decay} \times 10^1$ min^{-1}.
10,0	2,04	1,69	1,78
13,0	1,76	2,09	3,03
15,3	1,73	1,99	2,49
20,0	1,35	3,14	2,84
24,5	1,16	3,66	4,88
28,0	1,14	4,90	6,32

Table 24 Value of m in the equation $k = I^m + c$ for co-irradiated calcium azide powder

Temperature °C	Induction Period	Acceleratory Period	Decay Period
115,0	0,61	1,02	1,07

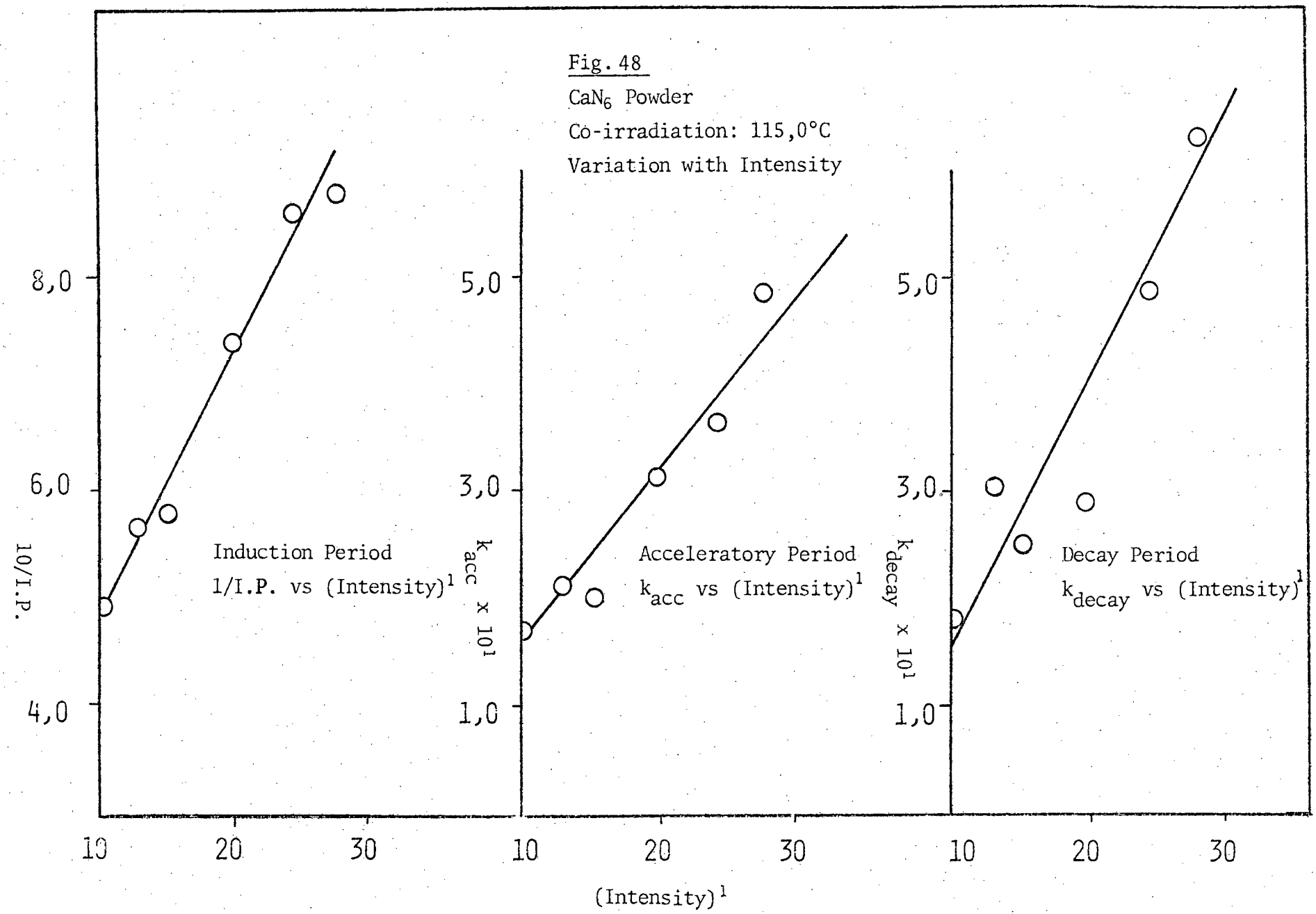

Fig. 48

CaN_6 Powder

Co-irradiation: 115,0°C

Variation with Intensity

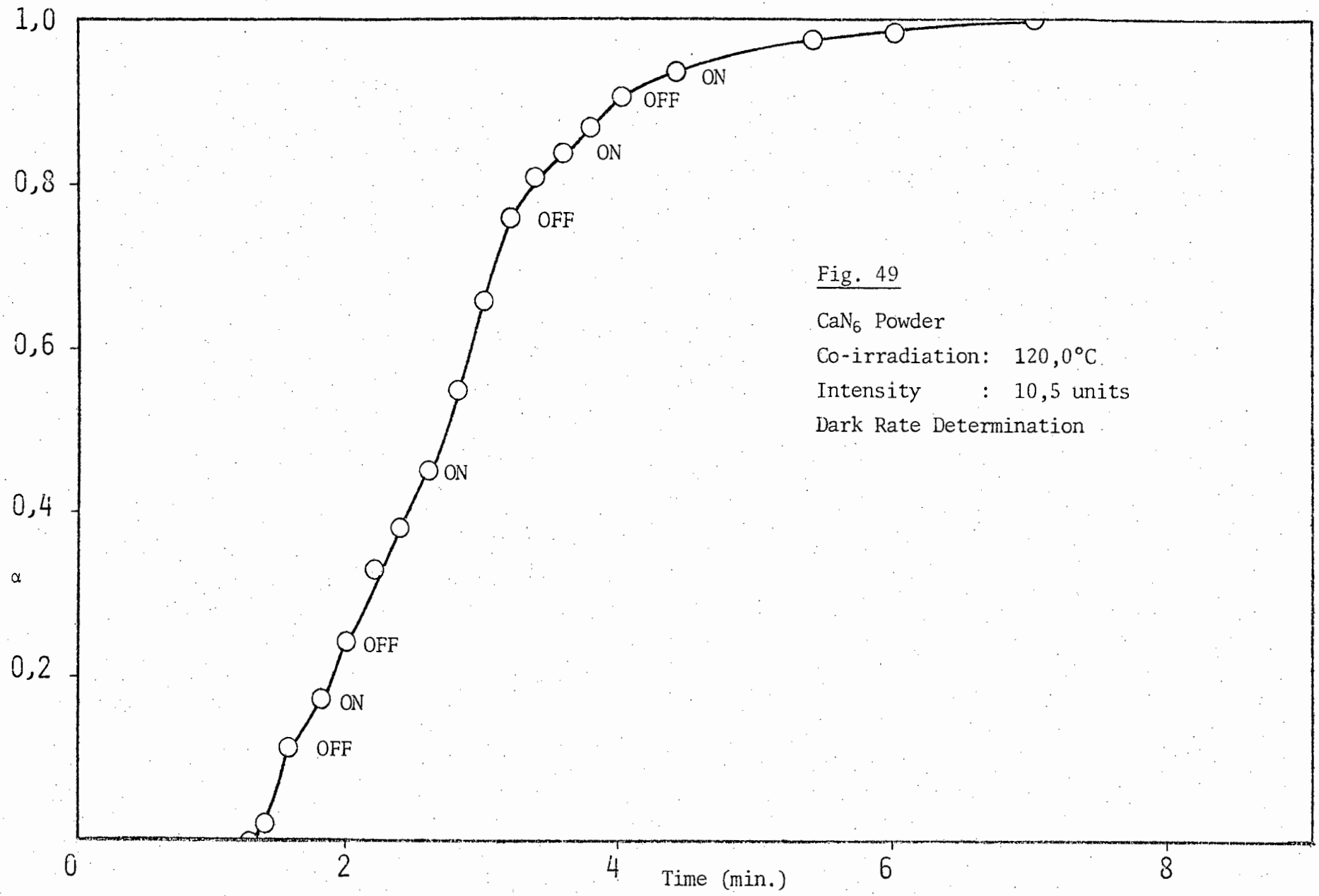

Fig. 49

CaN_6 Powder
Co-irradiation: 120,0°C
Intensity : 10,5 units
Dark Rate Determination

(iii.f) Interruption of a co-irradiated decomposition: dark rate determination

It was found that at temperatures greater than ±100,0°C decomposition did not cease when the source of ultraviolet radiation was removed i.e. the dark rate was considerable. It was also observed that when the ultraviolet source was removed, decomposition did not continue as would have been expected had the initial decomposition been entirely thermal. This was a result of the pre-irradiation effect which the ultraviolet radiation had on the subsequent thermal decomposition. Fig. 49 illustrates the dark rates at a decomposition temperature of 120,0°C. The light intensity used in this study was 10,5 units.

(iii.g) Admittance of water vapour following an interruption

At various stages of the co-irradiated decomposition of calcium azide, water vapour (17 torr pressure) was introduced in order to investigate the presence of metallic nuclei. The method used in this study has already been described in section 9 *(i.g)*. A decomposition temperature of 115,0°C and a light intensity of 2,0 units were used for the 'water interruptions'. The water vapour was allowed to react for 1 min. at the point of interruption. The water vapour was introduced at time t = 0 and at α values of 0,01; 0,10; 0,38 and 0,44.

The results were similar to those found for the corresponding reaction in the photolytic temperature range. Water vapour introduced at t = 0 had no effect on the subsequent co-irradiated reaction i.e. the run continued as though no interruption had occurred. Water vapour introduced at the end of the induction period and at positions further along the decomposition curve caused the subsequent reaction to proceed after a new induction period. The length of this induction period was initially shorter than that of an uninterrupted run but became progressively longer as the point of interruption along the decomposition curve increased. The acceleratory and decay

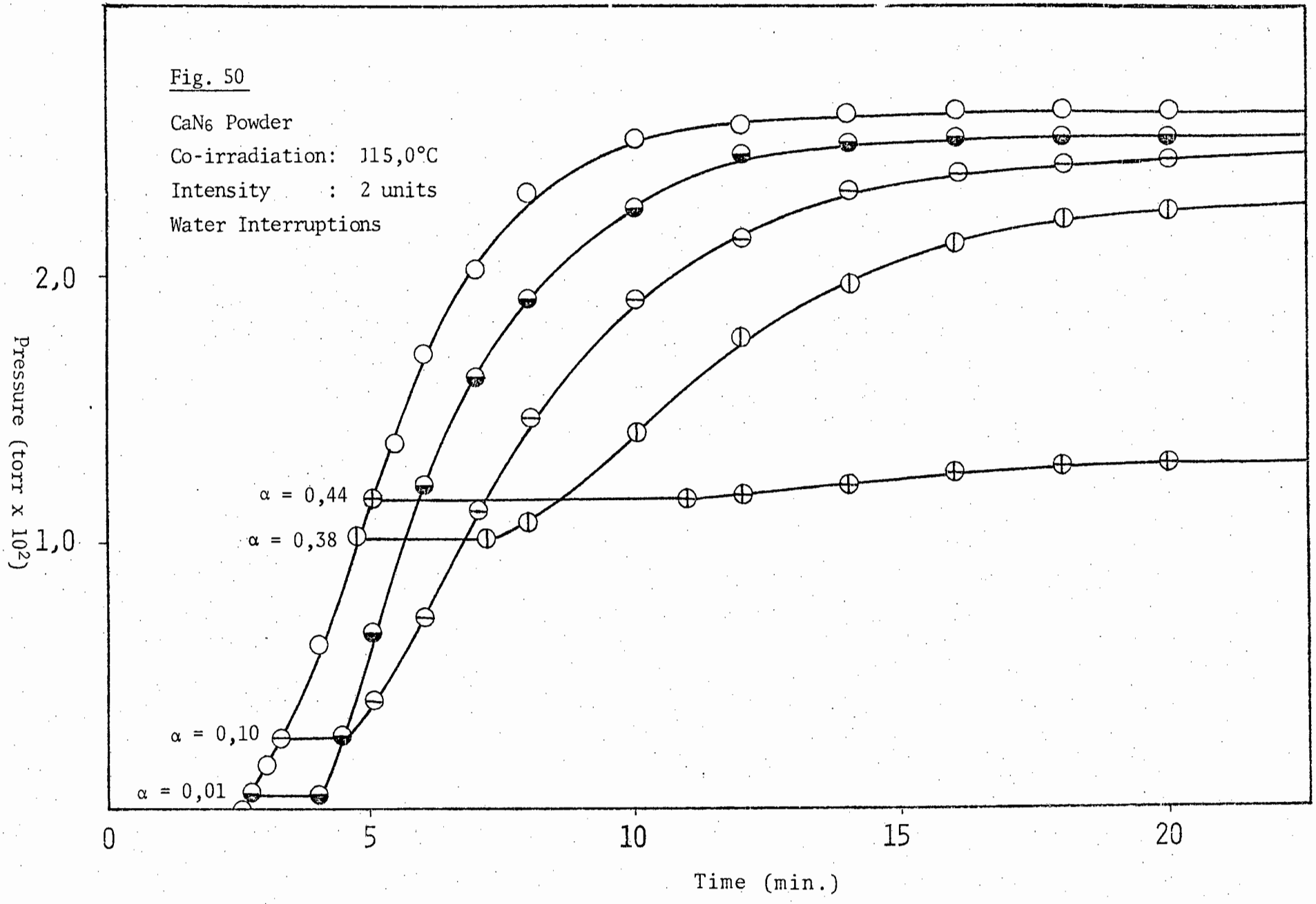
Fig. 50
CaN6 Powder
Co-irradiation: 115,0°C
Intensity : 2 units
Water Interruptions
2,0
1,0
Pressure (torr x 10²)
α = 0,44
α = 0,38
α = 0,10
α = 0,01
0
5
10
15
20
Time (min.)

reactions were also progressively slower than than of an uninterrupted decomposition. Water vapour introduced at the inflection point and beyond destroyed the subsequent reaction. The final pressure of the reactions following a 'water interruption' was much lower than that of an uninterrupted decomposition. The results are illustrated in Fig. 50 where the curve is a plot of pressure, not α, against time in order to illustrate the effect of introducing water vapour on the final pressure.

(iii.h) The effect of filtering the high intensity arc with blue and ultraviolet transmission filters

The effect of filtering the high intensity ultraviolet light source with various Schott filters was investigated in order to determine the most effective wavelengths for the co-irradiation of calcium azide. A decomposition temperature of 115,0°C and a light intensity of 20,0 units was used. The filters used and their Chance equivalents as well as the intensity of the transmitted wavelength are listed in Table 13 in section 9 *(i.h)*.

The results are shown in Fig. 51. The rate of the reaction decreased in the order of 3 mm UG5 - 1 mm UG1 - 5 mm BG12.

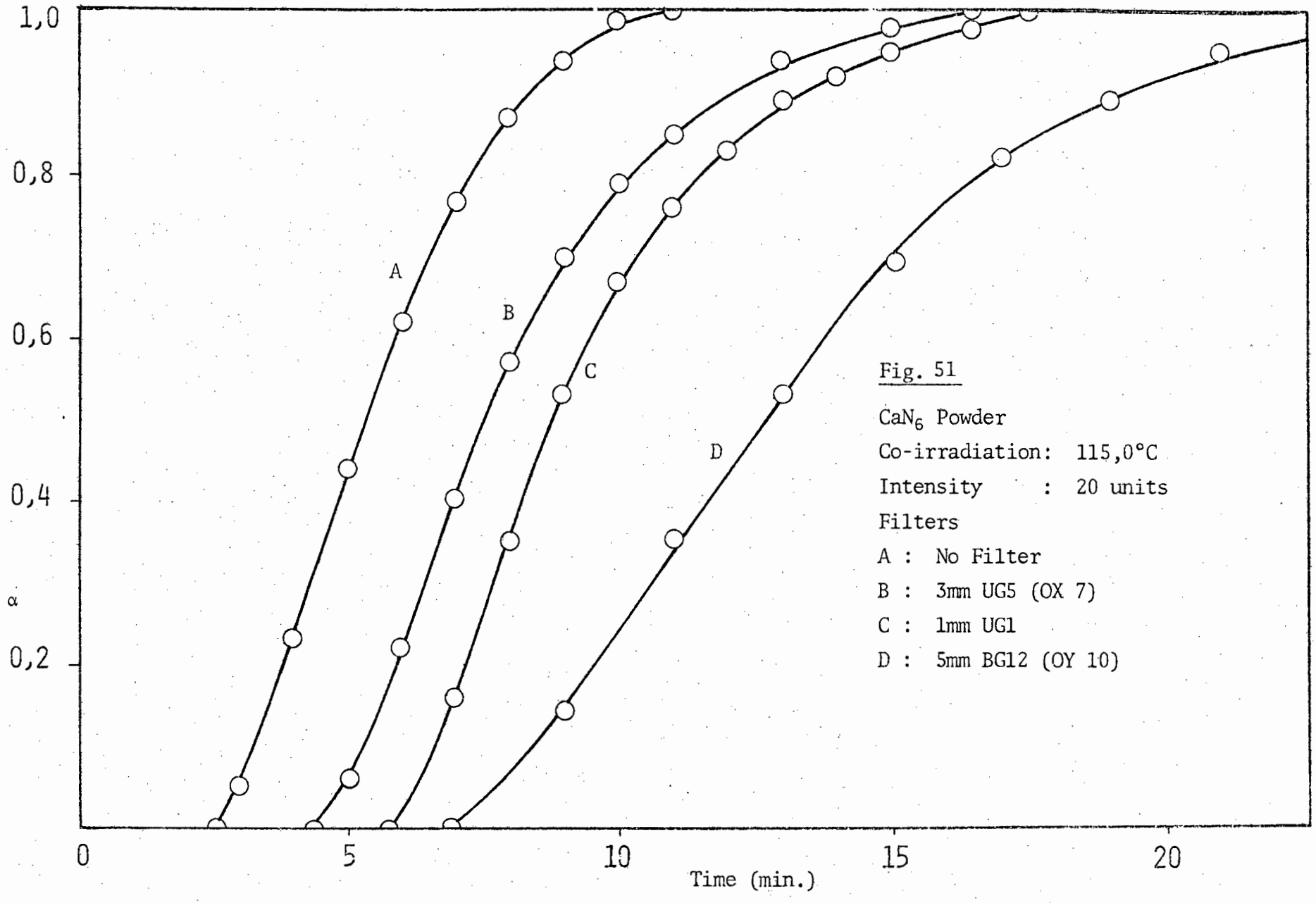

Fig. 51

CaN_6 Powder
Co-irradiation: 115,0°C
Intensity : 20 units
Filters
A : No Filter
B : 3mm UG5 (OX 7)
C : 1mm UG1
D : 5mm BG12 (OY 10)

(iv) IRRADIATION OF PELLETED CALCIUM AZIDE WITH ULTRAVIOLET LIGHT DURING THERMAL DECOMPOSITION (CO-IRRADIATION)

Irradiation of pelleted calcium azide with ultraviolet light during thermal decomposition was found to have the same effect as found with co-irradiated powder. The induction period shortened and there was an increase in the rate of the acceleratory and decay reactions. These decompositions were carried out on pellets of weight ±8,0 mg and diameter 5,0 mm and over the temperature range 100,0°- 130°C. A considerable dark rate reaction was observed in this temperature range due to the thermal decomposition of the pellet. Fig. 52 illustrates the difference between thermal decomposition and co-irradiation of calcium azide pelleted at a pressure of 1500 lb./sq.in. The percentage decomposition varied but on the average was 78,0%.

(iv.a) Reproducibility and mathematical analyses

The shapes of the co-irradiated decomposition curves of pellets of calcium azide decomposed at a temperature of 103,0°C and a light intensity of 0,2 units are shown in Fig. 53. The curves show the usual induction period followed by an acceleratory and a decay reaction.

The mathematical analyses for the curves were the same as those found for co-irradiated powder i.e. for the acceleratory period the Avrami-Erofeyev equation was used with n = 2 and for the decay period the unimolecular law. The inflection point occurred at $\alpha = 0,44$. The Avrami-Erofeyev equation fitted the curve in the range $0,02 < \alpha < 0,44$ and the unimolecular law in the range $0,44 < \alpha < 0,93$.

Fig. 54 shows a typical α vs t curve with analyses for a pellet of calcium azide at a decomposition temperature of 103,0°C and a light

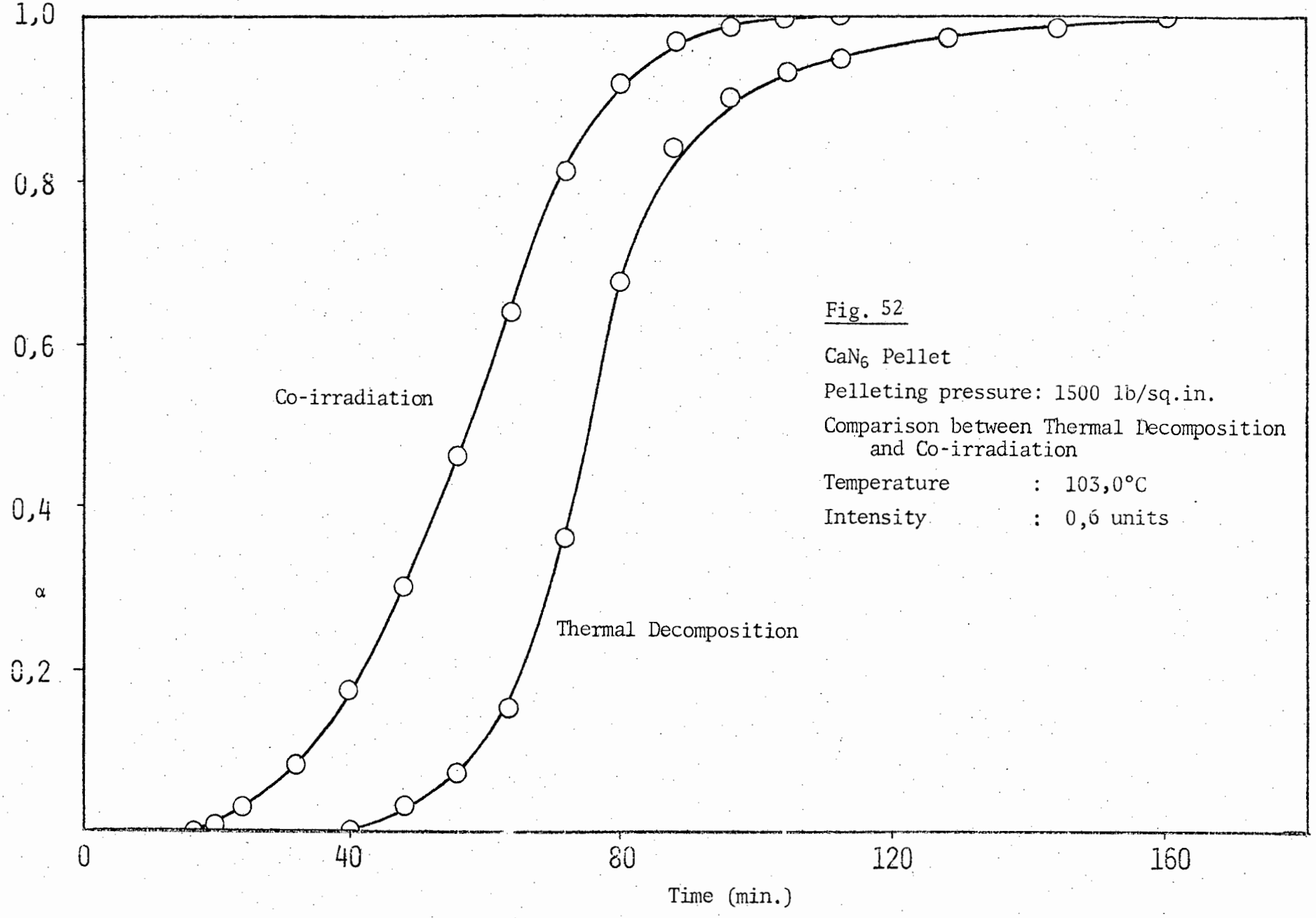

Fig. 52

CaN_6 Pellet

Pelleting pressure: 1500 lb/sq.in.

Comparison between Thermal Decomposition and Co-irradiation

Temperature : 103,0°C

Intensity : 0,6 units

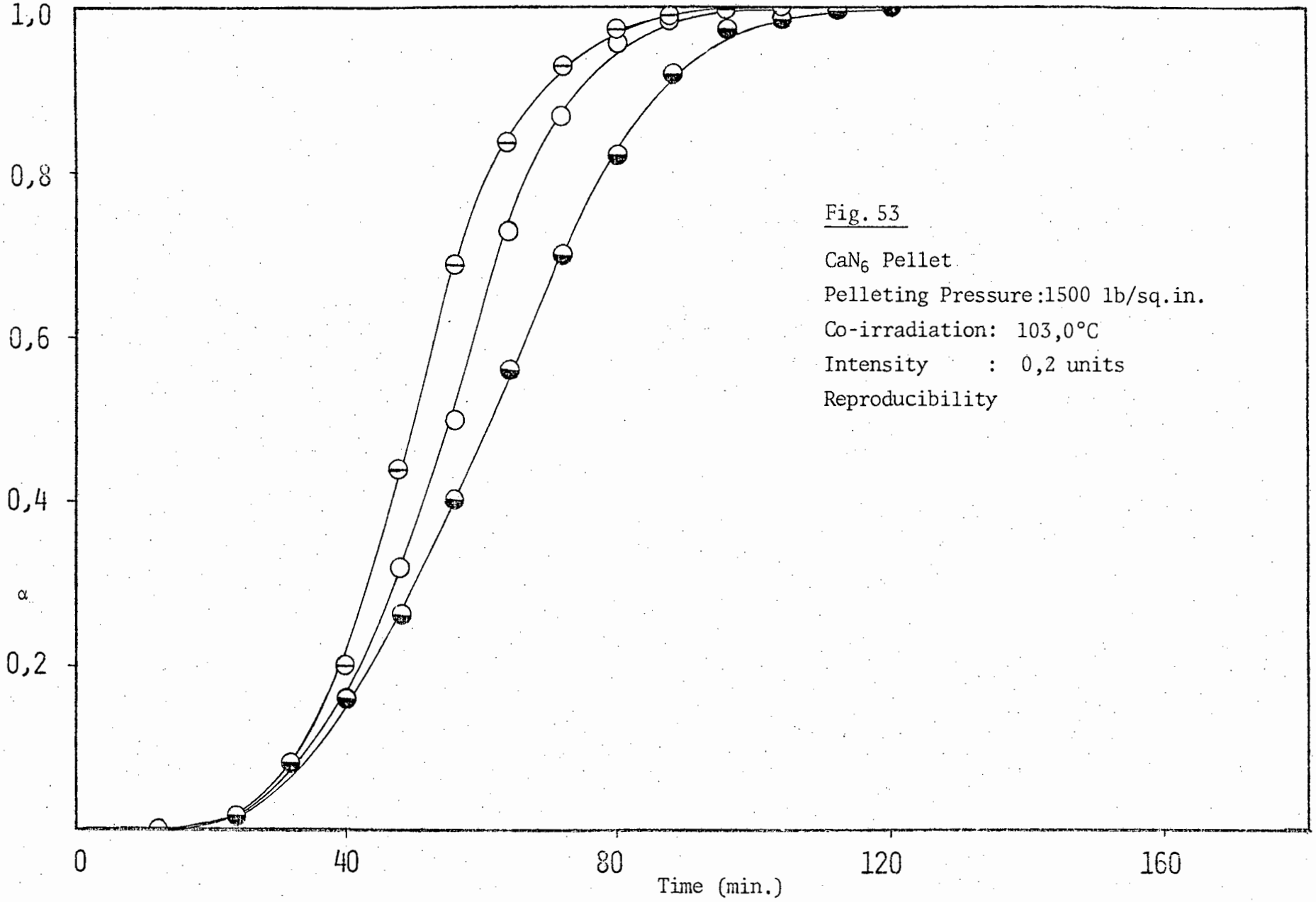

Fig. 53

CaN_6 Pellet
Pelleting Pressure:1500 lb/sq.in.
Co-irradiation: 103,0°C
Intensity : 0,2 units
Reproducibility

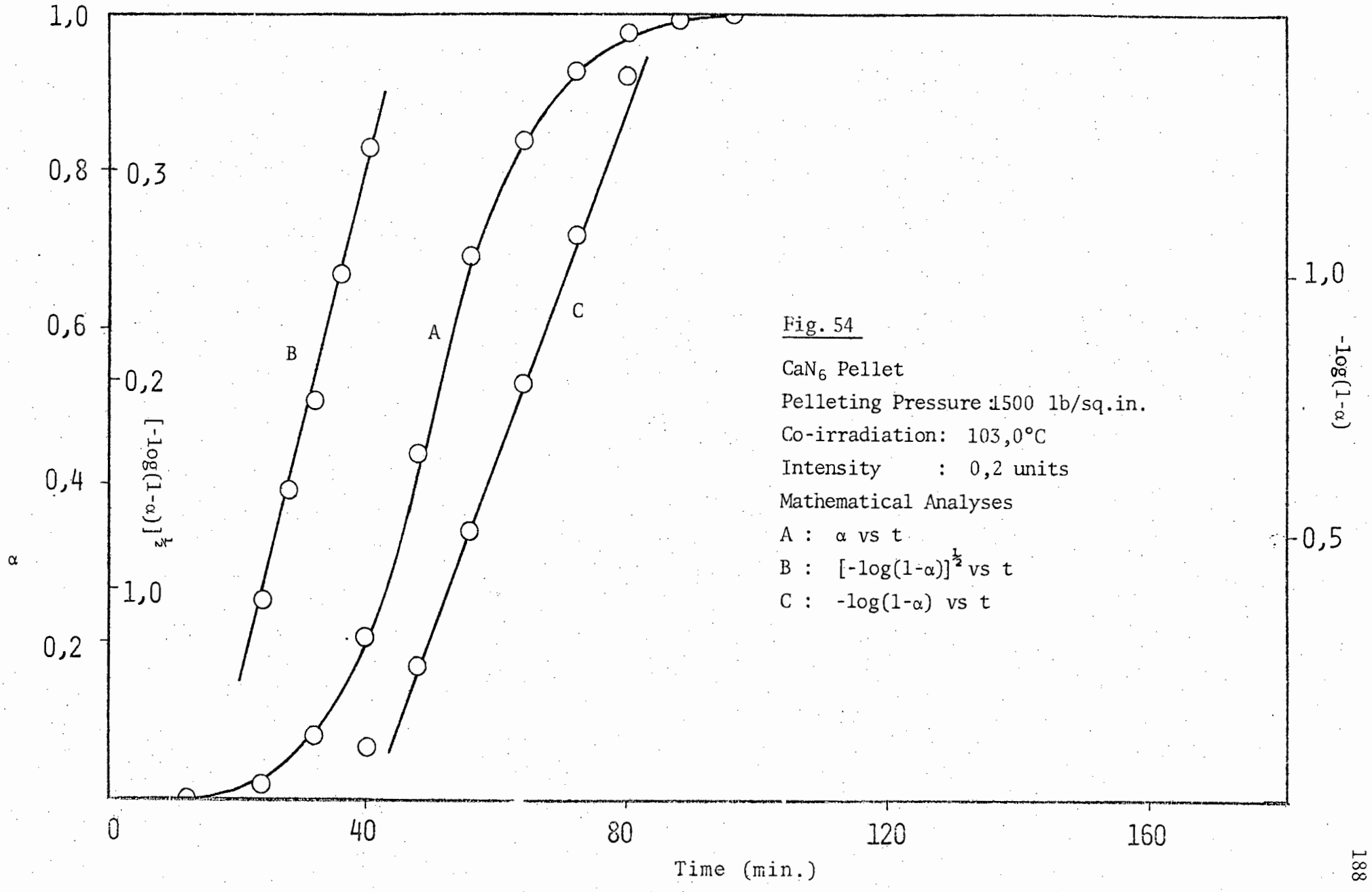

Fig. 54

CaN_6 Pellet

Pelleting Pressure : 1500 lb/sq.in.

Co-irradiation: 103,0°C

Intensity : 0,2 units

Mathematical Analyses

A : α vs t

B : $[-\log(1-\alpha)]^{\frac{1}{2}}$ vs t

C : $-\log(1-\alpha)$ vs t

intensity of 0,2 units. As is clearly shown in this figure and in Table 25 no highly reproducible results were obtainable for the co-irradiated decomposition of these pellets.

Table 25 Reproducibility constants for co-irradiated calcium azide pellets.

Pelleting pressure: 1500 lb./sq.in.

Temperature °C	Intensity Units	Induction Period min.	$k_{acc} \times 10^2$ min^{-1}.	$k_{decay} \times 10^2$ min^{-1}.
103,0	0,2	6,0	1,20	3,90
		8,0	1,30	3,00
		8,2	1,39	3,40

(iv.b)Evaluation of activation energies

Considerable efforts were made in order to determine the activation energies of co-irradiated decomposition of pelleted calcium azide. The lack of reproducibility illustrated above necessitated the use of the split-run technique in determining the activation energies. This method proved unsuccessful however as at temperatures beyond ±105,0°C the pellets exploded. Various pelleting pressures were used in order to overcome this. Pellets made at pressures 600, 1000, 1500 and 2000 lb./sq.in. were decomposed but at temperatures above 105,0°C these exploded. Another problem was that the dark rate was so great that in cases where explosion did not occur the pellet virtually completely decomposed during the period in which it was attaining the required temperature. Thus no rate constants could be determined and consequently no activation energies could be obtained.

(iv.c) Visual observations

A pellet of calcium azide pressed at a pressure of 1500 lb./sq.in. was decomposed at a temperature of 98,0°C and a light intensity of 2,5 units. At α = 0,10 the upper surface had turned a light grey colour. This surface then began turning a dark brown colour with greyish spots interspersed. Whereas the lower surface became light brown, darkening gradually. At $\alpha \approx 0,40$ the upper surface was a charcoal colour whilst the lower surface continued to darken progressively, until at $\alpha \approx 0,50$ the lighter spots disappeared. Beyond α = 0,50 the pellet was black on both surfaces.

(iv.d) Admittance of water vapour following an interruption

In order to investigate the presence of metallic nuclei, water vapour (17 torr pressure) was admitted at various stages of the decomposition. Pellets pressed at 1500 lb./sq.in. were decomposed at a temperature of 100,0°C and a light intensity of 1,0 units. The method employed and the results obtained were similar to those obtained for co-irradiated powder. Interruptions prior to the inflection point (α = 0,44) caused a new, ever-lengthening induction period to be observed with a lowering of the final pressure. Interruptions at α values greater than 0,44 virtually destroyed any subsequent reaction. Water vapour had no effect when introduced during the induction period.

(v) THERMAL DECOMPOSITION OF CALCIUM AND LITHIUM AZIDES

(v.a) Calcium azide

Calcium azide was thermally decomposed in order to determine the activation energies of the induction period and the subsequent acceleratory and decay reactions. These activation energies were necessary to facilitate the study of the differences between the mechanisms of photolysis and co-irradiation. It was also considered of interest to compare the values obtained with those of previous workers.

Two sets of decompositions were carried out. Freshly prepared calcium azide was thermally decomposed in the temperature range 100,0° - 130,0°C and then calcium azide which had been stored in vacuo over P_2O_5 for two years was thermally decomposed in the temperature range 110,0° - 140,0°C.

The reciprocal of the induction period was used as a rate constant for this part of the decomposition. The acceleratory reaction was analyzed using the Avrami-Erofeyev equation with n = 2. The decay reaction was analyzed using the unimolecular law. Previous workers[137,168] have used the equation $(1-\alpha)^{1/3} = kt + c$ in analyzing the decay reaction. As can be seen from Fig. 55 both equations fit equally well. It was decided to use the unimolecular law as this had already been successfully used in the study of the photolysis and co-irradiated decomposition of calcium azide powder. Tables 26 and 27 list the rate constants for the thermal decomposition of the fresh and aged material respectively. The activation energy was also calculated using the latter equation for comparison purposes.

Table 28 lists the values obtained for the activation energies for the induction, acceleratory and decay periods using the above analyses. Also listed are values obtained by previous workers for the purposes of comparison. A marked difference occurs in the values obtained for the decay reaction.

Table 26 Rate constants for the thermal decomposition of calcium azide powder (Fresh material)

Temperature °C	Induction Period min.	$k_{acc} \times 10^2$ min^{-1}.	$k_{decay} \times 10^2$ min^{-1}.
102,2	20,00	0,83	1,20
107,0	18,71	1,27	1,44
114,0	10,20	2,16	2,79
120,0	8,00	4,16	4,90
126,8	3,45	7,40	9,71

Table 27 Rate constants for the thermal decomposition of calcium azide powder (Material 2 years old)

Temperature °C	Induction Period min.	$k_{acc} \times 10^2$ min^{-1}.	$k_{decay} \times 10^2$ min^{-1}.
110,0	7,20	2,30	3,10
115,8	4,40	4,80	4,40
121,1	2,56	5,90	6,50
126,5	2,10	9,40	8,70
132,0	1,88	13,70	16,10
137,2	1,30	25,50	27,90

Table 29 Activation energies for the thermal decomposition of calcium azide powder

Material	Temperature Range °C	Induction Period Kcal./mol.	Acceleratory Period Kcal./mol.	Decay Period Kcal./mol.
(i) Freshly prepared	100,0 - 126,8	21,70	27,30	26,16 (a) 25,39 (b)
(ii) Aged (2 yrs.)	110,0 - 137,2	18,94	25,94	25,10
(iii) Aged (1 yr.) Ref.168	110,0 - 125,0	20,60	26,90	21,00
(iv) Freshly prepared Ref.137	105,0 - 130,0	18,00	26,90	21,40

(a) Unimolecular Law
(b) Contracting Sphere Equation.

Table 29 Activation energies for the thermal decomposition of lithium azide powder[174]

Temperature Range °C	Induction Period Kcal./mol.	Acceleratory Period Kcal./mol.	Decay Period Kcal./mol.
185,0 - 205,0	21,0	28,0	29,0

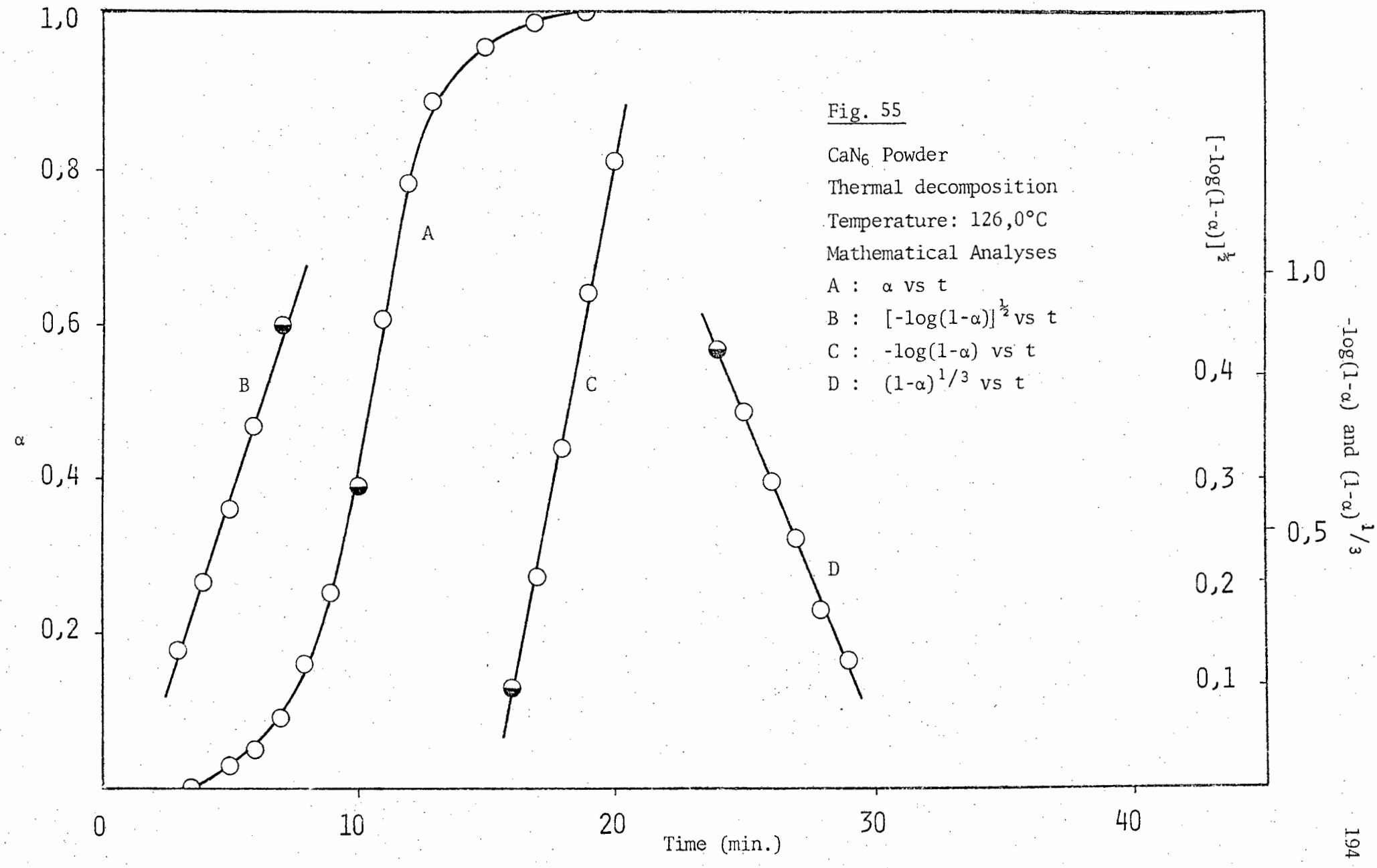
1,0
0,8
0,6
0,4
0,2
α
0
10
20
30
40
Time (min.)
A
B
C
D
Fig. 55
CaN6 Powder
Thermal decomposition
Temperature: 126,0°C
Mathematical Analyses
A : α vs t
B : [-log(1-α)]^½ vs t
C : -log(1-α) vs t
D : (1-α)^1/3 vs t
[-log(1-α)]^½
0,4
0,3
0,2
0,1
1,0
0,5
-log(1-α) and (1-α)^1/3

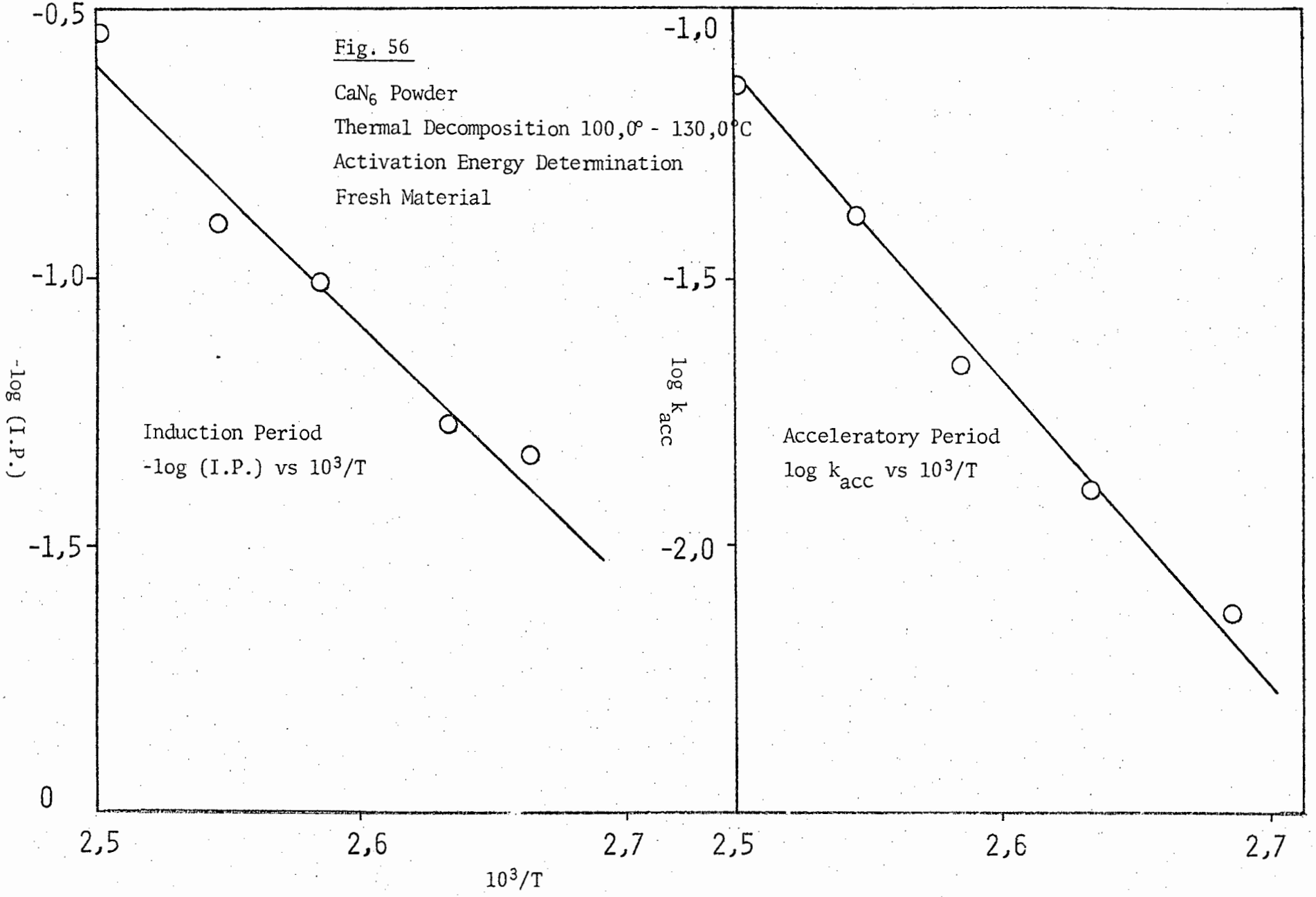
Fig. 56
CaN6 Powder
Thermal Decomposition 100,0° - 130,0°C
Activation Energy Determination
Fresh Material
Induction Period
-log (I.P.) vs 10³/T
Acceleratory Period
log kacc vs 10³/T
-log (I.P.)
log kacc
10³/T
-0,5
-1,0
-1,5
0
-1,0
-1,5
-2,0
2,5
2,6
2,7
2,5
2,6
2,7

Fig. 57

CaN_6 Powder
Thermal Decomposition: 100,0° - 140,0°C
Activation Energy Determination
Aged Material (2 yrs.)

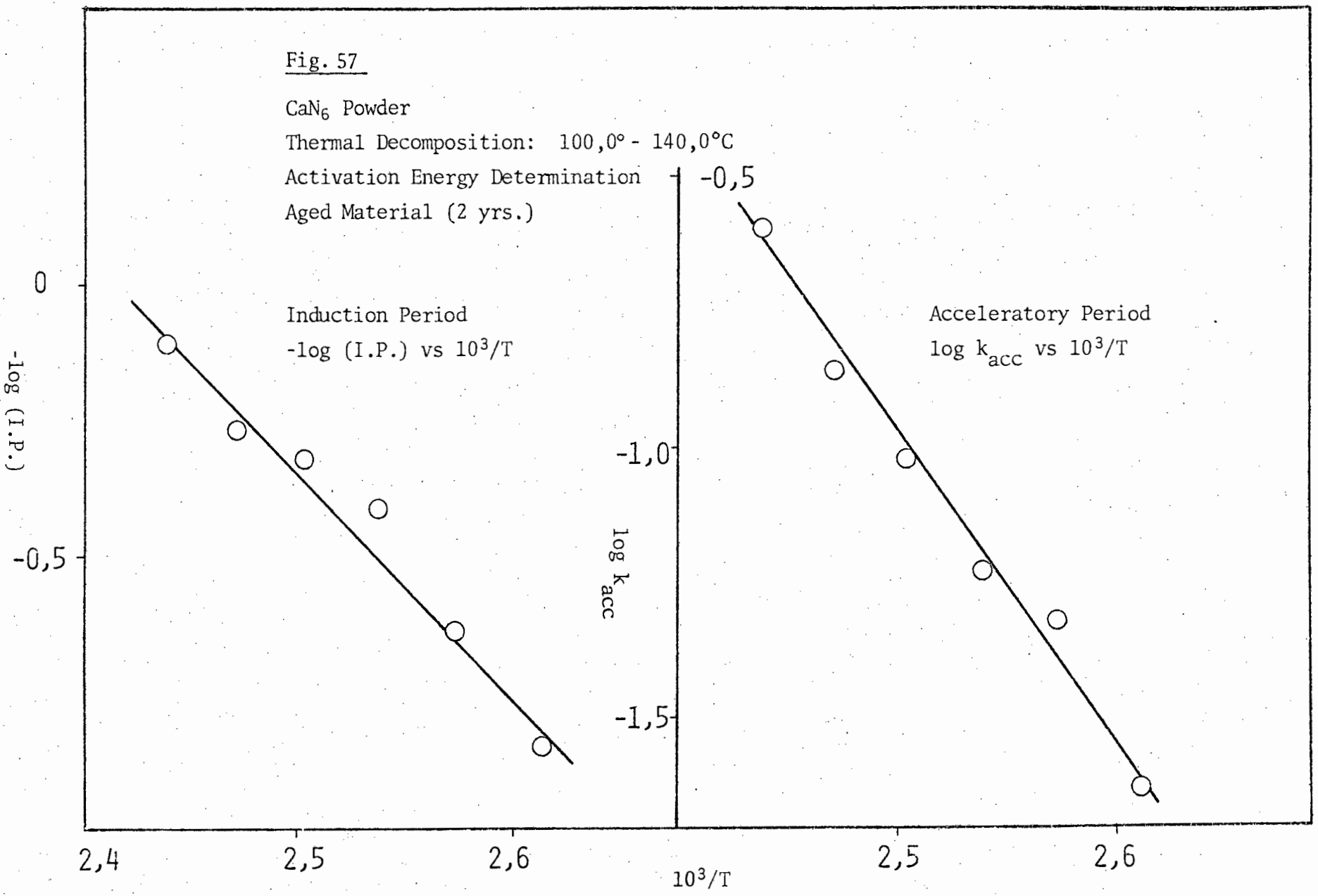

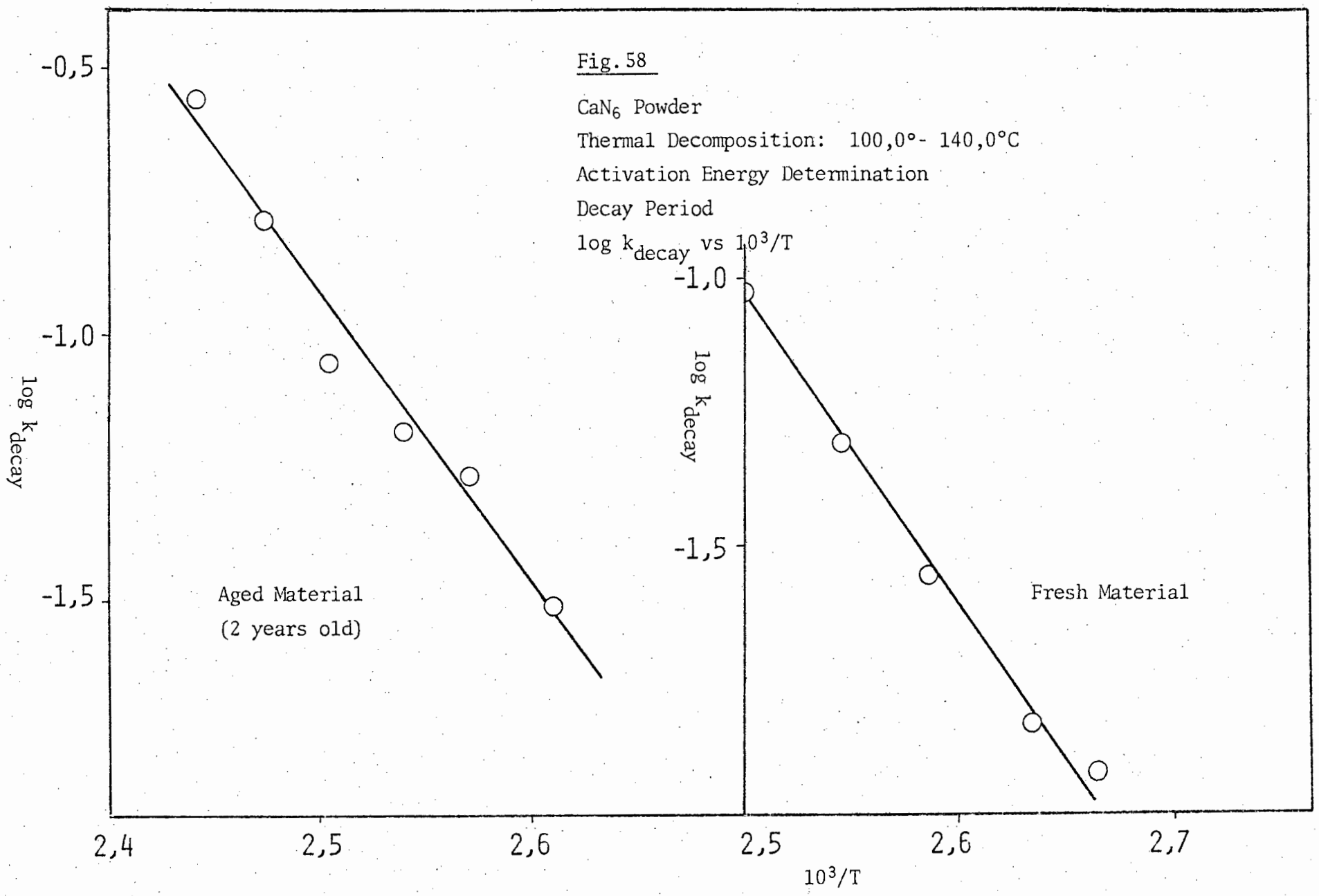

Fig. 58

CaN_6 Powder

Thermal Decomposition: 100,0°- 140,0°C

Activation Energy Determination

Decay Period

log k_{decay} vs $10^3/T$

Fig. 55 illustrates a typical α vs t curve for the thermal decomposition of powdered calcium azide at a temperature of 126,8°C. Also shown are analyses of the acceleratory and decay periods. Fig. 56 and 57 show the plots of -log(I.P.) and log k_{acc} vs $10^3/T$ for the fresh and aged material respectively and Fig. 58 shows plots of log k_{decay} vs $10^3/T$ for the fresh and aged material.

(v.b) Lithium azide

As referred to in section **9** *(ii.c)* the rate of photolysis of lithium azide powder at 170,0°C was so rapid as to make the rate of thermal decomposition at that temperature negligible. Hence it was decided not to make a study of co-irradiation of lithium azide. For this reason it was not considered necessary to determine the activation energies of the thermal decomposition of lithium azide. The values obtained by Prout and Liddiard[174] are given in Table 29 for reference purposes.

(vi) PHOTOLYSIS OF POWDERED CALCIUM, BARIUM, STRONTIUM AND LITHIUM AZIDES AT AMBIENT AND LOWER TEMPERATURES

The photolysis of calcium, barium, strontium and lithium azides was carried out in the temperature range -80,0°- 30,0°C. No dark rate was detected and thermal effects were thus negligible. The percentage decomposition for calcium azide was 62,0%, for barium azide 85,0%, for strontium azide 58,0% and for lithium azide 57,0%. These were lower than the values expected from decompositions at ambient temperatures.

(vi.a) Reproducibility

In the case of all four azides the crystals were ground for 5 minutes in a grindex and then sieved. The powder collected between sieves of mesh size 63μ and 125μ was selected for decomposition purposes. The powder thus obtained yielded reproducible results. Whole crystals or unsieved powder did not yield reproducible results. The barium and strontium azide powder used was from batches four years old. These had been stored in vacuo over P_2O_5. The calcium azide had been similarly stored for two years and the lithium azide was freshly prepared. The absence of any significant effect of aging on decomposition in previous photolysis studies of these compounds[180] enabled a comparable study to be made of these samples. In order to test the reproducibility, three decompositions of sieved samples were done at 30,0°C and -19,2°C for lithium azide at light intensities of 37,0 and 45,0 units respectively (Fig. 59 and 60); at 2,5°C and a light intensity of115,0 units for calcium azide (Fig. 61); at 4,0°C and a light intensity of 75,0 units for strontium azide (Fig. 62); and at 5,9°C and -12,8°C for barium azide at light intensities of 23,0 and 38,0 units respectively (Fig. 63 and 64). The rate constants obtained for these decompositions are listed in Table 30. The reciprocal of the induction period was used as a rate constant for this period and the Avrami-Erofeyev

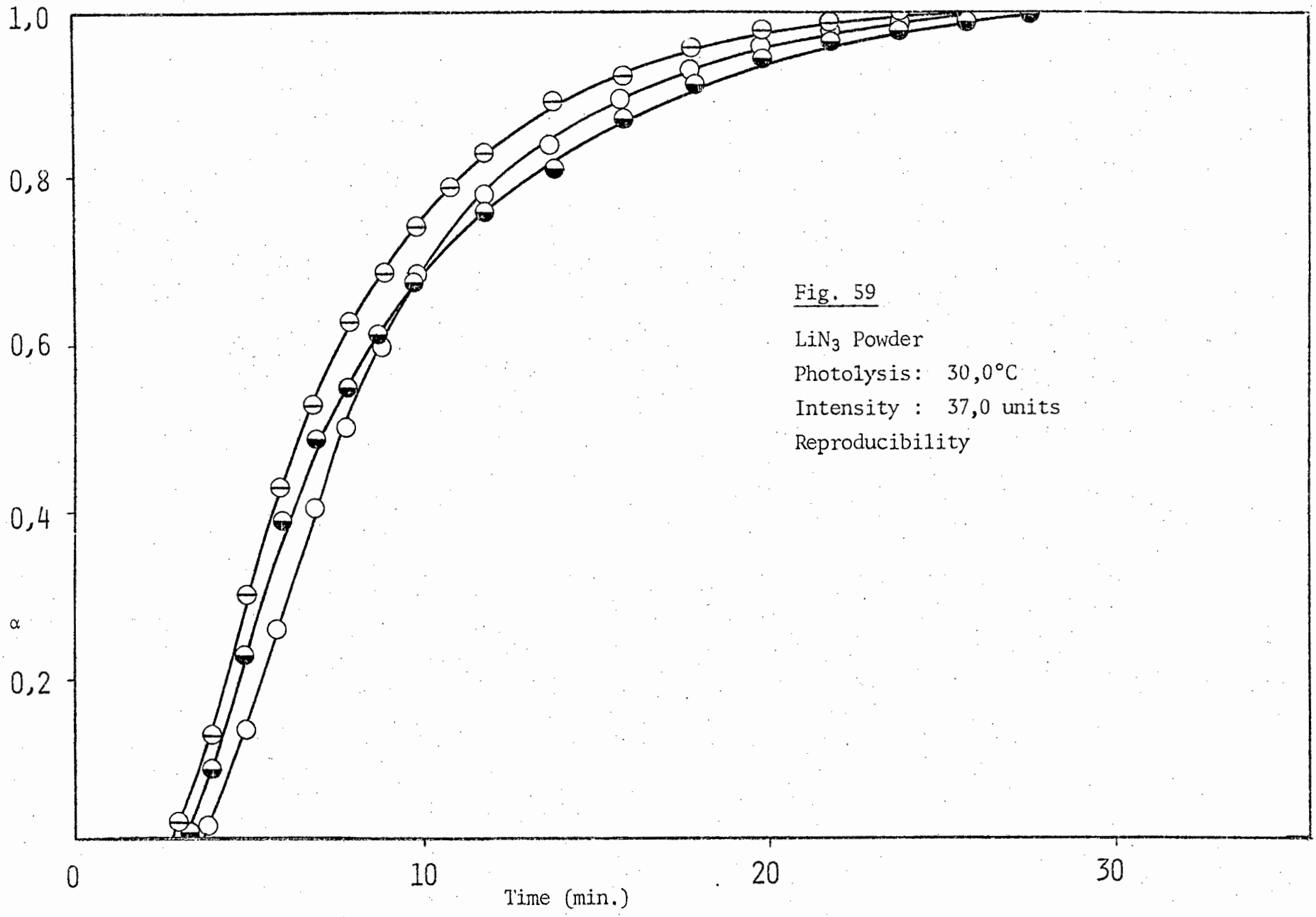

Fig. 59

LiN_3 Powder
Photolysis: 30,0°C
Intensity : 37,0 units
Reproducibility

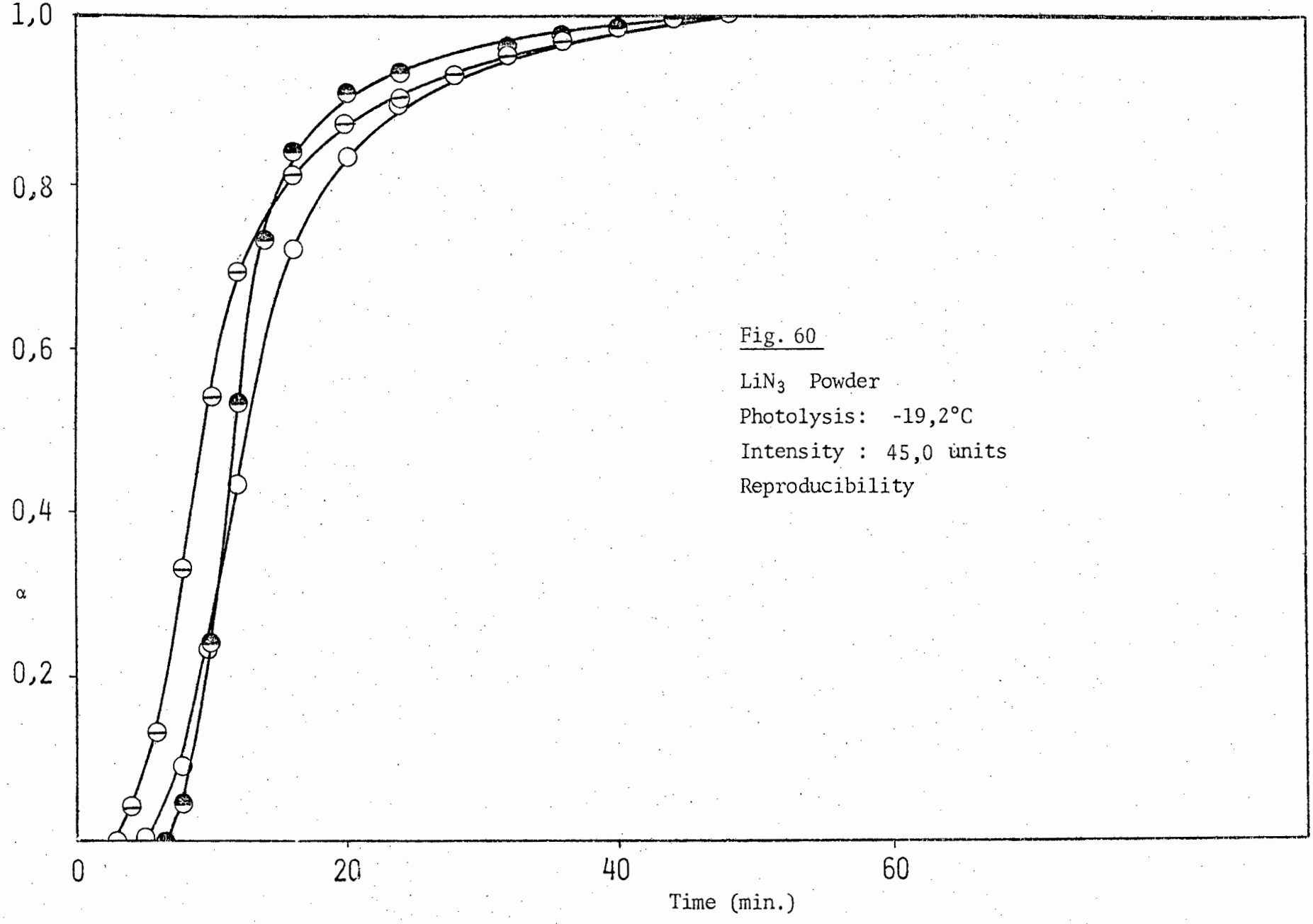

Fig. 60

LiN_3 Powder

Photolysis: -19,2°C

Intensity : 45,0 units

Reproducibility

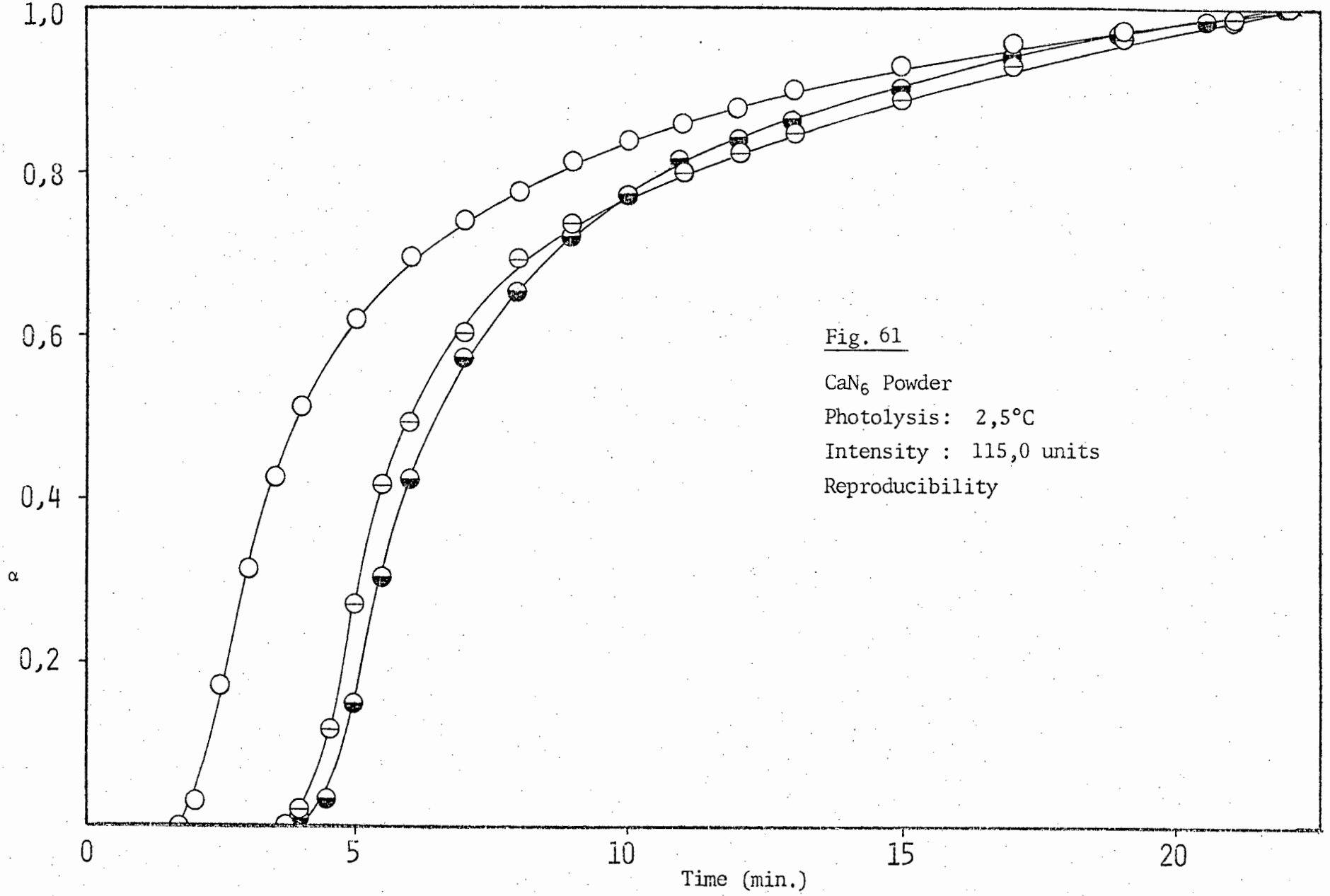

Fig. 61

CaN_6 Powder
Photolysis: 2,5°C
Intensity : 115,0 units
Reproducibility

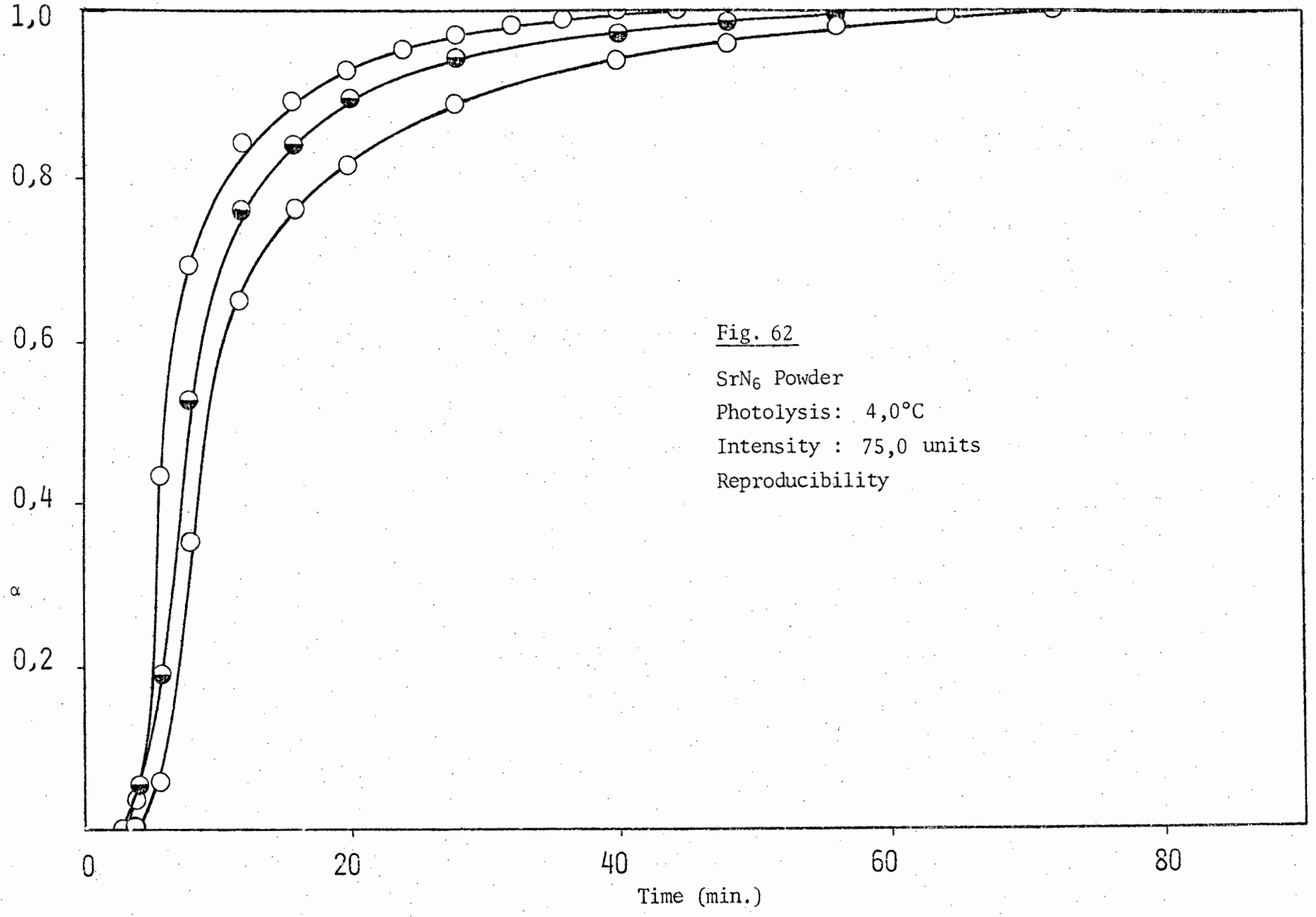

Fig. 62

SrN_6 Powder
Photolysis: 4,0°C
Intensity : 75,0 units
Reproducibility

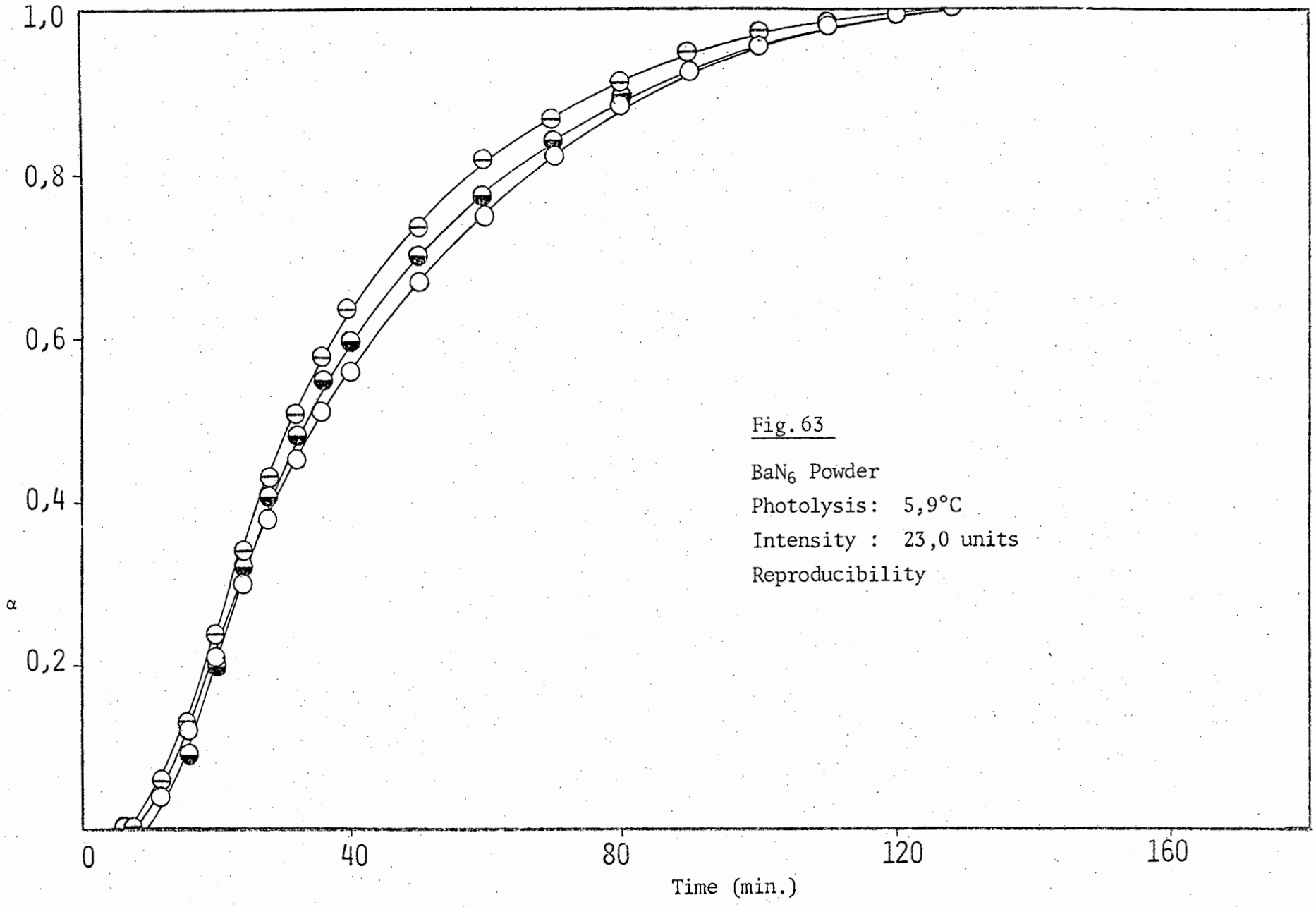

Fig. 63

BaN_6 Powder
Photolysis: 5,9°C
Intensity : 23,0 units
Reproducibility

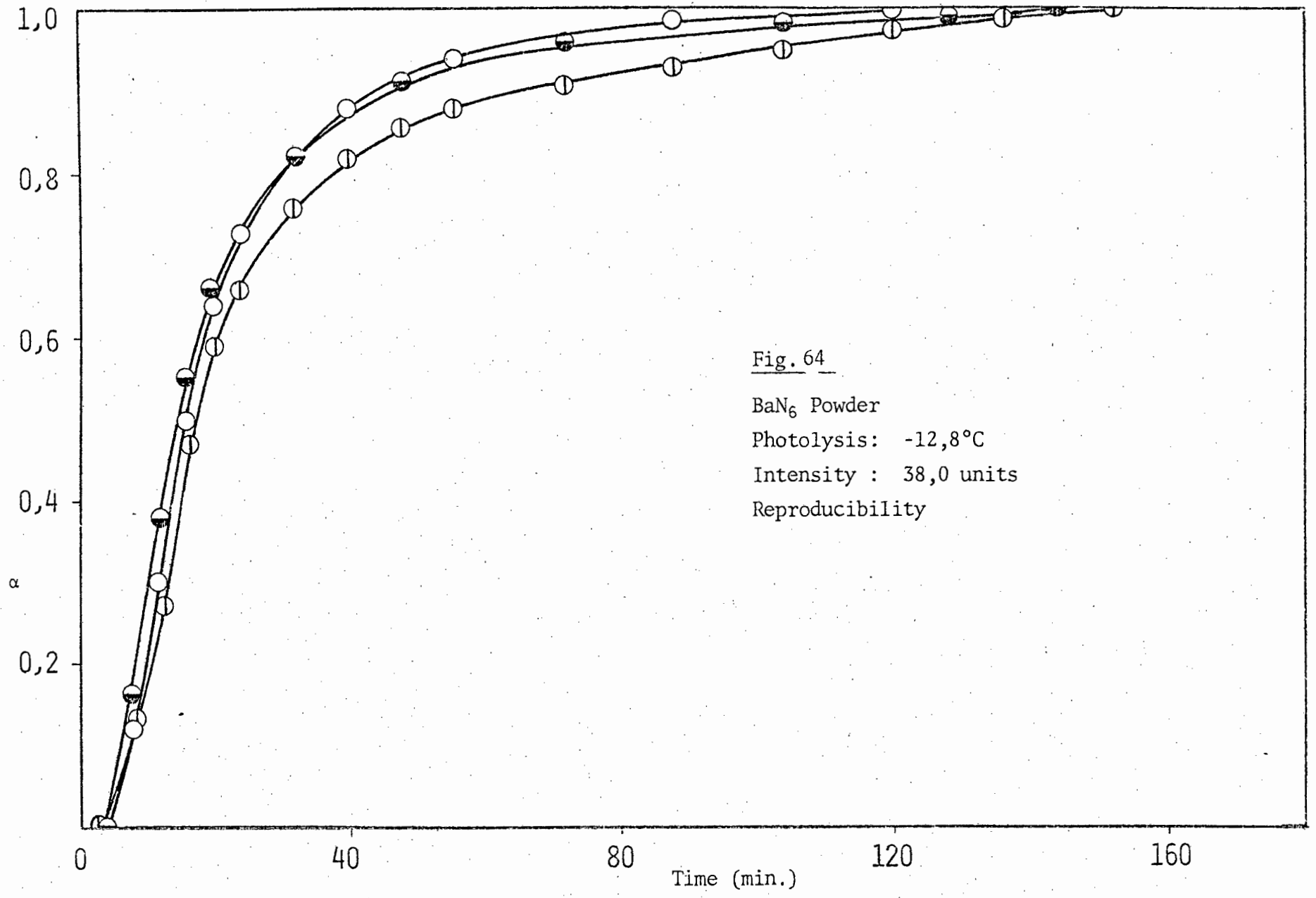

Fig. 64

BaN_6 Powder
Photolysis: -12,8°C
Intensity : 38,0 units
Reproducibility

equation with n = 2 and the unimolecular law were used to obtain rate constants for the acceleratory and decay reactions respectively. The applicability of these equations will be shown in the next section.

(vi.b) Mathematical analyses

Photolysis curves of all four azides in the temperature range -80,0°-30,0°C showed all the characteristics already observed in the studies of the photolysis of these compounds at ambient and higher temperatures (section 9 *(i.b)* and Ref. 50). There was a well defined induction period during which no measurable evolution of gas occurred. This was followed by an acceleratory reaction and a rather prolonged decay period.

The acceleratory reaction of all four azides was analyzed using the Avrami-Erofeyev equation with n = 2

$$\text{i.e.} \quad [-\log(1-\alpha)]^{\frac{1}{2}} = k_{acc}t + c \qquad \alpha = p/p_f$$

The determination of the final pressure was made difficult owing to the prolonged decay reaction particularly at the lower temperatures in the range. Fig. 65 illustrates a typical plot of recorder voltage against time for a decomposition of calcium azide at a temperature of 2,5°C and a light intensity of 115,0 units. Also illustrated is the method used for determining an estimated final pressure, p'_f, as opposed to the observed final pressure, p_f. The identical method was used on all four azides. In the case of barium and lithium azides the prolonged decay reaction was not as considerable as in the cases of calcium and strontium azides. However in all calculations the value of the final pressure used in the equations was determined in the manner shown above. No reference will be made henceforth to a value p'_f, it being presumed that, p_f, the final pressure, was either taken as observed (in the absence of a prolonged decay reaction) or as estimated as shown in the abovementioned figure.

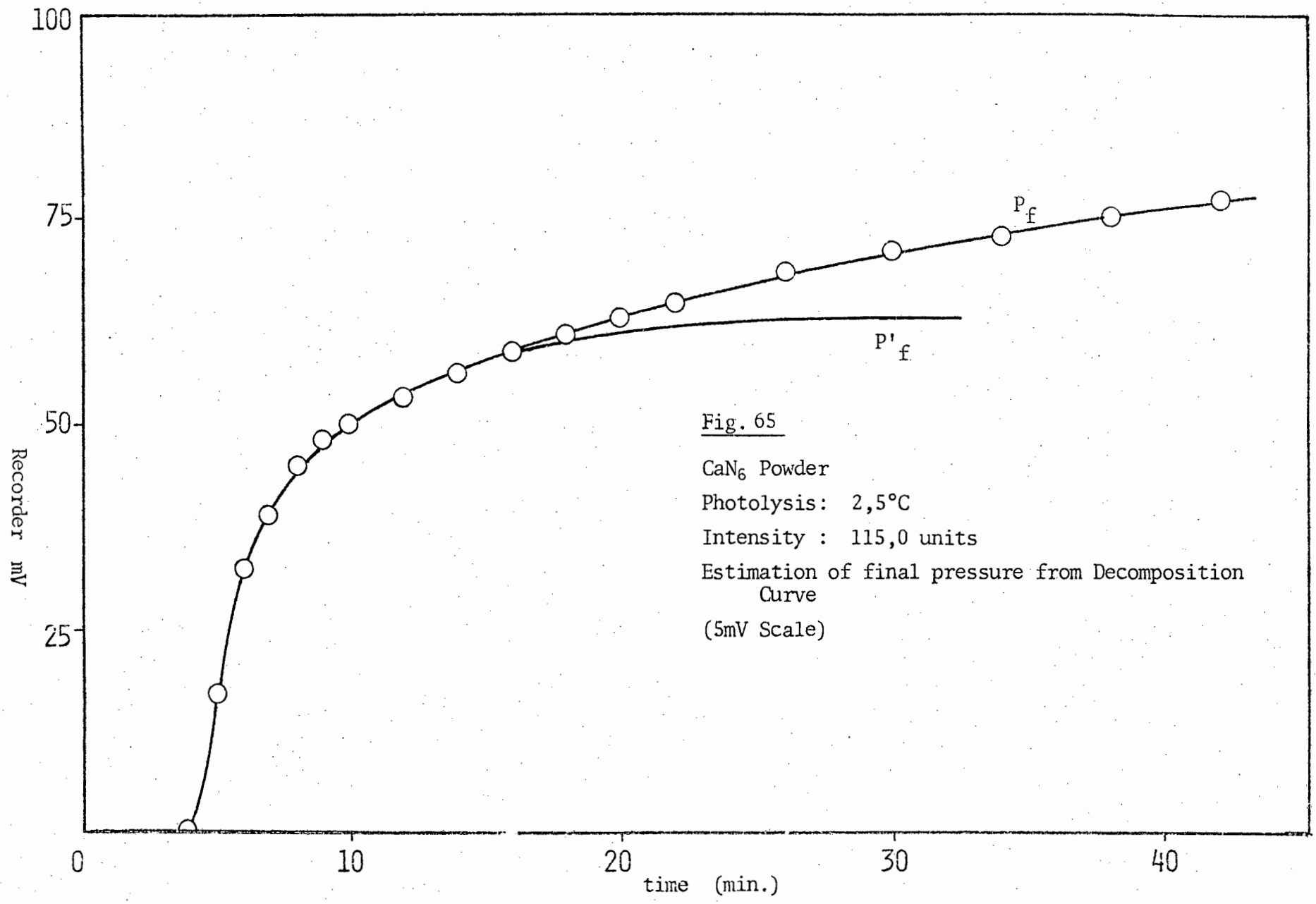

Fig. 65

CaN_6 Powder

Photolysis: 2,5°C

Intensity : 115,0 units

Estimation of final pressure from Decomposition Curve

(5mV Scale)

In all cases the unimolecular law

$$\text{i.e.} \quad -\log(1-\alpha) = k_{decay}t + c \qquad \alpha = p/p_f$$

was used to analyse the decay reaction. As mentioned earlier, the induction period was analyzed by using the reciprocal of the duration of the induction period as a rate constant. A typical α vs t curve for the photolysis of lithium azide powder, with mathematical analyses, is shown at -19,2°C and a light intensity of 45,0 units in Fig. 66. The inflection point occurs at α = 0,43. The Avrami-Erofeyev equation (n = 2) fits the acceleratory reaction in the range $0,03 < \alpha < 0,43$ and the unimolecular law fits the decay reaction in the range $0,43 < \alpha < 0,96$. Fig. 67 shows an α vs t curve, with mathematical analyses, for calcium azide at 2,5°C and a light intensity of 115,0 units. The inflection point occurs at α = 0,38 and the relevant equations fit in the ranges $0,03 < \alpha < 0,38$ and $0,38 < \alpha < 0,88$. Fig. 68 shows an α vs t curve, with mathematical analyses, for strontium azide at 4,0°C and a light intensity of 75,0 units. The inflection point occurs at α =0,43 and the relevant equations fit in the ranges $0,03 < \alpha < 0,43$ and $0,43 < \alpha < 0,95$. Fig. 69 and 70 show typical α vs t curves, with mathematical analyses, for barium azide at 5,9°C (light intensity 23,0 units) and -12,8°C (light intensity 38,0 units). The inflection point occurs at α = 0,32 and the equations for the acceleratory and decay reactions fit in the ranges $0,03 < \alpha < 0,32$ and $0,32 < \alpha < 0,90$.

Table 30 lists the reproducibility constants obtained using the above methods of analysis. Throughout this low temperature study, the degree of reproducibility was inferior to that obtained at higher temperatures. This was particularly so in the induction period. Notwithstanding this fact, all decompositions were analyzed in the induction period if only to illustrate the degree of irreproducibility. The results obtained for the

Table 30 Reproducibility constants for the photolysis of various azide powders

Substance	Temperature °C	Intensity Units	Induction Period min.	$k_{acc} \times 10^2$ min^{-1}.	$k_{decay} \times 10^2$ min^{-1}.
LiN_3	30,0	37	3,6 3,0 4,4	11,70 12,00 12,40	5,60 5,50 5,80
	-19,2	45	5,6 3,4 6,4	8,40 8,80 9,10	6,10 6,00 6,30
CaN_6	2,5	115	3,7 3,8 1,9	26,80 28,60 28,40	11,50 11,20 10,90
SrN_6	4,0	75	3,6 3,6 4,0	17,40 16,40 16,30	3,80 4,20 4,20
BaN_6	5,9	23	7,2 8,0 6,6	2,36 2,22 2,17	1,32 1,31 1,52
	-12,8	38	3,5 3,6 2,8	4,00 4,11 4,25	1,82 2,70 2,15

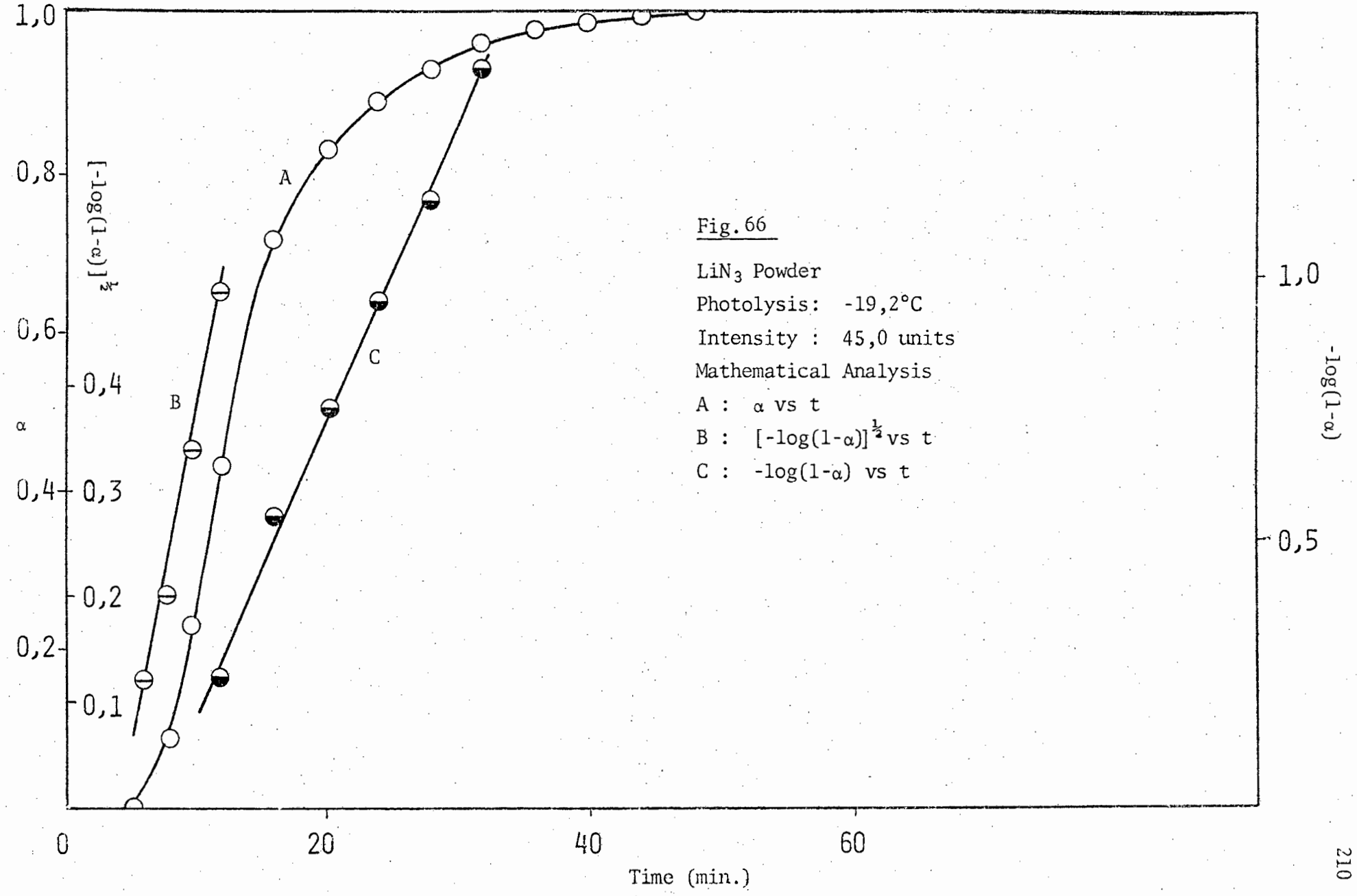

Fig. 66

LiN_3 Powder
Photolysis: -19,2°C
Intensity : 45,0 units
Mathematical Analysis
A : α vs t
B : $[-\log(1-\alpha)]^{\frac{1}{2}}$ vs t
C : $-\log(1-\alpha)$ vs t

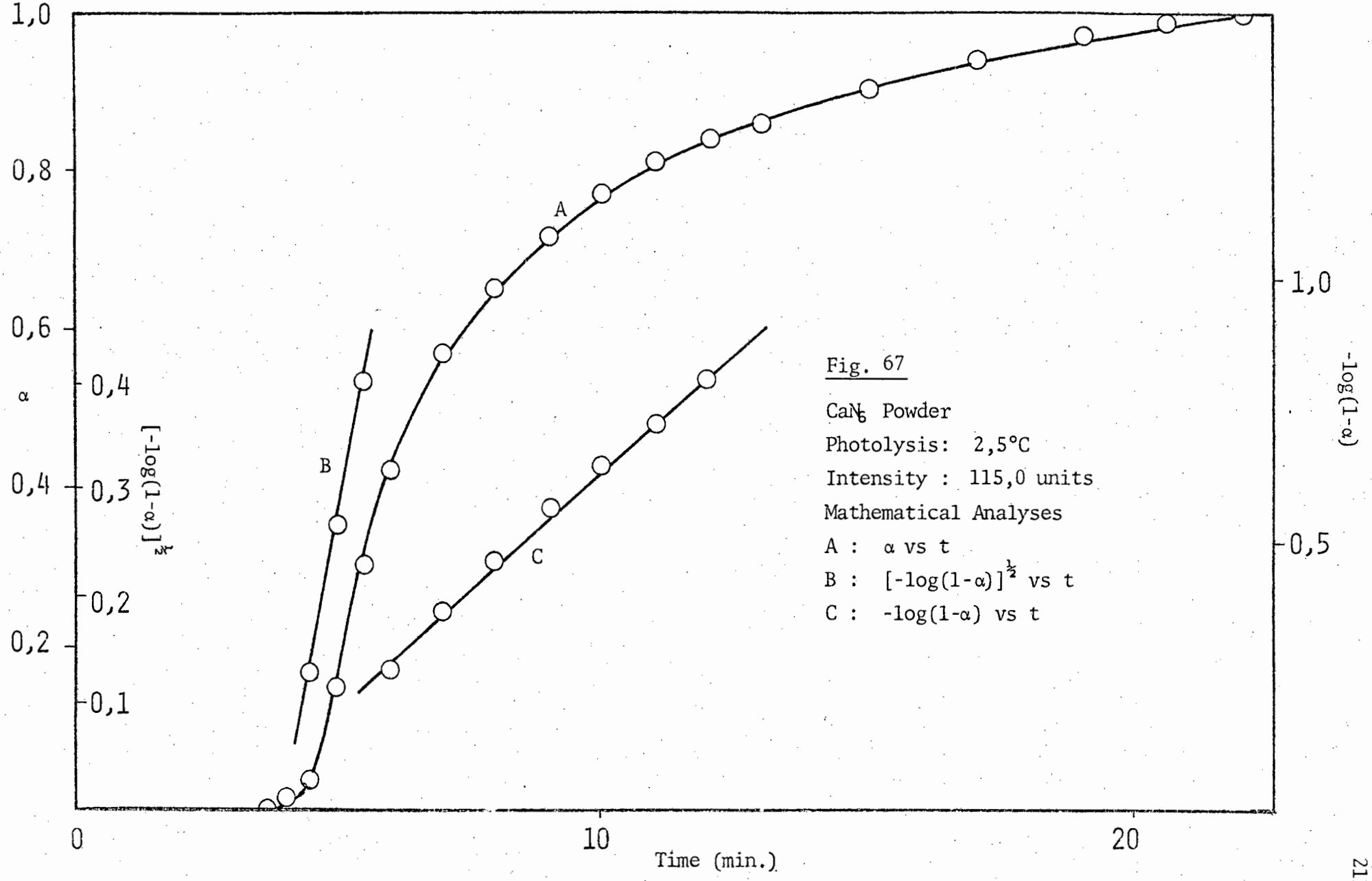

Fig. 67

CaN_6 Powder

Photolysis: 2,5°C

Intensity : 115,0 units

Mathematical Analyses

A : α vs t

B : $[-\log(1-\alpha)]^{\frac{1}{2}}$ vs t

C : $-\log(1-\alpha)$ vs t

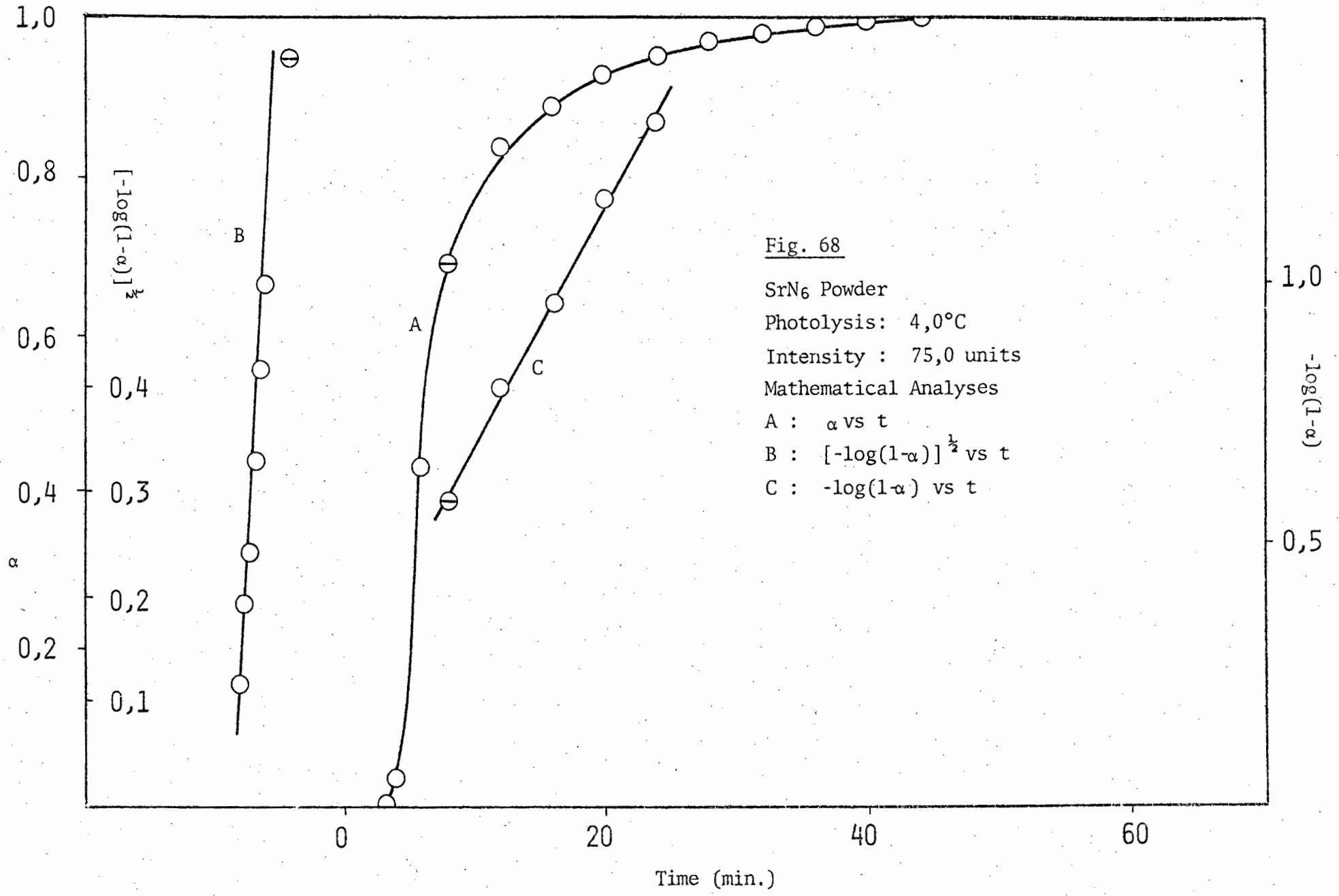

Fig. 68

SrN_6 Powder
Photolysis: 4,0°C
Intensity : 75,0 units
Mathematical Analyses
A : α vs t
B : $[-\log(1-\alpha)]^{\frac{1}{2}}$ vs t
C : $-\log(1-\alpha)$ vs t

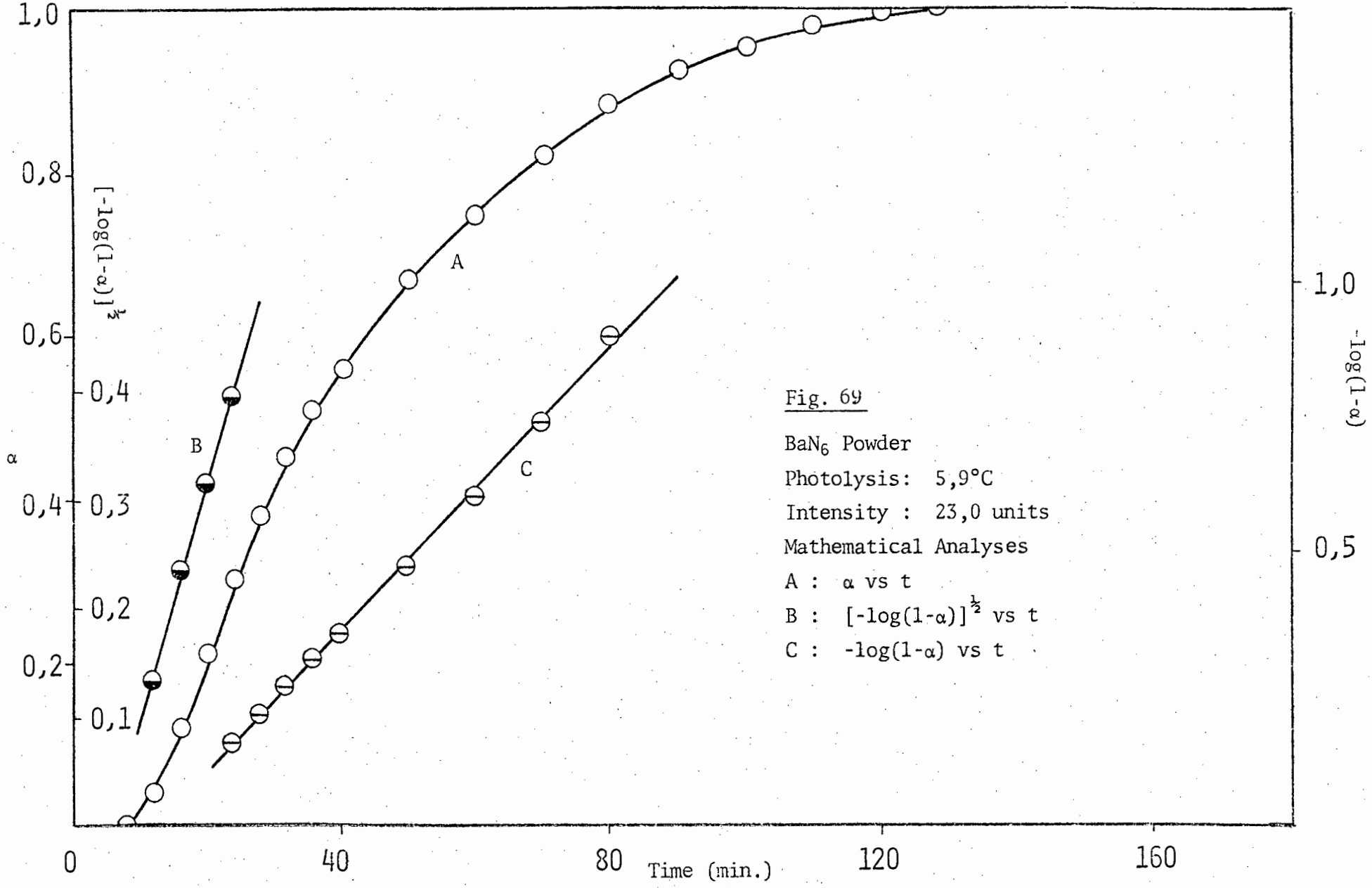

Fig. 69

BaN_6 Powder
Photolysis: 5,9°C
Intensity : 23,0 units
Mathematical Analyses
A : α vs t
B : $[-\log(1-\alpha)]^{\frac{1}{2}}$ vs t
C : $-\log(1-\alpha)$ vs t

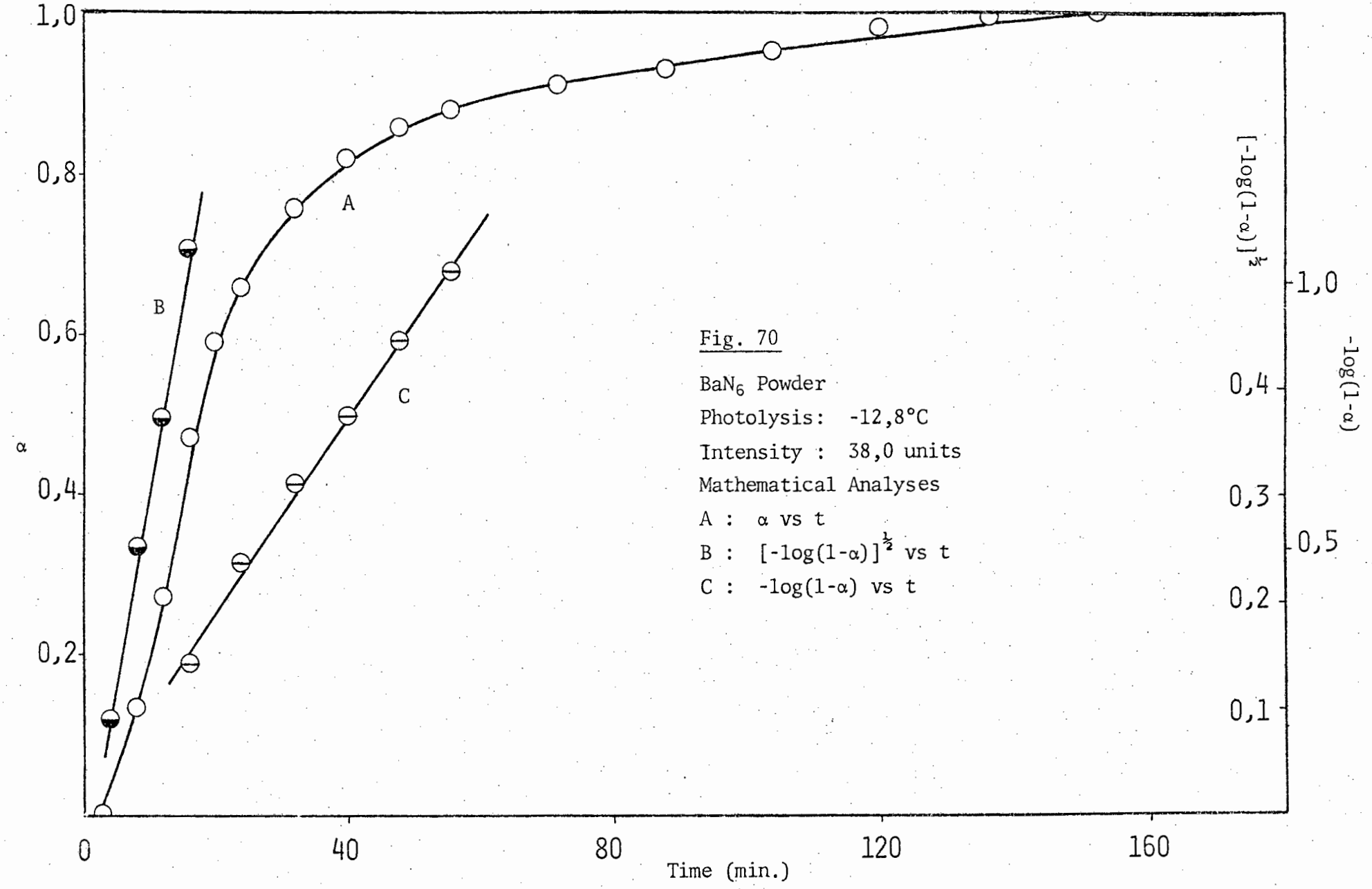

Fig. 70

BaN_6 Powder

Photolysis: -12,8°C

Intensity : 38,0 units

Mathematical Analyses

A : α vs t

B : $[-\log(1-\alpha)]^{\frac{1}{2}}$ vs t

C : $-\log(1-\alpha)$ vs t

induction period will thus be of less importance than those obtained for the acceleratory and decay reactions.

(vi.c) Evaluation of activation energies

Activation energies for all four azides were obtained by photolytically decomposing samples at various temperatures in the range under consideration. The light intensity was kept constant throughout the determination. As described in previous sections, the Arrhenius equation was applied to each of the three processes occurring during photolysis i.e. during the induction, acceleratory and decay periods. In each case the logarithm of the rate constant was plotted against $10^3/T$.

Constant light intensities of 14,0; 28,5; 35,0 and 14,0 units were used for calcium, barium, strontium and lithium azides respectively. In the case of calcium and barium azides a change occurred in activation energy in the region of 7,0°C and 17,0°C respectively, and in the case of strontium and lithium azides the change occurred in the region of -4,0°C and -19,0°C respectively. These changes were not always clearly defined and the temperature at which they are said to occur are really fairly accurate approximations.

Tables 31-34 list the rate constants and Tables 35-38 the activation energies for calcium, barium, strontium and lithium azides respectively. Fig. 71-81 illustrate the plots of -log(I.P.), log k_{acc} and $\log_{decay}$ against $10^3/T$ in the relevant temperature ranges for calcium, barium, strontium and lithium azides respectively.

(vi.d) The effect of variation of intensity of ultraviolet light source

The rates of photolysis of calcium, barium, strontium and lithium azides were measured at different light intensities with the temperature being kept constant for the purpose of determining the molecularity of the processes taking place. The method used to vary the intensity of the

Table 31 Rate constants for the photolysis of calcium azide powder

Temperature range: -70,0°- 22,0°C

Light intensity : 14 units

Temperature °C	Induction Period min.	$k_{acc} \times 10^2$ min^{-1}.	$k_{decay} \times 10^2$ min^{-1}.
-68,9	1,4	20,0	18,5
-62,2	0,7	26,0	15,0
-52,7	1,4	24,1	19,7
-42,6	1,4	27,5	17,1
-42,0	1,2	24,4	16,4
-34,5	0,6	24,4	16,6
-33,7	1,7	32,8	17,6
-20,5	0,7	28,0	18,5
-2,7	2,7	31,5	19,6
3,2	1,0	30,8	20,3
7,2	0,4	32,5	26,0
10,0	0,8	35,6	27,6
13,6	0,6	39,7	28,4
21,1	0,9	47,6	32,0

Table 32 Rate constants for the photolysis of barium azide powder

Temperature range: -70,0° - 35,0°C

Light intensity : 28,5 units

Temperature °C	Induction Period min.	$k_{acc} \times 10^2$ min^{-1}.	$k_{decay} \times 10^2$ min^{-1}.
-68,5	13,5	1,16	0,82
-63,0	10,0	1,36	0,88
-56,9	10,0	1,24	0,89
-41,8	10,0	1,20	1,07
-35,5	7,0	1,35	1,00
-27,9	8,9	1,54	1,24
-16,2	6,4	1,91	1,43
5,5	8,0	1,92	1,56
7,8	8,0	2,00	1,64
12,5	12,0	2,00	1,49
15,5	8,0	2,14	1,51
17,0	12,0	2,19	1,57
19,9	12,0	2,07	1,55
26,3	6,4	2,66	1,70
28,0	8,0	2,95	2,09
34,1	7,2	3,80	2,43

Table 33 Rate constants for the photolysis of strontium azide powder

Temperature range: -80,0°- 32,0°C

Light intensity : 35,0 units

Temperature °C	Induction Period min.	$k_{acc} \times 10^2$ min^{-1}.	$k_{decay} \times 10^2$ min^{-1}.
-78,0	44,0	4,33	3,55
-69,1	32,0	4,49	5,61
-62,2	4,0	5,62	4,06
-48,0	9,4	6,17	4,55
-40,0	8,0	8,34	4,33
-31,3	10,0	9,27	5,14
-19,5	8,4	10,30	5,45
4,0	7,6	15,14	6,90
5,0	6,0	14,29	9,81
9,2	6,4	16,94	6,97
14,1	6,8	20,75	9,55
18,8	6,8	22,49	7,01
23,1	3,45	24,43	10,99
27,0	4,0	24,43	10,42
31,5	3,9	26,67	13,71

Table 34 Rate constants for the photolysis of lithium azide powder

Temperature range: -72,0° - 17,0°C

Light intensity : 14,0 units

Temperature °C	Induction Period min.	$k_{acc} \times 10^2$ min^{-1}.	$k_{decay} \times 10^2$ min^{-1}.
-71,2	16,0	1,36	1,67
-62,2	16,0	1,85	1,82
-48,2	12,0	2,24	1,85
-40,2	6,4	2,43	2,07
-31,0	4,0	2,78	2,32
-18,8	4,0	3,60	2,70
-6,3	2,4	5,37	4,17
4,5	1,6	6,98	6,90
16,7	1,7	10,23	9,77

Table 35 Activation energies for the photolysis of calcium azide powder

Light intensity: 14,0 units

Temperature Range °C	Induction Period Kcal./mol.	Acceleratory Period Kcal./mol.	Decay Period Kcal./mol.
-70,0 - 7,0	0,34	0,56	0,42
7,0 - 22,0	5,70	4,18	3,76

Table 36 Activation energies for the photolysis of barium azide powder

Light intensity: 28,5 units

Temperature Range °C	Induction Period Kcal./mol.	Acceleratory Period Kcal./mol.	Decay Period Kcal./mol.
-70,0 - 17,0	0,24	0,82	0,97
17,0 - 35,0	6,48	5,47	5,19

Table 37 Activation energies for the photolysis of strontium azide powder

Light intensity: 35,0 units

Temperature Range °C	Induction Period Kcal./mol.	Acceleratory Period Kcal./mol.	Decay Period Kcal./mol.
-80,0 - -4,0	2,38	1,58	0,69
-4,0 - 32,0	4,00	3,73	3,96

Table 38 Activation energies for the photolysis of lithium azide powder

Light intensity: 14,0 units

Temperature Range °C	Induction Period Kcal./mol.	Acceleratory Period Kcal./mol.	Decay Period Kcal./mol.
-72,0 - -19,0	3,14	1,71	0,88
-19,0 - 17,0	4,98	4,25	5,44

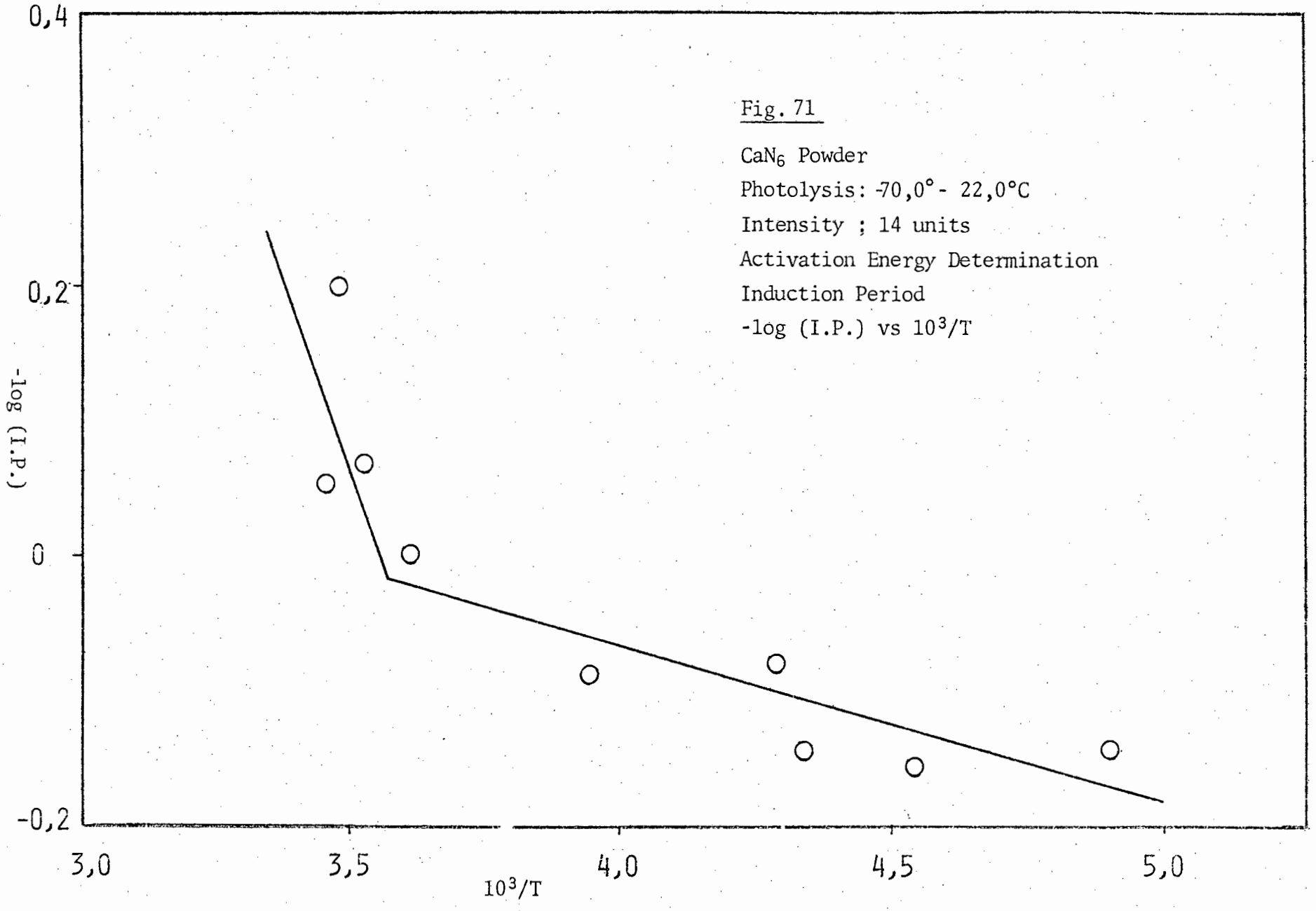

Fig. 71

CaN_6 Powder
Photolysis: -70,0° - 22,0°C
Intensity ; 14 units
Activation Energy Determination
Induction Period
-log (I.P.) vs $10^3/T$

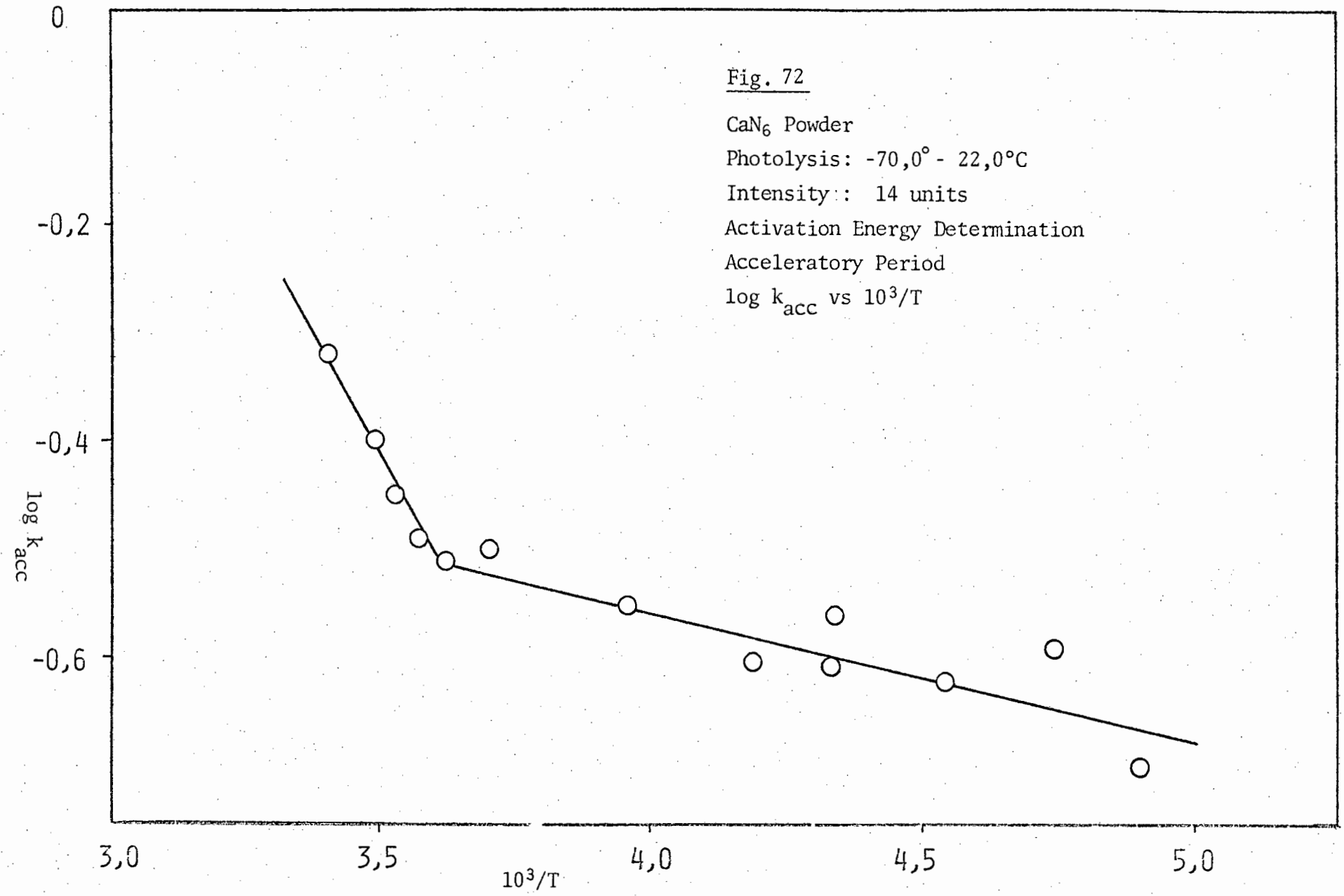

Fig. 72

CaN_6 Powder
Photolysis: -70,0° - 22,0°C
Intensity : 14 units
Activation Energy Determination
Acceleratory Period
log k_{acc} vs $10^3/T$

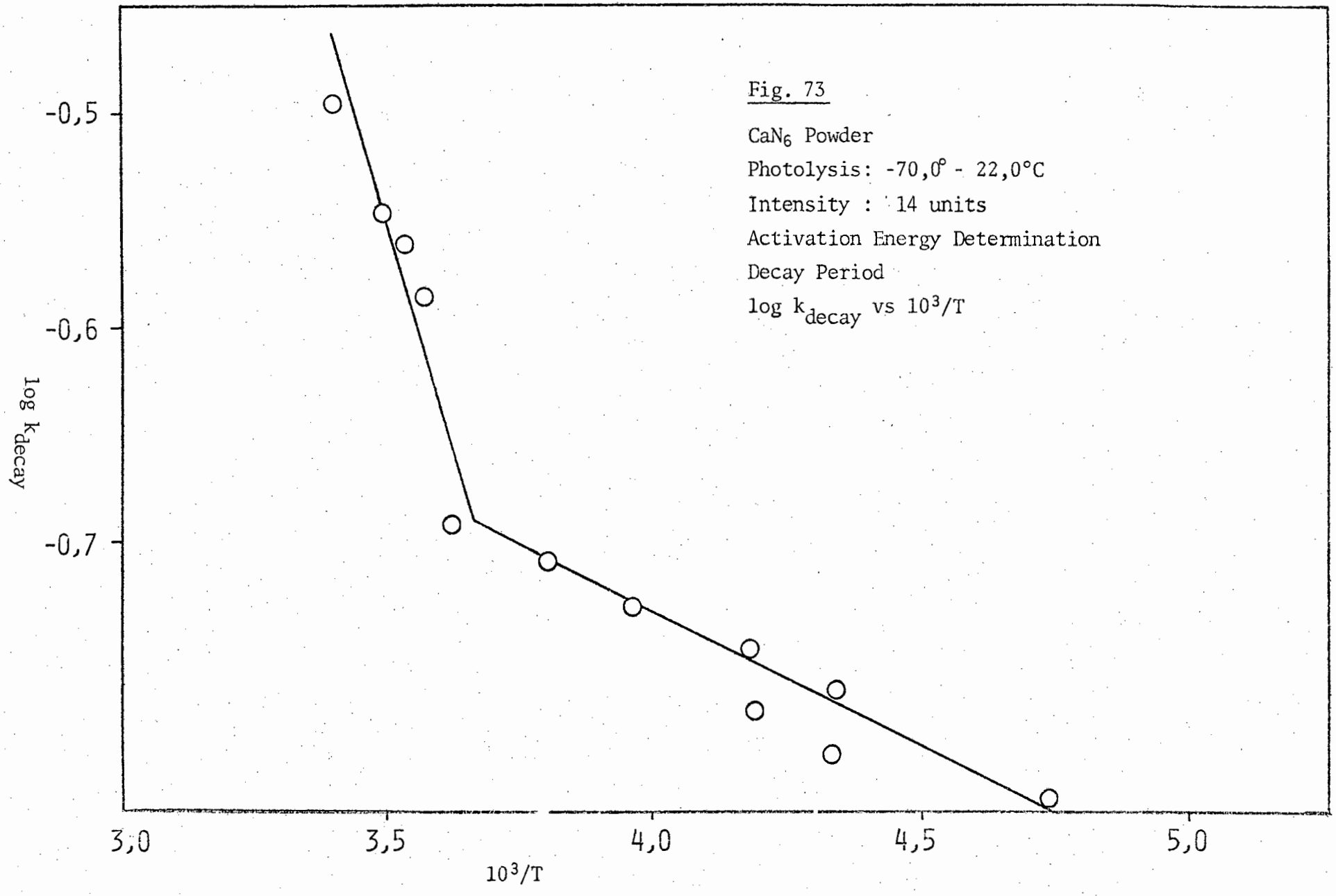

Fig. 73

CaN_6 Powder
Photolysis: -70,0° - 22,0°C
Intensity : 14 units
Activation Energy Determination
Decay Period
log k_{decay} vs $10^3/T$

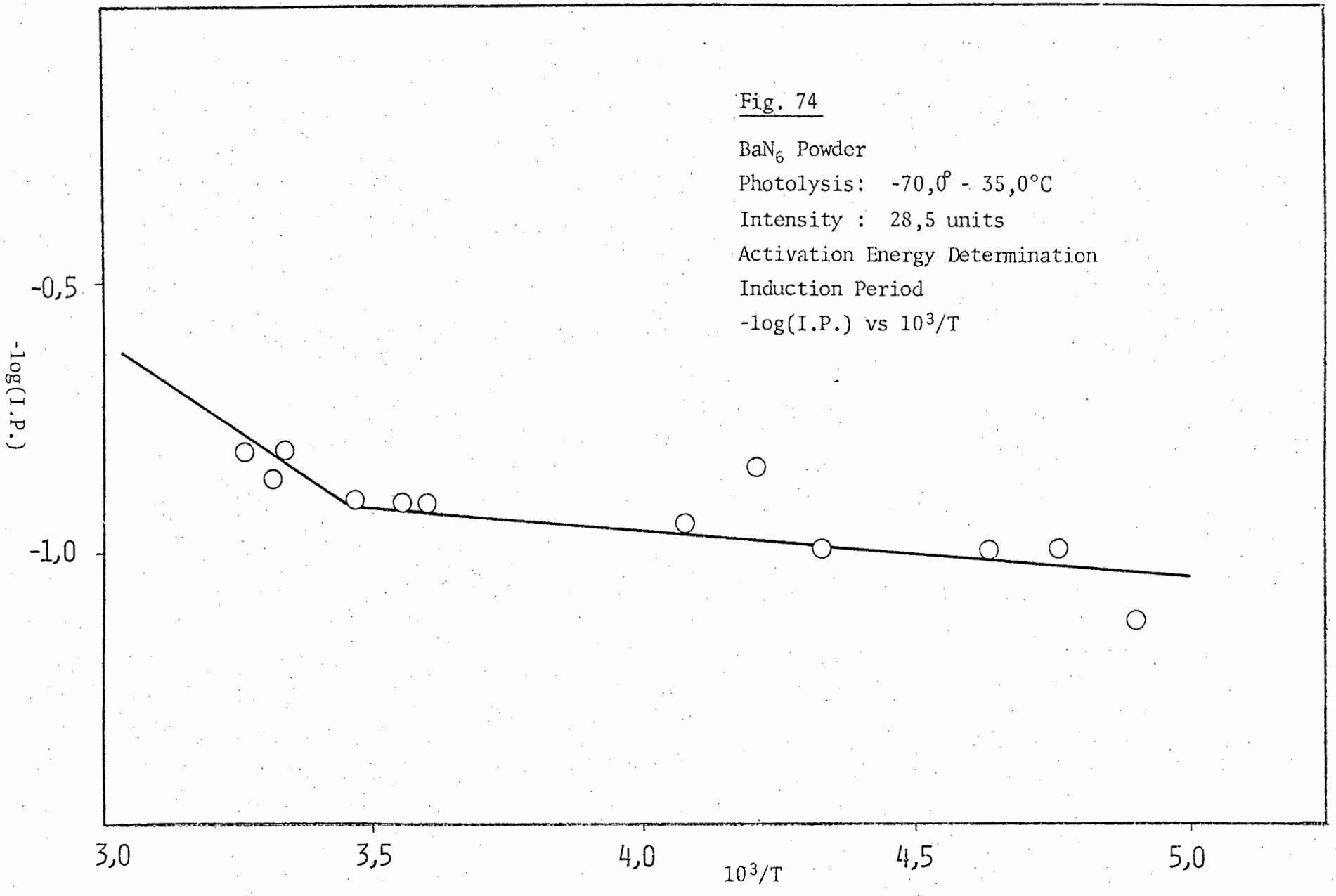

Fig. 74

BaN_6 Powder
Photolysis: -70,0° - 35,0°C
Intensity : 28,5 units
Activation Energy Determination
Induction Period
-log(I.P.) vs $10^3/T$

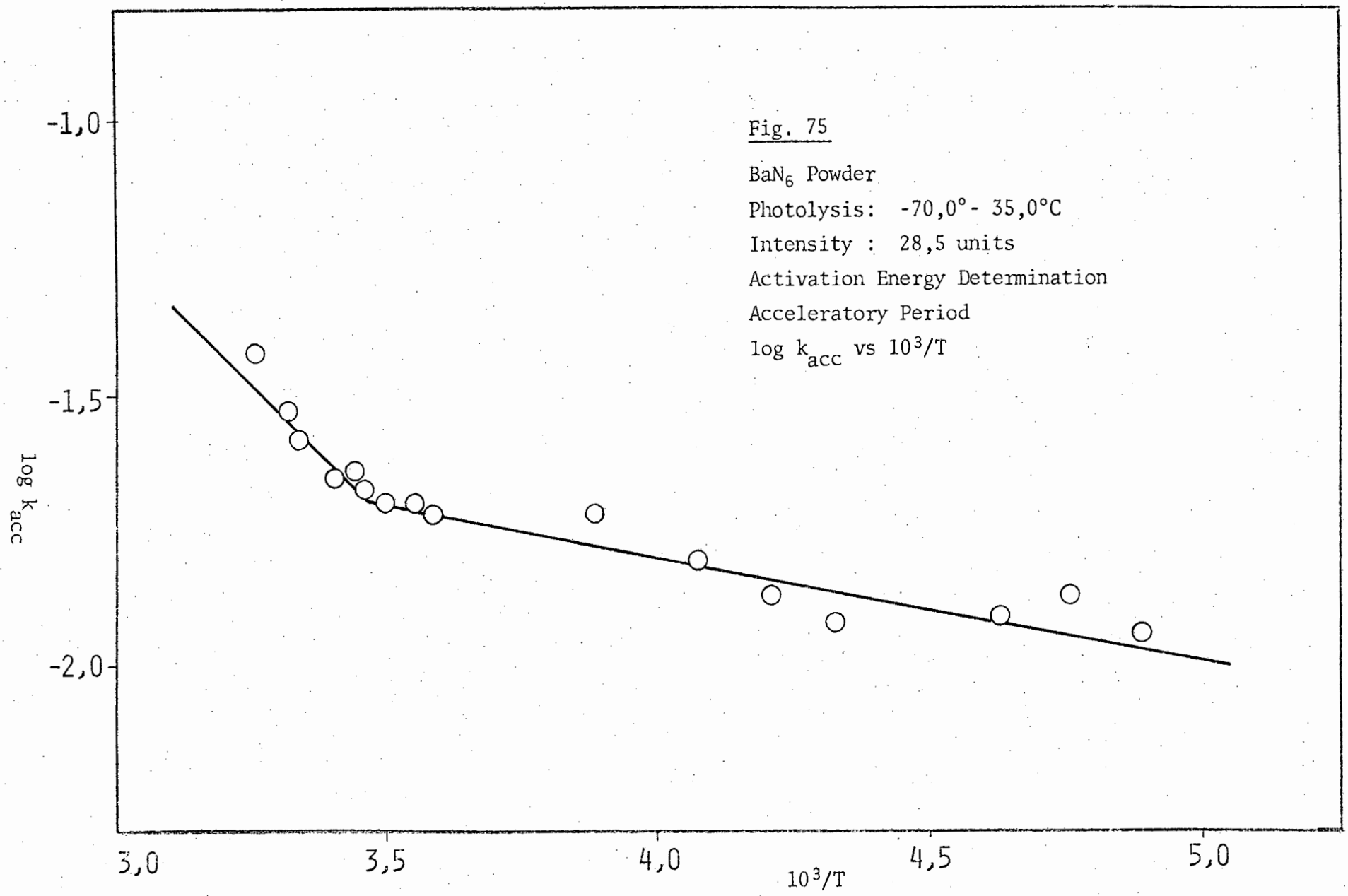

Fig. 75

BaN_6 Powder
Photolysis: -70,0°- 35,0°C
Intensity : 28,5 units
Activation Energy Determination
Acceleratory Period
log k_{acc} vs $10^3/T$

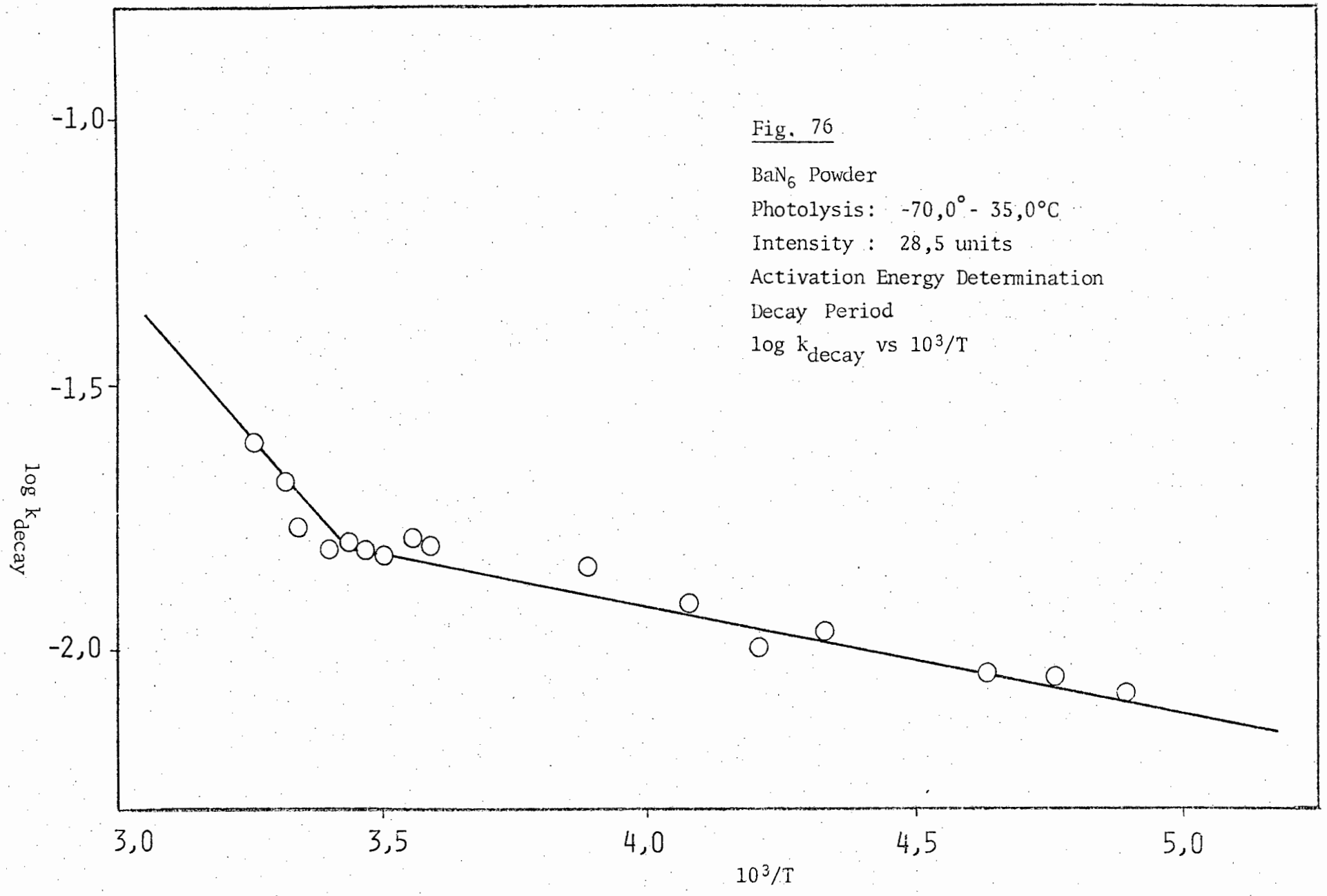

Fig. 76

BaN_6 Powder
Photolysis: -70,0° - 35,0°C
Intensity : 28,5 units
Activation Energy Determination
Decay Period
log k_{decay} vs $10^3/T$

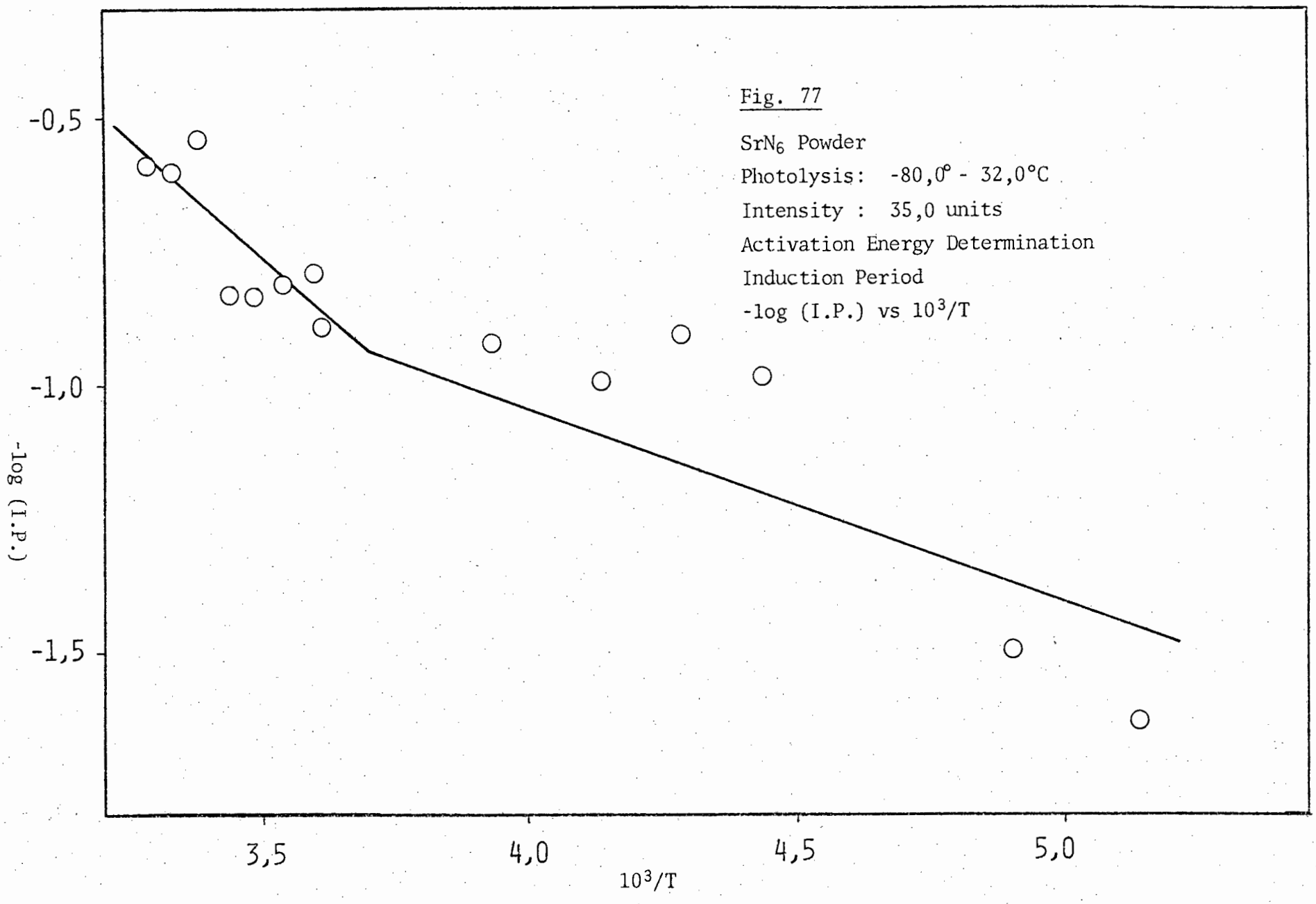

Fig. 77

SrN_6 Powder
Photolysis: -80,0° - 32,0°C
Intensity : 35,0 units
Activation Energy Determination
Induction Period
-log (I.P.) vs $10^3/T$

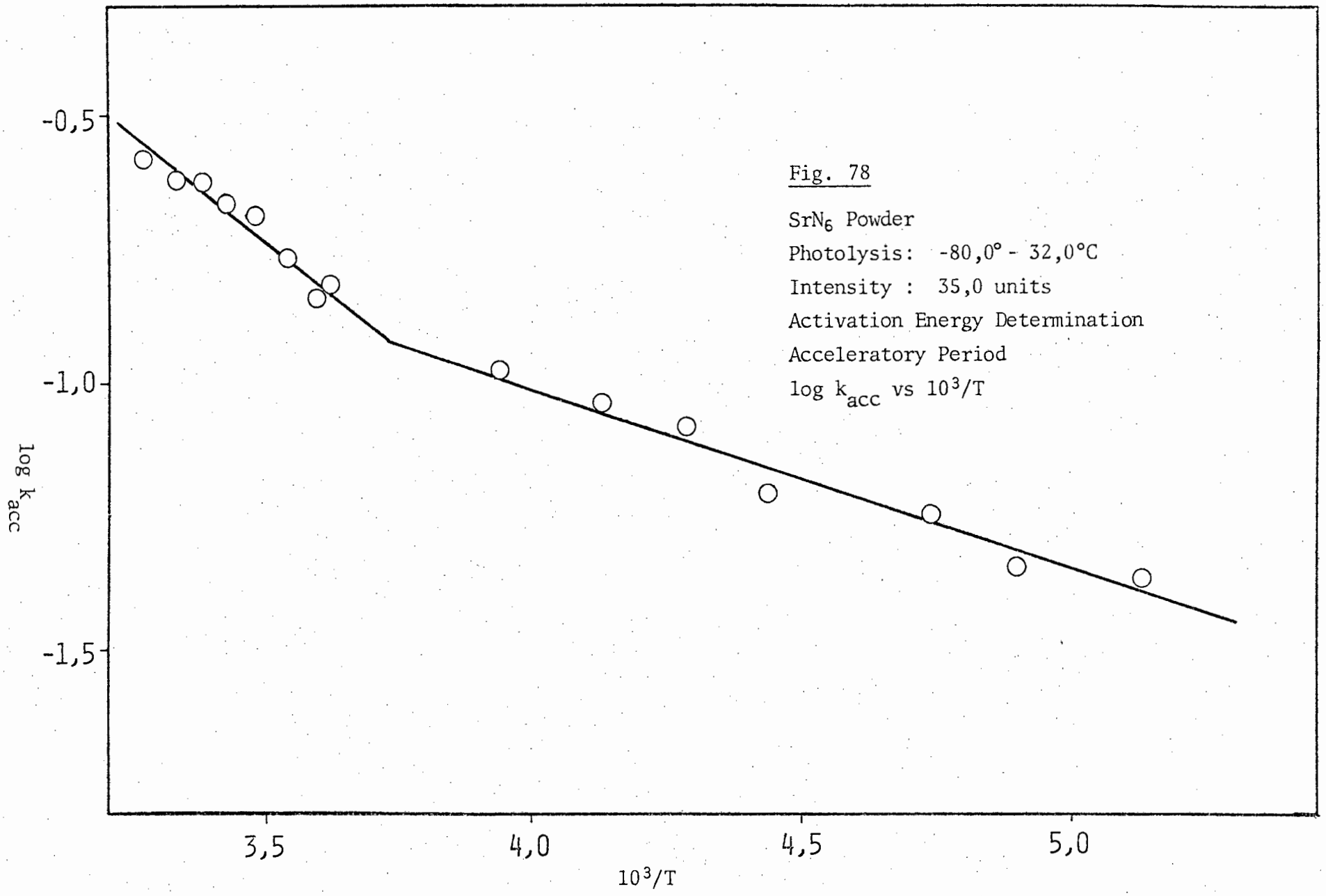

Fig. 78

SrN_6 Powder
Photolysis: -80,0° - 32,0°C
Intensity : 35,0 units
Activation Energy Determination
Acceleratory Period
log k_{acc} vs $10^3/T$

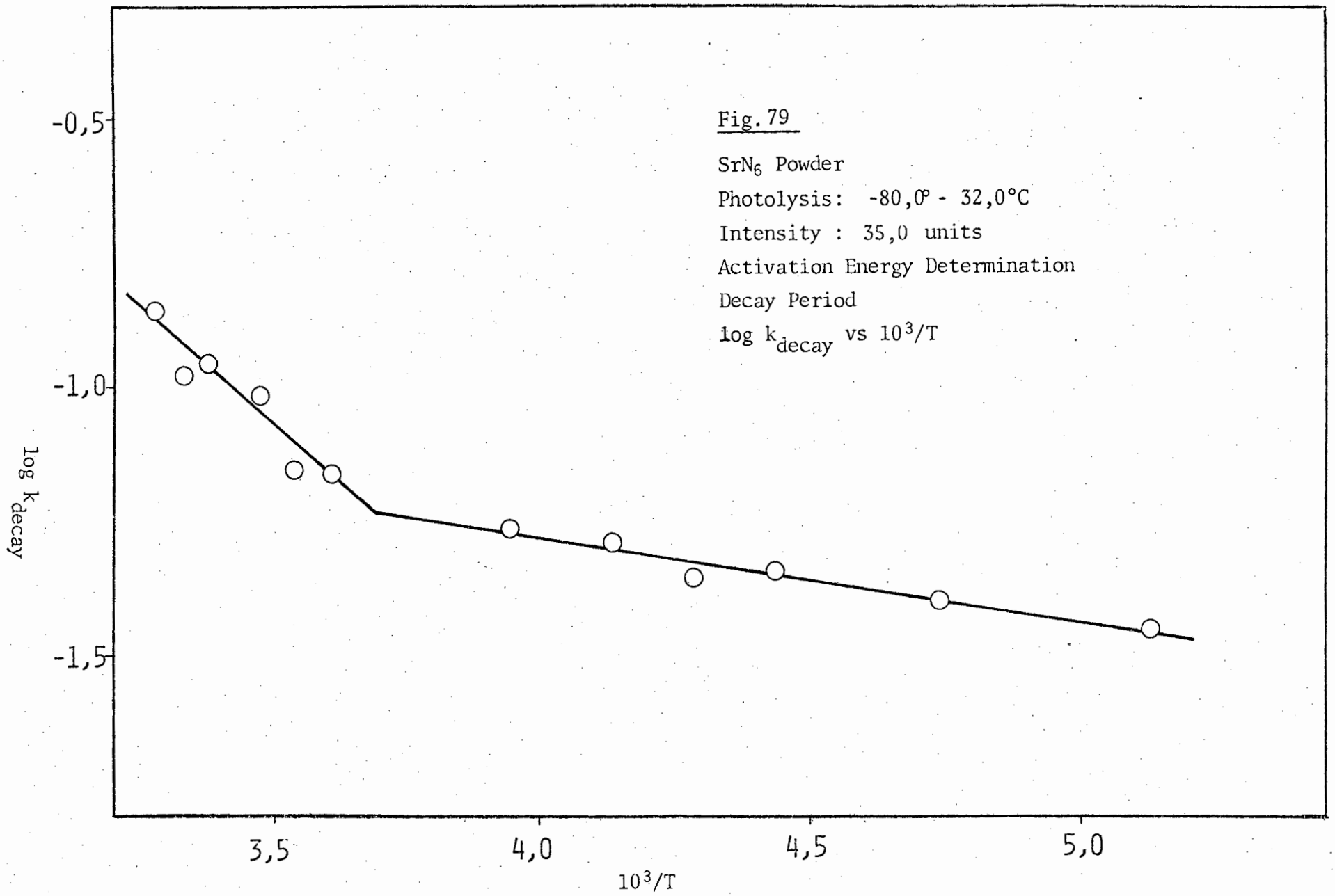

Fig. 79

SrN_6 Powder
Photolysis: -80,0° - 32,0°C
Intensity : 35,0 units
Activation Energy Determination
Decay Period
log k_{decay} vs $10^3/T$

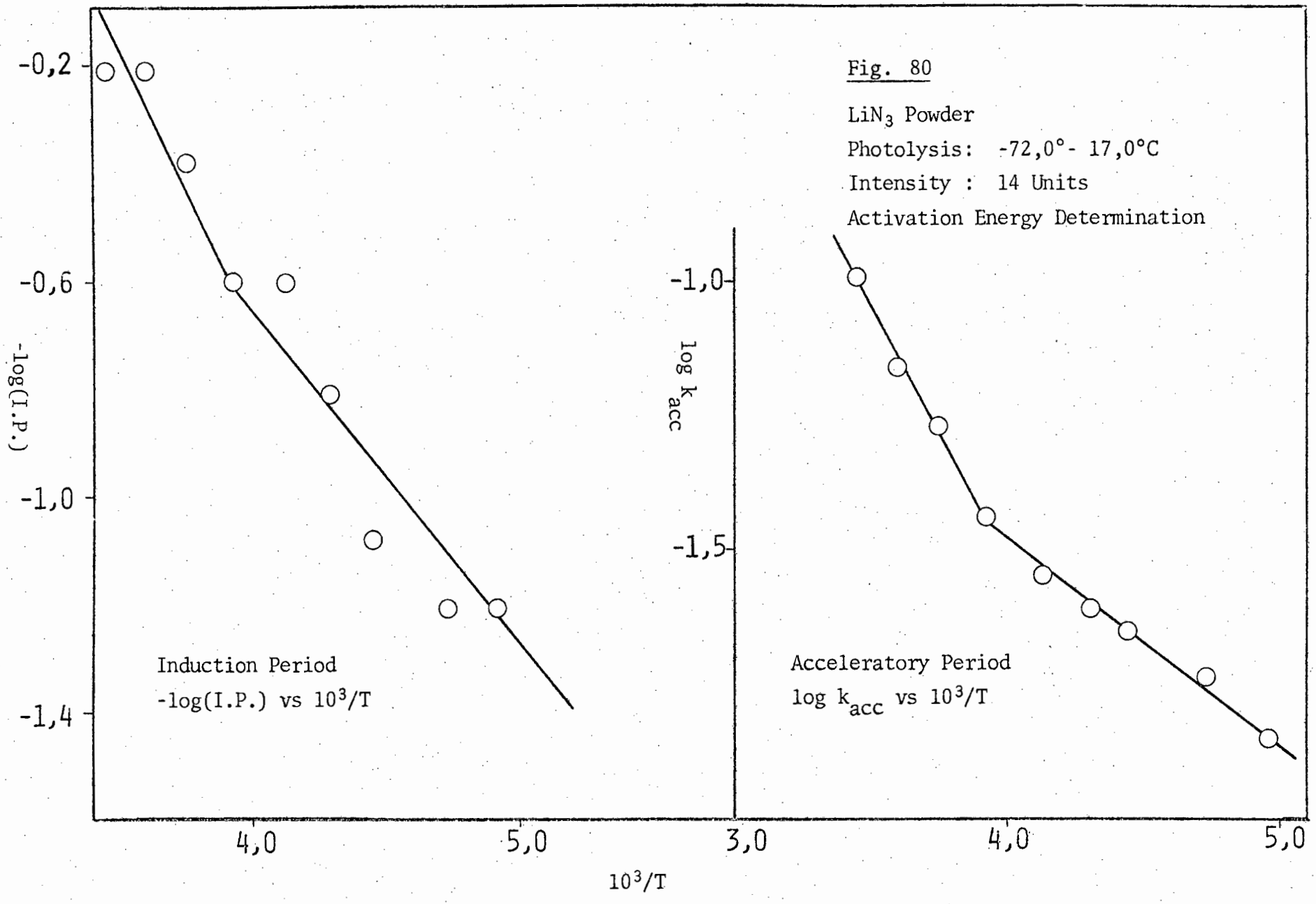

Fig. 80

LiN_3 Powder
Photolysis: -72,0°- 17,0°C
Intensity : 14 Units
Activation Energy Determination

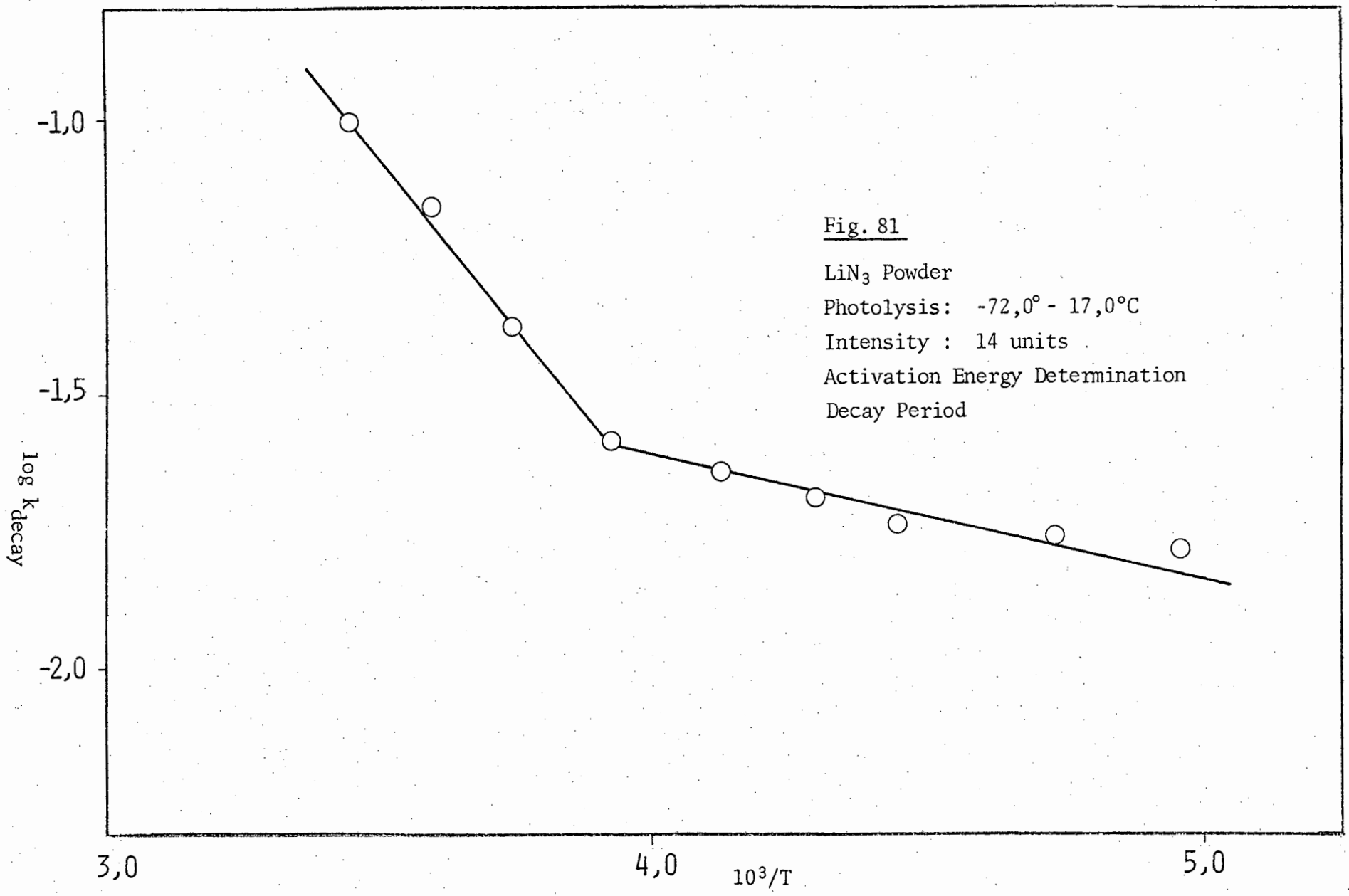

Fig. 81

LiN_3 Powder
Photolysis: -72,0° - 17,0°C
Intensity : 14 units
Activation Energy Determination
Decay Period

light has already been explained in section 8. The effect of variation of light intensity in the photolysis of calcium azide was studied at 19,5°C and -20,5°C; barium azide was studied at 22,0°C and -21,0°C; strontium azide at 18,2°C and -20,2°C and lithium azide at 30,0°C and -19,8°C.

The equation

$$k = I^m + c$$

was used to analyze the results. The value of m was obtained for each of the induction, acceleratory and decay reactions by plotting log k vs log I and determining the slope by a method of least squares.

Tables 39-42 give the rate constants for the induction period, the acceleratory and the decay reactions for the photolysis of calcium, barium, lithium and strontium azides at the abovementioned temperatures at various light intensities. Tables 43-46 give the values of m for calcium, barium, lithium and strontium azides respectively.

Fig. 82-89 show plots of k against I^m for calcium, barium, lithium and strontium azides respectively for the induction period and the acceleratory and decay reactions in each case. The values of m have been corrected to the nearest whole number for each azide.

(vi.e)Visual observations

The colour of the powder was observed at different stages of the photolytic decomposition. All observations were carried out at a temperature of -19,8°C. The results for all compounds were similar to observations made at higher temperatures. At the end of the induction period in the photolysis of calcium azide the powder had turned a pale brown colour which darkened as the decomposition progressed. As the inflection point was reached the upper surface turned dark brown and the lower surface was a somewhat lighter shade of brown. Beyond the inflection point the sample

Table 39 Rate constants for the photolysis of calcium azide powder at various light intensities

Temperature °C	Intensity Units	Induction Period min.	$k_{acc} \times 10^2$ min^{-1}.	$k_{decay} \times 10^2$ min^{-1}.
19,5	3,5	8,2	4,40	1,80
	6,5	6,4	13,90	8,60
	7,0	3,9	22,50	14,20
	9,5	2,6	41,90	16,10
-20,5	2,9	27,6	1,20	1,20
	4,0	4,4	2,50	2,30
	7,5	6,0	7,30	5,50
	9,0	3,4	18,20	8,70
	12,8	4,4	32,30	24,50

Table 40 Rate constants for the photolysis of barium azide powder at various light intensities

Temperature °C	Intensity Units	Induction Period min.	$k_{acc} \times 10^2$ min^{-1}.	$k_{decay} \times 10^2$ min^{-1}.
22,0	13,5	6,6	5,30	4,20
	15,5	2,0	5,20	4,80
	18,5	4,2	11,10	7,00
	22,0	2,0	15,80	13,80
	26,5	1,2	19,90	16,10
-21,0	2,7	16,0	1,80	1,30
	3,0	4,6	4,20	3,95
	4,5	1,3	4,00	3,80
	5,5	0,8	6,20	5,30
	6,7	0,4	20,80	10,70

Table 41 Rate constants for the photolysis of lithium azide powder at various light intensities

Temperature °C	Intensity Units	Induction Period min.	$k_{acc} \times 10^2$ min^{-1}.	$k_{decay} \times 10^2$ min^{-1}.
30,0	4,00	52,0	0,46	0,22
	6,50	67,6	0,70	0,50
	12,32	8,2	2,87	1,70
	13,03	15,2	3,50	1,70
	18,00	7,2	6,17	3,80
-19,8	5,10	78,0	0,82	0,25
	7,50	36,0	1,60	0,33
	11,00	22,0	2,80	0,81
	13,50	14,0	4,15	1,20

Table 42 Rate constants for the photolysis of strontium azide powder at various light intensities

Temperature °C	Intensity Units	Induction Period min.	$k_{acc} \times 10^2$ min^{-1}.	$k_{decay} \times 10^2$ min^{-1}.
18,2	5,5	16,0	3,10	2,30
	7,0	12,8	5,20	3,10
	9,5	7,0	7,40	5,30
	10,5	3,0	9,70	6,30
	13,0	1,3	23,30	8,80
-20,2	3,50	20,0	0,56	0,19
	6,50	40,0	1,80	1,20
	9,75	8,0	3,10	1,80
	11,85	9,9	10,80	5,10
	15,00	7,0	14,00	8,20

Table 43 Value of m in the equation $k = I^m + c$ for calcium azide powder

Temperature °C	Induction Period	Acceleratory Period	Decay Period
19,5	1,21	2,21	2,30
-20,5	1,00	2,23	2,00

Table 44 Value of m in the equation $k = I^m + c$ for barium azide powder

Temperature °C	Induction Period	Acceleratory Period	Decay Period
22,0	1,99	2,24	2,15
-21,0	2,50	2,02	1,69

Table 45 Value of m in the equation $k = I^m + c$ for lithium azide powder

Temperature °C	Induction Period	Acceleratory Period	Decay Period
30,0	1,54	1,81	1,86
-19,8	1,71	1,69	1,70

Table 46 Value of m in the equation $k = I^m + c$ for strontium azide powder

Temperature °C	Induction Period	Acceleratory Period	Decay Period
18,2	2,71	2,22	1,69
-20,2	0,75	2,12	2,35

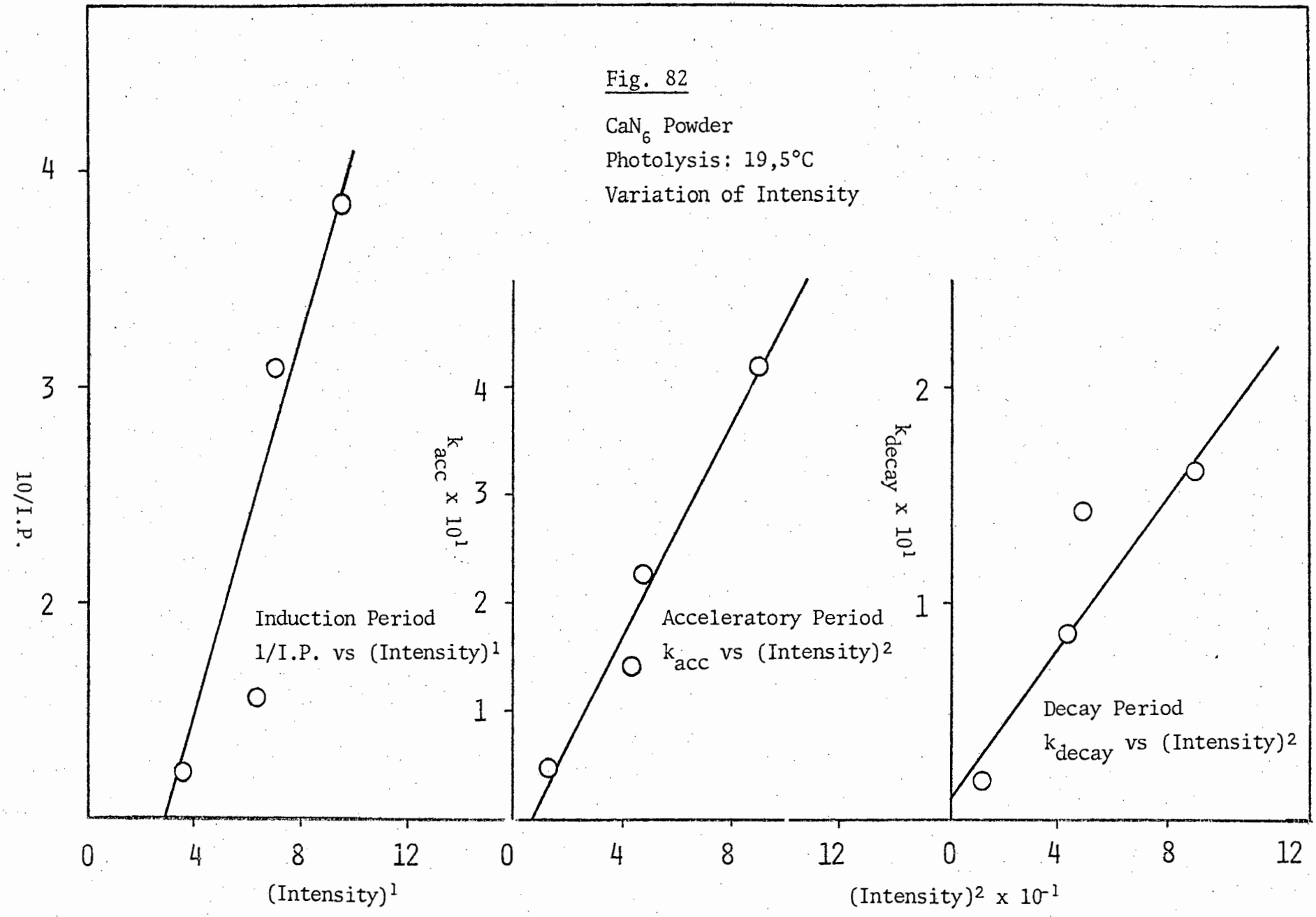
Fig. 82
CaN_6 Powder
Photolysis: 19,5°C
Variation of Intensity
1/I.P.
Induction Period
1/I.P. vs (Intensity)¹
(Intensity)¹
k_{acc} x 10¹
Acceleratory Period
k_{acc} vs (Intensity)²
k_{decay} x 10¹
Decay Period
k_{decay} vs (Intensity)²
(Intensity)² x 10⁻¹

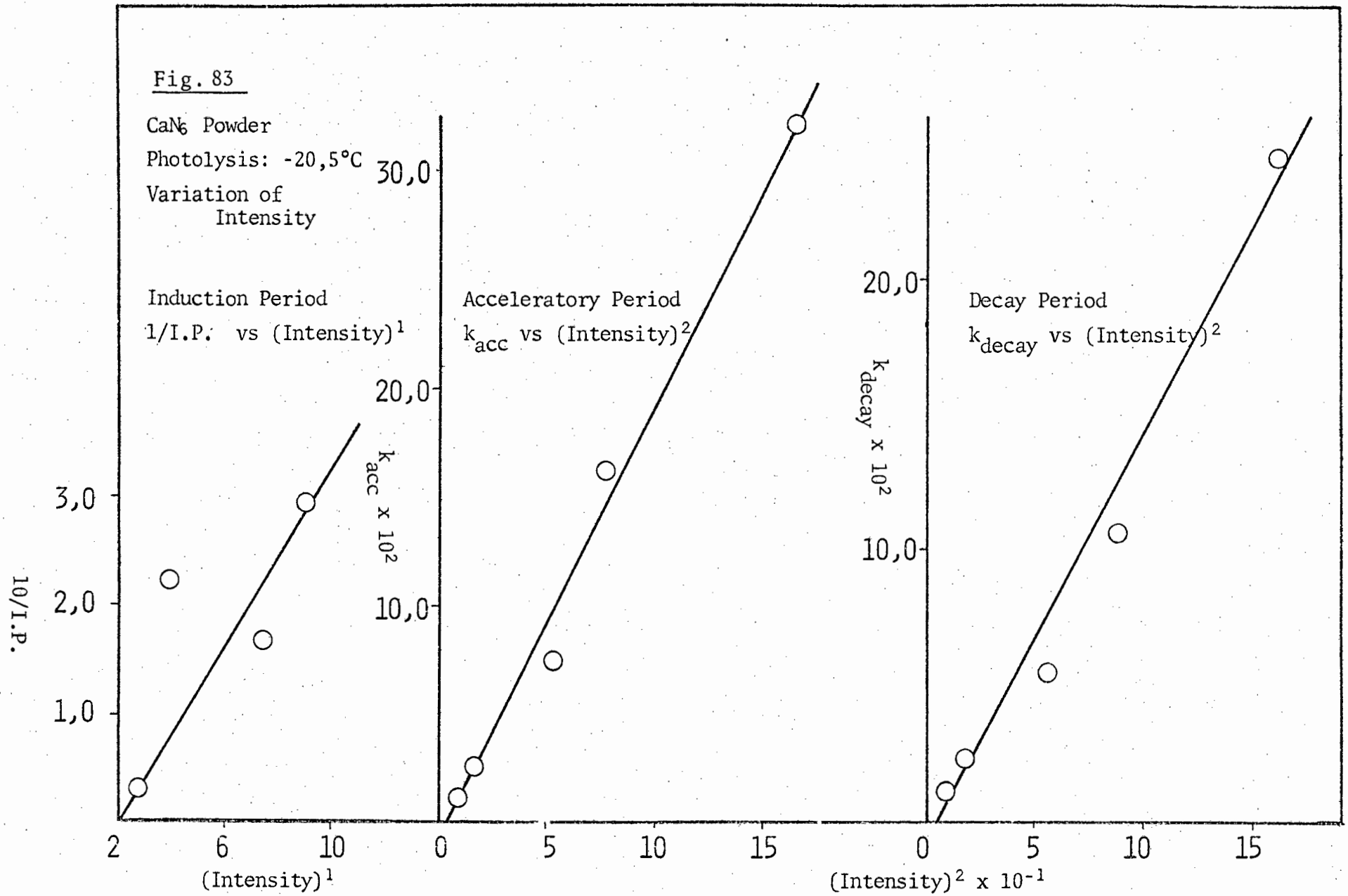
Fig. 83
CaN6 Powder
Photolysis: -20,5°C
Variation of Intensity
Induction Period
1/I.P. vs (Intensity)1
Acceleratory Period
kacc vs (Intensity)2
Decay Period
kdecay vs (Intensity)2
10/I.P.
3,0
2,0
1,0
kacc x 10²
30,0
20,0
10,0
kdecay x 10²
20,0
10,0
2
6
10
(Intensity)1
0
5
10
15
(Intensity)2 x 10-1

Fig. 84

BaN_6 Powder

Photolysis: 22,0°C

Variation of Intensity

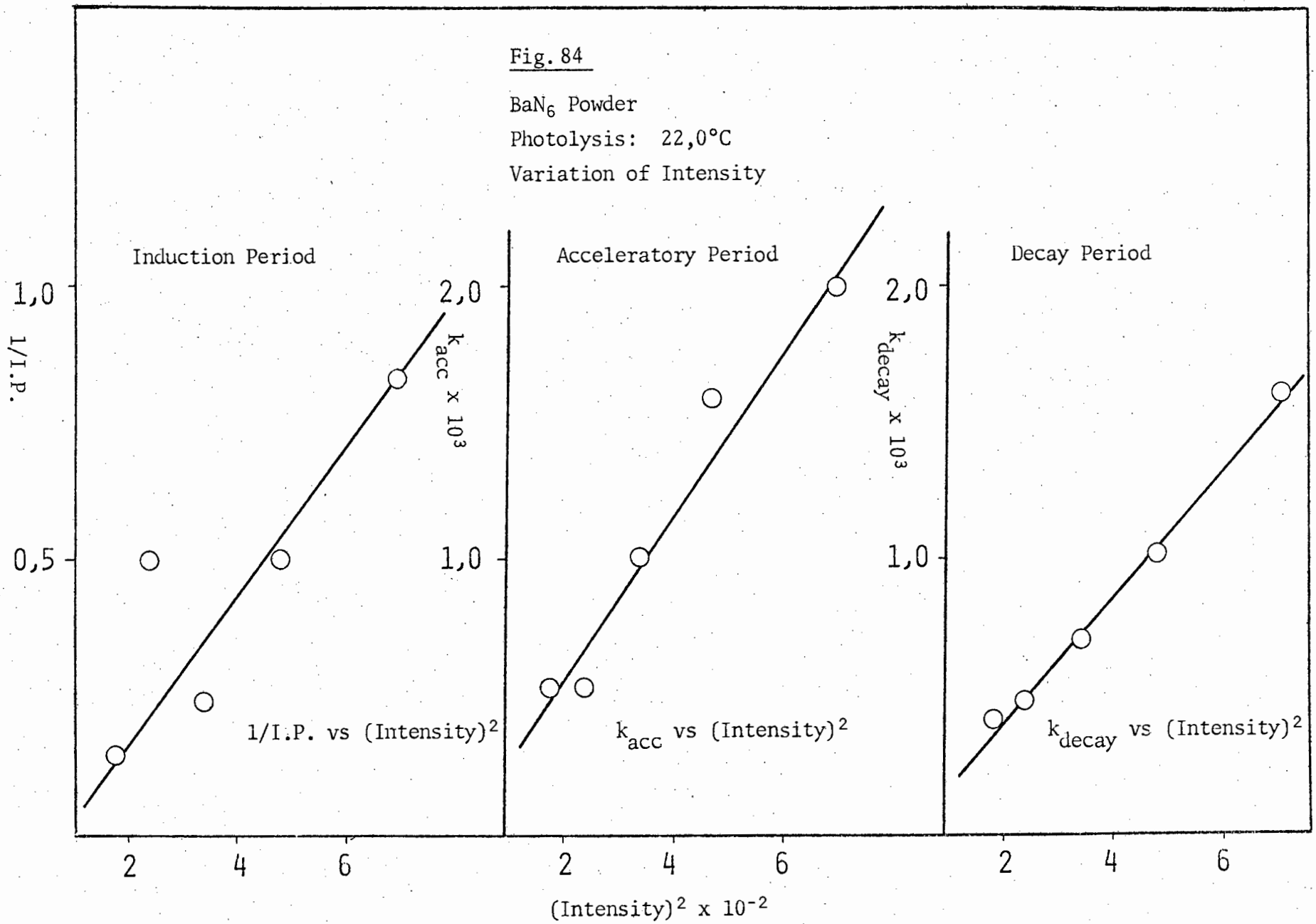

Fig. 85

BaN_6 Powder

Photolysis: -21,0°C

Variation of Intensity

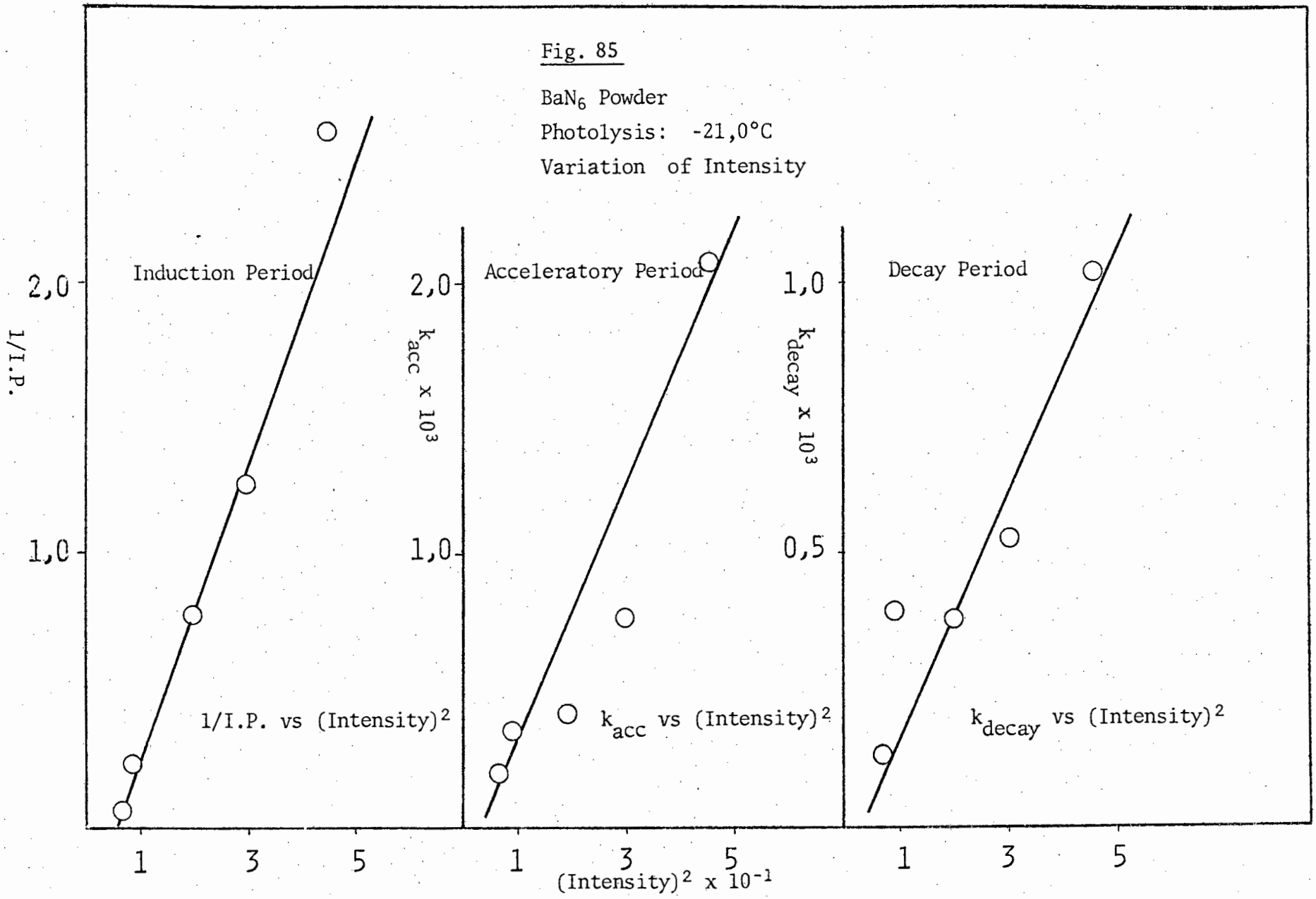

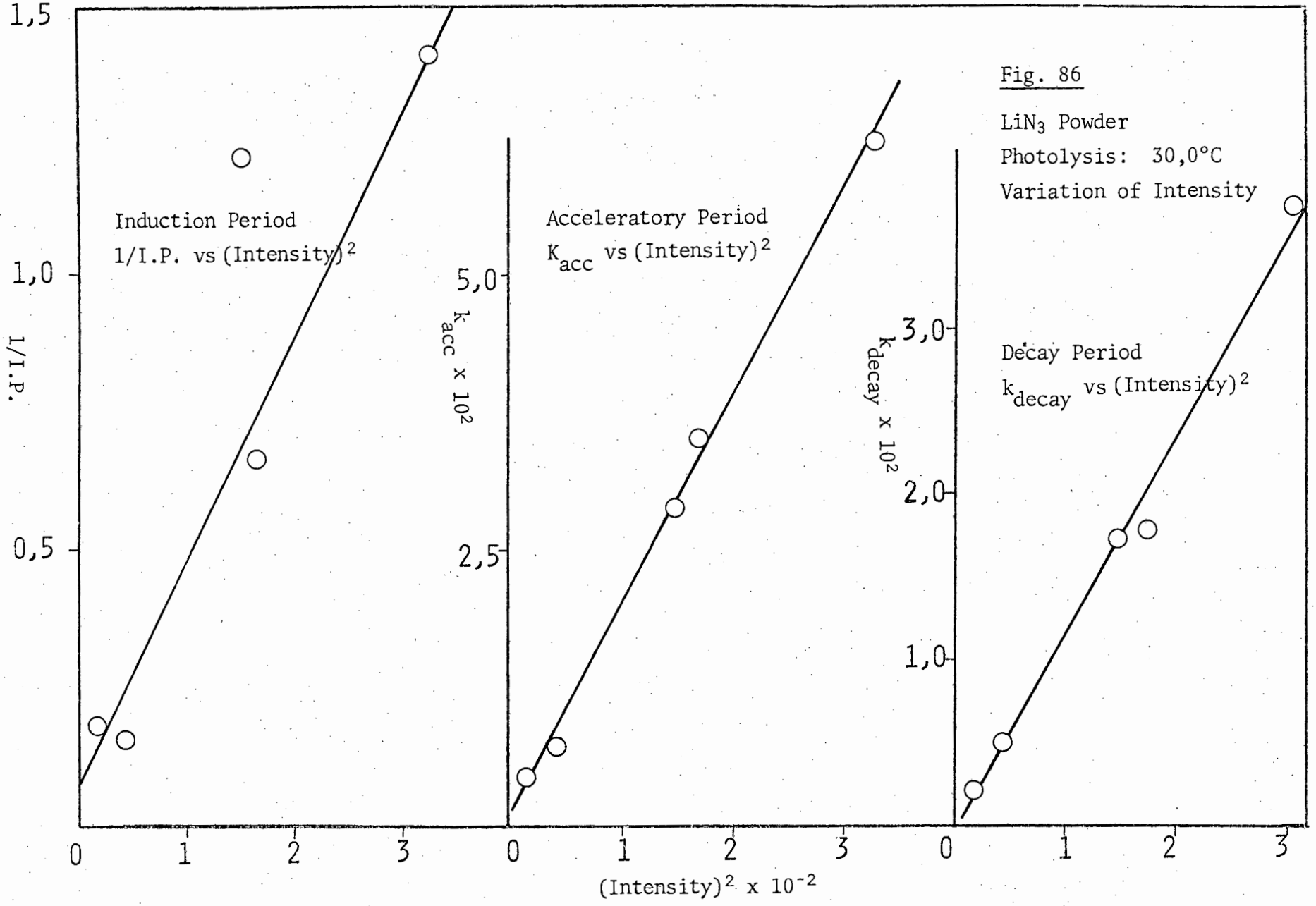

Fig. 86

LiN_3 Powder
Photolysis: 30,0°C
Variation of Intensity

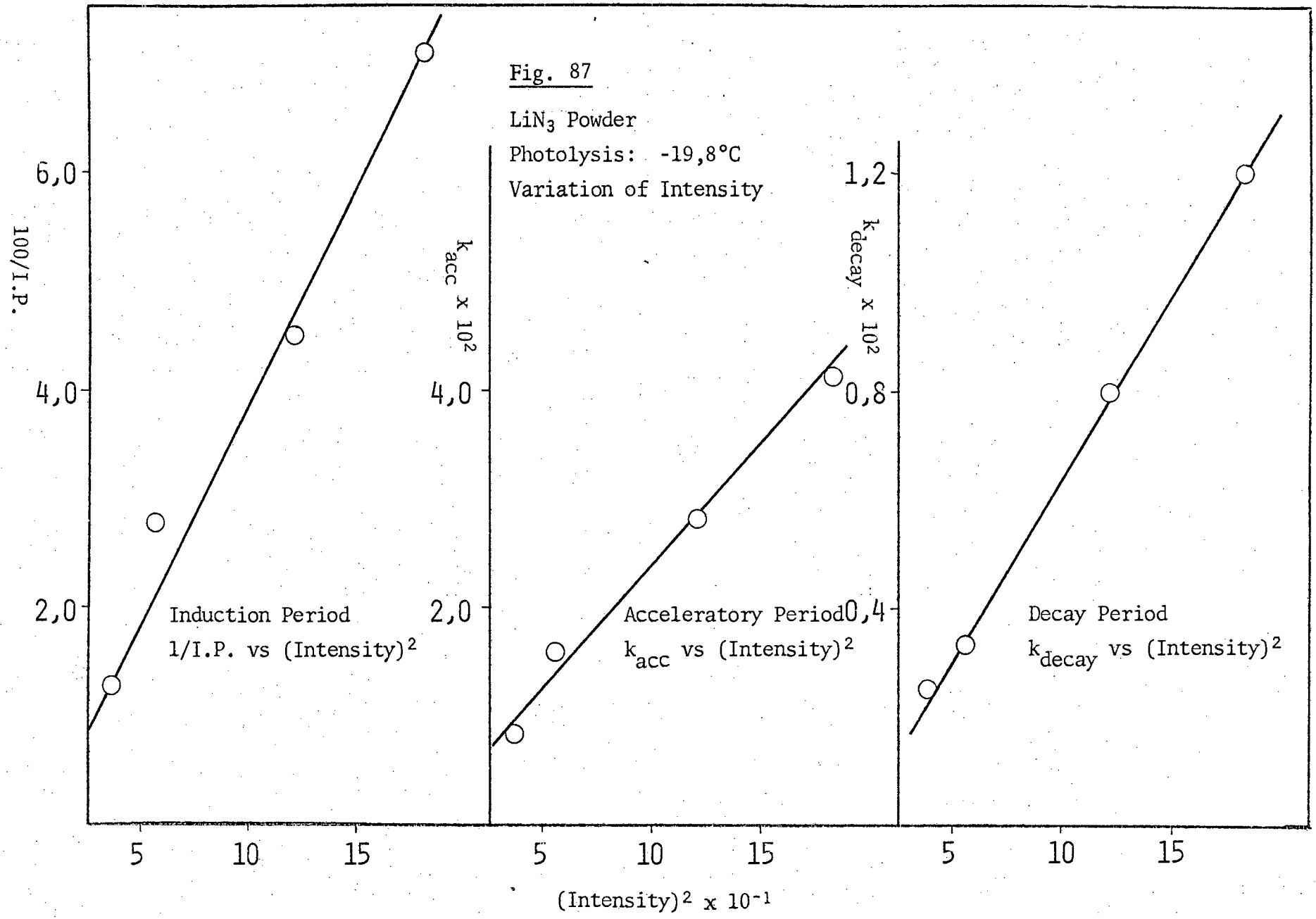
Fig. 87
LiN3 Powder
Photolysis: -19,8°C
Variation of Intensity
100/I.P.
6,0
4,0
2,0
Induction Period
1/I.P. vs (Intensity)2
kacc x 10²
4,0
2,0
Acceleratory Period
kacc vs (Intensity)2
kdecay x 10²
1,2
0,8
0,4
Decay Period
kdecay vs (Intensity)2
5
10
15
(Intensity)2 x 10-1

Fig. 88

SrN_6 Powder

Photolysis: 18,2°C

Variation of Intensity

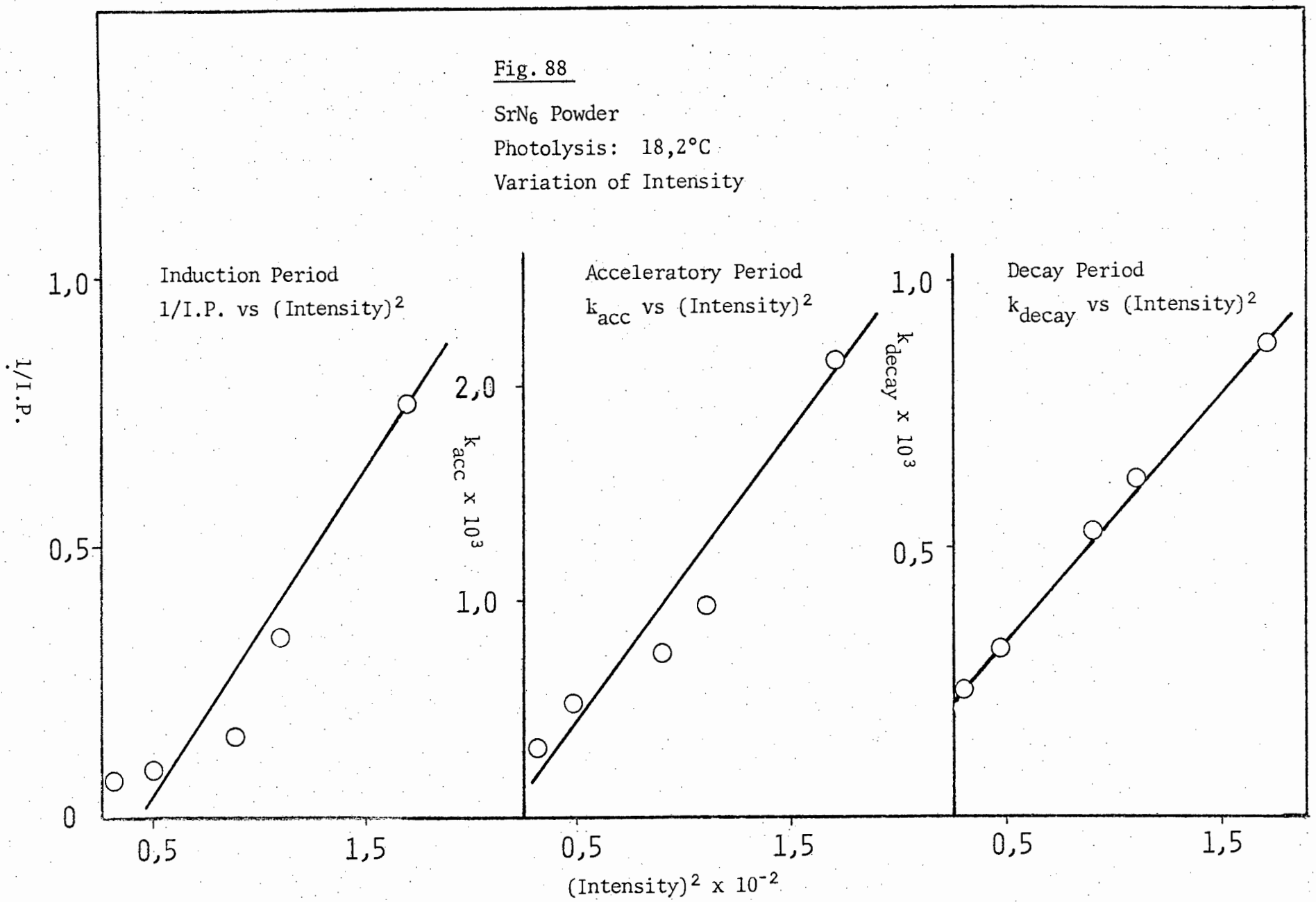

Fig. 89

SrN_6 Powder

Photolysis: -20,0°C

Variation of Intensity

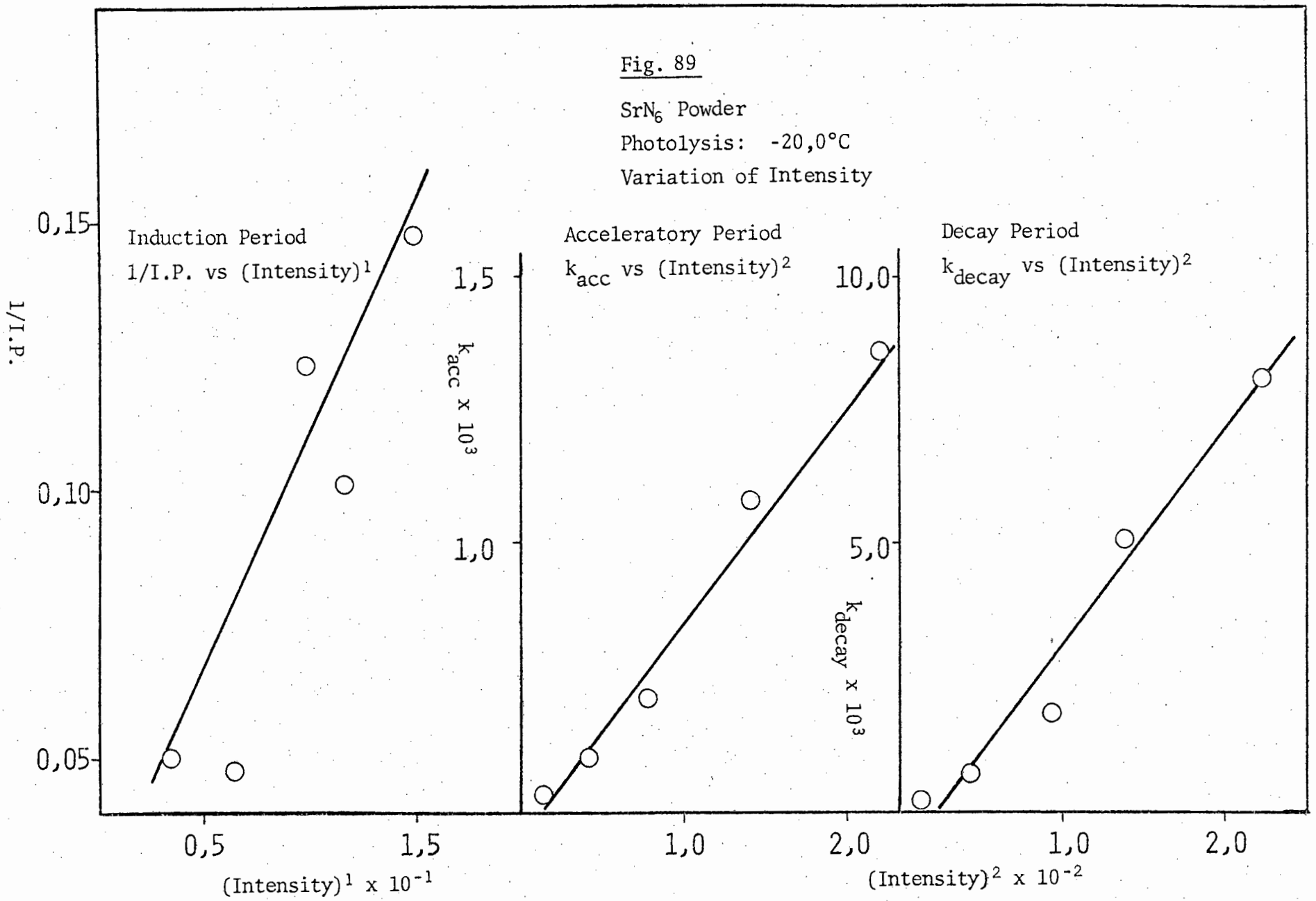

became a charcoal black colour and at the end of the decomposition the compound was dark brown/black wherever visible.

Barium azide showed similar colour changes to that described above for calcium azide as did strontium azide. Both compounds had turned a light brown at the end of the induction period and as the reaction proceeded violent explosions were observed and a continual darkening of the colour of the sample occurred. In the region of the inflection point the violence of the reaction diminished and the sample became a very dark brown colour. After prolonged exposure to ultraviolet radiation the sample eventually turned almost completely black. Lithium azide also showed similar characteristics to calcium azide. At the end of the decomposition the particles varied in colour from a very dark brown to black.

(vi.f) Interruption of a photodecomposition: dark rate determination

All photolytic decompositions of calcium, barium, strontium and lithium azides, in the temperature range under consideration, ceased the moment the source of the ultraviolet light was removed. No measurable dark rate could be observed in these ranges. On recommencing photolytic decompositions the runs continued as though no interruption had taken place.

(vi.g) Admittance of water vapour following an interruption

In order to investigate the presence of metallic nuclei at various stages of the photolytic decomposition of the four azides, water vapour (17 torr pressure) was introduced after the reaction had reached a certain point. These decompositions, called 'water interruptions', were carried out according to the method described in section 9 *(i.g)*. The prior investigation regarding the effect of an interruption on the subsequent

decomposition, as explained in section 9 *(i.e)*, was carried out. No effect was observed.

Water interruptions were carried out on calcium azide at a temperature of 25,0°C and a light intensity of 42,0 units. Fig. 90 illustrates the results for calcium azide. Water vapour was introduced for 1 minute at t = 0 and at α values of 0,02; 0,15; 0,30 and 0,52. Interruptions at t = 0 had no effect on the subsequent reaction. A new induction period, shorter than that of the uninterrupted run, was detected when water vapour was introduced at α = 0,01. The subsequent reaction showed a decrease in k_{acc} and k_{decay}. Water vapour introduced at positions further along the decomposition curve caused subsequent reactions to proceed after longer induction periods followed by acceleratory and decay reactions. The duration of the induction period became progressively greater and the rates of the acceleratory and decay reactions decreased as the point of interruption along the curve increased. Water vapour introduced at the inflection point and at various positions during the decay reaction destroyed any further reaction. The final pressure of decomposition which followed 'water interruptions' at α = 0,01 and at positions further along the decomposition curve, was reduced from that of an uninterrupted decomposition. Fig. 91 illustrates the results obtained for 'water interruptions' on strontium azide powder (temperature 25,0°C and light intensity 37,0 units) at α values of 0,04; 0,14 and 0,51. Fig. 92 illustrates the results of barium azide (temperature 23,0°C and light intensity 22,0 units) at α values of 0,01; 0,10; 0,36 and 0,52. Fig. 93 illustrates the results of lithium azide (temperature 30,0°C and light intensity 35,0 units) at α values of 0,13 and 0,49. As is clearly shown in these figures the effects of 'water interruptions' on these azides are almost identical to those obtained for calcium azide powder. Fig. 94

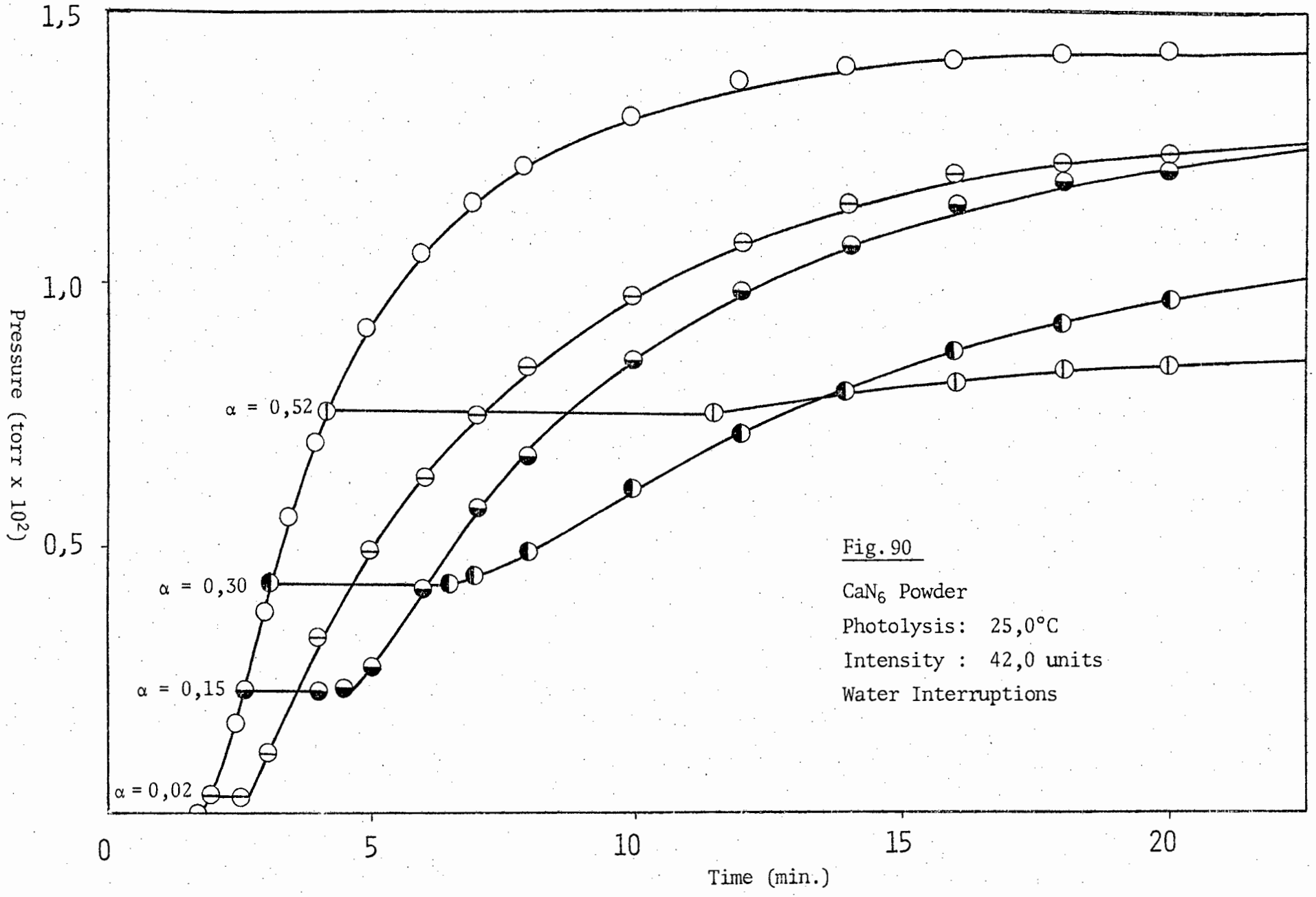

Fig. 90

CaN_6 Powder

Photolysis: 25,0°C

Intensity : 42,0 units

Water Interruptions

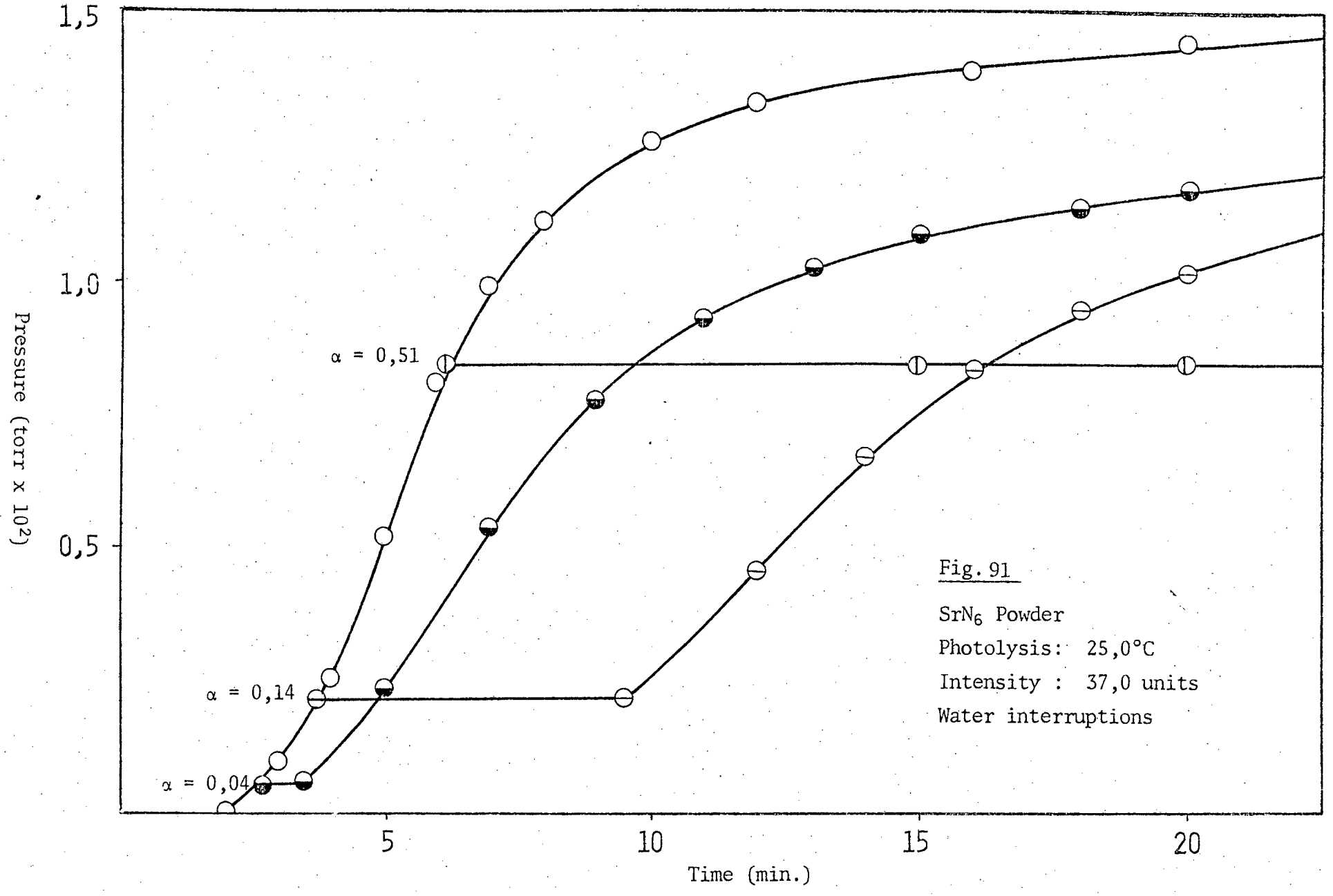

Fig. 91

SrN_6 Powder
Photolysis: 25,0°C
Intensity : 37,0 units
Water interruptions

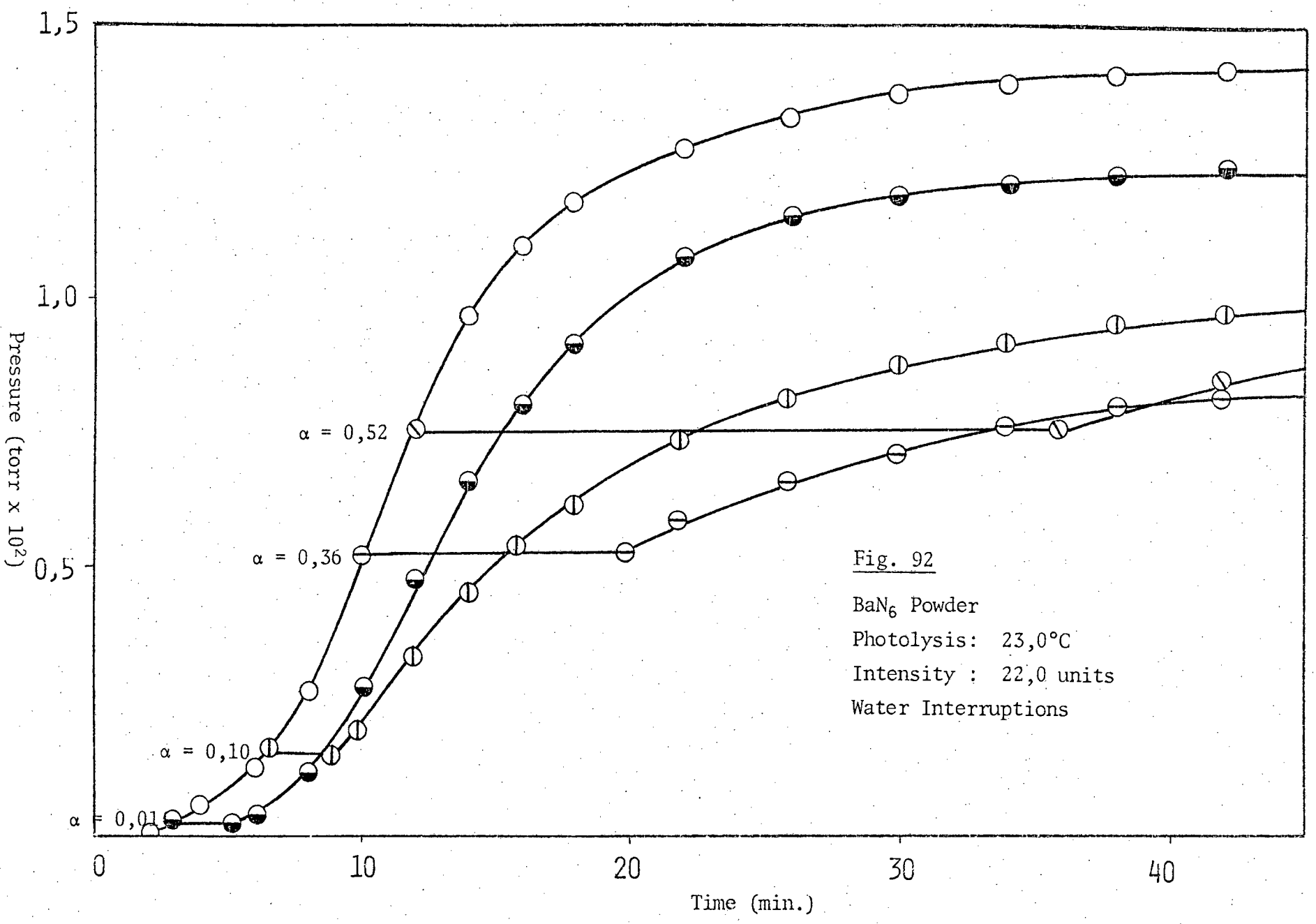

Fig. 92

BaN_6 Powder

Photolysis: 23,0°C

Intensity : 22,0 units

Water Interruptions

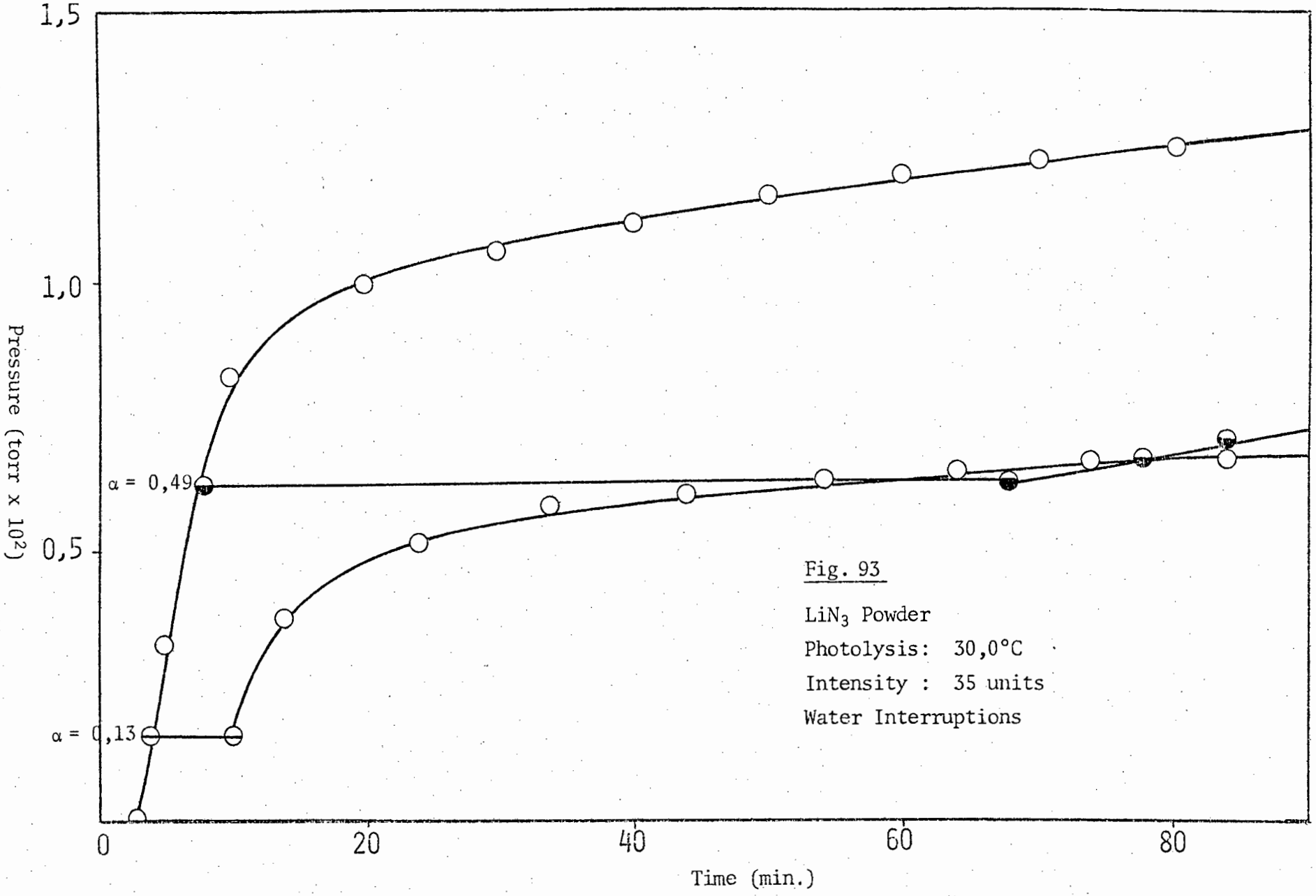

Fig. 93

LiN_3 Powder
Photolysis: 30,0°C
Intensity : 35 units
Water Interruptions

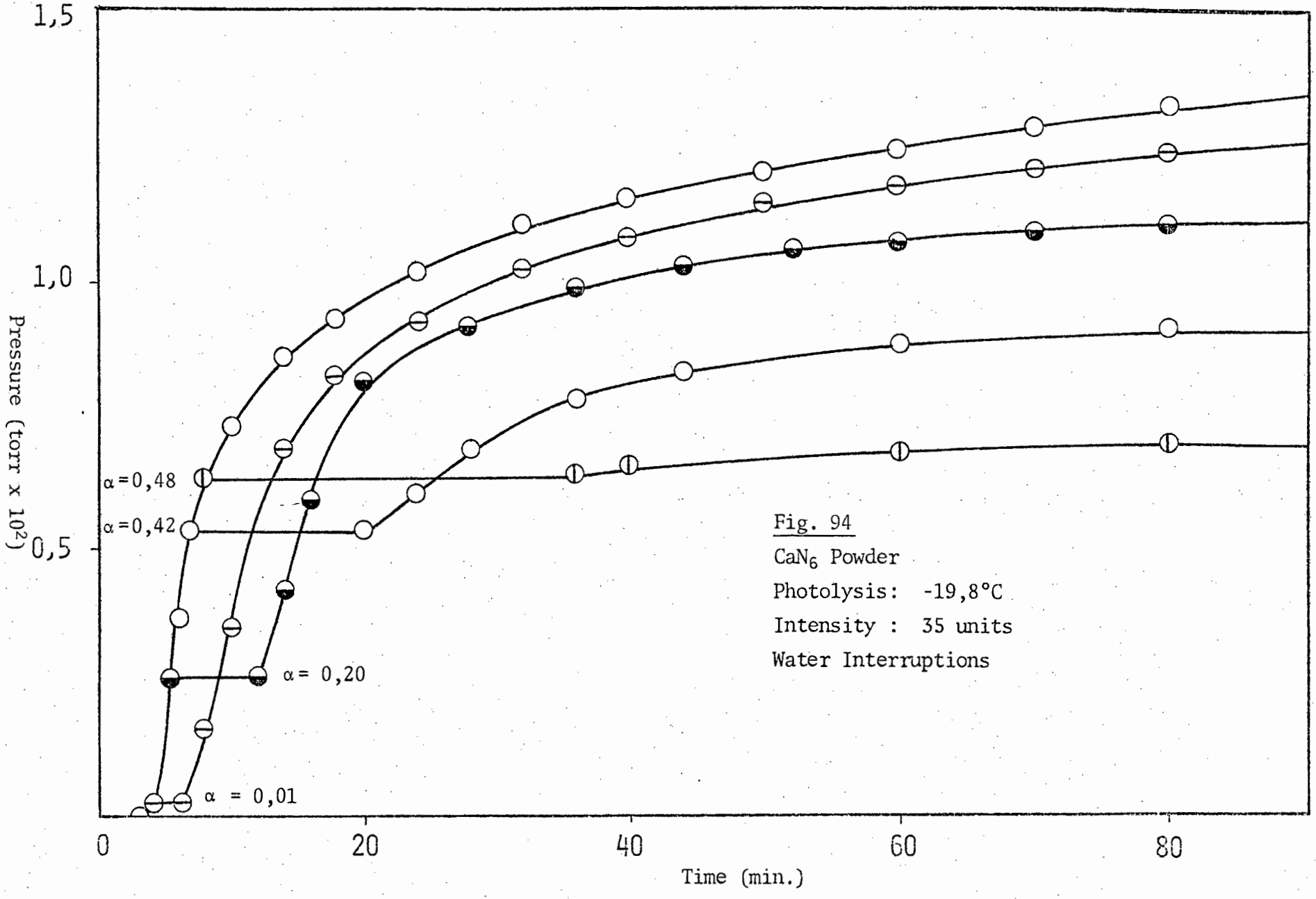

Fig. 94

CaN_6 Powder

Photolysis: -19,8°C

Intensity : 35 units

Water Interruptions

illustrates the results obtained for 'water interruptions' on calcium azide powder at α values of 0,01; 0,20; 0,42 and 0,48 for the decompositions at -19,8°C and a light intensity of 35,0 units. The effects of 'water interruptions' at this temperature are the same as at higher temperatures i.e decrease in the value of k_{acc} and k_{decay} and lengthening of the induction period at progressively greater values of α and a virtual destruction of the reaction when the interruption takes place beyond the inflection point. Water interruptions during the photolysis of barium, strontium and lithium azides at temperatures in the region of -20,0°C yielded similar results to those shown for calcium azide.

(vi.h) The effects of filtering the high intensity arc with blue and ultraviolet transmission filters.

Various Schott filters were employed in order to determine which wavelengths of ultraviolet radiation were most effective for the photolysis of calcium, barium, strontium and lithium azides at ambient and lower temperatures. The filters used, their Chance equivalents and the wavelengths and intensities transmitted have already been listed in Table 13.

Photodecompositions were carried out on calcium azide (decomposition temperatures 20,0°C and -20,0°C at light intensities of 50,0 units and 28,5 units respectively), lithium azide (decomposition temperatures of 30,0°C and -19,8°C at light intensities of 27,5 units and 35,0 units respectively), barium azide (decomposition temperatures of 21,5°C and -20,2°C and at light intensities of 33,0 units and 22,0 units respectively) and strontium azide (decomposition temperatures of 25,0°C and -19,5°C at a light intensity of 37,0 units in both cases).

The effect of the filters were in all cases a reduction in the reaction rate. With the 5 mm filter either no reaction or a negligibly slow reaction

occurred. In the case of barium, strontium and lithium azides the reaction with the 1 mm filter was considerably slower than that with the 3 mm filter. In the case of calcium azide the difference in the rates using these two filters was not as marked as with the other azides.

Fig. 95-102 illustrate the effect of filters on the photodecompositions of the various azides under the conditions described above.

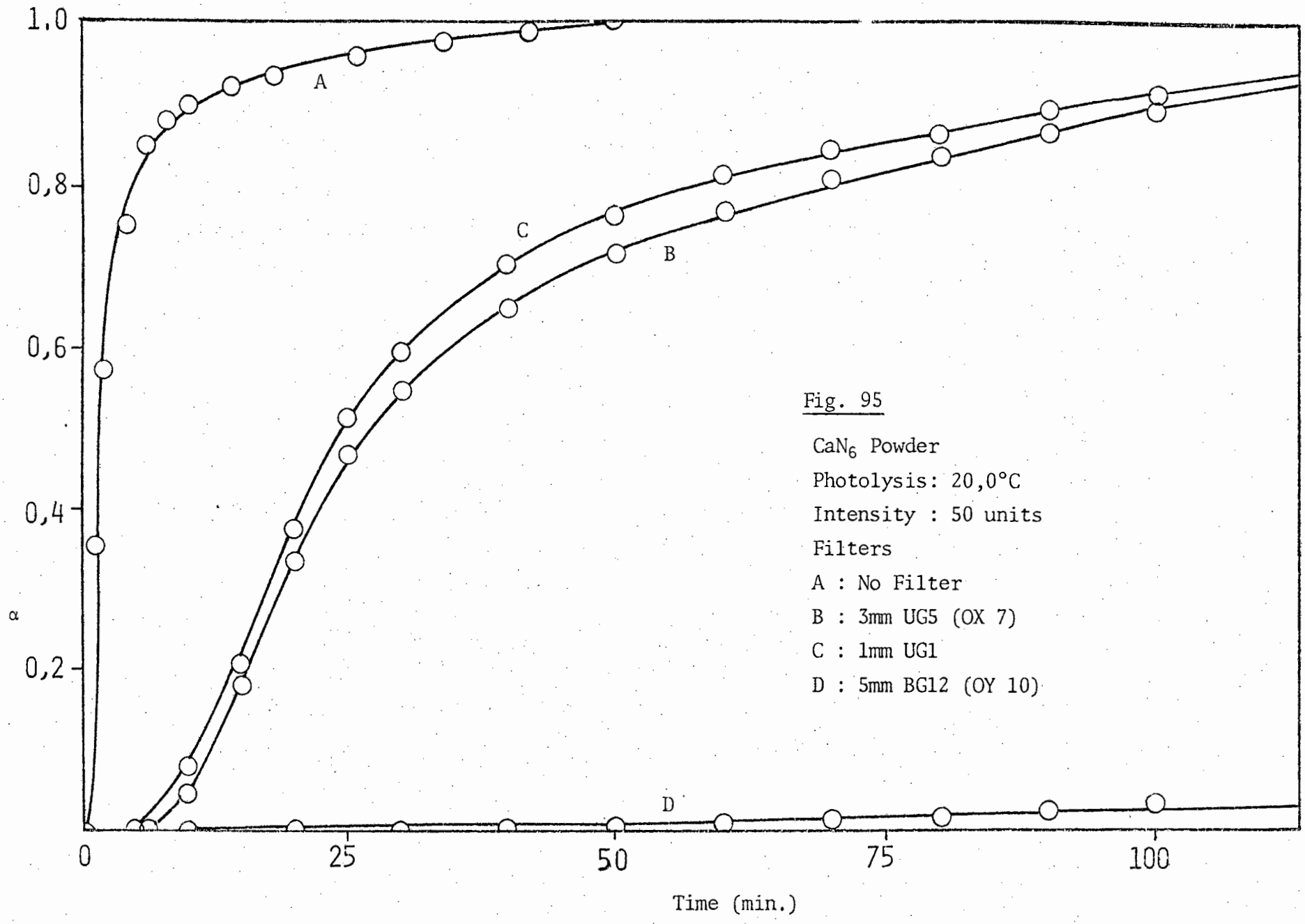

Fig. 95

CaN_6 Powder
Photolysis: 20,0°C
Intensity : 50 units
Filters
A : No Filter
B : 3mm UG5 (OX 7)
C : 1mm UG1
D : 5mm BG12 (OY 10)

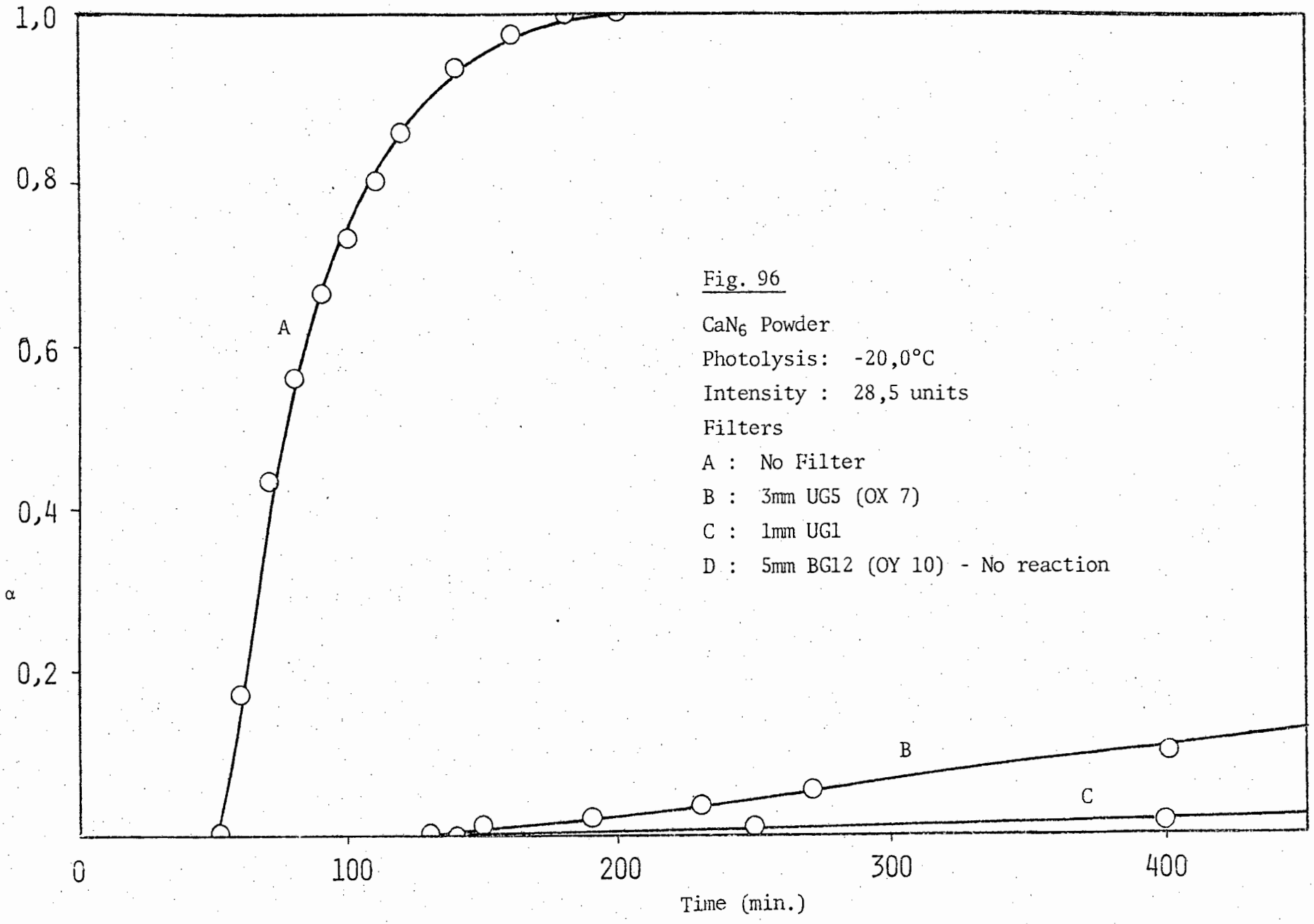

Fig. 96

CaN_6 Powder

Photolysis: -20,0°C

Intensity : 28,5 units

Filters

A : No Filter

B : 3mm UG5 (OX 7)

C : 1mm UG1

D : 5mm BG12 (OY 10) - No reaction

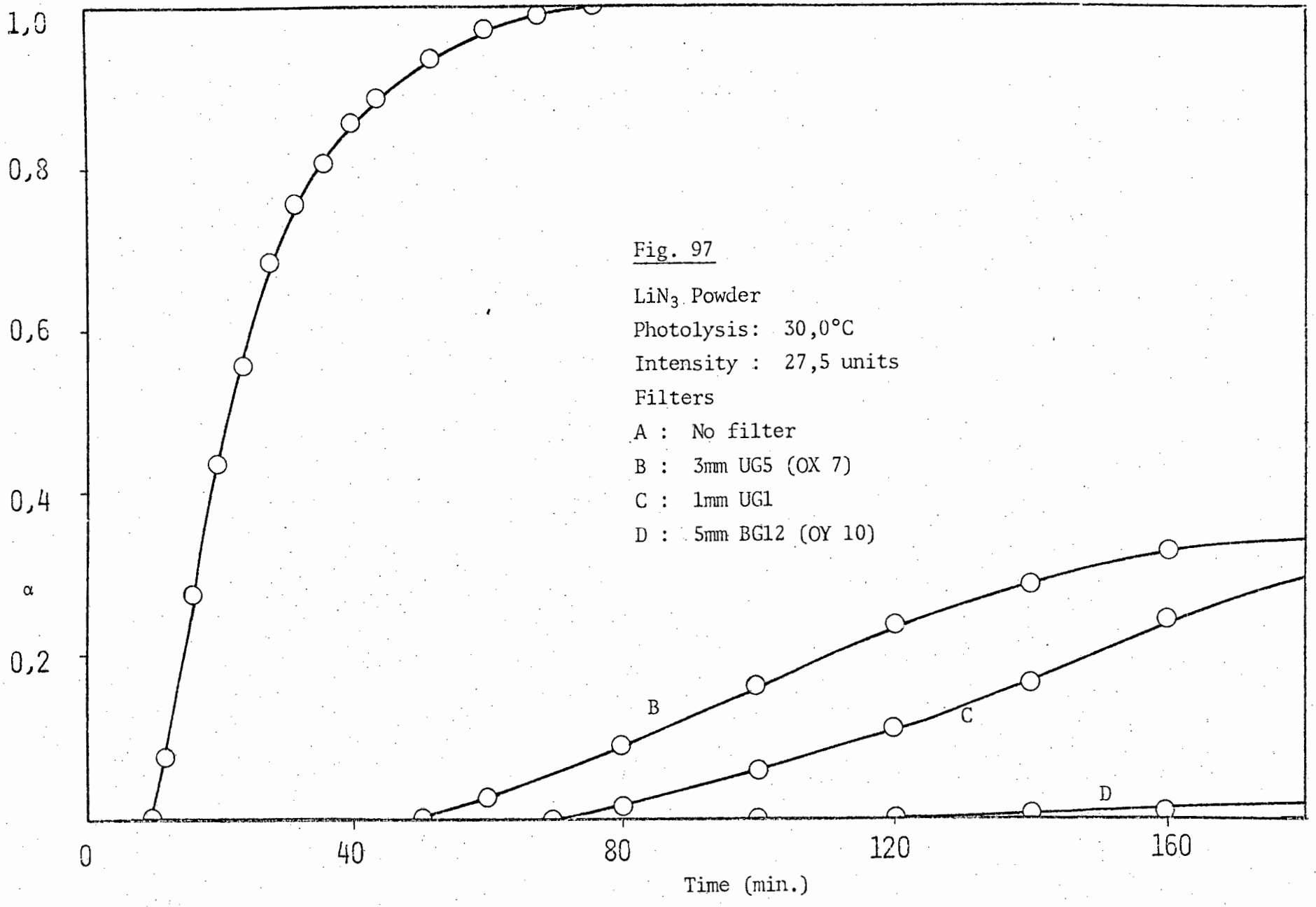

Fig. 97

LiN_3 Powder

Photolysis: 30,0°C

Intensity : 27,5 units

Filters

A : No filter

B : 3mm UG5 (OX 7)

C : 1mm UG1

D : 5mm BG12 (OY 10)

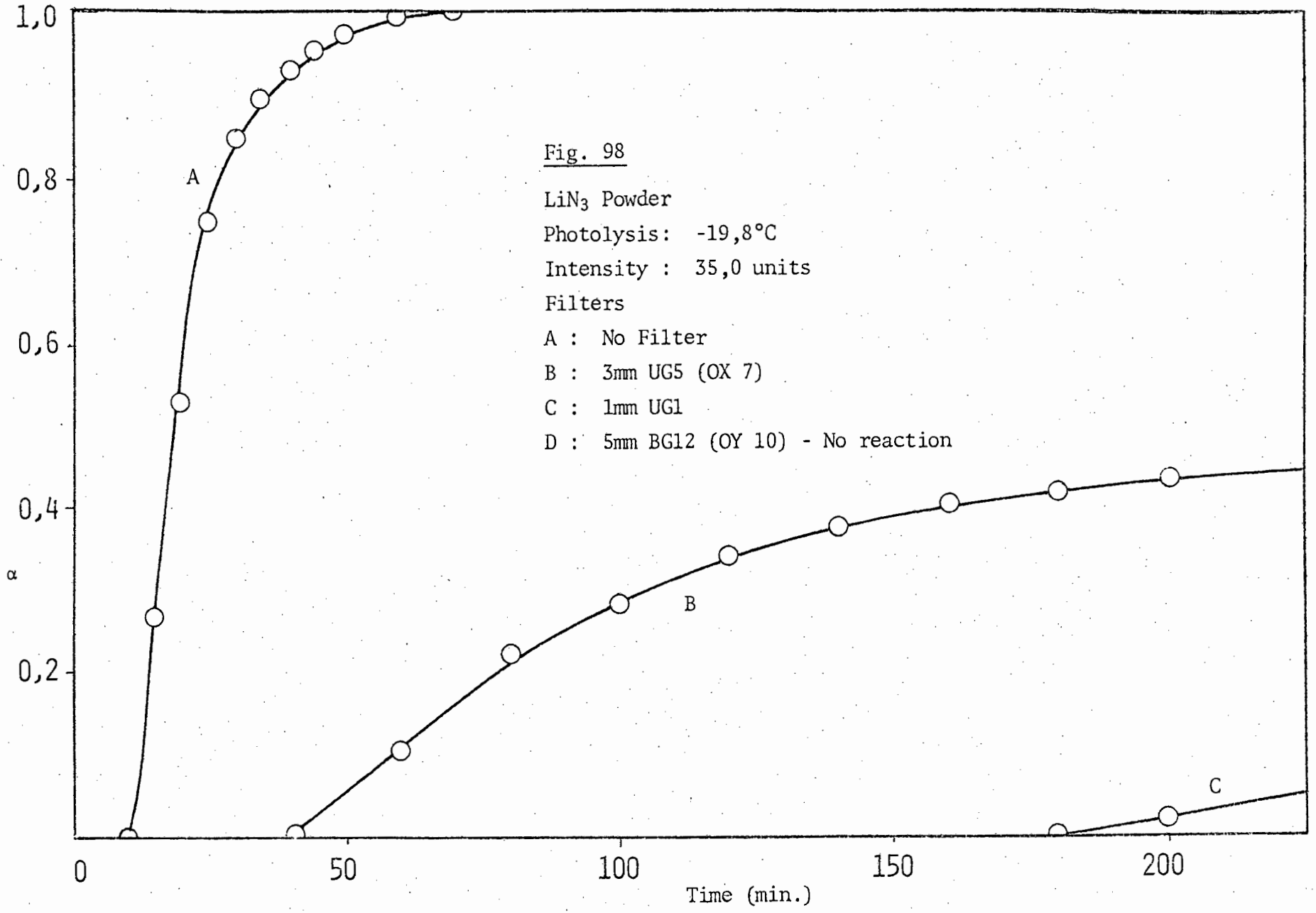

Fig. 98

LiN_3 Powder

Photolysis: -19,8°C

Intensity : 35,0 units

Filters

A : No Filter

B : 3mm UG5 (OX 7)

C : 1mm UG1

D : 5mm BG12 (OY 10) - No reaction

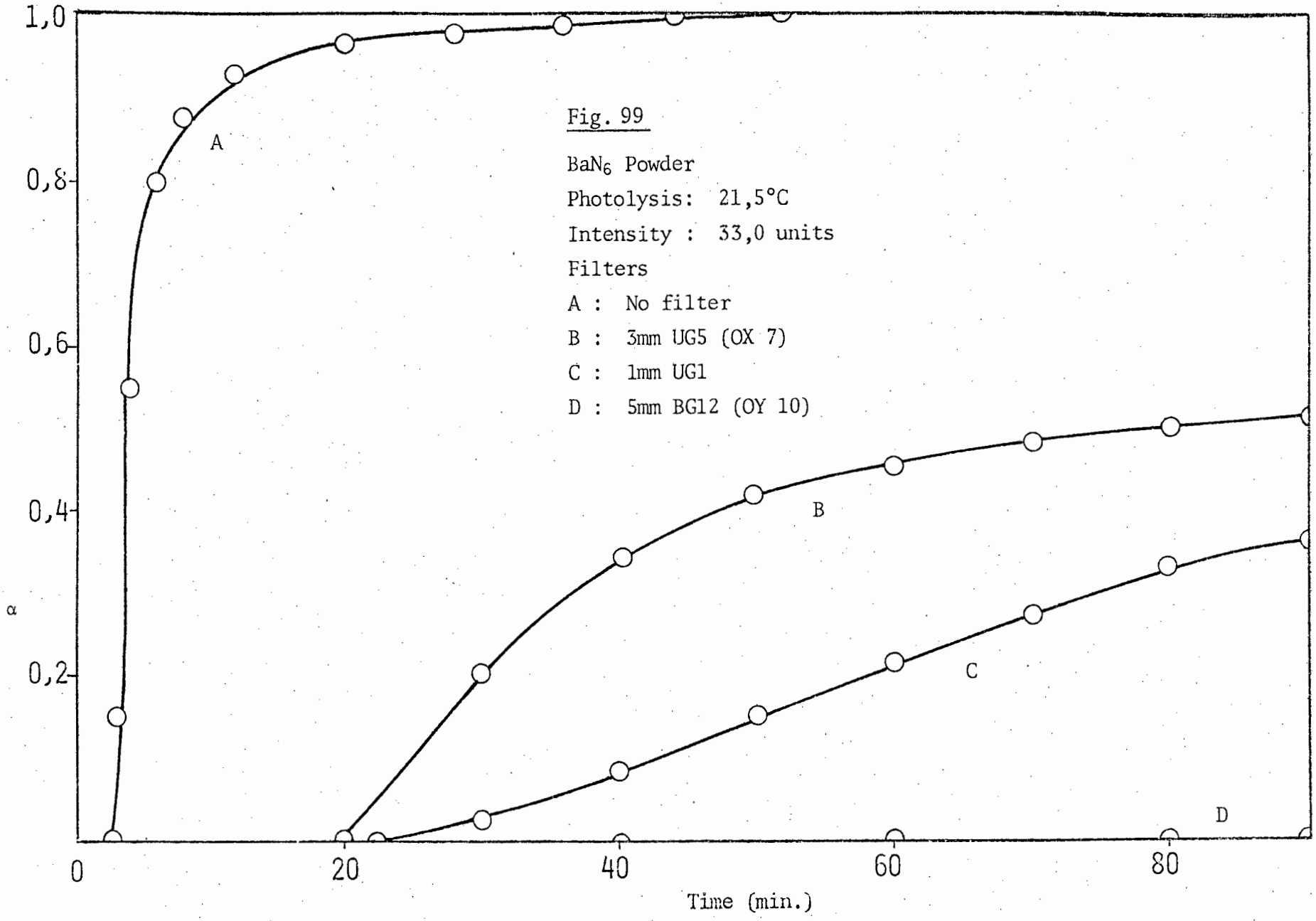

Fig. 99

BaN_6 Powder

Photolysis: 21,5°C

Intensity : 33,0 units

Filters

A : No filter

B : 3mm UG5 (OX 7)

C : 1mm UG1

D : 5mm BG12 (OY 10)

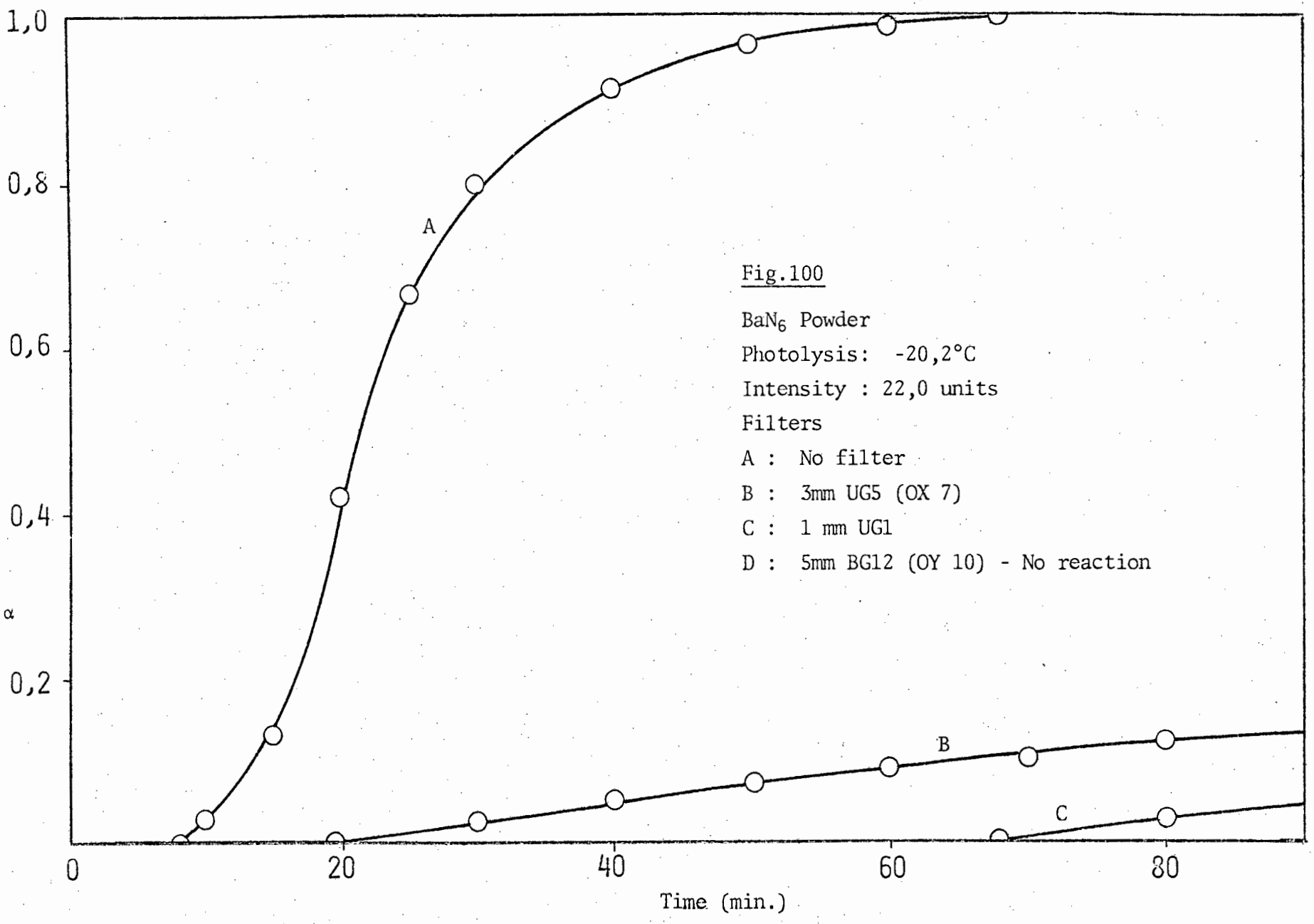

Fig.100

BaN_6 Powder

Photolysis: -20,2°C

Intensity : 22,0 units

Filters

A : No filter

B : 3mm UG5 (OX 7)

C : 1 mm UG1

D : 5mm BG12 (OY 10) - No reaction

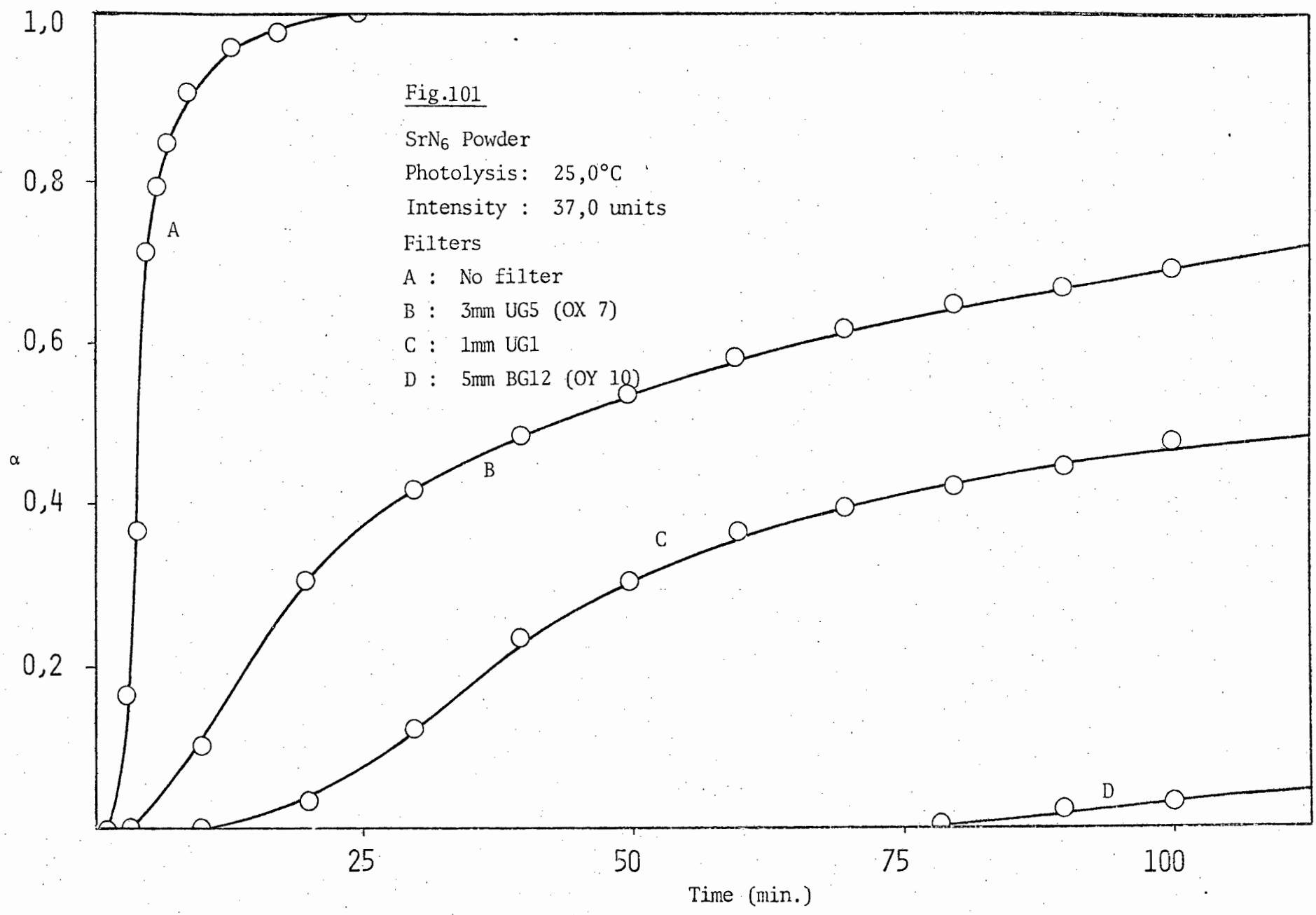

Fig.101

SrN_6 Powder

Photolysis: 25,0°C

Intensity : 37,0 units

Filters

A : No filter

B : 3mm UG5 (OX 7)

C : 1mm UG1

D : 5mm BG12 (OY 10)

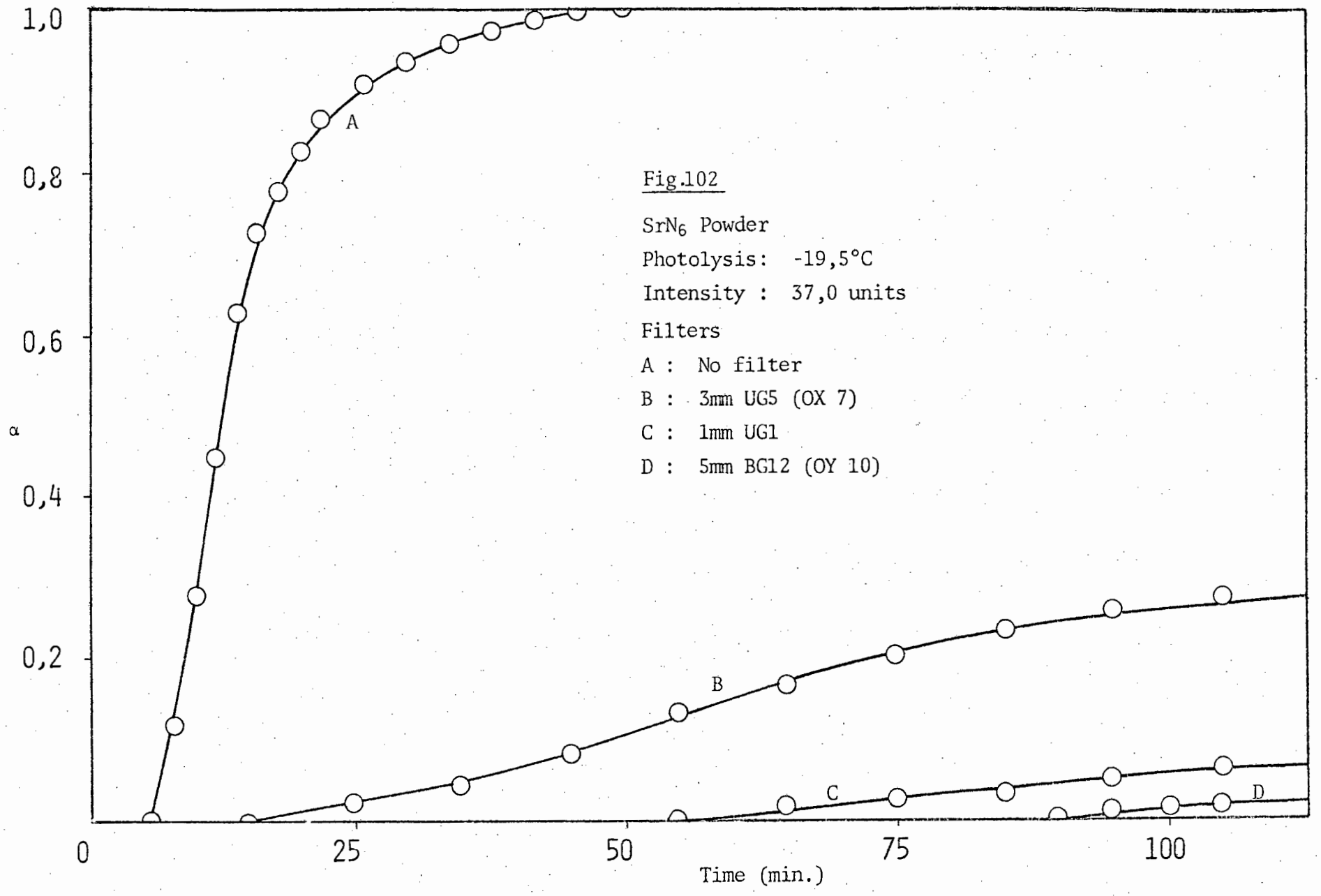

Fig.102

SrN_6 Powder

Photolysis: -19,5°C

Intensity : 37,0 units

Filters

A : No filter

B : 3mm UG5 (OX 7)

C : 1mm UG1

D : 5mm BG12 (OY 10)

10 DISCUSSION

Calcium and lithium azides were both subjected to ultraviolet radiation from a high intensity 100 watt "point source" high pressure mercury lamp. Photolytic decompositions took place in the temperature range 35,0° - 95,0°C in the case of powdered calcium azide and in the range 24,6° - 170,0°C in the case of powdered lithium azide. Co-irradiated decompositions were carried out on powdered calcium azide in the temperature range 110,0° - 140,0°C using the same source of ultraviolet radiation. Moreover, photolytic decompositions of pelleted calcium azide were carried out in the temperature range 25,0° - 90,0°C. Photolytic decompositions were also carried out on powdered calcium, barium, strontium and lithium azides at temperatures between -70,0° - 35,0°C. In these decompositions a 200 watt high pressure mercury arc lamp was used. Initially the results of the photolysis of each azide in the powdered form will be considered and then the photolysis of pelleted calcium azide and the co-irradiated decomposition of calcium azide will be discussed.

A. PHOTOLYSIS OF AZIDES IN THE POWDERED FORM

(i) PHOTOLYSIS OF BARIUM AZIDE

The photolysis of powdered barium azide has been studied by various workers over a wide range of temperatures.[5,37,40,48,50,188] The present study investigated the photolytic decomposition of barium azide in the temperature range -70,0° - 35,0°C.

The pressure-time plots obtained were sigmoid in shape and in this respect were similar to those obtained by previous workers.[48,50] As has already been seen in section 9*(vi)*, the reproducibility obtained for the acceleratory and decay reactions was good but that obtained for the induction period did not prove to be highly satisfactory and the results obtained for that part of the decomposition process should be treated accordingly. The unsatisfactory reproducibility is probably a result of a variation in the defect surfaces of the powders.

Photolysis over this temperature range was characterized by an induction period during which there was no measurable evolution of gas, followed by an acceleratory period which was analyzed by means of the Avrami-Erofeyev equation with n = 2. Finally there was a decay period which was analyzed by means of the unimolecular law.

The percentage decomposition at -20°C was found to be 85,0% which was slightly less than that obtained for a purely thermal decomposition at 130°C. Throughout the temperature range of this study no dark rate was detected and thus any purely thermal effects were negligible. Visual observations of the photolytic process indicated that the commencement of the decay reaction coincided with a blackening of the powder on all surfaces. No studies were carried out to determine the nature of the photolytic nuclei but previous workers[50] have found that, under conditions of decomposition similar to

those present in this study, thermal centres and photolytic centres were similar in nature.

In the temperature range -70,0° - 35,0°C two distinct activation energies were obtained for the photolysis of barium azide. The transition temperature occurred at 17,0°C. In the temperature range -70,0° - 17,0°C the activation energies for the induction, acceleratory and decay periods were found to be 0,24 Kcal./mol., 0,82 Kcal./mol. and 0,97 Kcal./mol. respectively. In the temperature range 17,0° - 35,0°C the activation energies for the same periods were found to be 6,48 Kcal./mol., 5,47 Kcal./mol. and 5,19 Kcal./mol. respectively.

The reciprocals of the duration of the induction period were found to be proportional to the intensity to the power of 2,50 for temperatures below 17,0°C and to the power of 1,99 for temperatures above 17,0°C. The value of 2,50 in the lower temperature range was approximated to 2,00. The ambiguous value was largely a result of poor reproducibility. The value of 3,00 was not considered feasible in view of the fact that a dependence of rate on the cube of the light intensity was extremely unlikely since no mechanism involving three excited azide ions or a triply excited ion was thought possible for this period. Thus over the whole temperature range the rate depended on the square of the light intensity during the induction period.

The rate of the acceleratory reaction was found to be proportional to $\text{Intensity}^{2,24}$ for temperatures above 17,0°C and to $\text{Intensity}^{2,02}$ for temperatures below 17°C. The rate of the decay reaction was proportional to $\text{Intensity}^{2,15}$ and $\text{Intensity}^{1,69}$ for temperatures above and below 17,0°C respectively. Thus throughout the temperature range in which the photolysis of barium azide was studied the rates of both the acceleratory and decay reactions were dependent upon the square of the light intensity. The results obtained in the two temperature ranges will be discussed separately.

(i.a) Photolysis in the temperature range -70,0° - 17,0°C

Visual observations made during photolysis in this temperature range showed a light brown colour at the end of the induction period. This is attributed to the presence of barium metal at the end of this period. It is assumed that decomposition sites are those where severe strain exists such as at surface cracks or lines. The grinding and dehydration of the powder cause these stresses to be present in increased concentrations, thus leading to the formation of dislocations. These eventually group to form high angle grain boundaries. The layered crystal structure of barium azide implies that a large number of incomplete planes of edge dislocations in an emergent grain boundary will contain only azide ions or barium ions. Thus decomposition will commence when azide ions at positions of stress on the surface or along the planes of the particles become optically excited.

In a study of the optical absorption spectrum of thin films of barium azide, Deb[43] has shown the presence of three bands with multiple structure in the region 140 - 250 nm. The spacings in the band structure closely corresponded with the fundamental vibration frequencies of the azide ion and each of the absorption bands was associated with the azide ion itself. The magnitude of the absorption coefficient of the peaks is low for an allowed electronic transition of an ionic crystal such as barium azide. Moreover, the appearance of a well resolved vibrational structure in these bands suggests that the transitions would be forbidden ones since such transitions would interact only weakly with the surroundings in the crystal.[191] By analogy with the electronic spectra of an isoelectronic molecule such as N_2O[192], the absorption bands of the azide ion in the range 140 - 250 nm may be interpreted in terms of transitions involving different excited states of the azide ion itself. The absence of any measurable photocurrent at wavelengths longer than 170 nm indicates that the electronic

transitions in this region involve bound excited states of the azide ion. The association of such transitions with vibrational structure implies that the excitons are in effect trapped on the molecules on which they are formed.[193]

Results obtained from filtering the high intensity ultraviolet arc showed that all three filters reduced the rate of decomposition relative to that obtained using unfiltered radiation. The lowered rate is to some extent due to the reduction in the arc intensity as a result of simple reflection from the polished filter surface. This factor can however be considered constant for all the filters. The most marked reduction in rate took place with the 5 mm BG12 filter and, only slightly less so, with the 1 mm UG1 filter. The effect of the 3 mm UG5 filter was much less drastic than that of the other two. This leads to the conclusion that the most effective wavelengths for the photolysis of barium azide are in the region 220 - 280 nm. Hence it follows that the mechanism of decomposition does not involve electrons and positive holes since these effective wavelengths represent energy less than that required for their formation. Thus it can be concluded that excited azide ions rather than excitons are formed, the absorbed energy being localized at favoured sites in the form of vibrational or internal electronic excitation. The reduced rates observed with the UG1 and BG12 filters are probable due to the very low absorption coefficient of long wavelengths compared with the shorter wavelengths and consequently are due to a low rate of excitation of the internal transition.

The rate of photolysis in this temperature range is considerably lower than at higher temperatures. This difference can be accounted for by postulating that at these lower temperatures fewer defects are produced. Moreover it must be noted that the rate-determining step at low temperatures could possibly be the diffusion of reactants to a reaction site or diffusion of product gas to the ambient.

Jacobs *et al.*[44] have suggested that, during the "warm-up" period at -35,0°C, following the ultraviolet irradiation of barium azide at -70,0°C, two holes, trapped at a common site, decompose to form N_4^- ions, nitrogen gas and an electron. They also proposed that at -5,0°C the N_4^- ion decomposed as follows:

$$N_4^- \rightarrow N_3^- + N$$

$$N + N \rightarrow N_2 \ .$$

Deb[63], in commenting on these mechanisms, observed that no nitrogen was evolved in this "warm-up" period following ultraviolet radiation. There is much speculation on the existence of the N_4^- ion. Some workers[3,44] postulate its existence as a product in the decomposition of barium azide but it has only been definitely observed in the photolysis of potassium and rubidium azides. Marinkas[194] has shown in e.s.r. studies that irradiation at low temperatures produces a new centre which is identified as N_3^{2-} rather than N_4^-. These ions result from electrons forsaking an N_2^- ion to reside on an N_3^- ion, the product, an $N_2^0 - N_3^{2-}$ complex, existing as a pair, thus:

$$N_2^- + N_3^- \rightleftarrows N_2^0 - N_3^{2-} \ .$$

These results therefore do not support mechanisms which propose N_4^- ions as products. The N_2^- ion, however, has been detected in the photolysis of barium azide at ambient and liquid nitrogen temperatures.[47] Thus mechanisms postulated for the photolysis of barium azide ought to incorporate the formation of this ion and, by implication, the $N_2^0 - N_3^{2-}$ complex.

Prout and Shephard[50] have proposed a mechanism for the induction period in the photolysis of barium azide at ambient temperature in which an excited azide ion is trapped at an anion vacancy together with a ground state azide

ion. This complex then reacts with a barium ion to produce a barium atom, three molecules of nitrogen and an anion vacancy. This step has an activation energy of 6,2 Kcal./mol. In the temperature range under discussion the activation energy is much less viz. 0,24 Kcal./mol. but the molecularity changes from one at ambient temperature to two. Hence the following mechanism is proposed:

$$N_3^- \overset{h\nu}{\rightleftarrows} N_3^{-*} \qquad (1)$$

$$N_3^{-*} \overset{h\nu}{\rightleftarrows} N_3^{-**} . \qquad (2)$$

This doubly excited ion is trapped at a trapping site, such as an anion vacancy, together with a ground state azide ion. This complex then reacts with a Ba^{2+} ion.

$$Ba^{2+} + N_3^- \, S \, N_3^{-**} \overset{\Delta}{\rightarrow} Ba + 3N_2 + S \qquad (3)$$

The activation energy of 0,24 Kcal./mol. is associated with step (3). Alternatively, the complex $[N_3^{-*} \, S \, N_3^{-*}]$ could have been postulated. This would have allowed for the dependence of the rate on the square of the light intensity. However, on the basis of Prout and Shephard's work the thermal energy required for this complex, involving two singly excited azide ions, to react with a Ba^{2+} ion to form barium atoms, would possibly be more than the 0,24 Kcal./mol. determined for the reaction taking place during the induction period. The doubly excited azide ion is assumed to be located at an imperfection and will presumably be relatively more stable at low temperatures. If located at an ideal lattice site it will return to its ground state or to a singly excited state.

This mechanism, proposed for the formation of barium metal nuclei, is in accordance with the observed dependence of the inverse of the duration of the induction period on the square of the light intensity, the duration

being dependent on the time required for the barium atoms to aggregate, through diffusion, to form barium metal nuclei, this occurrence in turn being dependent on the light source.

Experiments in which water vapour was introduced to the sample during a photolytic decomposition have indicated the presence of metal at the end of the induction period. Water vapour introduced at the end of the induction period caused the barium metal on the surface to be destroyed, the subsequent reaction continuing after a new, shorter induction period. This subsequent reaction presumably proceeds from growth nuclei still present in the bulk of the material. The absence of any difference in the pattern of decomposition subsequent to an interruption during an induction period, indicated that barium metal nuclei are formed only at the end of the induction period. This barium metal has characteristics which are the same as those of the bulk metal. At the end of the induction period nuclear growth commences and the reaction accelerates. The nitrogen gas evolved is not observed to escape during the induction period but is absorbed on the powder.

The acceleratory reaction was analysed using the Avrami-Erofeyev equation with n = 2. The inflection point occurred at $\alpha = 0,32$. Due to the very intense light source used in the low temperature studies the effect of the irradiation is very pronounced. Thus any linear increase in the number of nuclei during the acceleratory period would be much less significant than the large number of nuclei formed at the end of the induction period. Hence it is assumed that this value of n implies a two-dimensional growth of nuclei increasing from a fixed number of centres.

The metal nuclei are initially discrete but, with the progress of the acceleratory reaction, overlapping occurs, as indicated by the fact that the acceleratory reaction conforms to Avrami-Erofeyev type kinetics.

The acceleratory period has been found to be dependent upon the square of the light intensity over the temperature range under discussion and hence the overall mechanism must involve the decomposition of two singly excited azide ions or a single doubly excited ion.

Prout and Sears[48] have proposed a free radical type of reaction for temperatures below 0°C, involving the formation of F-centres and the reaction of holes and azide ions to form N_4^- and N_2. This mechanism, however, does not postulate any reactions resulting in the production of barium metal nuclei. Moreover, as stated above, the N_4^- ion has not been detected in the photolysis of barium azide and mechanisms postulating its production are not reliable. The following mechanism is proposed. Initially an azide ion is excited and is trapped at a trapping site S which is probably a defect such as an anion vacancy. Another singly excited ion is trapped at the same site. In each case the excited ion may revert to the ground state if located at an ideal lattice position. The two singly excited ions at a common trap then react with a barium ion formed via the photoelectric effect to form barium metal, two positive holes and an electron. The trapping site is regenerated. If this site is an anion vacancy it will form an F-centre with the electron. The positive holes react with ground state azide ions to produce N_2^- ions and nitrogen gas. These ions and molecules then react to form more nitrogen gas and F-centres. The F-centres formed may move through the lattice at a rate determined mainly by the mobility and concentration of such vacancies. When two F-centres meet, aggregation to double F-centres results because such aggregates are more stable than single F-centres as a result of the resonance energy of the electrons in the two identical defects. Ultimately, the F-centres collapse at a certain critical concentration. The electrons produced as a result of this collapse react with Ba^{2+} ions and the barium metal nuclei formed grows to the interface.

As mentioned previously, Marinkas *at al.*[47] have detected in e.s.r. studies the N_3^{2-} ion. Thus the N_2^- ion, postulated to be formed in this mechanism, will react to some extent, however small, with ground state azide ions to form the $N_2^0 - N_3^{2-}$ complex. Thus the mechanism proposed for the acceleratory reaction in the photolysis of barium azide in this temperature range is as follows:

$$N_3^- \underset{\leftarrow}{\overset{h\nu}{\rightarrow}} N_3^{-*} \qquad (1)$$

$$Ba_n \underset{\leftarrow}{\overset{h\nu}{\rightarrow}} Ba_n^+ + e \qquad (2)$$

$$Ba_n^+ + N_3^{-*} \; S \; N_3^{-*} \overset{\Delta}{\rightarrow} Ba_n + 2N_3 + e + S \qquad (3)$$

$$2N_3 + 2N_3^- \rightarrow 2N_2^- + 4N_2 \qquad (4)$$

$$N_2^- + N_3^- \underset{\leftarrow}{\rightarrow} N_2^0 - N_3^{2-} \qquad (5)$$

$$N_2^- + 2N_2 \rightarrow 3N_2 + \square + e \qquad (6)$$

$$\rightarrow 3N_2 + \boxdot \qquad (7)$$

$$2\boxdot \rightarrow 2\square + 2e \qquad (8)$$

$$Ba_n + Ba^{2+} + 2e \rightarrow Ba_{n+1} \qquad (9) \quad .$$

Step (3) is considered to be the rate determining step and has an activation energy of 0,82 Kcal./mol. associated with it. The mechanism is seen to be dependent on the square of the light intensity as determined experimentally. Step (4) appears to be a relatively fast step due to the coulombic attraction of the positive hole and the ground state ion. Moreover, step (3) must require some thermal energy since it is unlikely to take place spontaneously. The interpretation of the activation energy in this mechanism is difficult. The rate determining step, as has been stated earlier, could be the diffusion of the reactants to a reaction site

or the diffusion of the nitrogen to the ambient. Step (5), the formation of the N_2^0 -N_3^{2-} complex, occurs as a result of radiation of wavelength 325 nm.[194] The most effective wavelengths for photolysis of barium azide in this temperature range have been shown to lie between 220 - 280 nm. Hence this reaction is not critical to the overall photolytic process and will only occur to a minimal degree.

Water interruptions during the acceleratory period have illustrated the importance of metal nuclei during this period. The water vapour destroyed the reaction and a new induction period of duration shorter than that of an uninterrupted decomposition was observed. This duration increased as the position of interruption along the curve progressed. The rate of the subsequent acceleratory reaction decreased and the new reaction is presumed to begin from growth nuclei not destroyed by the water vapour. The growth nuclei are situated on the planes of the particles and the new induction period observed is the time required for these nuclei to grow to a critical size. Thus the water vapour is assumed to attack only those metal nuclei on the surface of the particles. The drop in the rate of the subsequent acceleratory reaction is due to the commencement of reaction from fewer centres.

Interruptions beyond the inflection point caused decomposition to cease. At and beyond the inflection point all the external surfaces of the particles were observed to be black. This indicated a complete layer of barium metal. Introduction of water vapour causes the formation of a layer of barium hydroxide which is opaque to ultraviolet light. Growth nuclei present under the surface are thus unable to be activated by the radiation and reaction ceases. Partial hydrolysis of the azide by introduction of water vapour at positions prior to the inflection point causes the observed final pressure to be lower than that expected. Hence,

during the acceleratory period, the concentration of the barium metal nuclei is increasing as indicated by the visual observations made and these metal nuclei are seen to have a catalytic effect as it were on the photolytic reaction.

The decay reaction commences when the two-dimensional nuclei overlap and the surface of the small particles is covered by reaction product. During this period the product interface penetrates into the particles. The decrease in molecular volume as the product forms causes the interface to collapse leaving isolated blocks of material in which no nuclei are present. This arises from the extensive growth of plate-like nuclei. In these isolated blocks each molecule has an equal probability of decomposition and the rate of reaction becomes proportional to the amount of unreacted substance. Thus the decay reaction conforms to the unimolecular decay law.

The activation energy for the decay reaction was found to be 0,97 Kcal./mol. and the rate of the reaction was dependent upon the square of the light intensity. These results were very similar or identical to those obtained for the acceleratory reaction. Hence it was assumed that the mechanism of the decay reaction is the same as that occurring during the acceleratory period. The reduced rate of production of nitrogen is a result of the gradual consumption of defects which are helpful to the reaction.

(i.b) Photolysis in the temperature range 17,0° - 35,0°C

As mentioned previously the activation energies for the photolysis of powdered barium azide changed at 17,0°C. The value for the induction period changed from 0,24 Kcal./mol. to 6,48 Kcal./mol., that for the acceleratory period from 0,82 Kcal./mol. to 5,47 Kcal./mol. and the value for the decay period from 0,97 Kcal./mol. to 5,19 Kcal./mol. The rates of

reaction for each period were found, as in the lower temperature range, to be dependent upon the square of the light intensity. The mathematical analyses, visual observations, the effect of filters and the effect of introducing water vapour at various stages of reaction were analogous to the results obtained in the temperature range -70,0° - 17,0°C. Moreover the results obtained were very similar to those found in a previous study over a similar temperature range by Prout and Shephard[50] except that in the induction period they found the rate to be linearly dependent on the light intensity. Activation energies found by them for the induction, acceleratory and decay reactions were 6,2 Kcal./mol., 7,2 Kcal./mol. and 6,6 Kcal./mol. respectively.

The mechanism for the formation of nuclei in this temperature range involves the trapping of two singly excited azide ions at a site, S, such as an anion vacancy. The complex $[N_3^{-*}\ S\ N_3^{-*}]$ then reacts with Ba^{2+} ions to form metal atoms which aggregate into nuclei at the end of the induction period.

$$N_3^- \xrightarrow{h\nu} N_3^{-*} \qquad (1)$$

$$Ba^{2+} + N_3^{-*}\ S\ N_3^{-*} \xrightarrow{\Delta} Ba + 3N_2 + S \quad . \qquad (2)$$

Step (2) is considered to be the rate determining step and has an activation energy of 6,48 Kcal./mol. associated with it. As mentioned above, some workers[44,3] have proposed the formation of the N_4^- ion in the photolysis of barium azide. No evidence exists for its presence, however. In any event, in the cases where it has been detected, viz. potassium and rubidium azides, it is not observed at room temperature.

The marked similarity which exists between the results shown in the present study and those obtained by Prout and Shephard[50] in previous work under similar conditions implies that the same mechanism of nuclear growth is occurring, viz.:

$$N_3^- \overset{h\nu}{\rightleftarrows} N_3^{-*} \quad (1)$$

$$Ba_n \overset{h\nu}{\rightleftarrows} Ba_n^+ + e \quad (2)$$

$$Ba_n^+ + N_3^{-*} \overset{\Delta}{\rightarrow} Ba_n + N_3 \quad (3)$$

$$N_3 + N_3^{-*} \rightarrow 3N_2 + 2\square + e \quad (4)$$

$$\rightarrow 3N_2 + \boxdot + \square \quad (5)$$

$$2\boxdot \rightarrow 2\square + 2e \quad (6)$$

$$Ba_n + Ba^{2+} + 2e \rightarrow Ba_{n+1} \quad (7)$$

Step (3) is considered to be the rate determining step and has an activation energy of 5,47 Kcal./mol. associated with it. The Ba^+ ion is formed in step (2) as a result of the photoelectric effect. The F-centres formed in step (5) will aggregate until they reach a critical concentration at which point they collapse as in step (6). The reaction is an acceleratory one in which the barium metal is regenerated. As has already been discussed in the section on the photolysis of barium azide in the low temperature range, there is much evidence for the existence of the N_2^- ion. This ion is a stable product in the photolysis of barium azide at room temperature, even partially surviving annealing at 100°C for 45 minutes.[181] Thus it is possible that, parallel with step (4), the following reactions take place:

$$N_3 + N_3^- \rightarrow N_2^- + 2N_2$$

$$\rightarrow 3N_2 + \square + e$$

$$\rightarrow 3N_2 + \boxdot$$

$$N_2^- + N_3^- \rightleftarrows N_2^0 - N_3^{2-} \quad .$$

These reactions will probably involve only a relatively small number of positive holes and step (4) will be the dominant reaction involving the N_3 radical. The mechanism is seen to be in accordance with the observed dependence of the rate of the reaction on the square of the light intensity.

The similarity in the values of the activation energy and the molecularity in the acceleratory and decay reactions leads to the conclusion that the same mechanism as proposed above for the acceleratory reaction is occurring during the decay reaction.

(ii) PHOTOLYSIS OF STRONTIUM AZIDE

The photolysis of powdered strontium azide has been investigated over the temperature range -80,0° - 32,0°C. The discussion of the results obtained in the photolysis of barium azide over this temperature range is, in general, applicable to strontium azide. The pressure-time plots were sigmoid in shape and the reproducibility was good over the acceleratory and decay periods but was not highly satisfactory over the induction period. Thus, as in the case of barium azide, mechanisms of photolytic decomposition postulated on the basis of data obtained during the induction period, need to be treated with caution. This unsatisfactory reproducibility was again probably a result of a variation in the defect surfaces of the powders.

The characteristics of the photolysis and the methods of mathematical analyses were the same as for barium azide. The methods of mathematical analyses were also the same as those used by Prout and Shephard[50] in their study of the photolysis of strontium azide over the temperature range 30,0° - 90,0°C. The percentage decomposition at -20,0°C was 58% which was 14% less than that obtained by other workers[50] during photolysis at higher temperatures. Throughout the temperature range under discussion no dark rate was observed and the visual observations made were almost identical to those made during the photolysis of barium azide in a similar temperature range. Prout *at al.*[50] have found that during photolysis at ambient and higher temperatures thermal centres and photolytic centres were similar in nature. It was assumed that this is also the case in the temperature range under discussion.

In the temperature range -80,0° - 32,0°C two distinct activation energies were found for the photolysis of strontium azide. The transition temperature occurred at -4 ,0°C. In the temperature range -80,0°- -4,0°C

the activation energies for the induction, acceleratory and decay reactions were found to be 2,38 Kcal./mol., 1,58 Kcal./mol. and 0,69 Kcal./mol. respectively. In the temperature range -4,0° - 32,0°C the activation energies for the same periods were 4,00 Kcal./mol., 3,73 Kcal./mol. and 3,96 Kcal./mol. respectively.

In determining the molecularities of the various stages of the reaction the exponent m in the equation $k = I^m + c$ was taken to the nearest whole number. The rates of reaction throughout the induction, acceleratory and decay periods were found to be dependent on the square of the light intensity with the exception of the induction period in the temperature range -80,0° - -4,0°C where the rate was found to be linearly dependent on the light intensity. A value of 2,71 was obtained for the induction period in the temperature range -4,0° - 32,0°C. This value was interpreted as representing a bimolecular reaction since it was considered unlikely that a triply excited ion would be involved in the mechanism of photolytic decomposition. Moreover, the value obtained by Prout *et al.*[50] in a similar study was 2,0. The poor reproducibility obtained during the induction period accounts for this inaccuracy and, in view of this known irreproducibility, this approximation to 2 is permissible. The results obtained in the two temperature ranges will be discussed separately.

(ii.a) Photolysis in the temperature range -80,0° - -4,0°C

The topography of the photolytic decomposition of strontium azide can be assumed to be analogous to that described for barium azide in the temperature range -70,0° - 17,0°C. This is reasonable since the kinetic equations used to describe and analyse the photolysis of strontium azide, the visual observations made, the effect of filters and the effect of the

interaction of water vapour at various stages of photolysis were identical or very similar to those obtained for barium azide.

The formation of metal nuclei was found to be linearly dependent on the light intensity. As indicated in the case of barium azide, mechanisms proposing the formation of the N_4^- ion must be treated with caution since there is no evidence for the existence of this ion in these compounds. Prout *et al.*[50], in their study of the photolysis of strontium azide at ambient temperatures, postulated a mechanism for the induction period in which the rate determining step involved the reaction of a strontium ion with the complex $[N_3^{-*}\ S\ N_3^{-*}]$ and had an activation energy of 2,60 Kcal./mol. associated with it. This value is very similar to that obtained in the temperature range under discussion and hence a similar mechanism is postulated in which the complex is $[N_3^-\ S\ N_3^{-*}]$ in order to allow for the linear dependence of the rate on the light intensity.

Initially a primary excitation corresponding to an internal transition on an azide ion occurs.

$$N_3^- \overset{h\nu}{\rightleftarrows} N_3^{-*} \qquad (1)$$

This excited azide ion is trapped at a surface defect S:

$$N_3^{-*} + S \rightleftarrows N_3^{-*}\ S \qquad (2)$$

where S is probably an anion vacancy.

The excited ion at the defect, if adjacent to a ground state ion, forms the complex $[N_3^-\ S\ N_3^{-*}]$ which reacts as follows with an Sr^{2+} ion.

$$Sr^{2+} + N_3^-\ S\ N_3^{-*} \overset{\Delta}{\rightarrow} Sr + 3N_2 + S \qquad (3)$$

Step (3) is considered to be the rate determining step and has an activation energy of 2,38 Kcal./mol. associated with it.

The formation of nuclei probably occurs at the point of emergence of dislocations on the surface of crystals. These will be mainly spiral dislocations and the discontinuities associated with the mosaic structure. The strontium atoms formed diffuse with time resulting in aggregation to produce strontium metal nuclei. This aggregation of metal atoms marks the end of the induction period. The mechanism proposed is in accordance with the observed dependence of the inverse of the duration of the induction period on the first power of the light intensity. The duration of the induction period is itself a measure of the time required for the strontium atoms to aggregate, through diffusion, to form strontium metal nuclei.

In the abovementioned study of the photolysis of strontium azide at ambient temperatures by Prout *et al.*[50], they postulated, for the acceleratory reaction, a mechanism in which a strontium ion, formed as a result of the photoelectric effect, reacts with a doubly excited azide ion viz.

$$Sr^{+} + N_3^{-**} \xrightarrow{\Delta} Sr + N_3 \quad .$$

This was considered the rate determining step and had an activation energy of 3,2 Kcal./mol. associated with it. In the same study an induction period mechanism

$$Sr^{2+} + N_3^{-*}\,S\,N_3^{-*} \xrightarrow{\Delta} Sr + 3N_2 + S$$

was postulated, having an activation energy of 2,6 Kcal./mol. In the present study of the photolysis of strontium azide in the temperature range -80,0° - -4,0°C, the activation energy for the acceleratory period is 1,58 Kcal./mol. The mechanism proposed earlier for the acceleratory reaction in the photolysis of barium azide in the temperature range

-70,0° - 17,0°C involves a complex: $[N_3^{-*}\ S\ N_3^{-*}]$ as in the second equation above. This complex reacts with a Ba_n^+ ion to form a barium atom, positive holes and an electron. This was considered to be the rate determining step. It is uncertain whether the change in activation energy in the case of strontium azide from 3,2 Kcal./mol. at ambient temperatures to 1,58 Kcal./mol. at lower temperatures is a result of a change in mechanism. As explained in the case of barium azide, interpretation of the activation energy is not simple and it could be associated with the rate determining step, the diffusion of reactants to a reaction site or the diffusion of molecular nitrogen to the ambient. In any event the mechanism postulated here must involve either two singly excited ions or a single doubly excited ion. Hence the following mechanism is proposed for the acceleratory reaction in the photolysis of strontium azide in this low temperature range. Two singly excited ions, present at a common defect site S, probably an anion vacancy, react with a strontium ion formed through the photoelectric effect to yield strontium metal, two positive holes and an electron. The trapping site is regenerated and, if an anion vacancy, will form an F-centre with the electron. The positive holes produced react with two adjacent ground state azide ions as in the case of barium azide. The products of this reaction are the N_2^- ion and molecular nitrogen. No e.s.r. studies of strontium azide have yet been carried out and hence the proposed reaction, involving the production of the N_2^- ion, is complete speculation. However, there appear to be sufficient similarities in the results obtained for the photolysis of barium and strontium azides to justify this proposed reaction which has already been postulated in the case of barium azide. The N_2^- ion reacts with an adjacent ground state azide ion to form, ultimately, nitrogen and an F-centre. The F-centres tend to aggregate as a result of the increased stability arising from the resonance of the electrons in the identical defects. At a

critical concentration the F-centres collapse and the electrons thus produced react with Sr^{2+} ions to form strontium atoms. These atoms aggregate forming metal nuclei which then add to the interface. Hence the following mechanism is proposed:

$$N_3^- \overset{h\nu}{\rightleftarrows} N_3^{-*} \quad (1)$$

$$Sr_n \overset{h\nu}{\rightleftarrows} Sr_n^+ + e \quad (2)$$

$$Sr_n^+ + N_3^{-*} \; S \; N_3^{-*} \overset{\Delta}{\rightarrow} Sr_n + 2N_3 + e + S \quad (3)$$

$$2N_3 + 2N_3^- \rightarrow 2N_2^- + 4N_2 \quad (4)$$

$$N_2^- + N_3^- \rightleftarrows N_2^0 - N_3^{2-} \quad (5)$$

$$N_2^- + 2N_2 \rightarrow 3N_2 + \square + e \quad (6)$$

$$\rightarrow 3N_2 + \boxed{\cdot} \quad (7)$$

$$2\boxed{\cdot} \rightarrow 2\square + 2e \quad (8)$$

$$Sr_n + Sr^{2+} + 2e \rightarrow Sr_{n+1} \; . \quad (9)$$

Step (3) is considered to be the rate determining step and has an activation energy of 1,58 Kcal./mol. associated with it. The mechanism is seen to be dependent on the square of the light intensity involving, as it does, two singly excited azide ions.

The small difference between the values of the activation energy for step (3) of the above mechanism and those of the rate determining steps mentioned above, as proposed by Prout *et al.*[50] at ambient temperature, make the assignment of this step difficult. It is not really possible to distinguish between the energies associated with the excited states $[N_3^{-**}]$ and $[N_3^{-*} \; S \; N_3^{-*}]$ since this excitation is associated with the ion

or complex as a whole. However, strontium ions, formed via the photoelectric effect, are more reactive than lattice Sr^{2+} ions. This possibly favours a lower value of activation energy for step (3) relative to the value of 2,6 Kcal./mol. obtained by Prout *et al.*[50] for the reaction of the same complex $[N_3^{-*} S\ N_3^{-*}]$ with Sr^{2+} as outlined above. The difference in these values is so slight, however, that any such comparative reasoning must be very tentative.

Since the activation energy and the molecularity for the decay reaction are either similar or identical to those values obtained for the acceleratory reaction, the same mechanisms as those proposed for the acceleratory period are proposed for this period.

(ii.b) Photolysis in the temperature range -4,0° - 32,0°C

The values of the activation energies obtained for the induction, acceleratory and decay periods in the temperature range -4,0° - 32,0°C, as well as the dependence of the rates of the reactions on the light intensity, have already been presented. The mathematical analyses, the visual observations, the effect of filters and the effect of introducing water vapour at various stages of decomposition were similar or identical to the results obtained for strontium azide over the lower temperature range. The values of activation energies obtained for the inducion, acceleratory and decay periods by Prout *et al.*[50] in a similar temperature range and under similar conditions were 2,6 Kcal./mol., 3,2 Kcal./mol. and 5,7 Kcal./mol. with the rate dependent throughout on the square of the light intensity. The similarities between their results and those in the present work are so marked that their postulated mechanisms are also proposed to occur in this temperature range.

The formation of the strontium metal nuclei at the end of the induction period is assumed to proceed via the following mechanism. Initially an azide ion is excited:

$$N_3^- \overset{h\nu}{\underset{\leftarrow}{\rightarrow}} N_3^{-*} \quad . \qquad (1)$$

This excited azide ion, corresponding to an internal transition on the ion, is then trapped at a common defect site S with another excited azide ion. This complex then reacts with an Sr^{2+} ion, thus:

$$Sr^{2+} + N_3^{-*} S N_3^{-*} \overset{\Delta}{\rightarrow} Sr + 3N_2 + S \qquad (2)$$

where S is probably an anion vacancy. This is the rate determining step and has an activation energy of 4,00 Kcal./mol.

Two mechanisms are proposed for the growth of nuclei during the acceleratory period. These mechanisms are virtually identical and both postulate the formation of a single doubly excited azide ion. The difference in the mechanisms lies in the manner in which this ion is formed. In the first case the doubly excited ion is produced as a result of the successive excitation of the same ion. In the second case the ion is formed as a result of the transfer of energy from one singly excited azide ion to another singly excited ion. The doubly excited ion then decomposes in the rate determining step to produce an excited hole and an electron. The electron thus generated through thermal ionization reacts with an Sr^+ ion formed via the photoelectric effect. The excited positive hole reacts with a ground state azide ion occupying a strained position to yield nitrogen, an F-centre and an anion vacancy. As explained above, these F-centres aggregate to a critical size at which point they collapse. Ultimately strontium metal atoms are formed and these add to the interface.

Thus:

$$Sr_n \overset{h\nu}{\rightleftarrows} Sr_n^+ + e \qquad \text{photoelectric effect} \qquad (1)$$

$$N_3^- \overset{h\nu}{\rightleftarrows} N_3^{-*} \qquad \text{primary excitation} \qquad (2)$$

$$N_3^{-*} \rightleftarrows N_3^- \qquad \text{de-excitation} \qquad (3)$$

$$\text{Then either (i)} \quad N_3^{-*} \overset{h\nu}{\rightleftarrows} N_3^{-**} \qquad \text{secondary excitation} \qquad (4)$$

$$\text{or (ii)} \quad N_3^{-*} + N_3^{-*} \rightleftarrows N_3^{-**} + N_3^- \qquad \text{energy transfer} \qquad (5)$$

$$N_3^{-**} \rightleftarrows N_3^{-*} \qquad \text{de-excitation} \qquad (6)$$

$$N_3^{-**} \overset{\Delta}{\rightarrow} N_3^* + e \qquad \text{decomposition} \qquad (7)$$

$$Sr_n^+ + e \rightarrow Sr_n \qquad (8)$$

$$N_3^* + N_3^- \rightarrow 3N_2 + 2\square + e \qquad (9)$$

$$\rightarrow 3N_2 + \boxed{\cdot} + \square \qquad (10)$$

$$2\boxed{\cdot} \rightarrow 2\square + 2e \qquad (11)$$

$$Sr_n + Sr^{2+} + 2e \rightarrow Sr_{n+1} \qquad (12)$$

The above mechanism can be shown to agree with the experimentally determined dependence of the rate on the square of the light intensity. The detailed calculations with respect to a similar mechanism are presented in section 10 *(iii.a)* in the discussion of the photolysis of calcium azide. Step (7) is considered to be the rate determining step and has an activation energy of 3,73 Kcal./mol. associated with it.

The values of the activation energy and the molecularity for the decay reaction are similar or identical to those obtained over the accelera-

tory period. Hence the same mechanisms as those postulated above for the acceleratory reaction are assumed to be applicable to the decay reaction.

(iii) PHOTOLYSIS OF CALCIUM AZIDE

No comprehensive studies have as yet been made of the photolytic decomposition of calcium azide. In the present work activation energies and molecularities were determined in the temperature range -70,0° - 95,0°C. Visual observations were made and the effects of filters and introduction of water vapour during photolysis were also examined. The reproducibility obtained was satisfactory over the acceleratory and decay reactions throughout this temperature range. At the lower temperatures, however, viz. below ambient temperature, the reproducibility obtained during the induction period was not good. This was probably due to variations in the defect surfaces of the powders. The induction period at higher temperatures was more reproducible. This improvement however appeared to be due to the fact that the short duration of this period at these temperatures disguised the irreproducibility.

The pressure-time plots obtained throughout this temperature range were sigmoid in shape and in this respect were similar to the decomposition curves obtained for the thermal decomposition of calcium azide by previous workers.[58,168,137] The curves showed a true induction period during which no measurable amount of nitrogen was evolved. The subsequent acceleratory period and decay period were described by the Avrami-Erofeyev equation with n = 2 and by the unimolecular law respectively. The percentage decomposition at ambient temperature of 90,0% was similar to that obtained for the thermal decomposition of calcium azide powder viz. 93,4%.[168] The point at which the decay reaction commenced occurred at $\alpha \sim 0{,}35$. Beyond this point the powder was observed to be completely black on all the external surfaces.

Throughout the temperature range -70,0° - 95,0°C no dark rate was observed, thus indicating the relative absence of any thermal effects.

A study of the photolytic decomposition subsequent to the end of the induction period of a purely thermal decomposition and vice versa revealed that the centres formed at the end of the induction period during photolysis and during thermal decomposition are similar in nature.

The photolysis of powdered calcium azide was studied over four distinct temperature ranges. The initial study took place in the range 35,0° - 95,0°C and revealed a change in the activation energy at 60,0°C. In the region 35,0° - 60,0°C the activation energies for the induction, acceleratory and decay periods were 7,78 Kcal./mol., 7,30 Kcal./mol. and 4,67 Kcal./mol. respectively and the molecularities (to the nearest whole number) 1, 2 and 2 respectively. The corresponding activation energies and molecularities for the temperature range 60,0° - 95,0°C were 10,80 Kcal./mol., 12,52 Kcal./mol., 17,36 Kcal./mol. and (to the nearest whole number) 1,1 and 1 respectively.

Subsequently the photolysis was studied in the temperature range -70,0° - 22,0°C. Two distinct activation energies were found with the transition temperature at 7,0°C. In the temperature range -70,0° - 7,0°C the activation energies for the induction, acceleratory and decay periods were 0,34 Kcal./mol., 0,56 Kcal./mol. and 0,42 Kcal./mol. respectively and the molecularities (to the nearest whole number) for the corresponding periods were 1, 2 and 2 respectively. The photolysis of calcium azide powder was also studied in the temperature range 7,0° - 22,0°C in order to investigate whether any other transitions in the activation energy occurred. Within the limits of experimental error it appeared that no changes in activation energies occurred until the previously mentioned transition

temperature of 60,0°C was reached. The activation energies for the induction, acceleratory and decay periods in this temperature range were 5,70 Kcal./mol., 4,18 Kcal./mol. and 3,76 Kcal./mol. and the molecularities (to the nearest whole number) for the corresponding periods were 1, 2 and 2 respectively. The results obtained in these four temperature ranges will be discussed separately.

(iii.a) Photolysis in the temperature range 35,0° - 60,0°C

Photolytic decomposition of powdered calcium azide is assumed to take place at specific sites in the crystal. These are sites where severe strain exists such as at surface cracks or at lines where mechanical damage has taken place resulting in a higher thermodynamic instability. Thus the chemical potential and stereochemical environment in the vicinity of a dislocation are not the same as at an ideal lattice site. Pairs of vacancies of opposite sign separated by a few unit cells, isolated vacancies near edge dislocations and, more particularly, vacancies near jogs in dislocations are in the most favourable positions energetically for photolytic decomposition to occur.

The grinding and dehydration of the calcium azide is thus beneficial to the decompositon process since many more imperfections are generated. Excited ions which migrate to jogs or dislocations will not revert to their ground state as would occur at an ideal lattice site. These defect centres are thus responsible for trapping charge carriers such as excitons and ultimately facilitate the decomposition process.

Calcium azide crystallizes in an orthorhombic F ddd space group[181] with eight molecules per unit cell. The molecular packing is a layer structure type. As a result of this, incomplete planes of the edge dislocations will contain only azide ions or calcium ions. These dislocations

could serve as reaction sites or generate vacancies. They may also trap electrons. Decomposition will commence when azide ions at positions of stress become optically excited.

No studies have been made of the optical absorption spectrum of calcium azide. Deb[43] has studied the photoconductivity and photoemission properties of some Group 1 azides as well as barium azide. Photocurrent is absent in each case at wavelengths greater than 170 nm. It can be assumed that since the band gap energies of these azides and of calcium azide are similar, no photocurrent will occur in the latter at wavelengths greater than 170 nm. Whatever photocurrent there is, is ascribed wholly to the motion of vacancies.[59] The band gap energy of calcium azide is 8,5 eV corresponding to 145,8 nm. Thus radiation at this wavelength would imply the promotion of electrons into the conduction band resulting in free electrons and positive holes and thus photoconductivity.

The filtering of the ultraviolet radiation in the photolysis of calcium azide has shown that the rate of decomposition decreases when filters are used. The lowered rate is not solely due to the change in the wavelength of irradiation but another contributory factor is the reduction in the arc intensity as a result of reflection from the polished filter surface. This factor is, however, considered constant for all three filters used. The 5 mm BG12 filter virtually caused the reaction to cease, implying that wavelengths greater than 330 nm played no role in the photolytic decomposition. The 1 mm UG1 filter had a slightly greater retarding effect than did the 3 mm UG5 filter. From these results it can be concluded that the most effective wavelengths for photolysis are those between 220 - 280 nm with a slightly reduced efficacy on the range 280 - 330 nm. These wavelengths are equivalent to an energy range of 5,63 eV - 4,43 eV - 3,76 eV which represent less energy than that required for the

formation of positive holes and electrons. Excitons are expected to form only at a wavelength of ≈ 170 nm (7,3 eV). Hence it can be concluded that the most effective wavelengths for photolytic decomposition are of less energy than that required for the formation of excitons. The most probable occurrence is an internal transition on the azide ion. This excitation will be the primary photochemical process on irradiation. The much lower rates which have been observed at long wavelengths are due to the very low absorption coefficient and consequently the low rate of excitation of the internal transition at these wavelengths.[44] The energy which is absorbed is thus localized at the favoured sites either in the form of vibrational energy or internal electronic excitation. Similar assumptions have been made for barium and strontium azides,[50] nitronium perchlorate[97] and sodium bromate[95] in which the primary excitations, which eventually lead to decomposition, result in the localization of energy in a trapped anion.

The following reaction mechanism is proposed for the formation of nuclei during the induction period:

$$N_3^- \overset{h\nu}{\rightleftarrows} N_3^{-*} \quad . \qquad (1)$$

If the excited azide ion N_3^{-*} is situated at an ideal lattice site it will decay to the ground state N_3^-. However, if located at a surface defect S, it will form the complex $[N_3^- \; S \; N_3^{-*}]$ with an adjacent ground state azide ion. The following reaction will then occur:

$$Ca^{2+} + N_3^- \; S \; N_3^{-*} \overset{\Delta}{\rightarrow} Ca + 3N_2 + S \qquad (2)$$

The measured activation energy of 7,78 Kcal./mol. for this period is associated with step (2) since only this step requires thermal energy. The pertinent defect in this reaction mechanism is probably an anion vacancy. This proposed mechanism is similar to those postulated by Jacobs

et al.[44] and Prout *et al.*[50] for other large band gap azides. Calcium atoms will be formed as calcium ions combine with freed electrons. Initially these atoms will be at the interatomic spacing of calcium atoms in calcium azide but when a critical concentration is reached, they will aggregate to form calcium metal. Thus a metal speck, with all the associated electronic properties of a metal, will be formed. Work on the structure and properties of thin films of metals[183] indicates that the structure of a metal in the thin film is the same as that of bulk metal, and that pseudomorphism is generally not known. Films are formed by lateral growth of nuclei and may become continuous at thicknesses as low as 5 nm. The character of the conductivity of such metal films corresponds very closely to that of the massive metal. Presumably, therefore, by the end of the induction period, very thin two-dimensional plates of metal nuclei, with electronic properties of the bulk metal, will form on the surface of the particles and along the planes of the crystal at discrete centres.

The duration of the induction period is proportional to the time taken for the calcium atoms to aggregate which, in turn, is dependent upon the temperature of the decomposition and the intensity of the light source used. The mechanism postulated presumes that the duration of the induction period will be inversely proportional to the light intensity and this is in accordance with the experimentally determined linear dependence of the rate on the light intensity.

The nitrogen gas evolved will not necessarily escape during the induction period but will be largely absorbed on the powder. If escape is not easy, this gas can cause strain at the reactant/product interface. Photolytic decompositions, which have been interrupted to allow for the introduction of water vapour, have indicated the presence of metal at the

end of the induction period. Water vapour introduced at the end of this period caused the calcium metal on the surface to be destroyed. The subsequent reaction proceeded after a new induction period shorter than that for an uninterrupted decomposition. This showed that water vapour only reacted with nuclei on the surface and left those in the bulk of the material intact. These nuclei, along the planes of the particles, are possibly newly formed and small. It is postulated that after the introduction of water vapour, reaction then proceeds from growth nuclei which are still present in the bulk of the material. The duration of the new induction period is a measure of the time required for these growing nuclei to aggregate and reach a significant critical size. In view of the fact that the reaction of water vapour with the powder before the end of the induction period had no effect on the subsequent photolytic decomposition, it is assumed that calcium metal nuclei are only formed at the end of this period.

Growth proper begins when the calcium metal atoms aggregate to form metal specks. This represents the end of the induction period and the reaction accelerates from the rapidly expanding reactant/product interface.

It has already been shown that the acceleratory period fits the Avrami-Erofeyev equation with the exponent taking the value $n = 2$. The value of n in this equation indicates the nature of the centres of decomposition which increase in number according to a fixed power of time and grow 1-, 2- or 3-dimensionally. The equation also includes the effects of ingestion of potential nucleus-forming sites by growing nuclei or by the overlapping of such nuclei. Thus the value of $n = 2$ indicates either one-dimensional growth of nuclei increasing in number linearly with time or two-dimensional growth of nuclei increasing from a fixed number of centres. The former alternative is considered highly

unlikely as any linear increase in the number of nuclei with time during the acceleratory period would be swamped by the very large number of nuclei formed at the end of the induction period. Moreover, it was considered highly unlikely that a one-dimensional growth could be sustained at such a high intensity of irradiation for the entire acceleratory period which represents 35% of the decomposition. Thus plate-like growth centres are postulated, these centres advancing along the grain boundaries in which they were initiated. During the initial stages of the acceleratory period these growth centres are discrete nuclei, but, as the reaction progresses, independent growth of the individual reaction centres is no longer ensured and overlapping occurs. This is indicated by the use of the Avrami-Erofeyev equation over the acceleratory period.

The rate of the acceleratory reaction was found to be dependent on the square of the light intensity thus indicating that the overall mechanism must involve either two singly excited azide ions or one doubly excited azide ion. There are three possible mechanisms which can be postulated.

(i) The possibility of photoemission from the metal nuclei formed at the end of the induction period (the photoelectric effect) has been widely postulated.[41,44] Calcium ions and electrons are thus formed. At the same time a singly excited azide ion is formed through the absorption of a photon. The absorbed electromagnetic energy is localized at favoured sites in the form of vibrational or internal electronic excitation. If this excited azide ion is located at an ideal lattice point, it will revert to the ground state by communication of its energy to the vibrational modes of adjacent ions. If located at a defect site, the imbalance of forces will allow the absorbed energy to be localized on

this particular ion long enough for it to undergo subsequent reaction. The relevant reaction occurring is that of the excited azide ion with a calcium ion, formed through the photoelectric effect, to give calcium metal and an azide radical (positive hole). This positive hole then reacts with an adjacent singly excited ion to give three molecules of nitrogen, an electron and two anion vacancies. The overall reaction is acceleratory in view of the fact that calcium metal is being regenerated. The electron is captured by an anion vacancy to form an F-centre. Although F-centres have no intrinsic mobility, by a process of association with a mobile anion vacancy and subsequent dissociation, they may move through the lattice at a rate determined mainly by the mobility and concentration of such vacancies. When two F-centres "collide" aggregation to double F-centres results because such aggregates are more stable than single F-centres since the electron in the two identical defects may resonate i.e. this centre is stabilized by reason of the resonance energy. Thus the F-centres tend to aggregate.[53] Ultimately the F-centre aggregate breaks away from the azide matrix. At a critical concentration, collapse of the F-centre occurs and electrons are produced. These react with calcium ions resulting in the growth of calcium metal nuclei to the interface. The reaction scheme is as follows:

$$N_3^- \overset{h\nu}{\rightleftarrows} N_3^{-*} \qquad (1)$$

$$Ca_n \overset{h\nu}{\rightleftarrows} Ca_n^+ + e \qquad (2)$$

$$Ca_n^+ + N_3^{-*} \overset{\Delta}{\rightarrow} Ca_n + N_3 \qquad (3)$$

$$N_3 + N_3^{-*} \rightarrow 3N_2 + 2\square + e \qquad (4)$$

$$\rightarrow 3N_2 + \boxdot + \square \qquad (5)$$

$$2\,[\cdot] \rightarrow 2\,[\,] + 2e \qquad (6)$$

$$Ca_n + Ca^{2+} + 2e \rightarrow Ca_{n+1} \qquad (7)$$

Jacobs *et al.*[184] and Prout *et al.*[50] have postulated a similar process for the growth of sodium and barium azides respectively. Recently de Panafieu[185] has proposed a similar mechanism for the photolysis of potassium azide. Jacobs *et al.*[42,44] and de Panafieu[185] have both proposed the formation of molecular nitrogen via the combination of two holes at the surface, viz.

$$2N_3 \text{ (surface)} \rightarrow 3N_2$$

Thomas and Tompkins[165] have considered this unlikely, however, in a discussion of the photolysis of barium azide. This reaction necessitates the radicals occupying adjacent anion sites and, while they remain incorporated in the lattice, they carry positive charges. Considerable activation would thus be required in order to overcome the high repulsive interaction between the radicals whereas the experimental value is only 7,30 Kcal./mol. If, however, as in step (4), the radical is to react with an excited azide ion, the centre as a whole will be neutral and there would be little steric hinderance to the reaction.

Most workers are in agreement that the acceleratory reaction is attributable to the development of metal nuclei which form after sufficient decomposition has occurred.

No comprehensive optical absorption or e.s.r. studies have been made of calcium azide. E.s.r. studies of barium, sodium and potassium azides have shown the presence of N_2^- and N_4^- ions.[47] If these are produced in this case they probably form as a result of the reactions:

$$N_3 + N_3^- \rightarrow N_4^- + N_2 \qquad (8)$$

and

$$N_3 + N_3^- \rightarrow N_2^- + 2N_2 \quad . \qquad (9)$$

These reactions are possible in view of the fact that the N_3 radical has a life time long enough to interact with a neighbouring ground state azide ion. There is, however, no experimental evidence for the formation of N_2^- and N_4^- in the photolysis of calcium azide. In any event step (4) of the reaction mechanism, in which the hole reacts with an excited azide ion, will be by far the dominant reaction involving the N_3 radicals formed in step (3).

Step (3) is considered to be the rate determining step during the acceleratory reaction and has an activation energy of 7,30 Kcal./mol. associated with it.

(ii) This mechanism involves the successive absorption of two photons by an azide ion. As in the first mechanism the calcium metal nuclei which are formed during the induction period undergo reaction via the photo-electric effect to produce calcium ions and electrons. Absorption of a photon results in a singly excited azide ion being formed. Two possibli-ties then exist for this excited ion. It may return to the ground state by the tunnel effect. This, as explained in the discussion of the previous mechanism, will only occur if the excited ion is located at an ideal lattice site. The second possibility is that it may become doubly excited by the absorption of another quantum of light energy. This will only happen if the excited ion is situated at a defect site. At such sites, e.g. jogs, dislocations, vacancies, etc., the imbalance of forces allows the absorbed energy to be localized on a particular ion long enough for secondary excit-ation to occur. The same possibilities, i.e. reversion to the singly

excited state or subsequent reaction depending on the site at which it is located, also exist for this doubly excited azide ion. If located at a defect site the subsequent reaction which occurs will be thermal ionization, resulting in the formation of an electron and an excited positive hole. The electron so produced reacts with the Ca^+ ion, produced as a result of the photoelectric effect, to form calcium metal. The excited positive hole reacts with an adjacent ground state azide ion to produce three molecules of nitrogen, an electron and two additional anion vacancies. The regeneration of calcium metal indicates the acceleratory nature of the mechanism. Thus the mechanism proposed is as follows:

$$Ca_n \overset{h\nu}{\underset{}{\rightleftarrows}} Ca_n^+ + e \qquad \text{photoelectric effect} \qquad (1)$$

$$N_3^- \overset{h\nu}{\underset{k_1}{\rightarrow}} N_3^{-*} \qquad \text{primary excitation} \qquad (2)$$

$$N_3^{-*} \overset{}{\underset{k_2}{\rightarrow}} N_3^- \qquad \text{de-excitation} \qquad (3)$$

$$N_3^{-*} \overset{h\nu}{\underset{k_3}{\rightarrow}} N_3^{-**} \qquad \text{secondary excitation} \qquad (4)$$

$$N_3^{-**} \overset{}{\underset{k_4}{\rightarrow}} N_3^{-*} \qquad \text{de-excitation} \qquad (5)$$

$$N_3^{-**} \overset{\Delta}{\underset{k_5}{\rightarrow}} N_3^* + e\,. \qquad \text{thermal ionization} \qquad (6)$$

Step (6) is considered to be the rate determining step. As explained above, the electron produced in step (6) combines with the Ca^+ ion formed in step (1),

$$Ca_n^+ + e \rightarrow Ca_n \qquad (7)$$

and the excited positive hole reacts with a ground state azide ion in

the strained region at the interface,

$$N_3^* + N_3^- \rightarrow 3N_2 + e + 2\square \qquad (8)$$

$$\rightarrow 3N_2 + \boxdot + \square \quad . \qquad (9)$$

Aggregation of F-centres then takes place. When a region consists almost exclusively of F-centres a collapse of the lattice occurs and colloidal metal is formed as follows:

$$2\boxdot \rightarrow 2\square + 2e \qquad (10)$$

$$Ca_n + Ca^{2+} + 2e \rightarrow Ca_{n+1} \quad . \qquad (11)$$

By applying steady state conditions we can assume that

$$\frac{d[N_3^{-*}]}{dT} = \frac{d[N_3^{-**}]}{dT} = 0 \quad . \qquad (i)$$

Now

$$\frac{d[N_3^{-*}]}{dT} = k_1[N_3^-]I - k_2[N_3^{-*}] - k_3[N_3^{-*}]I + k_4[N_3^{-**}] \qquad (ii)$$

and

$$\frac{d[N_3^{-**}]}{dT} = -k_4[N_3^{-**}] - k_5[N_3^{-**}] + k_3[N_3^{-*}]I \quad . \qquad (iii)$$

Thus it follows that, from (i) and (ii),

$$(k_2 + k_3I)[N_3^{-*}] = k_4[N_3^{-**}] + k_1[N_3^-]I$$

and, from (i) and (iii),

$$[N_3^{-*}] = \frac{(k_4 + k_5)[N_3^{-**}]}{k_3I} \quad . \qquad (iv)$$

Hence, by substituting the value of $[N_3^{-*}]$ from (iv) into (ii) we obtain:

$$[N_3^{-**}] = \frac{k_1 k_3 [N_3^-] I^2}{(k_2 + k_3 I)(k_4 + k_5)} \quad . \qquad (v)$$

Since step (6) is the rate determining step we can express the rate of the overall reaction as:

$$R = k_5 [N_3^{-**}] \quad . \qquad (vi)$$

Thus, from (v) and (vi) we obtain

$$R = \frac{k_1 k_3 k_5 [N_3^-] I^2}{(k_2 + k_3 I)(k_4 + k_5)} \quad . \qquad (vii)$$

The singly excited azide ion formed in step (2) will tend to revert to the ground state more readily than be doubly excited and thus $k_2 >> k_3 I$. Moreover since there is only a single experimental activation energy $k_4 >> k_5$. Thus (vii) reduces to the form

$$R = \frac{k_1 k_3 k_5 [N_3^-] I^2}{k_2 k_4}$$

and it follows that, according to this mechanism, the rate of the reaction is proportional to the square of the light intensity. This is in accordance with the observations made experimentally with respect to the relationship between rate and light intensity.

(iii) This scheme is similar to that described in (ii) above except that energy is transferred from one excited azide ion to another excited azide ion to form the doubly excited ion:

$$Ca_n \overset{h\nu}{\rightleftarrows} Ca_n^+ + e \qquad \text{photoelectric effect} \qquad (1)$$

$$N_3^- \xrightarrow[k_1]{h\nu} N_3^{-*} \qquad \text{primary excitation} \qquad (2)$$

$$N_3^{-*} \xrightarrow[k_2]{} N_3^- \qquad \text{de-excitation} \qquad (3)$$

$$N_3^{-*} + N_3^{-*} \xrightarrow[k_3]{} N_3^{-**} + N_3^- \qquad \text{energy transfer} \qquad (4)$$

$$N_3^{-**} \xrightarrow[k_4]{} N_3^{-*} \qquad \text{de-excitation} \qquad (5)$$

$$N_3^{-**} \xrightarrow[k_5]{\Delta} N_3^* + e \qquad \text{thermal ionization} \qquad (6)$$

The electron produced in step (6) reacts with the formed Ca ions in step (1) and the positive hole formed in step (6) reacts with an adjacent azide ion to give three molecules of nitrogen and an electron. Thus

$$Ca_n^+ + e \rightarrow Ca_n \qquad (7)$$

$$N_3^* + N_3^- \rightarrow 3N_2 + e + 2\square \qquad (8)$$

$$\rightarrow 3N_2 + \boxdot + \square \; . \qquad (9)$$

The F-centres aggregate, collapse and colloidal metal is formed.

$$2\boxdot \rightarrow 2\square + 2e \qquad (10)$$

$$Ca_n + Ca^{2+} + 2e \rightarrow Ca_{n+1} \; . \qquad (11)$$

Thus the calcium metal is regenerated and the whole process is acceleratory. By applying the steady state conditions it follows that

$$\frac{d[N_3^{-*}]}{dT} = \frac{d[N_3^{-**}]}{dT} = 0 \; . \qquad (i)$$

Now

$$\frac{d[N_3^{-*}]}{dT} = k_1[N_3^-]I - k_2[N_3^{-*}] - k_3[N_3^{-*}]^2 + k_4[N_3^{-**}] \qquad (ii)$$

and

$$\frac{d[N_3^{-**}]}{dT} = k_3[N_3^{-*}]^2 - k_4[N_3^{-**}] - k_5[N_3^{-**}] \quad . \qquad \text{(iii)}$$

From (iii) it follows that

$$[N_3^{-*}] = \left[\frac{k_4 + k_5}{k_3}\right]^{\frac{1}{2}} [N_3^{-**}]^{\frac{1}{2}} \quad . \qquad \text{(iv)}$$

Substitution of the value for $[N_3^{-*}]$ obtained in (iv) into equation (ii), yields

$$k_1[N_3^-]I = C_1[N_3^{-**}]^{\frac{1}{2}} + C_2[N_3^{-**}] \qquad \text{(v)}$$

where $C_1 = k_2(k_4 + k_5)^{\frac{1}{2}} \; k_3^{-\frac{1}{2}}$

and $C_2 = k_5$.

Being associated with the rate determining step, k_5 is very small and the term $C_2[N_3^{-**}]$ is negligible. The rate of the overall reaction is

$$R = k_5[N_3^{-**}] \qquad \text{(vi)}$$

and thus by substituting for $[N_3^{-**}]$ from equation (v) into equation (vi), it follows that

$$R = k_5.k_1^2.C_1^{-2}.\,[N_3^-]^2\, I^2 \quad .$$

This mechanism thus yields an equation in which the rate is seen to be directly proportional to the square of the light intensity. This is again in accordance with the relationship between rate and light intensity observed experimentally.

Mechanisms (2) and (3) have been proposed by a number of workers. Prout and Shephard[50] proposed both of these mechanisms for the accelera-tory reaction in the photolysis of strontium azide. The azide ion was

doubly excited in either of the two methods outlined and then the rate determining step was the thermal ionization of the N_3^{-**} ion which reacts with an Sr_n^+ ion. The latter ion had been formed as a result of the photoelectric effect. Thus the rate determining step in this mechanism is:

$$Sr_n^+ + N_3^{-**} \rightleftarrows Sr_n + N_3^* \quad . \qquad 3{,}20 \text{ Kcal./mol.}$$

Maycock *et al.*[97] proposed the transfer of energy between an excited ClO_4^- ion and a similarly excited ion trapped at a defect site in the photolysis of nitronium perchlorate. Herley and Levy[95] studied the photolysis of sodium bromate and proposed the following reactions:

$$BrO_3^- \overset{h\nu}{\rightleftarrows} BrO_3^{-*} \quad .$$

Then either: $BrO_3^{-*} \overset{h\nu}{\rightleftarrows} BrO_3^{-**}$

or: $BrO_3^{-*} + BrO_3^{-*} \rightleftarrows BrO_3^{-**}$.

The doubly excited site then undergoes decomposition

$$BrO_3^{-**} \rightarrow BrO^- + O_2 \quad .$$

Tompkins *et al.*[104] in studying the photolytic decomposition of silver oxalate, postulated the production of a singly excited oxalate ion by ultraviolet radiation such that the excited electron is still associated with the parent ion. The mobile exciton is trapped at an anion vacancy, a process that involves the capture of the excited electron by the vacancy which may accomodate two electrons. This complex may either be further excited by absorbing a second photon or may be destroyed by the electron returning, by the tunnel effect, form the anion vacancy back to a singly charged ion. Further this doubly excited oxalate radical may either revert to a singly excited state or decompose to give two

molecules of carbon dioxide. Briefly therefore they proposed:

$$[Ox^{2-}] \overset{h\nu}{\underset{\leftarrow}{\rightarrow}} [Ox^{2-}]^*$$

$$[Ox^{2-}]^* \overset{h\nu}{\underset{\leftarrow}{\rightarrow}} [Ox^{2-}]^{**}$$

$$[Ox^{2-}]^{**} \rightarrow 2CO_2 + 2e \quad .$$

Prout and Lownds[102] have proposed a similar mechanism in the photolysis of potassium permanganate. Two different dependencies of the rate on the light intensity were observed. Below 110,0°C the rate depended on the cube of the light intensity and above this temperature on the square of the light intensity. Thus the following mechanism was postulated where M represents the MnO_4^- ion:

$$M \overset{h\nu}{\underset{\leftarrow}{\rightarrow}} M^*$$

$$M^* \overset{h\nu}{\underset{\leftarrow}{\rightarrow}} M^{**}$$

at temperatures above 110,0°C. At temperatures below 110,0°C the reaction continued thus:

$$M^{**} \overset{h\nu}{\underset{\leftarrow}{\rightarrow}} M^{***}$$

Decomposition of the doubly or triply excited ion then occurs:

$$M^{**} \text{ or } M^{***} \overset{\Delta}{\rightarrow} \text{Products.}$$

Such mechanisms are thus considered feasible for photolytic decompositions involving either successive excitations of a single ion by direct absorption of photons or by transfer of energy from one excited ion to another in order to account for rate equations of the form $R \alpha I^n$ where $n > 1$.

In making a choice of one of the three mechanisms proposed it must be borne in mind that, at 60,0°C, the molecularity changes from two to one. This implies that in the lower temperature range either two singly excited azide ions or one doubly excited ion is involved in the photolytic process and that in the higher temperature range only one option exists viz. a singly excited azide ion. Hence it would appear more likely that mechanism (1), which involves singly excited azide ions, rather than (2) or (3), is operative in the photolytic decomposition of calcium azide in this temperature range. This is because mechanism (1) is more easily adaptable to the processes occurring in the higher temperature range in that in both temperature ranges only singly excited ions would be postulated. The case for accepting mechanism (1) is further strengthened when the results for calcium azide are compared with the results for barium azide obtained by Prout and Shephard.[50] The rate determining step in mechanism (1), viz.

$$Ca_n^+ + N_3^{-*} \overset{\Delta}{\rightarrow} Ca_n + N_3$$

has an activation energy of 7,30 Kcal./mol. In the mechanism of photolysis of barium azide proposed by these workers the rate determining step, viz.

$$Ba_n^+ + N_3^{-*} \overset{\Delta}{\rightarrow} Ba_n + N_3$$

has an activation energy of 7,60 Kcal./mol. Moreover in both compounds the molecularity changed from two to one in going from the acceleratory reaction at ambient temperatures to the acceleratory reaction at higher temperatures. Hence mechanism (1), identical to that proposed by these workers for barium azide, is postulated for calcium azide. Mechanisms (2) and (3) are rejected since they require a more drastic amendment at higher temperatures than does mechanism (1). These mechanisms have been

applied to the photolysis of strontium azide.[50] In this compound the molecularity of the acceleratory reaction throughout the temperature range 30,0° - 90,0°C is two. Hence no drastic change in mechanism was required to explain the reactions occurring in the temperature ranges above and below 60,0°C.

Introducing water vapour on to the sample during the acceleratory period of the photolytic decomposition has clearly illustrated the importance of metal nuclei during this period. Water vapour was found to destroy the reaction. A new induction period, shorter than that for an uninterrupted decomposition, followed and the acceleratory rate of the subsequent reaction decreased. Growth nuclei, situated on the planes of the particles, which were not destroyed by the water vapour, were considered to be the points of origin of the new reaction. The new induction period observed is the time required for these nuclei to grow to a critical size. The water vapour presumably only attacks metal nuclei on the surface of the particles. The decrease in the acceleratory rate after admission of water vapour is due to the fewer centres which are available from which the reaction may commence. The acceleratory rate constant is dependent on the number of nuclei present at the start of the reaction and a decrease in this number will decrease the rate of the reaction. When water vapour was introduced at or beyond the inflection point, the reaction was destroyed. This was presumably due to the fact that calcium hydroxide formed from the reaction of calcium metal with the water which was introduced, is opaque to ultraviolet light. Thus, if all the particles are covered with calcium metal at or beyond the inflection point, this will result in a complete covering of calcium hydroxide subsequent to the introduction of water vapour. Owing to the latter's opaqueness, growth nuclei present below the surface cannot be activated by the ultraviolet radiation and reaction ceases.

Another effect of introducing water vapour was a decrease in the observed final pressure . This was probably a result of the calcium azide being partially hydrolyzed. It would appear therefore that calcium metal nuclei have a 'catalytic' effect on the photolytic reaction and that during the acceleratory period the layer or coating of calcium metal is continually growing. At the end of the acceleratory period all the particles are coated with a layer of calcium metal.

The decay reaction commences when the two-dimensional nuclei overlap and the surface of the small particles are covered by the reaction product of calcium metal. It has been shown that during this period the penetration of the product interface into the particles takes place according to the unimolecular decay law. The product and reactant phases have different molecular volumes and the interface thus collapses leaving isolated blocks of material in which no nuclei are present. This occurs as a result of the extensive growth of plate-like nuclei. In these isolated blocks each molecule has an equal probability of decomposition and the rate of reaction thus becomes proportional to the amount of unreacted substance.

The activation energy and the molecularity of the decay reaction have been found to be 4,67 Kcal./mol. and 2,0 respectively. These values are very similar or identical to the values obtained for the acceleratory reaction. Hence the same mechanism as that proposed for the acceleratory reaction is proposed for the decay reaction. The reduced rate of production of nitrogen is a result of the gradual consumption of defects which are helpful to the reaction.

(iii.b) Photolysis in the temperature range 60,0° - 95,0°C

The photolysis of calcium azide in the temperature range 60,0° - 95,0°C was found to be linearly dependent throughout on the light intensity.

This linear dependence necessitates a change in the mechanisms postulated for photolytic decomposition in the temperature range 35,0° - 60,0°C. The activation energies are greater for each period. The activation energy for the induction period is 10,80 Kcal./mol., for the acceleratory period 12,52 Kcal./mol. and for the decay period 17,36 Kcal./mol. These increased values of activation energy also require postulating different mechanisms for photolysis.

In this temperature range the mathematical analyses, visual observations, the effect of filters and of introducing water vapour at various stages of decomposition were found to be analogous to the results obtained in the lower temperature range. As a result of this it is assumed that the topochemical decomposition in this temperature range is similar to that in the temperature range 35,0° - 60,0°C.

Formation of nuclei in the induction period initially involves the formation of a singly excited azide ion. The activation energy of 10,80 Kcal./mol. represents sufficient thermal energy for the transfer of an electron from a ground state azide ion to a Ca^{2+} ion. The positive hole formed as a result of this electron transfer then reacts with an adjacent singly excited azide ion to form three molecules of nitrogen and an electron. This electron then combines with a Ca^{+} ion formed earlier to yield calcium metal. Thus

$$N_3^- \overset{h\nu}{\underset{\leftarrow}{\rightarrow}} N_3^{-*} \qquad (1)$$

$$Ca^{2+} + N_3^- \overset{\Delta}{\rightarrow} Ca^+ + N_3 \qquad (2)$$

$$N_3 + N_3^{-*} \rightarrow 3N_2 + e \qquad (3)$$

$$Ca^+ + e \rightarrow Ca \quad . \qquad (4)$$

Step (2) is considered to be the rate determining step and has an activation energy of 10,80 Kcal./mol. The mechanism is seen to be in accordance

with the linear dependence of the inverse of the duration of the induction period on the light intensity.

As already mentioned nuclear growth has been found to be dependent on the first power of the light intensity and thus the mechanism proposed for the lower temperature range needs to be modified accordingly. Moreover the activation energy of 12,52 Kcal./mol. represents sufficient thermal energy to transfer an electron from an azide ion to an adjacent Ca_n^+ ion formed as a result of the photoelectric effect. This transfer of an electron results in the formation of a positive hole, the latter then reacting with an excited azide ion in a manner similar to that proposed in the lower temperature range. Thus:

$$N_3^- \overset{h\nu}{\rightleftarrows} N_3^{-*} \qquad (1)$$

$$Ca_n \overset{h\nu}{\rightleftarrows} Ca_n^+ + e \qquad (2)$$

$$Ca_n^+ + N_3^- \overset{\Delta}{\rightarrow} Ca_n + N_3 \qquad (3)$$

$$N_3 + N_3^{-*} \rightarrow 3N_2 + 2\square + e \qquad (4)$$

$$\rightarrow 3N_2 + \boxdot + \square \qquad (5)$$

$$2\boxdot \rightarrow 2\square + 2e \qquad (6)$$

$$Ca_n + Ca^{2+} + 2e \rightarrow Ca_{n+1} \; . \qquad (7)$$

Step (3) is considered to be the rate determining step and has an activation energy of 12,52 Kcal./mol. The mechanism postulated is seen to be in accordance with the observed linear dependence of the photolytic rate on light intensity.

The activation energy for the decay period in this temperature range is 17,36 Kcal./mol. This value is quite considerably higher than that for the acceleratory period. The mechanism is still linearly

dependent on the light intensity. The activation energy for thermal decomposition over this period is approximately 26,0 Kcal./mol. which is about the same as the value obtained for the thermal decomposition over the acceleratory period. The rate determining step in the thermal decomposition is

$$N_3^- \overset{\Delta}{\rightarrow} N_3 + \text{electron in conduction band}$$

The value of 17,36 Kcal./mol. is not considered sufficient for this thermal ionization to occur. Prout *et al.*[137,168] have obtained a value of 18,8 Kcal./mol. for the decay period in the thermal decomposition of calcium azide. They associated this activation energy with the reaction

$$N_3^- + N_3^- \rightarrow 3N_2 \quad .$$

They considered that the decay reaction commenced when the surface nuclei touch and reaction takes place at the contracting interface. The metal sheath around the azide particle exerts compressive stresses on the azide lattice and distortion of adjacent azide ions at the reactant/product interface is a maximum. The adjacent azide ions interact in this region of strain. Two separate studies (one on aged material and the other on fresh material) were carried out to determine the activation energy of the thermal decomposition of the sample of calcium azide used in this study. Using two different mathematical analyses on the fresh material, a value of $\approx$ 26,0 Kcal./mol. was obtained in the case of both the fresh and the aged material. Furthermore, the subsequent studies carried out on the co-irradiated decomposition of calcium azide powder yielded values for the activation energy of the decay reaction between 17,0 Kcal./mol. and 26,0 Kcal./mol. which are to be expected in the light of the value obtained in this photolytic study. If the value for

the thermal decomposition quoted above, viz. 18,8 Kcal./mol., were to be accepted, this would imply that the activation energy for co-irradiated decomposition was higher than that for purely thermal decomposition which is improbable. Hence the value of 17,36 Kcal./mol. obtained for the photolysis of calcium azide powder in the decay period over the temperature range under discussion is presumably associated with the reaction

$$Ca_n^+ + N_3^- \xrightarrow{\Delta} Ca_n + N_3$$

which is the rate determining step in the acceleratory period. The difference between this value of 17,36 Kcal./mol. and the value of 12,52 Kcal./mol. obtained for the acceleratory period could be due to experimental error. This difference in value is not very excessive when one considers, for example, the large discrepancies existing in the literature for the thermal decomposition of calcium azide.[58,137,168,195]

Possibly a more plausible reason for the discrepancy in the activation energies for the acceleratory and decay reaction - if the same mechanism is to be postulated for both periods - is that during the decay period reaction is taking place predominantly below the surface. It has already been shown that, beyond the inflection point, the surface of the particles is completely covered with metal. There is also evidence to show that many azides decompose either at the surface or at internal cracks.[196] It is, therefore, to some extent an oversimplification to base a mechanism, which is operating at an interface, on the bulk properties. For example, the optical energy of sodium chloride is ≈16,0 Kcal./mol. lower at the surface.[36] The difference between bulk and surface energies is expected to exist in azides as well and will be strongly dependent upon the crystallographic orientation of the decomposing sample. Moreover the process of diffusion of the gas to the surface requires energy. This

increase in the activation energy of the decay reaction at these temperatures is possibly due to the difficulty experienced by the nitrogen formed at internal cracks or dislocations to diffuse to the surface.

Thus the same mechanisms are postulated for both the acceleratory and decay reaction and the difference in the values of the activation energies is ascribed to the fact that during the decay period the reaction

$$Ca_n^+ + N_3^- \rightleftharpoons Ca_n + N_3$$

is taking place predominantly in the bulk of the material whereas during the acceleratory reaction it is taking place predominantly at the surface cracks, jogs or dislocations or along planes which emerge at the surface.

(iii.c) Photolysis in the temperature range -70,0° - 7,0°C

No previous work has been carried out on the photolytic decomposition of calcium azide in this temperature range nor have any pre-irradiation studies been made. No data exists from e.s.r. studies and thus mechanisms proposed will depend to a considerable extent on work done on other azides, notably barium azide.

Sigmoid pressure-time plots were obtained and the reproducibility was found to be good over the acceleratory and decay reactions but was not highly satisfactory over the induction period. This was probably a result of a variation in the defect surfaces of the powders. Results obtained during this period should thus be treated with caution and mechanisms proposed for the induction period should be similarly viewed.

The acceleratory reaction was analyzed by means of the Avrami-Erofeyev equation with n = 2 and the decay reaction was analyzed using the unimolecular law. The percentage decomposition at -20,0°C was 62%,

considerably less than the 93,4% obtained for a purely thermal decomposition. No dark rate was detected in this temperature range and thus a purely photolytic decomposition process was at work. Visual observations showed a continually darkening colour during the induction and acceleratory periods and beyond the inflection point the particles were completely black.

The activation energy for the induction period over this temperature range was 0,34 Kcal./mol. and the molecularity was 1,00. The activation energy for the acceleratory reaction was 0,56 Kcal./mol. and the molecularity 2,23. The rate of photolysis in this period can therefore be considered to vary as the square of the light intensity. The decay reaction activation energy was found to be 0,42 Kcal./mol. and the value of the molecularity 2,00. Again, the rate of photolysis varies as the square of the light intensity.

The visual observations referred to above indicate the presence of calcium metal at the end of the induction period and during the acceleratory period. The darkening of the colour indicates an ever increasing amount of metal present and the black colour of the sample subsequent to the inflection point indicates that the particles are covered on the surface with a calcium metal layer. These facts were further illustrated by introducing water vapour during a photolytic decomposition. Introducing water vapour on to the sample at the end of the induction period caused the calcium metal on the surface to be destroyed. The reaction continued after a new shorter induction period, the new reaction proceeding presumably from growth nuclei still present in the bulk of the material. Water vapour introduced during the induction period had no effect on the subsequent reaction, indicating that calcium metal nuclei were only formed at the end of this period. The thin film of calcium metal has the same characteristics as those of the bulk metal[183] and it appears that by the

end of the induction period very thin two-dimensional plates of metal nuclei, with electronic properties of the bulk metal, will form on the surface of the particles and along the planes of the crystal at discrete centres.

Filtering the ultraviolet radiation has shown a reduction in the rate of decomposition relative to that obtained for unfiltered decompositions. Reflection from the polished surfaces accounts partially for this reduction in rate but if this factor is considered constant for the three filters then it is observed that the 5 mm BG12 filter causes a virtual end to the photolytic decomposition. The 3 mm UG5 and 1 mm UG1 filters both lower the rate, the latter slightly more so. From this it can be concluded that the most effective wavelengths for the photolysis of calcium azide in this temperature range are in the region 220 - 330 nm. These wavelengths represent energies which are too small to cause the formation of positive holes and free electrons. Thus the mechanism must involve the formation of an excited azide ion. Low absorption coefficients at the longer wavelengths probably account for the reduced rates resulting in a lower rate of excitation of the internal transitions.

In the temperature range 35,0° - 60,0°C it was proposed that the rate determining step for the induction period involved the reaction between a Ca^{2+} ion and the $[N_3^- S N_3^-*]$ complex where S is probably an anion vacancy. This mechanism was linearly dependent on the light intensity and had an activation energy of 7,78 Kcal./mol. associated with it. In this low temperature range the molecularity is still one but the activation energy is only 0,34 Kcal./mol. The following basically similar mechanism is thus proposed. A more logical explanation of the decreased activation energy could have been postulated had the molecularity been 2. This would have required a doubly excited complex/ion and hence the smaller activation energy would have been more meaningful. The poor reproducibility during this period

makes this proposed mechanism suspect.

$$N_3^- \overset{h\nu}{\underset{\leftarrow}{\rightarrow}} N_3^{-*} \qquad (1)$$

$$N_3^- \; S \; N_3^{-*} \overset{\Delta}{\rightarrow} 2N_2^- + N_2 + S \qquad (2)$$

$$2N_2^- \rightarrow 2N_2 + 2e \qquad (3)$$

$$Ca^{2+} + 2e \rightarrow Ca \qquad (4)$$

This mechanism incorporates a reaction in which the N_2^- ion is produced. No e.s.r. or optical absorption spectrum studies have been made of calcium azide and hence no evidence exists for its production. It has been observed in the low-temperature photolysis of potassium, sodium and barium azides.[61,62,53,47] The many similarities which exist in the results obtained for the photolysis of barium and calcium azides do, however, support the proposed formation of this ion. The rate of formation of the N_2^- ion has been found to be linearly dependent on the light intensity as is the case in this mechanism. Moreover it was produced by radiation of wavelength 225 nm[47] which is within the range of wavelengths found experimentally to be effective for photolysis. Step (2) is considered to be the rate determining step and has an activation energy of 0,34 Kcal./mol. associated with it.

The equations used in the mathematical analyses of the photolysis of calcium azide are the same as those used in the case of barium and strontium azides at these low temperatures. Thus the topography of the photolytic reactions involved can be assumed to be the same as that for these two azides. Calcium atoms formed in step (4) are located on the surface and on the planes of the crystal. Eventually diffusion of the atoms results in aggregation to give calcium metal nuclei. This aggregation of atoms indicates the end of the induction period. Nitrogen gas evolved

will not necessarily escape during this period but will be largely absorbed on the powder.

The acceleratory reaction was analyzed using the Avrami-Erofeyev equation with n = 2. The pronounced effect of the intense irradiation at low temperatures leads to the assumption that the value of n = 2 implies a two-dimensional growth of nuclei increasing from a fixed number of centres. The visual observations made, the mathematical analyses, the effect of filters and the effect of introducing water vapour on to the sample are all found to be virtually identical to those found for barium and strontium azides in the same temperature range and thus the topography, once again, is considered to be the same.

The activation energy for the acceleratory reaction in this temperature range is 0,56 Kcal./mol. and the molecularity is two. The mechanism proposed for the growth of calcium metal nuclei is similar to that proposed for barium azide in this temperature range. A singly excited azide ion is trapped at a site S which is probably an anion vacancy. Another singly excited azide ion is trapped at the same site and the complex $[N_3^{-*}\square N_3^{-*}]$ reacts with a Ca_n^+ ion formed via the photoelectric effect to form a calcium atom, two positive holes and an electron. The defect S is regenerated. If this defect is an anion vacancy it will form an F-centre with the electron. The positive holes react with ground state azide ions to form nitrogen and N_2^- ions. Light of wavelength 325 nm will cause the reaction

$$N_2^- + N_3^{2-} \rightleftarrows N_2^0 - N_3^{2-}$$

to occur. The predominant reaction involving the N_2^- ion, however, will result in the formation of nitrogen and, ultimately F-centres. Eventually the metal nuclei grow to the interface when electrons, formed as a result

of the collapse of F-centres, react with Ca^{2+} ions to form calcium atoms. The excited ions are presumed to be located at defect sites since they will revert to the ground state if located at ideal lattice positions. The F-centres aggregate initially as a result of the increased stability due to resonance and then, at a critical concentration, collapse to produce vacancies and electrons. Thus the mechanism for the acceleratory reaction in this temperature range is as follows:

$$N_3^- \overset{h\nu}{\rightleftarrows} N_3^{-*} \quad (1)$$

$$Ca_n \overset{h\nu}{\rightleftarrows} Ca_n^+ + e \quad (2)$$

$$Ca_n^+ + N_3^{-*} \; S \; N_3^{-*} \overset{\Delta}{\rightarrow} Ca_n + 2N_3 + e + S \quad (3)$$

$$2N_3 + 2N_3^- \rightarrow 2N_2^- + 4N_2 \quad (4)$$

$$N_2^- + N_3^- \rightleftarrows N_2^0 - N_3^{2-} \quad (5)$$

$$N_2^- + 2N_2 \rightarrow 3N_2 + \square + e \quad (6)$$

$$\rightarrow 3N_2 + \boxdot \quad (7)$$

$$2\boxdot \rightarrow 2\square + 2e \quad (8)$$

$$Ca_n + Ca^{2+} + 2e \rightarrow Ca_{n+1} \quad . \quad (9)$$

Step (3) is considered to be the rate determining step and has an activation energy of 0,56 Kcal./mol. associated with it. The mechanism is in accordance with the dependence of the rate on the square of the light intensity.

The decay reaction commences when the two-dimensional nuclei overlap and the surface of the particles are covered with the reaction product. This period was analysed using the unimolecular decay law. Introducing

water vapour during the decay period caused the reaction to cease. This was presumably a result of the formation of a layer of calcium hydroxide on the surface. This layer is opaque to ultraviolet light and hence the reaction ceases. The visual observations, mathematical analyses and the effect of introducing water vapour is the same as that for barium azide and the topochemistry of the reaction is considered to be the same.

The mechanism proposed for the decay period is the same as that for the acceleratory period. The activation energy for the decay reaction is 0,42 Kcal./mol. and is very similar to that of the acceleratory reaction. The rate is also dependent on the square of the light intensity as in the case of the acceleratory reaction.

(iii.d) Photolysis in the temperature range 7,0° - 22,0°C

The activation energies obtained for the photolysis of calcium azide powder in this temperature range are 5,70 Kcal./mol., 4,18 Kcal./mol. and 3,76 Kcal./mol. for the induction, acceleratory and decay reactions respectively. The molecularities for these stages of the reaction are (to the nearest whole number) 1, 2 and 2 respectively. These values were obtained in a study completely independent from that carried out in the temperature range 35,0° - 60,0°C. The values for the activation energies and molecularities obtained in each temperature range are very similar or identical. The visual observations, mathematical analyses, the effect of the use of filters and the effect of introducing water vapour were also found to be the same. Hence it is concluded that the mechanisms proposed for the photolysis of calcium azide in the temperature range 35,0° - 60,0°C are also applicable in this temperature range, and the general discussion pertaining to these mechanisms is the same.

(iv) PHOTOLYSIS OF LITHIUM AZIDE

Powdered lithium azide was decomposed photolytically in the temperature range -70,0° - 170,0°C. Throughout this temperature range the photolysis was characterized by an initial induction period during which no measurable amount of nitrogen was evolved. This was followed by an acceleratory and decay reaction. The reproducibility obtained over the acceleratory and decay periods was good but no highly satisfactory reproducibility was obtained over the induction period, particularly at low temperatures. Powdered samples were ground and sieved repeatedly in an effort to improve reproducibility over this period but variations in the defect surfaces, crucial to the decomposition process, are not readily eliminated. The pressure-time graphs were sigmoid in shape. The acceleratory period was described by the Avrami-Erofeyev equation with n = 2 and the decay period was analyzed using the unimolecular decay law. The degree of fit of the mathematical equations was virtually the same at all temperatures under study and the inflection point occurred consistently in the region of α = 0,25 in the higher temperature range and at α = 0,43 in the lower temperature ranges. The percentage decomposition was 78% in the higher temperature range and 57% in the lower temperature range. These are to be compared with a value of 82% obtained in the thermal decomposition of lithium azide powder at 200°C.[174]

In the study carried out over the temperature range -70,0° - 17,0°C two distinct activation energies were determined, a change in the value occurring at -19,0°C. The activation energy for the induction period was 3,14 Kcal./mol. below -19,0°C and 4,98 Kcal./mol. above that temperature. The activation energy for the acceleratory period was 1,71 Kcal./mol. and 4,25 Kcal./mol. for the temperature ranges below and above -19,0°C respectively and for the corresponding temperature ranges

the activation energy for the decay period was 0,88 Kcal./mol. and 5,44 Kcal./mol. respectively. The values of m for the induction, acceleratory and decay periods respectively were 1,71, 1,69 and 1,70 in the temperature range below -19,0°C and 1,54, 1,81 and 1,86 in the temperature ranges above -19,0°C.

In the study carried out in the temperature range 24,6° - 170,0°C the activation energies were found to change at 71,8°C. Below this temperature the activation energies for the induction, acceleratory and decay reactions were found to be 6,10 Kcal./mol., 4,20 Kcal./mol. and 3,20 Kcal./mol. respectively. Above 71,8°C the activation energies were found to be 11,50 Kcal./mol., 9,90 Kcal./mol. and 11,60 Kcal./mol. The decay reaction was also analyzed using the split-run method. Below 78,0°C the activation energy was found to be 2,48 Kcal./mol. and above 78,0°C the activation energy was 8,44 Kcal./mol. The molecularity of the induction, acceleratory and decay reactions below 71,0°C were found to be 1,54, 1,81 and 1,86 respectively and above this temperature the molecularities for the corresponding reactions were 1,14, 1,14 and 1,18.

(iv.a) Photolysis in the temperature range 24,6° - 71,8°C

As stated above the photolysis commenced with an induction period, during which there was no measurable evolution of gas, followed by an acceleratory and decay period. The acceleratory period was analyzed using the Avrami-Erofeyev equation with n = 2. The value of n = 2 can be ascribed to one of the following types of nuclear growth :

(i) one-dimensional growth of nuclei, increasing in number linearly with time; or

(ii) two-dimensional growth of nuclei increasing from a fixed number of centres.

The first type of growth does not appear acceptable because the relatively high value of the inflection point implies that it is highly unlikely that a one-dimensional growth could be sustained at such a high intensity of irradiation for the entire acceleratory period.

It is during the induction period that the formation of nuclei takes place. Metallic nuclei were not present at the commencement of heating since admission of water vapour at t = 0 had no effect on the subsequent photolysis other than to lower the final pressure. This latter phenomenon was probably due to the partial hydrolysis of azide by the water vapour. Introducing water vapour at subsequent points during the induction period similarly had no effect on the photolysis. However, introduction of water vapour at the end of the induction period had the effect of causing a new induction period to occur with a subsequent lowering of the acceleratory rate. This indicates that it was only at the end of the induction period that metallic nuclei were formed. The nuclei are considered to be surface ones and are discrete. Clustering of nuclei occurs at the end of the induction period and the sites preferred for this are on the surface of the particles, such as surface cracks or lines of strain where disorganization or mechanical damage has taken place and where there is a higher thermodynamic instability and unsaturation of cohesive forces.[174] This mechanical damage is enhanced by the grinding and dehydration process which precedes decomposition. Grinding produces a large number of dislocations which group to form high angle grain boundaries.

It was found that the effect of filtering the ultraviolet radiation caused the rate of the reaction to decrease. The extent of the decrease in rate depended on the type of filter used. The decrease in rate experienced with all three filters was partially a result of simple reflection of the radiation from the highly polished surface. Disregarding this, however,

as being a constant factor, it was found that there was a much greater decrease in rate when the 1 mm UG1 was used compared to the 3 mm UG5. The 5 mm BG12 filter had such a dramatic decreasing effect that the photolytic decomposition virtually appeared to cease. The conclusions that are drawn from these observations are that the most effective wavelengths for photolysis are those in the range 220 - 280 nm. As has been explained previously in the discussion on the photolytic decompositions of the other azides, these wavelengths do not represent energies of the magnitude required for the formation of free electrons and holes and it is considered that the ultraviolet radiation causes a transition of low probability to a low-lying excited state of the azide ion.[9] This absorbed energy is localized at the favoured sites in the form of vibrational or internal electronic excitation. This primary excitation which ultimately leads to decomposition, thus results in the localization of energy in a trapped anion.

The mechanism proposed for the formation of nuclei during the induction period must be in accordance with the observed dependence of the rate on the square of the light intensity. Since no e.s.r. or optical absorption spectrum studies have been carried out on lithium azide to date, the proposition that certain specific ions or colour centres are products of photolysis is speculative. Lithium azide has the same crystal structure as α-sodium azide and is similar in structure to barium azide. All three are monoclinic, barium azide being $P2_1/m$ and the other two are $C2/m$.[182] Lithium and sodium azides are both basically distorted sodium chloride type crystals, in which the azide ions stack perpendicularly. No photocurrent has been observed with sodium azide at the wavelengths which were found to be effective for photolysis of lithium azide. This observation strengthens the proposal that excited azide ions are formed in lithium azide. F-centres have been observed in the halides as well as in sodium

and many other azides. Sodium and lithium azides have also been shown to have virtually identical properties in vibrational studies.[182]

Prout and Liddiard[174], in a study of the thermal and pre-irradiated decomposition of lithium azide, have proposed an induction period mechanism involving the decomposition of two azide ions to give three molecules of nitrogen and two electrons. The activation energy determined for this is 22,0 Kcal./mol. The activation energy of photolysis for the same period in the temperature range under discussion is much less and thus the rate determining step is clearly different. Initial absorption of a photon leads to the formation of an excited azide ion. This excited ion is probably trapped at a defect such as an anion vacancy. A second excited azide ion is trapped at the same site in a manner analogous to that postulated for barium, strontium and calcium azides. Reaction then takes place with a Li^+ ion to form the metal. Nitrogen gas produced is probably absorbed on the very large surface of the particles of the powder. The defect S is regenerated. Thus

$$N_3^- \overset{h\nu}{\rightleftarrows} N_3^{-*} \qquad (1)$$

$$2Li^+ + N_3^{-*} \; S \; N_3^{-*} \overset{\Delta}{\rightarrow} 2Li + 3N_2 + S \qquad (2)$$

The rate determining step is step (2) and the activation energy of 6,10 Kcal./mol. is associated with this step. As already stated, introducing water vapour at the end of the induction period causes a new induction period to appear but does not markedly alter the subsequent rate of decomposition. This indicates firstly that metal atoms are present at the end of the induction period and secondly that the water vapour does not affect the decomposition sites.

The lithium atoms formed in step (4) diffuse over the surface and, at a critical concentration, aggregate to form lithium metal nuclei with

all the associated electronic properties of a metal. The structure of a metal in a thin film has been shown to be identical to the bulk metal. The films, formed by lateral growth of nuclei, may become continuous at thicknesses as low as 5 nm. The character of the conductivity of such metal films corresponds very closely to that of the massive metal. Thus it will be possible for a very thin two-dimensional metal nucleus with the electronic properties of the bulk metal to form on the surface of the particles at discrete centres.

At the end of the induction period growth of the nuclei commences and the reaction accelerates. During this period reaction occurs at a rapidly expanding reactant/product interface and an increasing number of nuclei.

The acceleratory period has a rate which is dependent on the square of the light intensity. Thus a mechanism must be postulated involving the decomposition of two excited azide ions. Prout and Sears[74] in a study of the photolysis of lithium azide in the temperature range -60,0° - 20,0°C have found a dependence throughout this range on the square of the light intensity. They have proposed a mechanism which involves the bimolecular reaction between two excited ions each trapped at a different anion vacancy. ' The complex formed, viz. $[N_3 \square_2 N_3]^{-*}$, subsequently decomposes to yield two positive holes and two F-centes. The F-centres eventually aggregate, collapse and react with Li^+ ions to form lithium metal. It is not clear, however, to which specific period of the decomposition nor to which part of the temperature range studied this mechanism was applied. If it is assumed that in general lithium and sodium azides can be treated analogously then the mechanism postulated should preferably account for the formation of F-centres and F_2^+-centres both of which have been detected in sodium azide. The latter has also been observed in the photolysis of

potassium and barium azides.[47,61,62,70,190] Thus a mechanism can be proposed in which an excited azide ion reacts with an Li_n^+ ion, formed via the photoelectric effect, to produce Li_n and the positive hole N_3. A second excited azide ion would react with an adjacent ground state azide ion to produce nitrogen and, ultimately, F-centres. The positive hole decomposes to yield eventually, with a ground state azide ion, two molecules of nitrogen and an N_2^- ion.

However, there is no evidence for the formation of the N_2^- ion in the photolysis of lithium azide and, if anything, it is more likely to be produced at low temperatures where it has been detected in the case of sodium, potassium and barium azides. F- and F_2^+-centres have been observed in the photolysis of sodium azide and the former in the photolysis of virtually all inorganic azides. F_2^+-centres are, however, not stable at ambient temperature and are not postulated to form here. Hence, the following mechanism is proposed for the acceleratory reaction in the photolysis of lithium azide. Initially a ground state azide ion is excited by absorption of a photon. This excitation is an internal transition on the ion itself. If it is situated at an ideal lattice site it will revert to the ground state. If situated at a defect site, the excited ion will be stable and will then react with a lithium ion formed as a result of the photoelectric effect. A second singly excited azide ion reacts with a positive hole to form three molecules of nitrogen, two anion vacancies and an electron. Electrons are then trapped at single anion vacancies to form F-centres. These centres aggregate because of the increased stability thus obtained as a result of resonance of the electrons between identical defects. The aggregate collapses on reaching a critical size and the electrons thus produced react with lithium ions to form lithium atoms. Eventually metal nuclei form and these grow to the interface.

Hence the mechanism proposed is:

$$N_3 \overset{h\nu}{\rightleftharpoons} N_3^{-*} \quad (1)$$

$$Li_n \overset{h\nu}{\rightleftharpoons} Li_n^{+} + e \quad (2)$$

$$Li_n^{+} + N_3^{-*} \overset{\Delta}{\rightarrow} Li_n + N_3 \quad (3)$$

$$N_3 + N_3^{-*} \rightarrow 3N_2 + 2\square + e \quad (4)$$

$$\rightarrow 3N_2 + \boxed{\cdot} + \square \quad (5)$$

Collapse of the F-centres produces anion vacancies and electrons, the latter reacting as follows:

$$Li_n + Li_n^{+} + e \rightarrow Li_{n+1} \quad (6)$$

Step (3) is considered to be the rate determining step and has an activation energy of 4,2 Kcal./mol. associated with it. Similar mechanisms have been proposed by Prout and Shephard in the case of barium and strontium azides,[50] and by Jacobs *et al.* in the case of sodium azide[44] and in the present work in the case of calcium azide.

The importance of the metal nucleus during the acceleratory period has been illustrated by the experiments in which water vapour has been introduced on to the sample. Exposure to water vapour during this period caused the reaction to be destroyed and resulted in a new induction period slightly shorter than that for an uninterrupted decomposition. The rate constant of the subsequent reaction decreased. The destruction of the reaction implies the presence of metallic nuclei on the surfaces of particles. The new induction period implies that new nuclei had to form to enable the reaction to continue and the lowering of the rate constant is considered to be due to the removal of potential nuclei forming sites by the water vapour.

Interruptions at the inflection point and at positions further along the decomposition curve destroy any further reaction, thus indicating that no new growth nuclei are possible beyond this stage of the decomposition. Visual observations made indicate that all surfaces are very dark brown after the inflection point indicating that all particles are covered with a layer of lithium metal. Introduction of water vapour during the decay reaction causes lithium hydroxide to be formed. This is opaque to ultraviolet radiation and thus no new growth nuclei can be formed and the reaction ceases.

The decay reaction commences when the surface nuclei touch and the surfaces of the small particles are covered by reaction product. The value of n = 2 used during the acceleratory reaction in the application of the Avrami-Erofeyev equation has indicated that the growth centres of the metal are plate-like in nature advancing along the grain boundaries in which they were initiated. This results ultimately in a difference in molecular volume between product and reactant phases. The interface may then collapse leaving isolated blocks of material in which no nuclei are present. If each molecule in these isolated blocks has an equal probability for decomposition, then the rate of reaction is simply proportional to the amount of substance undecomposed. This is the topography associated with the unimolecular law which has been found to fit the decay reaction.

The activation energy for the decay period was 3,2 Kcal./mol. and the molecularity was two. These values are very similar or identical to the values obtained during the acceleratory period. Hence, the same mechanism as that proposed for the acceleratory reaction is postulated for the decay reaction. The evolution of nitrogen is decreased as a result of the gradual consumption of defects which are helpful to the reaction.

(iv.b) Photolysis in the temperature range 71,8° - 170,0°C

In this temperature range the activation energies for the induction, acceleratory and decay reactions were 11,50 Kcal./mol., 9,90 Kcal./mol. and 11,60 Kcal./mol. respectively. The rates of induction, acceleratory and decay reactions were linearly dependent on the light intensity.

The mathematical analyses, visual observations and the effect of the introduction of water vapour at various stages of the reaction were found to be analogous to the results obtained in the temperature range 24,6° - 71,8°C. It is consequently assumed that the topochemical decomposition in the higher temperature range is similar to that in the temperature range below 71,8°C.

The rate of the induction period changes at 71,8°C from a dependence on the square of the light intensity to a linear dependence on the light intensity. In order to account for this change as well as to account for the increase in the activation energy from 6,10 Kcal./mol. to 11,50 Kcal./mol. an alternative mechanism is proposed. The rate determining step is considered to be one in which an electron is transferred from an azide ion to a lithium ion. Sufficient thermal energy is available for this to take place. The resultant positive hole reacts with an excited azide ion to produce nitrogen and an electron. The electron then reacts with another lithium ion.

$$N_3^- \overset{h\nu}{\underset{\leftarrow}{\rightarrow}} N_3^{-*} \qquad (1)$$

$$Li^+ + N_3^- \overset{\Delta}{\rightarrow} Li + N_3 \qquad (2)$$

$$N_3^{-*} + N_3 \rightarrow 3N_2 + e \qquad (3)$$

$$Li^+ + e \rightarrow Li \quad . \qquad (4)$$

Step (2) is the rate determining step and has an activation energy of 11,50

Kcal./mol. associated with it. The mechanism is seen to be in accordance with the observed linear dependence of the rate on the light intensity.

The acceleratory reaction in this temperature range is also linearly dependent on the light intensity as opposed to the dependence on the square of the light intensity below 71,8 °C. This change in molecularity as well as the increase in activation energy from 4,20 Kcal./mol. to 9,90 Kcal./mol. necessitates a new mechanism. As in the induction period, sufficient thermal energy is considered to be available for the transfer of an electron from a ground state azide ion to an ion of lithium which has been formed via the photoelectric effect. The positive hole thus formed reacts with an excited azide ion to form three molecules of nitrogen, two anion vacancies and an electron. Eventually there is an aggregation and a subsequent collapse of F-centres at a critical concentration. Ultimately lithium metal nuclei form and grow to the interface.

$$N_3^- \overset{h\nu}{\underset{\leftarrow}{\rightarrow}} N_3^{-*} \qquad (1)$$

$$Li_n \overset{h\nu}{\underset{\leftarrow}{\rightarrow}} Li_n^+ + e \qquad (2)$$

$$Li_n^+ + N_3^- \overset{\Delta}{\rightarrow} Li + N_3 \qquad (3)$$

$$N_3 + N_3^{-*} \rightarrow 3N_2 + 2\square + e \qquad (4)$$

$$\rightarrow 3N_2 + \boxdot + \square \qquad (5)$$

$$\boxdot \rightarrow \square + e \qquad (6)$$

$$Li_n + Li^+ + e \rightarrow Li_{n+1} \qquad (7)$$

Step (3) is considered to be the rate determining step and has an activation energy of 9,90 Kcal./mol. associated with it. The mechanism is in accordance with the linear dependence of the rate on the light intensity.

The mechanism of photolytic decomposition during the decay reaction is considered to be the same as that occurring during the acceleratory reaction. The activation energy of 11,60 Kcal./mol. is very similar to that obtained during the acceleratory period and the dependence of the rate on the light intensity is also the same. This mechanism is the same as that proposed by Prout and Shephard for the photolysis of barium azide in a similar temperature range[50] and the same as that proposed for calcium azide in the present work in the range 60,0° - 95,0°C.

(iv.c) Photolysis in the temperature range -70,0° - -19,0°C

The photolysis of lithium azide powder in this temperature range has been found to have most of the characteristics that have already been seen to be associated with the photolysis of calcium, barium and strontium azides in this temperature range. The general mathematical analyses of the various parts of the photolytic decomposition are the same. The reciprocal of the duration of the induction period was taken as the rate constant for this part of the reaction. The acceleratory period was analyzed using the Avrami-Erofeyev equation with n = 2. The decay reaction was analyzed using the unimolecular decay law. In a comparative study of the photolysis of lithium azide by Prout and Sears[74] the acceleratory reaction was analyzed using the Avrami-Erofeyev equation with n = 3. Prout and Liddiard[169] in a study of the thermal decomposition of lithium azide also used the Avrami-Erofeyev equation with n = 3 to analyze the acceleratory reaction. The latter workers, however, in a study of the thermal decomposition of lithium azide pre-irradiated with γ-rays, X-rays and ultraviolet radiation, used in each case a value of n = 2. Attempts were made to analyze the acceleratory reaction using a value of n = 3 but the fit was not as good as with n = 2. This latter value implied therefore a two-dimensional

growth of nuclei from a fixed number of centres. In the photolytic study referred to above[74] the decay reaction was analyzed using the equation $\log \alpha = kt + c$. This effectively yields the same results as the unimolecular decay law. This law is based on the principle that the rate of a reaction is proportional to the amount of substance undecomposed whereas the above equation has as its basis the dependence of the rate on the amount of substance decomposed.

The activation energies for the induction, the acceleratory and the decay reactions for the photolysis of lithium azide in this temperature range are 3,14 Kcal./mol., 1,71 Kcal./mol. and 0,88 Kcal./mol. respectively. The molecularities for the same periods in the same temperature range are 1,71, 1,69 and 1,70 respectively.

The visual observations, the effect of filters and the effect of introducing water vapour during a decomposition were all similar to the observations made in the cases of calcium, barium and strontium azides in the same temperature range. The discussion of the topography of the photolytic decomposition for each period will therefore be the same as for the other azides.

The rate of the reaction during the induction period is dependent on the square of the light intensity and hence the mechanism postulated must involve either two singly excited azide ions or a single doubly excited ion. The rate determining step in the formation of nuclei at ambient temperatures involves the reaction between a complex containing two singly excited ions and a lithium ion and has an activation energy of 6,10 Kcal./mol. In the present temperature range the decreased value of the activation energy viz. 3,14 Kcal./mol. is thought to imply a reaction with a single doubly excited ion. Thus nuclear growth is proposed to occur according to the following mechanism:

$$N_3^- \overset{h\nu}{\rightleftarrows} N_3^{-*} \quad (1)$$

$$N_3^{-*} \overset{h\nu}{\rightleftarrows} N_3^{-**} \quad (2)$$

The doubly excited ion is trapped at a trapping site, such as an anion vacancy, together with a ground state azide ion. This complex then reacts with a lithium ion.

$$2Li^+ + N_3^- \, S \, N_3^{-**} \xrightarrow{\Delta} 2Li + 3N_2 + S \quad (3)$$

where S is a trapping site, probably an anion vacancy. Step (3) is the rate determining step and has an activation energy of 3,14 Kcal./mol. associated with it.

The acceleratory reaction also depends on the square of the light intensity. Both the molecularity and the activation energy for the acceleratory reaction in this temperature range are identical or very similar to the values obtained for calcium, barium and strontium azides in this temperature range. Prout and Sears[74] also found the rate to be dependent on the square of the light intensity and, in this temperature range, found the activation energy for the acceleratory reaction to be 0,82 Kcal./mol. The mechanism proposed by them has already been discussed in the previous section. It basically involves free radicals. The mechanism proposed here is similar to that already proposed earlier in the cases of barium, strontium and calcium azides. Initially an azide ion is excited and is trapped at a defect site S, such as an anion vacancy. Another singly excited ion, trapped at the same site, forms the complex $[N_3^{-*} \, S \, N_3^{-*}]$. This complex reacts with an Li_n^+ ion, formed via the photo-electric effect, to yield a lithium atom, two positive holes and an electron. The defect site is regenerated. If it is an anion vacancy it will form an F-centre with the electron produced. The two holes formed

react with two ground state azide ions to produce N_2^- ions and molecular nitrogen. The N_2^- ion has been detected in the photolysis of both sodium and potassium azides. The N_2^- ions react to a very small extent with N_3^- ions to yield the $N_2^0 - N_3^{2-}$ complex. The ion reacts mainly, however, with molecular nitrogen to yield more nitrogen and F-centres or F_2^+-centres. These reactions, involving the N_2^- ions, have been postulated in the case of calcium, barium and strontium azides. The F_2^+- and F-centres aggregate, reach a critical size and then collapse to produce electrons and anion vacancies. These electrons react with lithium ions to form lithium metal nuclei which grow to the interface. Thus the mechanism is:

$$N_3^- \overset{h\nu}{\rightleftarrows} N_3^{-*} \tag{1}$$

$$Li_n \overset{h\nu}{\rightleftarrows} Li_n^+ + e \tag{2}$$

$$Li_n^+ + N_3^{-*} \; S \; N_3^{-*} \overset{\Delta}{\rightarrow} Li_n + 2N_3 + e + S \tag{3}$$

$$2N_3 + 2N_3^- \rightarrow 2N_2^- + 4N_2 \tag{4}$$

$$N_2^- + N_3^- \rightleftarrows N_2^0 - N_3^{2-} \tag{5}$$

$$N_2^- + 2N_2 \rightarrow 3N_2 + 2\square + 2e \tag{6}$$

$$\rightarrow 3N_2 + 2\boxdot \tag{7}$$

$$\underline{\text{or}} \quad \rightarrow 3N_2 + \square\boxdot + e \tag{8}$$

$$\boxdot \rightarrow \square + e$$

$$\underline{\text{or}} \quad \square\boxdot \rightarrow 2\square + e \tag{9}$$

$$Li_n + Li^+ + e \rightarrow Li_{n+1} \tag{10}$$

The F-centre formed in step (7) and the F_2^+-centre formed in step (8)

are both relatively stable and will tend to aggregate as a result of the increased stablilty arising from resonance of the electron. Ultimately, however, they collapse to yield electrons which combine with the lithium ion as shown in step (10). Step (3) is considered to be the rate determining step and has an activation energy of 1,71 Kcal./mol. associated with it. The effects of introducing water vapour during photolysis and of filtering the ultraviolet radiation are identical to those observed at ambient temperatures and thus the discussion outlined in Secion 10 *(iv.a)* is equally applicable here.

The decay reaction is also dependent on the square of the light intensity and has an activation energy of 0,88 Kcal./mol. Prout and Sears[74] have obtained similar dependence on light intensity and an activation energy of 0,85 Kcal./mol. for this period. The values obtained in this work are identical or similar to those obtained for the acceleratory reaction and consequently the same mechanism is postulated.

(iv.d) Photolysis in the temperature range -19,0° - 17,0°C

The activation energies found for the photolysis of powdered lithium azide in this temperature range were 4,98 Kcal./mol., 4,25 Kcal./mol. and 5,44 Kcal./mol. for the induction, acceleratory and decay periods respectively. These values were very similar to the values of 6,1 Kcal./mol., 4,2 Kcal./mol. and 3,2 Kcal./mol. obtained for the same periods in the temperature range 24,6° - 71,8°C. The value of the molecularity of the induction, acceleratory and decay periods in the temperature ranges -19,0° - 17,0°C and 24,6° - 71,8°C was two throughout. In view of the marked similarities between the results obtained in these two temperature ranges and the similarities in the topochemistry as indicated by the use of the same equations in the mathematical analyses, it is proposed that the same mechanisms as postulated in Section 10 *(iv.a)* for the temperature range 24,8° - 71,6°C are also applicable in this temperature range.

B. PHOTOLYSIS OF PELLETED CALCIUM AZIDE

The photolysis of pelleted calcium azide was carried out in the temperature range 25,0° - 90,0°C. The pressure-time plots showed similar characteristics to those obtained for powdered samples. They were sigmoid in shape and showed distinctive induction, acceleratory and decay periods. During the induction period there was no measurable evolution of gas. The acceleratory period was analyzed using the Avrami-Erofeyev equation with n = 2 and the unimolecular law was used to analyze the decay period. The reproducibility obtained was not very good notwithstanding the use of different pelleting pressures.

The poor reproducibility is presumed to be a result of the randomness of the effects resulting from the pelleting process. When the powdered azide is pelleted large numbers of crystal defects are created. New high angle grain boundaries will also arise as a result of an accumulation of dislocations. Thus a pellet with a high concentration of point and line defects will result but the concentration of these defects will vary from pellet to pellet in a random manner. Thus the decomposition of the pellet, which is highly dependent on the concentration of defects will vary accordingly and hence the observed unsatisfactory reproducibility. The phenomenon of pellets exploding can be ascribed to a particularly high concentration of defects.

The mechanism whereby the calcium metal nuclei form during the induction period is presumed to be the same as that postulated for the powdered form in the temperature range 35,0° - 95,0°C. The metal nuclei form on the surface of the pellet at emergent grain boundaries and also along internal grain boundaries and dislocations in the pellet. The duration of the induction period is proportional to the time required for the calcium metal atoms, formed initially at the interatomic spacing of calcium azide, to

aggregate to calcium metal specks. The process of decomposition commences when azide ions, present at defect sites, become excited by the absorption of a photon. Visual observations made of the pellet during photolysis show the appearance of a brown colour at the end of the induction period. This is presumably an indication of the presence of calcium metal at the end of this period. Introducing water vapour on to the pellet at various stages of the induction period provided further evidence of this. The effect of water vapour introduced at the commencement of the induction period as well as half-way along this period had no effect on subsequent decomposition, indicating that no metal nuclei exist at these stages. Water vapour introduced at the end of the induction period, however, caused a new induction period to appear of duration almost equal to that of the original period. This phenomenon indicated the presence of calcium metal at the end of the induction period.

The acceleratory period was analyzed in the same way as in the case of the powdered form. A difference was observed in the position of the inflection point. In the case of the powder this point occurred at 0,35 and in the case of the pellet at 0,27. Two reasons can be proposed for this observation which implies that the decay reaction commences more rapidly in the pelleted form than in the powdered form. The decay reaction, as has been seen in the study of the powdered azide, commences when all the particles are covered on the surface with metallic calcium. Clearly the surface to volume ratio of pellets is small compared to that for powder and thus the time taken to cover the surface of the pellet with metallic nuclei will be considerably less than that observed in the case of powder. This time will represent a considerably smaller fraction of the time taken for complete decomposition to occur than in the case of powder. The other factor which can account for the rapid onset of the decay reaction is that, as a result of the pelleting process, there will be extreme disorganization of the

surfaces of the particles as they are pressed together, thus forming new "internal surfaces". These regions are considered to be likely zones for the formation of F-centres. In addition some F-centres will also form at the grain boundaries in the individual particles, and it is assumed that the concentration of centres in the new "internal surfaces" is very high. By postulating for pellets the same mechanism as that proposed for the acceleratory period of powdered calcium azide, it can be seen that a higher concentration of F-centres will lead to a more rapid formation of calcium atoms which then crystallize to form metal nuclei.

The decay reaction commences when the two-dimensional nuclei overlap and the product interface moves into the pellet obeying the unimolecular decay law. The pellet was observed to be black wherever visible. This was due to the layer of metal on the surface as was shown by experiments in which water vapour was introduced onto the sample during the decomposition. This caused the reaction to cease completely presumably as a result of the formation of calcium hydroxide which, being opaque to untraviolet light, causes photolysis to cease. Interruptions at values of α less than 0,27 caused a new, progressively longer, induction period to occur and in all cases the final pressure was lower than that of an uninterrupted run. This was probably due to hydrolysis of the azide.

As has already been outlined in the results section, both 'separate run' and split-run' techniques were used to determine the activation energies. The pressure at which the pellets were pressed was also varied in these studies. In the temperature range 25,0° - 50,0°C the activation energy of the induction period was 6,39 Kcal./mol. compared to a value of 7,78 Kcal./mol. for powdered calcium azide in the same temperature range. The activation energy for the acceleratory period in the 25,0° - 50,0°C range was 7,07 Kcal./mol. compared to 7,30 Kcal./mol. in the same temperature range for the powdered calcium azide. It would seem therefore that pelleting the

sample has little or no effect on the activation energy for the induction and acceleratory periods of the reaction although the poor reproducibility during the induction period necessitates the value for that region being treated with caution.

The average value of the activation energy for the decay period in the temperature range 25,0° - 60,0°C was approximately 13,5 Kcal./mol. and the average value in the temperature range 60,0° - 90,0°C was approximately 24 Kcal./mol. No marked differences could be detected in the values when the pelleting pressure changed from 1500 lb./sq.in. to 2000 lb./sq.in. The activation energy for the powdered form in the corresponding temperature ranges is 4,67 Kcal./mol. and 17,36 Kcal./mol. respectively. Prout and Shephard[50] in a comparable study of pelleted barium and strontium azides in these temperature ranges have noted similar trends in the activation energy of the decay period. They also observed a fairly marked increase in the activation energy with increased pelleting pressure.

The photolytic decomposition of pellets will occur in the bulk of the pellet and on the external surface. The particles comprising the pellet behave as if they were isolated particles. The increase observed in the activation energy on pelleting the sample may be due to the formation of pockets of nitrogen in the bulk of the pellet implying that energy is required for diffusion as well as for the relevant reaction.

In general therefore it is proposed that the same mechanism postulated for the photolysis of powdered calcium azide in the temperature range 35,0° - 95,0°C are applicable to the photolysis of pelleted calcium azide in the temperature range under discussion.

C. CO-IRRADIATED DECOMPOSITION OF CALCIUM AZIDE

(i) POWDER

A study of the co-irradiated decomposition of calcium azide powder produced results which resembled in the various ways the results obtained for the photolysis of powdered calcium azide at high temperature i.e. 60,0° - 95,0°C and those obtained for the purely thermal decomposition of powdered calcium azide. This particular study was carried out in the temperature range 110,0° - 140,0°C. The essential feature of this decomposition is the existence of a dark rate at all temperatures in the decomposition temperature range. This dark rate which is observed is basically a result of the phenomenon of pre-irradiation which means that, when the azide is irradiated prior to thermal decomposition, the latter occurs at an increased rate for reasons which have been explained in sections 5 and 6.

The co-irradiated decompositions were found to yield satisfactory reproducibility. The Avrami-Erofeyev equation with n = 2 was found to fit the acceleratory reaction as it had in the case of pure photolysis. The decay reaction also was analyzed in the same manner as in the case of pure photolysis i.e. the unimolecular law was used. The inflection point occurred at a slightly higher value than in the case of photolytic decompositions. Activation energies were determined at three different intensities. These results indicated clearly that the lower the intensity the closer the value of the activation energy approximated that for a purely thermal decomposition. For the induction period the activation energy of photolysis in the temperature range 60,0° - 95,0°C was 10,80 Kcal./mol. and the activation energy of thermal decomposition in the temperature range 110,0° - 140,0°C was approximately 20,0 Kcal./mol. The value obtained for co-irradiated

decompositions in the temperature range 110,0° - 140,0°C varied from 21,31 Kcal./mol. at an intensity of 7,0 units to 14,04 Kcal./mol. at an intensity of 17,5 units. The activation energy for the acceleratory reaction in photolysis in the temperature range 60,0° - 95,0°C is 12,52 Kcal./mol. and the corresponding value for thermal decomposition in the temperature range 110,0° - 140,0°C is approximately 26,70 Kcal./mol. The values for the co-irradiated decomposition in the temperature range 110,0° - 140,0°C varied from 24,01 Kcal./mol. at an intensity of 7,0 units to 23,18 Kcal./mol. at an intensity of 17,5 units. Similar trends occurred over the decay period where the activation energy for photolysis (60,0° - 95,0°C) was 17,36 Kcal./mol., for thermal decomposition (110,0° - 140,0°C) was 26,0 Kcal./mol. and for co-irradiated decomposition (110,0° - 140,0°C) was 27,51 Kcal./mol. (intensity 7,0 units) and 21,66 Kcal./mol. (intensity 17,5 units). From these results it can be concluded, as was done by Prout and Shephard[50], that two concurrent mechanisms are taking place during co-irradiation. As the intensity of the ultraviolet radiation decreases the thermal decomposition mechanism becomes dominant in the light of the activation energy trends. Conversely, as the intensity of ultraviolet radiation increases the photolytic mechanism tends to dominate. The mathematical analyses of the acceleratory reaction in the thermal decomposition made use of the Avrami-Erofeyev equation with n = 2 which had been used to analyze photolytic decomposition. Previous workers[137,168] had used the equation $(1-\alpha)^{1/3} = kt + c$ but the former equation was found to fit equally well. Therefore it was concluded that the topology of the reactions in thermal decomposition, photolysis and co-irradiation is the same in view of the fact that the same equation was used to analyze all three reactions. Similarly, the decay reaction was analyzed throughout using the unimolecular law.

As had been found in the photolysis of calcium azide in the temperature range 60,0° - 95,0°C, the rate of the induction, acceleratory and decay reactions were linearly dependent on the light intensity in the co-irradiated decomposition. This evidence serves to strengthen the proposal that the same mechanisms as those occurring during high temperature photolytic decomposition are taking place during co-irradiation together with thermal decomposition processes.

The percentage decomposition for co-irradiated photolytic and thermal decompositions were all very much the same. Many of the effects already observed in pre-irradiation studies[137,168] were characteristic of co-irradiated decomposition. These included a shortening of the induction period and an increase in the rate of the acceleratory and decay reactions.

Prout and Brown[137] have made a detailed study of the thermal decomposition - both unirradiated and pre-irradiated - of calcium azide. The process of formation of nuclei is observed to take place on the external surface and, to a lesser extent, within the crystal. Formation may be preferred at certain sites such as surface cracks or lines of strain where disorganization has taken place and where there is a higher thermodynamic instability and unsaturation of cohesive forces. They proposed that the induction period during thermal decomposition is really a slow decomposition in which nitrogen is slowly liberated, thus:

$$2N_3^- \overset{\Delta}{\rightarrow} 3N_2 + 2e \quad . \qquad (1)$$

The freed electrons combine with calcium ions to form calcium atoms which eventually aggregate to form metal specks with all the associated electronic properties of a metal.. Thus:

$$Ca^{2+} + 2e \rightarrow Ca \quad . \qquad (2)$$

Step (1) is considered to be the rate determining step. No measurable amount of nitrogen is seen to be evolved in view of the fact that it is absorbed on the powder. In a study of the thermal decomposition of calcium azide subsequent to pre-irradiation with ultraviolet radiation, the same workers observed that the shortening of the induction period following irradiation was a result of the effect of the aggregation at the surface of the vacancies which the radiation produces. These alter the surface topography and thus additional centres are created at which strained azide radicals will decompose. Therefore the time taken to reach the critical concentration of calcium atoms for aggregation to a metal nucleus will be shortened. The additional anion vacancies result in a larger number of surface clusters which are transformed to active growth nuclei by the capture of electrons.

The mechanism of nucleus formation during photolysis in the temperature range 60,0° - 95,0°C has been shown to involve, as the rate determining step, the thermal transfer of an electron from a ground state azide ion to a calcium metal ion, Ca^{2+}. The result of this reaction is the formation of a Ca^{+} ion and a positive hole, N_3. The latter then reacts with an adjacent singly excited azide ion to give three molecules of nitrogen and an electron. The freed electron then combines with the Ca^{+} ion to form calcium metal atoms. These atoms, formed in thin plates on the surface and moving down the core of the dislocation, aggregate to form calcium metal nuclei at the end of the induction period. This mechanism is consistent with the observed linear dependence of the rate on the light intensity. Both the thermal decomposition and photolytic decomposition mechanism are therefore seen to result eventually in the aggregation of calcium atoms to give calcium metal nuclei and both mechanisms are postulated to occur concurrently during co-irradiation.

It has been observed in the present study that the duration of the induction period during co-irradiation is much shorter that that during thermal decomposition. It is not clear, however, whether the increased rate is due to the more rapid appearance of reaction nuclei or whether an additional number of nuclei is formed by accumulation of photolytic products. In both cases the change in the decomposition velocity is due to the appearance in the initial substance of decomposition products which catalyze the process. For the same reasons the transition from induction period to acceleratory period is very much more dramatic in the case of co-irradiation than in the case of thermal decomposition.

In summary, therefore, the calcium metal nuclei formed at the end of the induction period are a result of separate thermal and photolytic mechanisms, although the end result is the same. The ultraviolet radiation has not changed the thermal effects, nor the temperature affected the photolytic processes. The two mechanisms are additive as shown by the relative activation energies of the photolytic, thermal and co-irradiated decompositions. The results of introducing water vapour have shown that at the end of the induction period calcium metal is present as also have the visual observations which were made. Thus two mechanisms are proposed to take place simultaneously during the induction period in the co-irradiated decomposition of powdered calcium azide.

(i) Photolytic:

$$N_3^- \overset{h\nu}{\rightleftarrows} N_3^{-*}$$

$$Ca^{2+} + N_3^- \overset{\Delta}{\rightarrow} Ca^+ + N_3$$

$$N_3 + N_3^{-*} \rightarrow 3N_2 + e$$

$$Ca^+ + e \rightarrow Ca$$

(ii) Thermal:

$$2N_3^- \overset{\Delta}{\rightarrow} 3N_2 + 2e$$

$$Ca^{2+} + 2e \rightarrow Ca \quad .$$

The acceleratory period commences when the metal nuclei are formed. In the purely thermal process[137] nitrogen is evolved by a mechanism in which an electron from the azide ion is elevated into the conduction band of the metal, followed by the reaction of a adjacent azide ion and the azide radical when the former receives sufficient thermal energy. As a result of this reaction nitrogen and F-centres are formed. The latter will aggregate as in the case of photolysis and eventually collapse to produce anion vacancies and electrons. The electrons react with Ca^{2+} ions to form calcium atoms which add on to the interface. The rate determining step is considered to be the first step i.e. transfer of an electron to the conduction band and has an activation energy of 26,70 Kcal./mol. associated with it. Water interruptions have illustrated the presence of calcium metal during this period and the effects are the same as those usually associated with photolysis studies.

Previous workers[137,168,57] have used a third power law in analyzing the acceleratory reaction in the thermal decomposition of calcium azide and have concluded that this implies the two-dimensional growth of nuclei increasing in number, linearly with time. In the present study the acceleratory reaction in the thermal decomposition was analyzed using the Avrami-Erofeyev equation with n = 2 which implies, most likely, a two-dimensional growth of nuclei increasing from a fixed number of centres. The third power law was also used[136] in the analysis of the acceleratory reaction in the thermal decomposition of calcium azide subsequent to ultraviolet radiation. Tompkins and Young[58] found that when pre-irradiated

material is decomposed above 97,0°C the cubic law ceased to apply and was replaced by a contracting envelope topochemistry. Prout and Moore[168] found that with higher doses of ultraviolet radiation the power law with n = 2 applied which represents the same topochemistry as the Avrami-Erofeyev equation with n = 2. The latter equation has also been used by Prout and Liddiard[169] in a study of the thermal decomposition of lithium azide subsequent to ultraviolet radiation. The present study thus seems to indicate that in the co-irradiated decomposition of calcium azide the predominant feature of the growth of nuclei is two-dimensional growth from a fixed number of nuclei. The irradiation effect is very pronounced since a high intensity light source is employed. Irrespective of the validity of the cubic or square laws in the thermal decomposition or pre-irradiation studies, the growth of these nuclei from fixed centres would swamp the latter effect and in general cause an acceleration of the decomposition and decrease the time required to reach the decay stage of the reaction. These growing centres are considered to by plate-like in nature advancing along the grain boundaries in which they were initiated.

The mechanism of photolytic decomposition in the temperature range 60,0° - 95,0°C has been seen to involve the thermal transfer of an electron from a ground state azide ion to a positively charged Ca^+ ion. The Ca^+ ion results from the metal nuclei formed at the end of the induction period being subjected to the photoelectric emission of an electron. Hence, calcium metal and a positive hole, N_3, are formed. This positive hole then reacts with an adjacent azide ion which has absorbed energy from a photon and three molecules of nitrogen, an F-centre and an anion vacancy are formed. Aggregation and subsequent collapse of the F-centres results in formation of calcium metal atoms which then add to the nucleus. The mechanism is consistent with the linear dependence of the rate on the light

intensity. The same dependence was found with the co-irradiated decomposition. The discussion pertaining to formation of excitons, excited azide ions or free holes and electrons as explained in photolysis is equally applicable here. The results of using filters are the same as in the case of photolytic decompositions although the decrease in rate is less dramatic because of the thermal effects at the higher temperature. Nevertheless it is clear that the most effective wavelengths during co-irradiation are in the 220 - 300 nm range. This precludes the possibility of electrons being excited to the conduction band or of excitons being formed. It is postulated therefore that, as in the case of the induction period, the mechanism of photolysis and thermal decomposition are taking place concurrently.

The mechanism proposed for thermal decomposition involves, as the rate determining step, the promotion of an electron from an azide ion into the conduction band of the metal nucleus requiring an activation energy of 26,7 Kcal./mol. The rate determing step in photolysis involves the thermal transfer of an electron from an azide ion to a Ca^+ ion, which has been formed via the photoelectric effect. This process requires 12,52 Kcal./mol. In either case the mechanism involves an azide ion losing an electron to form a positive hole. Ultimately, also, in either case the net result is the formation of calcium metal via either thermal ionization or thermal transfer. For a particular reactant - product topography at a particular temperature the measured rate is thus proportional to the concentration of positive holes. Two parallel reactions are responsible for the creation of this N_3 radical. Therefore the measured reaction rate of a co-irradiated decomposition at a particular temperature can be expressed as

$$R = R_T + R_{CO}$$

where

R_T = rate of decomposition if *thermal ionization* of an electron from a ground state azide ion into the conduction band of calcium metal nucleus occurs exclusively, and

R_{CO} = rate of decomposition if *thermal transfer* of an electron from a ground state azide ion to a Ca^+ ion occurs exclusively.

It has already been shown experimentally that the rate constant of the acceleratory period of a co-irradiated decomposition is proportional to the light intensity. It is necessary to examine the relationship between the experimental rate constant and the corresponding measured rate constant at a particular value of α.

In view of the similarities of the values of the activation energies for the acceleratory and decay reactions at a particular light intensity in co-irradiated and thermal decomposition, it can be assumed that the kinetic processes outlined for a co-irradiated decomposition occur both during the acceleratory and decay periods. Hence at a particular value of α greater than the value of the inflection point, the unimolecular law describes the rate of decomposition.

$$\text{i.e. } -\log(1-\alpha) = kt$$

$$\therefore \frac{d\alpha}{dt} = R = k(1-\alpha) \quad .$$

It is seen, therefore, that the rate of the reaction is proportional to the amount of undecomposed material. Thus the measured rate for a value of α in the decay stage is directly proportional to the experimental rate constant.

The rate constant was found to be linearly dependent on the light intensity throughout the co-irradiated decomposition. Hence the relationship between k and I is

$$k = a_1 I + c_1$$

and since R is proportional to k

$$R = a_2 I + c_2$$

where a_1, a_2, c_1 and c_2 are constants.

It has been seen that the overall rate of the reaction is the sum of the rates of two parallel reactions. Therefore

$$R_T + R_{CO} = a_2 I + c_2 .$$

Since at all light intensities, at constant temperature, R_T at a particular value of α is constant, the rate vs intensity relationship can then be rewritten as

$$R_{CO} = a_2 I + c_3 .$$

The above argument implies that the rate, at a particular value of α, of the reaction

$$N_3^- \overset{h\nu}{\underset{\leftarrow}{\rightarrow}} N_3^{-*}$$

$$\overset{N_3}{\rightarrow} 3N_2 + 2\square + e$$

$$\rightarrow 3N_2 + \boxdot + \square$$

is directly proportional to the light intensity. Thus it is seen that only one optical excitation process occurs before the reaction with the positive hole occurs. This is in agreement with the observed linear dependence of reaction rate on light intensity. The reaction mechanism during the acceleratory and decay periods are identical and thus it is to be expected that R_{CO}, at a particular value of α less than the value of the inflection point, is directly proportional to the light intensity.

The above mechanism is consistent with the observed behaviour of the Arrhenius activation energy for the acceleratory and decay reactions when

calcium azide is irradiated with ultraviolet light during thermal decomposition. The study of the photolytic decomposition in the temperature range 60,0° - 95,0°C has shown that the energy required for the reaction

$$Ca^{+} + N_3^{-} \overset{\Delta}{\rightarrow} Ca + N_3$$

is 12,52 Kcal./mol., while the energy required for the reaction

$$N_3^{-} \rightarrow N_3 + (\text{electron in conduction band of calcium metal nucleus}),$$

which takes place during thermal decomposition, is 26,70 Kcal./mol. Therefore the energy required for co-irradiation, during which both these reactions are occurring concurrently, should lie between 12,52 Kcal./mol. and 26,70 Kcal./mol. The observed activation energy of the co-irradiated decomposition was intensity dependent but varied from 23,0 - 24,0 Kcal./mol. Clearly the Arrhenius equation applying to parallel reactions of this type should be written

$$k_T + k_{CO} = A_T \exp(-\frac{E_T}{RT}) + A_{CO} \exp(-\frac{E_{CO}}{RT})$$

where the subscripts T and CO have their previous meanings provided that the rate constants are obtained from the same rate equation. As the light intensity increases, k_{CO} increases with respect to k_T and the measured activation energy of the parallel reactions should approach E_{CO}. This fact has been verified experimentally as has been shown by the values of the activation energy for co-irradiation at different intensities quoted at the beginning of this section.

Prout and Lownds[144], in a study of co-irradiated potassium permanganate, adopted a similar approach in explaining the decomposition process. The rate determining step of the thermal decomposition was

$$MnO_4^- \overset{\Delta}{\rightarrow} MnO_4^0 + e \qquad (1)$$

which had an activation energy of 39 Kcal./mol. The rate determining step in the photolysis of potassium permanganate at high temperatures, i.e. just below the range in which thermal decomposition occurred, was

$$(MnO_4^-)^{**} \overset{\Delta}{\rightarrow} MnO_4^0 + e \qquad (2)$$

which had an activation energy of 14 Kcal./mol. This mechanism involved the double excitation of an MnO_4^- ion whereas the co-irradiated decomposition was linearly dependent on light intensity. Thus the co-irradiated decomposition involved

$$MnO_4^- \overset{h\nu}{\rightarrow} (MnO_4^-)^* \overset{\Delta}{\rightarrow} MnO_4^0 + e \qquad (3)$$

Thus both reactions (1) and (3) were postulated to occur and the activation energy of reaction (3) was expected to lie within the range 14,0 - 39,0 Kcal./mol. The experimental values, dependent as in the case of calcium azide on the light intensity, were found to lie between 29,0 Kcal./mol. and 33,0 Kcal./mol.

Prout and Shephard[50], in a study of the co-irradiated decomposition of barium and strontium azides, also postulated mechanisms on the basis of a concurrently occurring photolytic and thermal process. In the case of both azides the rate determining step in the photolytic decomposition below the range in which thermal decomposition occurred was

$$M_n^+ + N_3^- \overset{\Delta}{\rightarrow} M_n + N_3 \qquad (4)$$

where M represents the relevant metal. The thermal decomposition process as postulated by other workers[168] has as its rate determining step

$$M + N_3^- \overset{\Delta}{\rightarrow} \text{(electron in conduction band of metal)} + N_3 \cdot \quad (5)$$

The activation energy associated with step (4) was approximately 11,5 Kcal./mol. for the two azides and that associated with step (5) was approximately 25,5 Kcal./mol. for each azide. The value expected for the co-irradiated decomposition, in which both steps were proposed to occur concurrently, was between these purely thermal and purely photolytic values. The activation energies obtained experimentally were again dependent on the light intensity and were in the region of 20,0 Kcal./mol.

In view of the similarity between the activation energies and dependence on light intensity for the acceleratory reaction and for the decay reaction in the co-irradiated decomposition at a fixed light intensity, the same mechanisms are postulated to occur during the decay period. Thus it is proposed that the following mechanism holds during the acceleratory and decay periods of co-irradiation:

(i) Photolytic:

$$N_3^- \overset{h\nu}{\underset{\leftarrow}{\rightarrow}} N_3^{-*} \quad (1)$$

$$Ca_n \overset{h\nu}{\underset{\leftarrow}{\rightarrow}} Ca_n^+ + e \quad (2)$$

$$Ca_n^+ + N_3^- \overset{\Delta}{\rightarrow} Ca_n + N_3 \quad (3)$$

$$N_3 + N_3^{-*} \rightarrow 3N_2 + 2\square + e \quad (4)$$

$$\rightarrow 3N_2 + \boxdot + \square \quad (5)$$

$$2\boxdot \rightarrow 2\square + 2e \quad (6)$$

$$Ca_n + Ca^{2+} + 2e \rightarrow Ca_{n+1} \quad (7)$$

(ii) Thermal:

$$N_3^- + Ca(metal) \overset{\Delta}{\rightarrow} N_3 + (electron\ in\ conduction\ band\ of\ calcium\ metal) \quad (8)$$

$$N_3 + N_3^- \rightarrow 3N_2 + 2\square + e \quad (9)$$

$$\rightarrow 3N_2 + \boxdot + \square \quad (10)$$

$$2\boxdot \rightarrow 2\square + 2e \quad (11)$$

$$Ca_n + Ca^{2+} + 2e \rightarrow Ca_{n+1} \quad (12)$$

The decay reaction was analyzed using the unimolecular decay law. This had also been used in the analyses of purely photolytic and thermal decompositions. Andreev[197] and Marke[194] in previous studies of the thermal decomposition of calcium azide had also used the unimolecular decay law. The use of this law implies that the extensive growth of plate-like nuclei has caused a difference in molecular volume between the product and reactant phases. This results in collapse of the interface leaving isolated blocks of material in which no nuclei are present. If each molecule in these isolated blocks has an equal probability for decomposition, then the rate of reaction is simply proportional to the amount of substance undecomposed. This situation is described by the unimolecular decay law.

Other workers[137,168] have used the contracting sphere equation in analyzing unirradiated or pre-irradiated thermal decomposition. This is due to the rapid efficient surface nucleation of the particles, causing them to become coated with a layer of product on the surface only. The decay reaction corresponds to the penetration of the continuous interface into the particles according to the contracting sphere equation. In the case of co-irradiation the high intensity light source used causes nuclei to form on the surface and on the planes of particles resulting in a different topochemistry.

Introducing water vapour on to the sample at various stages of co-irradiated decomposition has shown the same effects as were observed in the case of photolysis. At the end of the induction period and at values of α below the inflection point, the water vapour destroyed the metal nuclei which had formed on the surface by forming calcium hydroxide. The subsequent reaction involved a new induction period and a decrease in the rate of the acceleratory and decay reactions. The new reaction commences from nuclei in the bulk of the sample which have not been destroyed. The new induction period represents the time required for these nuclei to grow to critical size and the decreased acceleratory and decay rates are a result of the reaction commencing from relatively fewer centres.

Visual observations were also similar to those made in the case of photolysis. The sample was seen to darken gradually and beyond the inflection point was black on all surfaces. This was interpreted to indicate that all surfaces were covered with a metal layer. Introducing water vapour beyond the inflection point virtually destroyed any subsequent reaction presumably due to the formation of a coating of calcium hydroxide which is opaque. Any subsequent reaction, however small, which occurred is a result of thermal decomposition. In all cases of water interruptions the final pressure was less than that for an uninterrupted run as a result of the partial hydrolysis of the calcium azide.

(ii) PELLETS

The co-irradiated decomposition of pelleted calcium azide showed similar differences relative to photolyzed pellets as had been observed in the comparison of co-irradiated and photolyzed powdered calcium azide. The induction period shortened, the rate of the acceleratory and decay reactions increased considerably and a definite dark rate was observed. The decomposition curves were analyzed using the Avrami-Erofeyev equation with n = 2 for the acceleratory reaction and the unimolecular decay law for the decay reaction. These equations had been used in the photolytic decompositions of the powdered azide. Thus the topochemical aspects of the co-irradiated decomposition of pellets are identical to those of the powdered form.

The reproducibility obtained was not satisfactory. Hence a split-run method was used in an attempt to determine activation energies. This proved unsuccessful, however, since at temperatures greater than 105,0°C the pellets exploded. Moreover, in cases where the pellets remained intact, the dark rate was so great that the pellet decomposed thermally while attaining the desired temperature.

In general it is thought that the discussion pertaining to the photolytic decomposition of pelleted calcium azide also applies to the co-irradiated decomposition. It is probable that the same mechanisms proposed for the co-irradiated decomposition of powdered calcium azide are also applicable to the pelleted form.

11. SUMMARY OF RESULTS AND DISCUSSION

(i) PHOTOLYSIS OF AZIDES IN THE POWDERED FORM AT LOW AND AMBIENT TEMPERATURES

COMPOUND	BaN_6	SrN_6	CaN_6	LiN_3
Kinetic equations used for analyses	*(i) Induction Period* : The rate constant is the inverse of the duration of the induction period *(ii) Acceleratory Period:* Avrami-Erofeyev equation: $[-\log(1-\alpha)]^{\frac{1}{2}} = k_{acc}t + c$ *(iii) Decay Period* : Unimolecular law : $-\log(1-\alpha) = k_{decay}t + c.$			
Inflection Point α_i	0,32	0,43	0,38	0,43
Fit of Analyses	*(i) Acceleratory Period* $0,03 < \alpha < 0,32$ *(ii) Decay Period* $0,32 < \alpha < 0,90$	*(i) Acceleratory Period* $0,03 < \alpha < 0,43$ *(ii) Decay Period* $0,43 < \alpha < 0,95$	*(i) Acceleratory Period* $0,03 < \alpha < 0,38$ *(ii) Decay Period* $0,38 < \alpha < 0,88$	*(i) Acceleratory Period* $0,03 < \alpha < 0,43$ *(ii) Decay Period* $0,43 < \alpha < 0,96$
Activation Energies (Kcal./mol.)	*Temperature Range* *(i)* -70,0° - 17,0°C *Induction Period* 0,24 *Acceleratory Period* 0,82 *Decay Period* 0,97 *(ii)* 17,0° - 35,0°C *Induction Period* 6,48 *Acceleratory Period* 5,47 *Decay Period* 5,19	*Temperature Range* *(i)* -80,0° - -4,0°C *Induction Period* 2,38 *Acceleratory Period* 1,58 *Decay Period* 0,69 *(ii)* -4,0° - 32,0°C *Induction Period* 4,00 *Acceleratory Period* 3,73 *Decay Period* 3,96	*Temperature Range* *(i)* -70,0° - 7,0°C *Induction Period* 0,34 *Acceleratory Period* 0,56 *Decay Period* 0,42 *(ii)* 7,0° - 22,0°C *Induction Period* 5,70 *Acceleratory Period* 4,18 *Decay Period* 3,76	*Temperature Range* *(i)* -70,0° - -19,0°C *Induction Period* 3,14 *Acceleratory Period* 1,71 *Decay Period* 0,88 *(ii)* -19,0° - 17,0°C *Induction Period* 4,98 *Acceleratory Period* 4,25 *Decay Period* 5,44

Dependence on light intensity (m in the equation $k = I^m + c$)	*Temperature* *(i)* -21,0°C *Induction Period* 2,50 *Acceleratory Period* 2,02 *Decay Period* 1,69 *(ii)* 22,0°C *Induction Period* 1,99 *Acceleratory Period* 2,24 *Decay Period* 2,15	*Temperature* *(i)* -20,2°C *Induction Period* 0,75 *Acceleratory Period* 2,12 *Decay Period* 2,35 *(ii)* 18,2°C *Induction Period* 2,71 *Acceleratory Period* 2,22 *Decay Period* 1,69	*Temperature* *(i)* -20,5°C *Induction Period* 1,00 *Acceleratory Period* 2,23 *Decay Period* 2,00 *(ii)* 19,5°C *Induction Period* 1,21 *Acceleratory Period* 2,21 *Decay Period* 2,30	*Temperature* *(i)* -19,8°C *Induction Period* 1,71 *Acceleratory Period* 1,69 *Decay Period* 1,70 *(ii)* 30,0°C *Induction Period* 1,54 *Acceleratory Period* 1,81 *Decay Period* 1,86
Type of nuclei	Two-dimensional growth of plate-like nuclei increasing from a fixed number of centres. Marked overlap and ingestion of nuclei.	As for barium azide.	As for barium azide.	As for barium azide.
Mechanism *(i) Induction Period* (Formation of nuclei)	*Temperature Range* *(i)* -70,0° - 17,0°C $N_3^- \overset{h\nu}{\rightleftarrows} N_3^{-*}$ $N_3^{-*} \overset{h\nu}{\rightleftarrows} N_3^{-**}$ $Ba^{2+} + N_3^- S N_3^{-**} \overset{\Delta}{\rightarrow} Ba + 3N_2 + S$	*Temperature Range* *(i)* -80,0° - -4,0°C $N_3^- \overset{h\nu}{\rightleftarrows} N_3^{-*}$ $Sr^{2+} + N_3^- S N_3^{-*} \overset{\Delta}{\rightarrow} Sr + 3N_2 + S$	*Temperature Range* *(i)* -70,0° - 7,0°C $N_3^- \overset{h\nu}{\rightleftarrows} N_3^{-*}$ $N_3^- S N_3^{-*} \overset{\Delta}{\rightarrow} 2N_2^- + N_2 + S$ $2N_2^- \rightarrow 2N_2 + 2e$ $Ca^{2+} + 2e \rightarrow Ca$	*Temperature Range* *(i)* -70,0°C - -19,0°C $N_3^- \overset{h\nu}{\rightleftarrows} N_3^{-*}$ $N_3^{-*} \overset{h\nu}{\rightleftarrows} N_3^{-**}$ $2Li^+ + N_3^- S N_3^{-**} \overset{\Delta}{\rightarrow} 2Li + 3N_2 + S$

(i) Induction Period (Formation of nuclei) (cont.)	*(ii)* 17,0° - 35,0°C	*(ii)* -4,0° - 32,0°C	*(ii)* 7,0° - 22,0°C	*(ii)* -19,0° - 17,0°C
	$N_3^- \overset{h\nu}{\rightleftarrows} N_3^{-*}$	$N_3^- \overset{h\nu}{\rightleftarrows} N_3^{-*}$	$N_3^- \overset{h\nu}{\rightleftarrows} N_3^{-*}$	$N_3^- \overset{h\nu}{\rightleftarrows} N_3^{-*}$
	$Ba^{2+} + N_3^{-*} \; S \; N_3^{-*}$	$Sr^{2+} + N_3^{-*} \; S \; N_3^{-*}$	$Ca^{2+} + N_3^- \; S \; N_3^{-*}$	$2Li^+ + N_3^{-*} \; S \; N_3^{-*}$
	$\overset{\Delta}{\rightarrow} Ba + 3N_2 + S$	$\overset{\Delta}{\rightarrow} Sr + 3N_2 + S$	$\overset{\Delta}{\rightarrow} Ca + 3N_2 + S$	$\overset{\Delta}{\rightarrow} 2Li + 3N_2 + S$
(ii) Acceleratory Period (Growth of nuclei)	*Temperature Range* *(i)* -70,0° - 17,0°C	*Temperature Range* *(i)* -80,0° - -4,0°C	*Temperature Range* *(i)* -70,0° - 7,0°C	*Temperature Range* *(i)* -70,0° - -19,0°C
	$N_3^- \overset{h\nu}{\rightleftarrows} N_3^{-*}$	$N_3^- \overset{h\nu}{\rightleftarrows} N_3^{-*}$	$N_3^- \overset{h\nu}{\rightleftarrows} N_3^{-*}$	$N_3^- \overset{h\nu}{\rightleftarrows} N_3^{-*}$
	$Ba_n \overset{h\nu}{\rightleftarrows} Ba_n^+ + e$	$Sr_n \overset{h\nu}{\rightleftarrows} Sr_n^+ + e$	$Ca_n \overset{h\nu}{\rightleftarrows} Ca_n^+ + e$	$Li_n \overset{h\nu}{\rightleftarrows} Li_n^+ + e$
	$Ba_n^+ + N_3^{-*} \; S \; N_3^{-*}$	$Sr_n^+ + N_3^{-*} \; S \; N_3^{-*}$	$Ca_n^+ + N_3^{-*} \; S \; N_3^{-*}$	$Li_n^+ + N_3^{-*} \; S \; N_3^{-*}$
	$\overset{\Delta}{\rightarrow} Ba_n + 2N_3 + e + S$	$\overset{\Delta}{\rightarrow} Sr_n + 2N_3 + e + S$	$\overset{\Delta}{\rightarrow} Ca_n + 2N_3 + e + S$	$\overset{\Delta}{\rightarrow} Li_n + 2N_3 + e + S$
	$2N_3 + 2N_3^- \rightarrow 2N_2^- + 4N_2$	$2N_3 + 2N_3^- \rightarrow 2N_2^- + 4N_2$	$2N_3 + 2N_3^- \rightarrow 2N_2^- + 4N_2$	$2N_3 + 2N_3^- \rightarrow 2N_2^- + 4N_2$
	$N_2^- + N_3^- \overset{\rightarrow}{\leftarrow} N_2^0 - N_3^{2-}$	$N_2^- + N_3^- \overset{\rightarrow}{\leftarrow} N_2^0 - N_3^{2-}$	$N_2^- + N_3^- \overset{\rightarrow}{\leftarrow} N_2^0 - N_3^{2-}$	$N_2^- + N_3^- \overset{\rightarrow}{\leftarrow} N_2^0 - N_3^{2-}$
	$N_2^- + 2N_2 \rightarrow 3N_2 + \square + e$	$N_2^- + 2N_2 \rightarrow 3N_2 + \square + e$	$N_2^- + 2N_2 \rightarrow 3N_2 + \square + e$	$N_2^- + 2N_2 \rightarrow 3N_2 + 2\square + 2e$
	$\rightarrow 3N_2 + \boxdot$	$\rightarrow 3N_2 + \boxdot$	$\rightarrow 3N_2 + \boxdot$	$\rightarrow 3N_2 + 2\boxdot$
				or $\rightarrow 3N_2 + \boxdot\boxdot + e$
	$2\boxdot \rightarrow 2\square + 2e$	$2\boxdot \rightarrow 2\square + 2e$	$2\boxdot \rightarrow 2\square + 2e$	$\boxdot \rightarrow \square + e$
				or $\boxdot\boxdot \rightarrow 2\square + e$
	$Ba_n + Ba^{2+} + 2e \rightarrow Ba_{n+1}$	$Sr_n + Sr^{2+} + 2e \rightarrow Sr_{n+1}$	$Ca_n + Ca^{2+} + 2e \rightarrow Ca_{n+1}$	$Li_n + Li^+ + e \rightarrow Li_{n+1}$

(ii) Acceleratory Period (Growth of nuclei) (cont.)	*(ii)* 17,0° - 35,0°C $N_3^- \overset{h\nu}{\underset{}{\rightleftarrows}} N_3^{-*}$ $Ba_n \overset{h\nu}{\rightleftarrows} Ba_n^+ + e$ $Ba_n^+ + N_3^{-*} \overset{\Delta}{\rightarrow} Ba_n + N_3$ $N_3 + N_3^{-*} \rightarrow 3N_2 + 2\square + e$ $\rightarrow 3N_2 + \boxdot + \square$ $2\boxdot \rightarrow 2\square + 2e$ $Ba_n + Ba^{2+} + 2e \rightarrow Ba_{n+1}$	*(ii)* -4,0° - 32,0°C $N_3^- \overset{h\nu}{\underset{}{\rightleftarrows}} N_3^{-*}$ $Sr_n \overset{h\nu}{\rightleftarrows} Sr_n^+ + e$ either $N_3^{-*} \overset{h\nu}{\rightleftarrows} N_3^{-**}$ or $N_3^{-*} + N_3^{-*} \rightleftarrows N_3^{-**} + N_3^-$ $Sr_n^+ + N_3^{-**} \overset{\Delta}{\rightarrow} Sr_n + N_3^*$ $N_3^* + N_3^- \rightarrow 3N_2 + 2\square + e$ $\rightarrow 3N_2 + \boxdot + \square$ $2\boxdot \rightarrow 2\square + 2e$ $Sr_n + Sr^{2+} + 2e \rightarrow Sr_{n+1}$	*(ii)* 7,0° - 22,0°C $N_3^- \overset{h\nu}{\underset{}{\rightleftarrows}} N_3^{-*}$ $Ca_n \overset{h\nu}{\rightleftarrows} Ca_n^+ + e$ $Ca_n^+ + N_3^{-*} \overset{\Delta}{\rightarrow} Ca_n + N_3$ $N_3 + N_3^{-*} \rightarrow 3N_2 + 2\square + e$ $\rightarrow 3N_2 + \boxdot + \square$ $2\boxdot \rightarrow 2\square + 2e$ $Ca_n + Ca^{2+} + 2e \rightarrow Ca_{n+1}$	*(ii)* -19,0° - 17,0°C $N_3^- \overset{h\nu}{\underset{}{\rightleftarrows}} N_3^{-*}$ $Li_n \overset{h\nu}{\rightleftarrows} Li_n^+ + e$ $Li_n^+ + N_3^{-*} \overset{\Delta}{\rightarrow} Li_n + N_3$ $N_3 + N_3^{-*} \rightarrow 3N_2 + 2\square + e$ $\rightarrow 3N_2 + \boxdot + \square$ or $\rightarrow 3N_2 + \square\boxdot$ $\boxdot \rightarrow \square + e$ or $\square\boxdot \rightarrow 2\square + e$ $Li_n + Li^+ + e \rightarrow Li_{n+1}$
(iii) Decay Period	*Temperature Range* *(i)* -70,0° - 17,0°C A continuation of the reaction occurring during the acceleratory period. *(ii)* 17,0° - 35,0°C A continuation of the reaction occurring during the acceleratory period.	*Temperature Range* *(i)* -80,0° - -4,0°C A continuation of the reaction occurring during the acceleratory period. *(ii)* -4,0° - 32,0°C A continuation of the reaction occurring during the acceleratory period.	*Temperature Range* *(i)* -70,0° - 7,0°C A continuation of the reaction occurring during the acceleratory period. *(ii)* 7,0° - 22,0°C A continuation of the reaction occurring during the acceleratory period.	*Temperature Range* *(i)* -70,0° - -19,0°C A continuation of the reaction occurring during the acceleratory period. *(ii)* -19,0° - 17,0°C A continuation of the reaction occurring during the acceleratory period.

(ii) PHOTOLYSIS OF AZIDES IN THE POWDERED FORM AT AMBIENT AND HIGHER TEMPERATURES

COMPOUND	CaN_6	LiN_3
Kinetic equations used for analyses	*(i) Induction Period* : The rate constant is the inverse of the duration of the induction period *(ii) Acceleratory Period:* Arvami-Erofeyev equation: $[-\log(1-\alpha)]^{\frac{1}{2}} = k_{acc}t + c$ *(iii) Decay Period* : Unimolecular law : $-\log(1-\alpha) = k_{decay}t + c$	
Inflection Point α_i	0,35	0,25
For of analyses	*(i) Acceleratory Period* $0,01 < \alpha < 0,35$ *(ii) Decay Period* $0,35 < \alpha < 0,90$	*(i) Acceleratory Period* $0,01 < \alpha < 0,25$ *(ii) Decay Period* $0,25 < \alpha < 0,90$
Activation Energies (Kcal./mol.)	*Temperature Range* *(i)* 35,0° - 60,0°C *Induction Period* 7,78 *Acceleratory Period* 7,30 *Decay Period* 4,67 *(ii)* 60,0° - 95,0°C *Induction Period* 10,80 *Acceleratory Period* 12,52 *Decay Period* 17,36	*Temperature Range* *(i)* 24,6° - 71,8°C *Induction Period* 6,10 *Acceleratory Period* 4,20 *Decay Period* 3,20 *(ii)* 71,8° - 170,0°C *Induction Period* 11,50 *Acceleratory Period* 9,90 *Decay Period* 11,60

Dependence on light intensity (m in the equation $k = I^m + c$)	*Temperature* *(i)* 55,0°C *Induction Period* 1,46 *Acceleratory Period* 1,70 *Decay Period* 2,00 *(ii)* 90,0°C *Induction Period* 0,99 *Acceleratory Period* 0,84 *Decay Period* 0,90	*Temperature* *(i)* 30,0°C *Induction Period* 1,54 *Acceleratory Period* 1,81 *Decay Period* 1,86 *(ii)* 127,0°C *Induction Period* 1,14 *Acceleratory Period* 1,14 *Decay Period* 1,18
Type of nuclei	Two-dimensional growth of plate-like nuclei, increasing from a fixed number of centres. Marked overlap and ingestion of nuclei.	As for calcium azide.
Mechanism *(i) Induction Period* (Formation of nuclei)	*Temperature Range* *(i)* 35,0° - 60,0°C $N_3^- \overset{h\nu}{\rightleftarrows} N_3^{-*}$ $Ca^{2+} + N_3^- S N_3^{-*} \overset{\Delta}{\rightarrow} Ca + 3N_2 + S$ *(ii)* 60,0° - 95,0°C $N_3^- \overset{h\nu}{\rightleftarrows} N_3^{-*}$ $Ca^{2+} + N_3^- \overset{\Delta}{\rightarrow} Ca^+ + N_3$	*Temperature Range* *(i)* 24,6° - 71,8°C $N_3^- \overset{h\nu}{\rightleftarrows} N_3^{-*}$ $2Li^+ + N_3^{-*} S N_3^{-*} \overset{\Delta}{\rightarrow} 2Li + 3N_2 + S$ *(ii)* 71,8° - 170,0°C $N_3^- \overset{\nu}{\rightleftarrows} N_3^{-*}$ $Li^+ + N_3^- \overset{\Delta}{\rightarrow} Li + N_3$

(i) Induction Period (Formation of nuclei) (cont.)	$N_3 + N_3^{-*} \rightarrow 3N_2 + e$ $Ca^+ + e \rightarrow Ca$	$N_3^{-*} + N_3 \rightarrow 3N_2 + e$ $Li^+ + e \rightarrow Li$
(ii) Acceleratory Period (Growth of nuclei)	*Temperature Range* *(i)* 35,0°-60,0°C $N_3^- \overset{h\nu}{\underset{\leftarrow}{\rightarrow}} N_3^{-*}$ $Ca_n \overset{h\nu}{\underset{\leftarrow}{\rightarrow}} Ca_n^+ + e$ $Ca_n^+ + N_3^{-*} \overset{\Delta}{\rightarrow} Ca_n + N_3$ $N_3 + N_3^{-*} \rightarrow 3N_2 + 2\square + e$ $\rightarrow 3N_2 + \boxdot + \square$ $2\boxdot \rightarrow 2\square + 2e$ $Ca_n + Ca^{2+} + 2e \rightarrow Ca_{n+1}$. *(ii)* 60,0° - 95,0°C $N_3^- \overset{h\nu}{\underset{\leftarrow}{\rightarrow}} N_3^{-*}$ $Ca_n \overset{h\nu}{\underset{\leftarrow}{\rightarrow}} Ca_n^+ + e$ $Ca_n^+ + N_3^- \overset{\Delta}{\rightarrow} Ca_n + N_3$	*Temperature Range* *(i)* 24,6° - 71,8°C $N_3^- \overset{h\nu}{\underset{\leftarrow}{\rightarrow}} N_3^{-*}$ $Li_n \overset{h\nu}{\underset{\leftarrow}{\rightarrow}} Li_n^+ + e$ $Li_n^+ + N_3^{-*} \overset{\Delta}{\rightarrow} Li_n + N_3$ $N_3 + N_3^{-*} \rightarrow 3N_2 + 2\square + e$ $\rightarrow 3N_2 + \boxdot + \square$ $\boxdot \rightarrow \square + e$ $Li_n + Li^+ + e \rightarrow Li_{n+1}$ *(ii)* 71,8° - 170,0°C $N_3^- \overset{h\nu}{\underset{\leftarrow}{\rightarrow}} N_3^{-*}$ $Li_n \overset{h\nu}{\underset{\leftarrow}{\rightarrow}} Li_n^+ + e$ $Li_n^+ + N_3^- \overset{\Delta}{\rightarrow} Li + N_3$

(ii) Acceleratory Period (Growth of nuclei) (cont.)	$N_3 + N_3^{-*} \rightarrow 3N_2 + 2\,\square + e$ $\rightarrow 3N_2 + \boxdot + \square$ $2\,\boxdot \rightarrow 2\,\square + 2e$ $Ca_n + Ca^{2+} + 2e \rightarrow Ca_{n+1}$	$N_3 + N_3^{-*} \rightarrow 3N_2 + 2\,\square + e$ $\rightarrow 3N_2 + 2\,\boxdot + \square$ $\boxdot \rightarrow \square + e$ $Li_n + Li^+ + e \rightarrow Li_{n+1}$
(iii) Decay Period	*Temperature Range* *(i)* 35,0° - 60,0°C A continuation of the reaction occurring during the acceleratory period. *(ii)* 60,0° - 95,0°C A continuation of the reaction occurring during the acceleratory period.	*Temperature Range* *(i)* 24,6° - 71,8°C A continuation of the reaction occurring during the acceleratory period. *(ii)* 71,8° - 170,0°C A contiuation of the reaction occurring during the acceleratory period.

(iii) CO-IRRADIATED DECOMPOSITION OF CALCIUM AZIDE | PHOTOLYSIS OF CALCIUM AZIDE

FORM	POWDERED CaN_6	PELLETED CaN_6	PELLETED CaN_6
Kinetic equations used for analysis	*(i) Induction Period* : The rate constant is the inverse of the duration of the induction period *(ii) Acceleratory Period:* Avrami-Erofeyev equation: $[-\log(1-\alpha)]^{\frac{1}{2}} = k_{acc}t + c$ *(iii) Decay Period* : Unimolecular law : $-\log(1-\alpha) = k_{decay}t + c$		
Inflection Point α_i	0,52	0,44	0,27
Fit of analyses	*(i) Acceleratory Period* $0,05 < \alpha < 0,52$ *(ii) Decay Period* $0,52 < \alpha < 0,95$	*(i) Acceleratory Period* $0,02 < \alpha < 0,44$ *(ii) Decay Period* $0,44 < \alpha < 0,93$	*(i) Acceleratory Period* $0,01 < \alpha < 0,27$ *(ii) Decay Period* $0,27 < \alpha < 0,90$
Activation Energies (Kcal./mol.)	*Temperature Range* 110,0° - 140,0°C *(i)* Intensity 7,0 units *Induction Period* 21,31 *Acceleratory Period* 24,01 *Decay Period* 27,51	*Temperature Range* > 100,0°C *Induction Period* - *Acceleratory Period* - *Decay Period* -	*Temperature Range* *(i)* 25,0° - 50,0°C Pelleting pressure 1500 lb./sq.in. *Induction Period* 6,39 *Acceleratory Period* 7,07 *Decay Period* 12,11

	(ii) Intensity 11,5 units *Induction Period* 20,65 *Acceleratory Period* 22,64 *Decay Period* 25,60 *(iii)* Intensity 17,5 units *Induction Period* 14,04 *Acceleratory Period* 23,18 *Decay Period* 21,66		*(ii)* 30,0° - 60,0°C Pelleting pressure 1500 lb./sq.in. *Decay Period (30,0 units)* 12,87 *Decay Period (41,0 units)* 15,34 Pelleting pressure 2000 lb./sq.in. *Decay Period (41,0 units)* 12,25 *(iii)* 60,0° - 90,0°C Pelleting pressure 1500 lb./sq.in. *Decay Period (30,0 units)* 22,75 *Decay Period (12,0 units)* 26,06 Pelleting pressure 2000 lb./sq.in. *Decay Period (15,0 units)* 22,75
Dependence on light intensity (m in the equation $k = I^m + c$)	*Temperature* 115,0°C *Induction Period* 0,61 *Acceleratory Period* 1,02 *Decay Period* 1,07	-	-
Type of nuclei	Two-dimensional growth of plate-like nuclei, increasing from a fixed number of centres. Marked overlap and ingestion of nuclei.	(i) Probably as for co-irradiated calcium azide powder. (ii) The mechanism for co-irradiated decomposition of pelleted calcium azide is probably as for the powder as outlined below.	As for powdered calcium azide.

Mechanism	*Temperature Range* 110,0° - 140,0°C	
(i) Induction Period (Formation of nuclei)	The following two processes occur concurrently: *(i)* $2N_3^- \overset{\Delta}{\rightarrow} 2N_3 + 2e$ $Ca^{2+} + 2e \rightarrow Ca$	*(ii)* $N_3^- \overset{h\nu}{\rightleftarrows} N_3^{-*}$ $Ca^{2+} + N_3^- \overset{\Delta}{\rightarrow} Ca^+ + N_3$ $N_3 + N_3^{-*} \rightarrow 3N_2 + e$ $Ca^+ + e \rightarrow Ca$
(ii) Acceleratory Period (Growth of nuclei)	*(i)* N_3^- + Ca(metal) $\overset{\Delta}{\rightarrow}$ N_3 + electron in the conduction band of calcium metal. $N_3 + N_3^- \rightarrow 3N_2 + 2\square + e$ $\rightarrow 3N_2 + \boxdot + \square$ $2\boxdot \rightarrow 2\square + 2e$ $Ca_n + Ca^{2+} + 2e \rightarrow Ca_{n+1}$	*(ii)* $N_3^- \overset{h\nu}{\rightleftarrows} N_3^{-*}$ $Ca_n \overset{h\nu}{\rightleftarrows} Ca_n^+ + e$ $Ca_n^+ + N_3^- \overset{\Delta}{\rightarrow} Ca_n + N_3$ $N_3 + N_3^{-*} \rightarrow 3N_2 + 2\square + e$ $\rightarrow 3N_2 + \boxdot + \square$ $2\boxdot \rightarrow 2\square + 2e$ $Ca_n + Ca^{2+} + 2e \rightarrow Ca_{n+1}$
(iii) Decay Period	A continuation of the reactions occurring during the acceleratory period.	

Assumed to be the same as that occurring during the corresponding reactions of photolysed powder.

(iv) THERMAL DECOMPOSITION OF AZIDES

COMPOUND	CaN_6	LiN_3[174]
Kinetic equations used for analyses	*(i) Induction Period* : The rate constant is the inverse of the duration of the induction period *(ii) Acceleratory Period:* Avrami-Erofeyev equation: $[-\log(1-\alpha)]^{\frac{1}{2}} = k_{acc}t + c$ *(iii) Decay Period* : Unimolecular law: $-\log(1-\alpha) = k_{decay}t + c$	*(i) Induction Period* : The rate constant is the inverse of the duration of the induction period *(ii) Acceleratory Period:* Avrami-Erofeyev equation: $[-\log(1-\alpha)]^{1/3} = k_{acc}t + c$ *(iii) Decay Period* : Contracting sphere equation: $1-(1-\alpha)^{1/3} = k_{decay}t$
Inflection point α_i	0,40	0,50
Fit of analyses	*(i) Acceleratory Period* $0,05 < \alpha < 0,40$ *(ii) Decay Period* $0,40 < \alpha < 0,95$	*(i) Acceleratory Period* $0,02 < \alpha < 0,50$ *(ii) Decay Period* $0,50 < \alpha < 0,95$
Activation Energies (Kcal./mol.)	*Temperature Range* *(i)* 100,0° - 126,8°C (Fresh material) *Induction Period* 21,70 *Acceleratory Period* 27,30 *Decay Period* 26,16	*Temperature Range* *(i)* 185,0° - 205,0°C *Induction Period* 21,0 *Acceleratory Period* 28,0 *Decay Period* 29,0

Activation Energies (Kcal/mol) (cont.)	*(ii)* 110,0° - 137,2°C (Aged material) *Induction Period* 18,94 *Accelerator Period* 25,94 *Decay Period* 25,10	—

12 COMPARATIVE DISCUSSION OF THE PHOTOLYTIC, CO-IRRADIATED AND THERMAL DECOMPOSITION OF CALCIUM, BARIUM, STRONTIUM AND LITHIUM AZIDES

In Table 47 the values of the activation energies and the molecularities in the photolytic, co-irradiated and thermal decomposition of calcium, barium, strontium and lithium azides obtained in both the present work and by previous workers are listed. The values for photolytic and co-irradiated decomposition are of particular interest because they have been obtained using ultraviolet sources of extremely high intensity causing, in most instances, remarkably high percentage decompositions.

A study of the activation energies reveals that these values increase with increasing temperature. In various temperature ranges different mechanisms are proposed to occur. In all four azides the first transition in activation energy occurs in the region of 0°C and the second in the region of 60°C. At the same time the dependence of the rate of the reaction on the light intensity (molecularity) changes, in general, from 2 at lower temperatures to 1 at higher temperatures. This implies that at higher temperatures mechanisms involving singly excited azide ions together with increased activation energies are applicable to the process of photolytic decomposition. In virtually all cases the values of molecularity and activation energy obtained for the acceleratory and decay reactions were identical or similar and hence the same mechanisms are thought to be operative during these two periods.

The pressure-time curves were sigmoid in shape in all temperature ranges. Each curve showed a distinct induction period during which there was no measurable evolution of gas. This was followed by an acceleratory and decay period. The inverse of the duration of the induction period was taken as a measure of the rate of reaction during this period. The

acceleratory reaction was in all cases analysed using the Avrami-Erofeyev equation with n = 2 and the decay reaction was analysed using the unimolecular law. This implies that during photolysis of all four azides the nuclei are plate-like in nature growing two-dimensionally from a fixed number of centres. There is marked overlap and ingestion of nuclei. During the induction period atoms form on the surface and on the planes of of the crystal, each plane starting at the surface at an emergent grain boundary. Eventually nuclei form by aggregation at the end of this period.

A comparison of the values obtained for the azides of the alkaline-earth elements with those of the azides of monovalent lithium do not indicate that the mechanisms of photolysis are related to the charge or nature of the cation. All four compounds are, however, large band gap azides. Moreover there appears to be no correlation between the process of photolytic decomposition and crystal structure. Calcium and strontium azides have identical structures (orthorhombic, F ddd, D_{2h}^{24}) and barium and lithium azides are both monoclinic. No similar correlations exist in the corresponding values of activation energy and molecularity. These crystal structures are, however, not very different from each other and they may account for the general overall similarities of activation energies and molecularities.

Co-irradiation studies yielded activation energies which were greater than those obtained for photolysis in the higher temperature ranges but less than those obtained during a purely thermal decomposition. This implied that during co-irradiation two parallel mechanisms were taking place - one photolytic and one thermal.

Therefore it can be concluded that a large number of similarities are observed when calcium, barium, strontium and lithium azides are photolyzed using sources of high intensity ultraviolet light and, in general, similar

mechanisms of photolytic and co-irradiated decomposition are postulated for all these azides in a particular temperature range.

Table 47. Activation energies and molecularities for all four azides

Compound			Calcium Azide	Barium Azide	Strontium Azide	Lithium Azide
Photolysis	Activation Energy (Kcal./mol.)					
	(i) Low Temperature	*Induction Period*	0,3	0,2	2,4	3,1
		Acceleratory Period	0,6	0,8	1,6	1,7
		Decay Period	0,4	1,0	0,7	0,9
	(ii) Ambient Temperature	*Induction Period*	7,8	$6,2^{50}$	$2,6^{50}$	6,1
		Acceleratory Period	7,3	7,6	3,2	4,2
		Decay Period	4,7	6,6	5,7	3,2
	(iii) High Temperature	*Induction Period*	10,8	$11,4^{50}$	$6,5^{50}$	11,5
		Acceleratory Period	12,5	11,3	12,9	9,9
		Decay Period	17,4	12,9	12,9	11,6
	Dependence on Light Intensity					
	(i) Low Temperature	*Induction Period*	1,0	2,5	0,7	1,7
		Acceleratory Period	2,2	2,0	2,1	1,7
		Decay Period	2,0	1,7	2,3	1,7

Photolysis (cont.)	*(ii) Ambient Temperature*	*Induction Period*	1,2	0,7[50]/2,0	2,0[50]	1,5
		Acceleratory Period	2,2	2,0	2,3	1,8
		Decay Period	2,3	2,1	1,9	1,9
	(iii) High Temperatures	*Induction Period*	1,0	0,6[50]	1,6[50]	1,1
		Acceleratory Period	0,8	1,0	1,8	1,1
		Decay Period	0,9	1,2	1,9	1,2
Co-irradiation	Activation Energy (Kcal./mol.)	*Induction Period*	14,0	16,5[50]	15,4[50]	-
		Acceleratory Period	23,2	19,2	18,8	-
		Decay Period	21,2	15,6	20,9	-
	Dependence on Light Intensity	*Induction Period*	0,6	0,7[50]	0,8[50]	-
		Acceleratory Period	1,0	0,7	0,6	-
		Decay Period	1,1	0,7	0,8	-
Thermal Decomposition	Activation Energy (Kcal./mol.)	*Induction Period*	21,7	26,5[115]	23,0[199]	21,0[174]
		Acceleratory Period	27,3	26,8	25,0	28,0
		Decay Period	26,2	26,1	21,7	29,0

Percentage Decomposition	*(i) Photolysis*	*(i) Low Temperature*	62%	85%	58%	57%
		(ii) Ambient Temperature	90%	95%[50]	71%[50]	78%
	(ii) Co-irradiation		91%	95%[50]	71%[50]	-
	(iii) Thermal Decomposition		90%	93%[168]	71%[168]	89%[174]

13 REFERENCES

1. Young, *Decomposition of Solids: International Encyclopaedia of Physical Chemistry and Chemical Physics*, Topic 21, Vol. 1.
2. Levy, Herley, *Material Science Research, 4*, 156, Chap. 8, 1969.
3. Tompkins, *Welch Found. Conf. XIV*, 203-4, 1970.
4. Dodd, *J. Chem. Phys., 35*, 1815, 1961.
5. Jacobs, Tompkins, *Proc. Roy. Soc. (Lond.), A215*, 254, 1952.
6. Hannay, *Solid State Chemistry*, Prentice-Hall, 1967.
7. Azaroff, *Introduction to Solids*, McGraw-Hill, 1960
8. Seitz, *Point Imperfections in Solids: Supp. del Nuovo Cimento*, Vol VII, Serie X, 2, 1958.
9. Deb, *J. Chem. Phys., 35*, 2122, 1961.
10. Deb, Yoffe, *Proc. Roy. Soc. (Lond.), A256*, 514, 1960.
11. McLaren, Rogers, *Proc. Roy. Soc. (Lond.), A240*, 484, 1957.
12. Rees, *Chemistry of the Defect Solid State*, Methuen, 1954.
13. Garner (Ed.), *Chemistry of the Solid State*, Butterworth, 1955.
14. Seitz, *Rev. Mod. Phys., 26*, 7, 1954.
15. Tamm, *Phys. Z. U.S.S.R., 1*, 733, 1932.
16. de Boer, *Rec. Trav. Chim. Pays. Bas., 56*, 301, 1937.
17. Witt, *Nachr. Akad. Wiss. Gottingen*, 17, 1952.
18. Mott, Littleton, *Trans. Far. Soc., 34*, 485, 1938.
19. Swank, Brown, *Phys. Rev., 130*, 34, 1963.
20. Pekar, *Journ. Phys. U.S.S.R., 10*, 341-7, 1946.
21. Pohl, *Physik. Zeits, 39*, 36, 1938.
22. Carlson, King, Miller, *J. Chem. Phys., 33*, 1266, 1960.
23. Cunningham, Tompkins, *Proc. Roy. Soc. (Lond.), A251*, 27, 1959.
24. King, Miller, Carlson, McMillan, *J. Chem. Phys., 35*, 1442, 1961.
25. Mollwo, *Nachr. Akad. Wiss. Gottingen*, 215, 1935.

26. Mollwo, *Ann. Phys., 29,* 394, 1937.

27. Pick, *Ann. d. Phys., 31,* 365, 1938.

28. Hilsch, Pohl, *Zeits. f. Phys., 68,* 721, 1931.

29. Delbecq, Pringsheim, Yuster, *J. Chem. Phys., 19,* 574, 1951; *ibid, 20,* 746, 1952.

30. Amelincx, *Rad. Damage nei Solidi, Scu.Int.di Fis.XVIII Corso,* 438, 1962.

31. Martienssen, Pohl, *Z. Phys., 131,* 488, 1952.

32. Molnar, Unpublished work quoted by Seitz, *Rev. Mod. Phys., 23,* 328, 1951.

33. Burnstein, Oberly, *Phys. Rev., 76,* 1254, 1949.

34. Duerig, Markham, *Phys. Rev., 88,* 1043, 1952.

35. Thomas, *Am. Phys., 38,* 601, 1940.

36. Mott, Gurney, *Electronic Processes in Ionic Crystals,* O.U.P., p.143.

37. Mott, *Proc. Roy. Soc., A172,* 325, 1939.

38. Garner, Maggs, *Proc. Roy. Soc., A172,* 299, 1939.

39. Wischin, *Proc. Roy. Soc., A172,* 314, 1939.

40. Thomas, Tompkins, *Proc. Roy. Soc., A209,* 550, 1951.

41. Baidins, *Disc. Fara. Soc., 28,* 248, 1959.

42. Jacobs, Tompkins, Young, *Disc. Fara. Soc., 28,* 234, 1959.

43. Deb, *Trans. Fara. Soc., 59,* 1423, 1963.

44. Jacobs, Tompkins, Pai Verneker, *J. Phys. Chem., 66,* 1113, 1962.

45. Boldyrev, Medvinskii, *Kin. i. Kat., 6,* 3, 550, 1965.

46. Pai Verneker, *J. Phys. Chem., 72,* 1733, 1968.

47. Marinkas, Bartram, *J. Chem. Phys., 48,* 927, 1968.

48. Prout, Sears, *J. Inorg. Nucl. Chem., 35,* 2163, 1973.

49. Owen, *J. Phys. Chem. Solids, 88,* 2646, 1971.

50. Prout, Shephard, Unpublished work (Shephard, Ph.D. Thesis, U.C.T., 1974).

51. Claxton, Overhill, Symons, *Mol. Phys.,* 75-80, 1973.

52. Brown, Milligan, Pimentel, *J. Chem. Phys., 25,* 1080, 1956.

53. Anderson, Horst, Milligan, *J. Phys. Chem. Solids, 23,* 157, 1962.

54. Ginns, Symons, *J. Chem. Soc. Far. Trans. 2, 68(4),* 631, 1972.

55. Begum, Symons, *J. Chem. Soc. A ,* 2062, 1971.

56. Maggs, *Trans. Fara. Soc., 35,* 433, 1939.

57. Garner, Reeves, *Trans. Fara. Soc., 51,* 694, 1955.

58. Tompkins, Young, *Trans. Fara. Soc., 61,* 1470, 1965.

59. Tompkins, Young, *Disc. Fara. Soc., 23,* 202-10, 1957.

60. Jacobs, Shephard, Tompkins, *International Symposium on the Reactivity of Solids, R5-45,* 509, 1964.

61. Brezina, Gelerinter, *J. Chem. Phys., 49,* 3293, 1968.

62. Gelerinter, Silsbee, *J. Chem. Phys., 45,* 1703, 1966.

63. Deb, *Trans. Fara. Soc., 59,* 1414, 1963.

64. Tompkins, Young, *Proc. Roy. Soc., A236,* 10, 1956.

65. Heal, Pringle, *J. Phys. Chem. Solids, 15,* 261, 1960.

66. Papazian, *J. Phys. Chem. Solids, 21,* 81, 1961.

67. Miller, *J. Chem. Phys., 33,* 889, 1960.

68. King, Carlson, Miller, McMillan, *J. Chem. Phys., 34,* 1499, 1961.

69. Shuskus, Young, Gilliam, Levy, *J. Chem. Phys., 33,* 622, 1960.

70. Wylie, Shuskus, Young,Gilliam, Levy, *Phys. Rev., 125,* 451, 1962.

71. Owens, *Physics Letters, 33A,* 41, 1970.

72. Owens, *Phys. Rev. B , 2,* 2064, 1970.

73. Jacobs, Tariq Kureishy, *J. Chem. Soc.,* 4723, 1964.

74. Prout, Sears, *Inorg. Nucl. Chem. Let., 9,* 31, 1973.

75. Pai Verneker, *J. Phys. Chem., 72,* 1733, 1968.

76. Marcantonio, Thekkendam, *J. Amer. Chem. Soc., 93,* 6, 1524, 1971.

77. Deb, Yoffe, Unpublished work (1958) quoted by Evans, Yoffe, Gray, *Chem. Rev., 59,* 515, 1959.

78. Yoganarasimhan, Sood, *J. Solid State Chem., 10(4),* 323, 1974.

79. Mitchell, *J. Phot. Sci, 5,* 49, 1957.

80. Mitchell, *Z. Phys., 138,* 381, 1954.

81. Vorob'eva, Sviridov, *Chem. Abs., 83,* 139761, 1975.

82. Saunders, *J. Opt. Soc. Am., 67(6),* 830, 1977.

83. Ovsyankin, Feofilov, *Chem. Abs., 83,* 69053, 1975.

84. Fujwara, Hada, *Chem. Abs. 85,* 134164, 1976.

85. Luckey, *J. Phys. Chem., 57,* 791, 1953.

86. Verwey, *J. Phys. Chem. Solids, 31,* 163, 1970.

87. Arends, Verwey, *Phys. Status Solidi, 23,* 137, 1967.

88. Schoonman, *Physica, 39,* 244, 1968.

89. Levine, Mark, *Phys. Rev., 144,* 751, 1966.

90. Kröger, *The Chemistry of Imperfect Crystals,* Amsterdam, 1964.

91. Reber, Steiger, *Surface Science, 49,* 236-252, 1975.

92. Kaldor, Somojai, *J. Phys. Chem., 70,* 3538, 1966.

93. Dawood, Forty, Tubbs, *Proc. Roy. Soc., 284,* 272, 1965.

94. Albrecht, Green, *J. Phys. Chem. Solids, 38(3),* 297, 1977.

95. Herley, Levy, *J. Chem. Phys., 46,* 627, 1967.

96. Herley, Levy, *6th Int. Symp. on React. Solids,* 1968.

97. Maycock, Pai Verneker, Witten, *J. Phys. Chem., 71,* 2107, 1967.

98. Pai Verneker, Maycock, *J. Phys. Chem., 72,* 2798, 1968.

99. Boldyrev, *J. Solid State Chem., 17,* 213, 1976.

100. Herley, Levy, *J. Chem. Phys., 62(1),* 177, 1975.

101. Copperthwaite, Lloyd, *J. Chem. Soc. Dalton Trans.,* 1117, 1977.

102. Prout, Lownds, *Inorg. Nucl. Chem. Lett., 9,* 377, 1973.

103. Shu-ti Lee, *Univ. Microfilms,* Ann Arbor, Mich., 6711878.

104. Finch, Jacobs, Tompkins, *J. Chem. Soc.,* 2053, 1954.

105. Boldyrev, *Kin. i. Kat., 1,* 203, 1960.

106. Hill, *Proc. Roy. Soc., A291,* 208, 1966.

107. Boldyrev, Kabanov, Trubitsyn, Oblivantsev, Uskov, Chelyshev, *Zh. Fiz. Khim., 41,* 1783, 1967.

108. Yoffe, *Developments in Inorganic Nitrogen Chemistry*, Ed. Colburn, p. 125, Elsevier (1966).

109. Bartlett, Tompkins, Young, *J. Chem. Soc.*, 3323, 1956.

110. Singh, *Trans. Fara. Soc.*, *52*, 1623, 1956.

111. Bowden, MacAuslan, *Nature*, *178*, 408, 1956.

112. Menter, *Proc. Roy. Soc.*, *A236*, 119, 1956.

113. Thomas, Renshaw, *J. Chem. Soc.*, 2058, 1967.

114. Bartlett, Tompkins, Young, *Proc. Roy. Soc.*, *A246*, 206, 1958.

115. Prout, Moore, *ASTM Spec. Tech. Pub. No. 400*, 45, 1966.

116. Boldyrev, London, Zhuravlev, *Phys. Status Solidi*, *30*, K13, 1968.

117. Secco, *J. Phys. Chem. Solids*, *24*, 469, 1963.

118. Bright, Garner, *J. Chem. Soc.*, 1872, 1934.

119. Hume, Colvin, *Proc. Roy. Soc.*, *A125*, 635, 1929.

120. Jacobs, Tompkins, *Proc. Roy. Soc.*, *A215*, 265, 1952.

121. Garner, Tanner, *J. Chem. Soc.*, 47, 1930.

122. Hill, Richardson, Rodger, *Proc. Roy. Soc.*, *A201*, 208, 1966.

123. Freeman, Anderson, Campisi, *J. Phys. Chem.*, *64*, 1727, 1960.

124. Komarov, Boldyrev, Zhuravlev, Ivanov, *Kin. i. Kat.*, *7*, 788, 1966.

125. Herley, Prout, *Nature*, *184*, 445, 1959.

126. Erofeyev, Protashchik, *Dokl. Akad. Nauk. S.S.S.R.*, *172*, 1129, 1967.

127. Groocock, Tompkins, *Proc. Roy. Soc.*, *A223*, 267, 1954.

128. Jach, Griffel, *J. Phys. Chem.*, *68*, 737, 1964.

129. Flanagan, *J. Phys. Chem. 66*, 416, 1962.

130. Bright, Garner, *J. Chem. Soc.*, 1872, 1934.

131. Herley, Jacobs, Levy, *Proc. Roy. Soc.*, *A318*, 197, 1970.

132. Herley, Jacobs, Levy, *J. Chem. Soc.*, *A*, 434, 1971.

133. Herley, Levy, *7th Int. Symp. on React. Solids*, 1972.

134. Herley, Levy, CFSTI, BNL, 15654, 1970.

135. Prout, Liddiard, *J. Phys. Chem.*, *72*, 2281, 1968.

136. Prout, Brown, *Nature, 205,* 1314, 1965.

137. Prout, Brown, Unpublished work (Brown, Ph.D. Thesis, Rhodes Univ., 1965).

138. Yankwich, Zavitsanos, *J. Phys. Chem., 68,* 457, 1964.

139. Leiga, *J. Phys. Chem., 70,* 3254, 3260, 1966.

140. Garner, Hailes, *Proc. Roy. Soc., A139,* 576, 1933

141. Hailes, *Trans. Fara. Soc., 29,* 544, 1933.

142. McDonald, *J. Chem. Soc.,* 839, 1936.

143. Herley, Prout, *J. Phys. Chem., 66,* 961, 1962.

144. Prout, Lownds, *Inorg. Nucl. Chem. Letters, 9,* 617, 1973.

145. Maycock, Pai Verneker, *J. Phys. Chem., 71,* 4077, 1967.

146. Phillips, Taylor, *J. Chem. Soc. A ,* 5583, 1963.

147. Markowitz, Boryta, *Chem. Abs., 55,* 26618, 1961.

148. Herley, Levy, *Nature, 211,* 1287, 1966.

149. Avrami, *J. Chem. Phys., 7,* 1103, 1939; *8,* 212, 1940; *9,* 177, 1941.

150. Erofeyev, *Acad. Sci. U.S.S.R., 52,* 511, 1946.

151. Boldyrev, Eroshkin, Zakharov, *Nauk. Dokl. Vysshikh. Shoklei,* 3, 1959.

152. Boldyrev, Zakharov, Eroshkin, Sokolova, *Dokl. Akad. Nauk., 129,* 365, 1959.

153. Protashchik, Erofeyev, *Dokl. Akad. Nauk. Beloruss. S.S.R., 10,* 658. 1966.

154. Ishkin, Dubil, *Zh. Prikl. Khim., 41,* 52, 1968.

155. Galway, Jacobs, *Proc. Roy. Soc., A254,* 455, 1960.

156. Acheson, Galway, *J. Chem. Soc.,* 1174, 1967.

157. Davies, Jacobs, Russel-Jones, *Trans. Fara. Soc., 63,* 1737, 1967.

158. Bond, Jacobs, *J. Chem. Soc., A9,* 1265, 1966.

159. Herley, Levy, *J. Chem. Phys., 49,* 1500, 1968.

160. Bel'kevich, Osinovik, *Chem. Abs., 50,* 11790, 1956.

161. Prout, Tompkins, *Trans. Fara. Soc., 42,* 482, 1946.

162. Prout, Brown, *ASTM Spec. Tech. Pub. No. 359,* 38, 1964.

163. Jacobs, Tariq Kureishy, *J. Chem. Soc.,* 4718, 1964.

164. Boldyrev, Oblivantsev, *Kin. i. Kat., 3,* 887, 1962.

165. Thomas, Tompkins, *Proc. Roy. Soc., A210,* 111, 1951.

166. Herley, Levy, *J. Phys. Chem., 75,* 191, 1971.

167. Boldyrev, Pinaerskaya,Boldyreva, Zakharov, Konyshev, *Kin. i. Kat., 2,* 184, 1961.

168. Prout, Moore, Unpublished Work (Moore, Ph.D. Thesis, Rhodes Univ., 1966).

169. Prout, Liddiard, *J. Inorg. Nucl. Chem., 35,* 2183, 1973.

170. Prout, Tompkins, *Trans. Fara. Soc., 43,* 148, 1947.

171. Benton, Cunningham, *J. Am. Chem. Soc., 57,* 2227, 1935.

172. Tompkins, *Trans. Fara. Soc., 44,* 206, 1948.

173. Haynes, Young, *Disc. Fara. Soc., 31,* 229, 1961.

174. Prout, Liddiard, Unpublished work (Liddiard, Ph.D. Thesis, U.C.T., 1969).

175. Garner, Moon, *J. Chem. Soc.*, 1398, 1933.

176. Boldyrev, Skorik, *Fiz. Shchel. Kristallov, Latv. Gos. Univ., Tr 2-go Vses. Soveshch., Riga,* 527, 1961.

177. Boldyrev, Skorik, *Dokl. Akad Nauk. SSSR, 156,* 1143, 1964.

178. Skorik, Boldyrev, Komarov, *Kin. i. Kat., 8,* 1258, 1967.

179. Frenkel, Anastosevich, *Zh ETF 11, 1,* 127, 1941.

180. Hannay (Ed.), *Treatise on Solid State Chemistry Vol. 4,* p 229.

181. Fair, Walker (Ed.), *Energetic Materials Vol. 1,* p. 110, Plenum Press (1977).

182. Nuegebauer (Ed.), *The Structure and Properties of Thin Films,* Wiley (1959).

183. Jacobs, Tariq Kureishy, *Can. J. Chem., 44,* 1733, 1968.

184. de Panafieu, Thesis, Princeton University, Princeton N.J., 1974.

185. Evans, Yoffe, Gray, *Chem. Rev., 59,* 515, 1959.

186. Schulman, Compton, *Colour Centres in Solids,* MacMillan, New York, 1962.

187. Young, *Progress in Solid State Chemistry, 5,* 427, 1971.

188. Tompkins, *Ind. and Eng. Chemistry, 44, 6,* 1336, 1952.

189. Owens, Vogel, *J. Chem. Phys., 56,* 2487, 1972.

190. Mason, *Quart. Rev., 15,* 287, 1961.

191. Walsh, *J. Chem. Soc.,* 2266, 1953.

192. Seitz, *Imperfections in Nearly Perfect Crystals,* John Wiley and Sons New York (1952).

193. Marinkas, *J. Chem. Phys., 52, 10,* 5144, 1970.

194. Marke, *Trans. Fara. Soc., 33,* 770, 1937.

195. Garner, Haycock, *Trans. Fara. Soc., 51,* 694, 1955.

196. Pai Verneker, Forsyth, *J. Phys. Chem., 71,* 3736, 1967.

197. Andreev, *Physik. Z. Soviet Union, 6,* 1121, 1934.

198. Owens, *J. Phys. Chem. Solids, 32,* 2646, 1971.

199. Prout, Moore, *J. Inorg. Nucl. Chem., 31,* 1595, 1969.